DM

Application of Phage Display Technology on the Diagnosis of Infectious Diseases

Discovery of Zika-Specific Peptides

MASTER DISSERTATION

Helena Cristina Silva Chá-Chá

MASTER IN APPLIED BIOCHEMISTRY

UNIVERSIDADE da MADEIRA

A Nossa Universidade

www.uma.pt

October | 2021

Application of Phage Display Technology on the Diagnosis of Infectious Diseases

Discovery of Zika-Specific Peptides

MASTER DISSERTATION

Helena Cristina Silva Chá-Chá
MASTER IN APPLIED BIOCHEMISTRY

ORIENTATION
Helena Paula de Freitas Caldeira Araújo

CO-ORIENTATION
Helena Maria Pires Gaspar Tomás

DECLARAÇÃO

O plágio consiste na apresentação, como sendo suas/seus e mesmo que tenha havido tradução, de ideias, opiniões, frases/textos, resultados ou conclusões de outros. A prática de plágio constitui uma grave violação da ética académica, além de poder levar à reprovação ou à retirada do grau, assim como a responsabilidade civil, criminal e disciplinar.

Assim, declaro por minha honra que a presente dissertação de mestrado é da minha exclusiva autoria, é original, e nela referenciei e citei todas as fontes utilizadas.

01/10/2021

Helena Cristina Silva Chá-Chá

Application of Phage Display Technology on the Diagnosis of Infectious Diseases: Discovery of Zika-Specific Peptides

Dissertation submitted to the University of Madeira in fulfilment of the requirements for the degree of Master in Applied Biochemistry

By Helena Cristina Silva Chá-Chá

Work developed under the supervision of

Professor Doctor Helena Paula de Freitas Caldeira Araújo

Co-supervised by Professor Doctor Helena Maria Pires Gaspar Tomás

Faculdade de Ciências Exatas e de Engenharia,

Centro de Química da Madeira,

Campus Universitário da Penteada,

Universidade da Madeira

Funchal – Portugal

2021

Acknowledgements

First of all, I would like to thank Professor Helena Caldeira and Professor Helena Tomás for the opportunity to work on this project under their supervision and for the chance to present it in various conferences. I would also like to recognize all their support, assistance and guidance throughout the development of this dissertation.

Also, a very sincere thank you to Doctor Mariana Vieira, for all the support, patience and advice given during the development of this project. I am very grateful for all the assistance and guidance given throughout these years, and also for the constant availability in helping, all the motivating words and the endless attention.

Additionally, I would like to thank laboratory technicians Paula Andrade and Teresa Abreu, for the assistance and availability in providing the necessary tools during the development of this project.

Likewise, I am deeply grateful for all the contributions and support given by all the CQM colleagues and personnel, namely Filipe Olim, Fátima Mendes, Fátima Moreira, Ana Olival, Onofre Figueira, Gonçalo Martins, Lydia dos Orfãos, Duarte Fernandes and João Serina, and by the friends Francisca Costa, Andreia Luís and Alex Faria. Thank you so much for your advice and contribution for this project, and for the valuable friendships built during these years.

Moreover, I am very appreciative of all the love and support given by my family, namely my dad Luís, my mom Helena and my sister Luísa. Thank you so much for your endless and continuous support and encouragement, I could never thank you enough. This was only possible because of you.

I would also like to thank my boyfriend Moeketsi Guy Maeyane, for all the constant support and words of encouragement, and for always being there for me when I was needing it the most. Thank you so very much for all the motivation and for never giving up on me. I love you.

Finally, I would like to thank CQM and all the professors for the tools and the support provided during the development of this dissertation.

This work was supported by FCT - Fundação para a Ciência e a Tecnologia (CQM Base Fund - UIDB/00674/2020 and Programmatic Fund - UIDP/00674/2020), ARDITI - Agência Regional para o Desenvolvimento da Investigação, Tecnologia e Inovação (Project M1420-01-0145-FEDER-000005-Centro de Química da Madeira-CQM+, Madeira 14-20 Programme), the Post-Doctoral Research Grant ARDITI-CQM-2017-009-PDG and the Bachelor Research Grant ARDITl-CQM-2019-015-BDG.

Oral and poster presentations in scientific meetings in the scope of this dissertation:

- Chá-Chá, H., Vieira, M., Rodrigues, J., Tomás, H., Caldeira, H. (2019), Application of the Phage Display Technology to the Development of Bionanosensors for the Diagnostic of Infectious Diseases, 6th CQM Annual Meeting.
- Chá-Chá, H., Vieira, M., Rodrigues, J., Tomás, H., Caldeira, H. (2019), Development of Bionanosensors for the Diagnosis of Infectious Diseases using the Phage Display Technology, XXVI Encontro Nacional da SPQ – XXVIENSPQ.
- Chá-Chá, H., Vieira, M., Rodrigues, J., Tomás, H., Caldeira, H. (2020), Development of Bacteriophage-Based Bionanosensors for the Diagnosis of Infectious Diseases using the Phage Display Technique, 7th CQM Annual Meeting.

Abstract

Zika is an infectious viral disease which had a recent worldwide outbreak. This illness is caused by the Zika virus (ZIKV), a flavivirus transmitted by the *Aedes aegypti* mosquito. Currently, there are still no vaccines to prevent Zika infection nor pharmacological agents to treat it. A routine and accurate assay for the diagnosis of Zika is also not presently available. Current diagnostic tools for this disease include serological/molecular studies and antigen and/or genome detection, which are time-consuming methods that occasionally present low specificity and require specialized and expensive laboratory equipment.

The phage display technique is based on the presentation of randomized molecule libraries on the surface of bacteriophages. In this technique, a gene encoding a protein of interest is inserted into a phage coat protein gene, allowing for a direct linkage between phage phenotype and genotype. Using this technology, large peptide sequences can be displayed in the phage surface and used for affinity screening of specific target molecules. Phages bound to a specific target go through several repeated cycles in order to produce a phage mixture enriched with the relevant phage-displayed peptides that specifically recognize disease target molecules with high sensitivity and selectivity.

Thus, the main purpose of this project was to develop an approach, based on the phage display technology, that would allow for an early, rapid and differential routine diagnosis of Zika. During this project, a commercially available phage-displayed peptide library was screened against two specific antibodies for Zika, in order to identify the phage-displayed peptides that specifically recognized their targets with high sensitivity and selectivity. The desired future outcome is the development of an innovative biosensing method for non-invasive, rapid and in real time diagnosis of the disease.

Keywords: Phage Display, Zika, Bacteriophage, Antibody, Peptide.

Resumo

A Zika é uma doença viral infeciosa que teve um recente surto mundial. A doença é causada pelo vírus Zika (ZIKV), um flavivírus transmitido pelo mosquito *Aedes aegypti*. Atualmente, ainda não existem vacinas para prevenir a infeção pelo vírus Zika nem estão disponíveis medicamentos para tratá-la. De momento, também ainda não estão disponíveis ensaios precisos e de rotina para o diagnóstico da Zika. As ferramentas de diagnóstico atuais para esta doença incluem estudos serológicos/moleculares e de deteção de antigénios e/ou genomas, que são métodos morosos, que muitas vezes apresentam baixa especificidade e que requerem, na sua maioria, equipamentos laboratoriais especializados e dispendiosos.

A técnica de disposição em fagos é baseada na apresentação de bibliotecas de moléculas aleatórias na superfície de bacteriófagos. Nesta técnica, um gene que codifica uma proteína de interesse é inserido num gene de uma proteína de revestimento do fago, permitindo estabelecer uma ligação direta entre o fenótipo e o genótipo do fago. Usando esta tecnologia, grandes sequências de péptidos podem ser exibidas na superfície de bacteriófagos e usadas para o rastreio de afinidade de moléculas alvo específicas. Os fagos ligados a um alvo específico passam por vários ciclos repetidos para produzir uma mistura de fagos enriquecida com os péptidos exibidos em fagos relevantes que reconhecem especificamente as moléculas alvo da doença com alta sensibilidade e seletividade.

Assim, o principal objetivo deste projeto foi o desenvolvimento de uma abordagem, baseada na tecnologia de exposição em bacteriófagos, que permitisse um diagnóstico de rotina precoce, rápido e diferencial da Zika. Durante este projeto, uma biblioteca de péptidos exibidos em fagos, que está disponível no mercado, foi testada contra dois anticorpos específicos para o vírus Zika, a fim de identificar os péptidos exibidos em fagos que reconheciam especificamente as moléculas alvo da doença com alta sensibilidade e seletividade. O resultado futuro desejado é o desenvolvimento de um método inovador de biossensores para o diagnóstico não invasivo, rápido e em tempo real da doença.

Palavras-Chave: Phage Display, Zika, Bacteriófago, Anticorpo, Péptido.

Index

Acknowledgements.....2
Abstract.....4
Keywords.....4
Resumo.....5
Palavras-Chave.....5
Abbreviations.....14
1. Introduction.....15
1.1. Zika Virus.....16
1.1.1. Virology.....16
1.1.2. Transmission.....17
1.1.2.1. Mosquito.....18
1.1.2.2. Sexual.....19
1.1.2.3. Pregnancy.....19
1.1.2.4. Blood Transfusions.....20
1.1.3. Pathogenesis.....21
1.1.4. Zika Fever.....21
1.1.4.1. Vaccine Development.....22
1.1.4.2. Treatment Strategies.....23
1.1.4.3. Laboratory Diagnosis.....24
1.2. Phage Display Technology.....25
1.2.1. Brief History.....25
1.2.2. Principle of the Technique.....26
1.2.3. Bacteriophages – Phage Display Vectors.....27
1.2.3.1. Filamentous Phages.....28
1.2.3.1.1. M13 Filamentous Phages.....28
1.2.4. Display of Foreign Peptides on Filamentous Phages.....30
1.2.5. Types of Phage Display Systems.....31
1.2.6. Types of Displayed Peptides and Proteins.....32
1.2.6.1. Display of Antibody Fragments.....33
1.2.7. General Principles of Selection.....35
1.2.7.1. General Protocol.....36
1.2.7.2. Affinity Selection.....37
1.2.8. Applications.....37
1.2.8.1. Disease Therapeutics.....38
1.2.8.1.1. Transfusion Medicine.....38
1.2.8.1.2. Autoimmune Diseases.....39
1.2.8.1.3. Neurological Disorders.....40
1.2.8.1.4. Tissue Targeting and Anti-Angiogenic Therapies.....41
1.2.8.1.5. Molecular Imaging and Tumor Targeting.....41
1.2.8.2. Target Receptors used in Affinity Selection.....44
1.2.8.2.1. Epitope Mapping and Mimicking.....44
1.2.8.2.2. Identification of New Receptors and Natural Ligands.....45
1.2.8.2.3. Drug Discovery.....46
1.2.8.2.4. Epitope Discovery.....46

1.2.8.2.5. Selection of DNA-Binding Proteins.....47
1.3. Thesis Objectives.....48
2. Materials and Methods.....50
2.1. General Materials.....51
2.1.1. Phage Display Peptide Library Kit.....51
2.1.2. *E. coli* ER2738 Host Strain.....51
2.1.3. Anti-Zika Virus NS1 Antibodies.....51
2.1.4. Media and Solutions.....52
2.1.5. Laboratory Equipment.....53
2.2. General Methods.....53
2.2.1. Strain Maintenance.....53
2.2.2. Avoiding Phage Contamination.....53
2.2.3. Phage Titering.....54
2.2.4. Storage of Phage Solutions.....55
2.3. Surface Panning Procedure with Direct Target Coating.....55
2.3.1. Biopanning against Streptavidin Target.....55
2.3.2. Biopanning against Anti-Zika Virus NS1 Antibody Target.....56
2.4. Solution-Phase Panning with Affinity Bead Capture.....58
2.4.1. Biopanning against Streptavidin Target.....58
2.4.2. Biopanning against Anti-Zika Virus NS1 Antibody Target.....58
2.4.2.1. Biopanning with Protein A and Protein G Agarose Beads.....59
2.4.2.2. Biopanning with Protein G Agarose Beads and Negative Selection Step.....60
2.4.2.3. Biopanning with Protein A Agarose Beads and Negative Selection Step.....62
2.5. Phage ELISA Binding Assay with Direct Target Coating.....63
2.5.1. Plaque Amplification for ELISA.....63
2.5.2. ELISA Assay.....64
2.5.2.1. ELISA Assay against Streptavidin Target.....65
2.5.2.2. ELISA Assay against Anti-Zika Virus NS1 Antibody Target.....65
2.6. Sequencing of Phage DNA.....66
2.6.1. Plaque Amplification for Sequencing.....66
2.6.2. Rapid Purification of Sequencing Templates.....67
2.6.3. DNA Quantification of PCR Templates.....67
2.6.4. PCR Amplification.....68
2.6.5. Purification of PCR Products.....68
2.6.5.1. Ethanol/Isopropanol Precipitation.....69
2.6.5.2. PCR Purification Kit.....69
2.6.6. DNA Quantification of PCR Products.....70
2.6.7. Agarose Gel Electrophoresis.....70
2.6.8. Phage DNA Sequencing.....71
2.6.8.1. Analysis of Results using Bioinformatic Tools.....71
3. Results and Discussion.....72
3.1. Surface Panning Procedure with Direct Target Coating.....73
3.1.1. Biopanning against Streptavidin Target.....73
3.1.2. Biopanning against Anti-Zika Virus NS1 Antibody Target.....74
3.2. Solution-Phase Panning with Affinity Bead Capture.....75

3.2.1. Biopanning against Streptavidin Target.....75
3.2.2. Biopanning against Anti-Zika Virus NS1 Antibody Target.....76
3.2.2.1. Biopanning with Protein A and Protein G Agarose Beads.....76
3.2.2.2. Biopanning with Protein G Agarose Beads and Negative Selection Step.....77
3.2.2.3. Biopanning with Protein A Agarose Beads and Negative Selection Step.....79
3.3. Phage ELISA Binding Assay with Direct Target Coating.....80
3.3.1. ELISA Assay against Streptavidin Target.....80
3.3.2. ELISA Assay against Anti-Zika Virus NS1 Antibody Target.....82
3.4. PCR Amplification of Phage DNA.....86
3.4.1. DNA Quantification of PCR Templates.....86
3.4.2. DNA Quantification of PCR Products.....90
3.5. Agarose Gel Electrophoresis.....100
3.6. Sequencing of Phage DNA.....108
Conclusions and Future Work.....116
Bibliography.....117
Annexes.....138
Annex 1: QIAGEN® "QIAquick® PCR Purification Kit / QIAquick® PCR & Gel Cleanup Kit" Protocol...138
Annex 2: Tables.....141
Annex 3: Figures.....163

Figures Index

Figure 1 – "Zika virus" capsid model, colored by chains (21). 17
Figure 2 – Global map of Zika virus infection (Centers for Disease Control and Prevention, September of 2018) (28). 18
Figure 3 – A baby with microcephaly (left) compared to a baby with a typical head size (right) (48). 20
Figure 4 – Principle of filamentous bacteriophage M13 phage display using a phagemid vector (117). 27
Figure 5 – Schematic structure of bacteriophage M13 (132). 30
Figure 6 – Panning with a pentavalent peptide library displayed on pIII (205). 37
Figure 7 – Absorbances registered on the ELISA assay conducted for the phage stocks amplified from the biopanning experiments performed against Streptavidin (Experiment S1 and Experiment S2). ... 81
Figure 8 – Absorbances registered on the ELISA assay conducted for the phage stocks amplified from the biopanning experiments performed against the Anti-Zika Virus NS1 Antibodies (Experiment Z1, Experiment Z2, Experiment Z3 and Experiment Z4). 83
Figure 9 – DNA concentrations obtained before PCR amplification and after PCR amplification and purification for the Experiment S1 clones. 90
Figure 10 – DNA concentrations obtained before PCR amplification and after PCR amplification and purification for the Experiment S2 clones. 91
Figure 11 – DNA concentrations obtained before PCR amplification and after PCR amplification by PCR Experiment 1, PCR Experiment 2 and PCR experiment 3 and purification for the Experiment Z1 clones. 92
Figure 12 – DNA concentrations obtained before PCR amplification and after PCR amplification and purification for the Experiment Z2 clones. 95
Figure 13 – DNA concentrations obtained before PCR amplification and after PCR amplification before and after purification for the Experiment Z3.1 clones. 96
Figure 14 – DNA concentrations obtained before PCR amplification and after PCR amplification before and after purification for the Experiment Z3.2 clones. 98
Figure 15 – DNA concentrations obtained before PCR amplification and after PCR amplification before and after purification for the Experiment Z4 clones. 99
Figure 16 – Photograph of the 1% agarose gel from the electrophoresis assay conducted for the 10 DNA samples from Experiment S1 after PCR amplification and after purification. Order of the samples: 100 bp DNA ladder; Clones S1.1-S1.10 101
Figure 17 – Photograph of the 1% agarose gel from the electrophoresis assay conducted for the 10 DNA samples from Experiment S2 after PCR amplification and after purification. Order of the samples: 100 bp DNA ladder; Clones S2.1-S2.10; 100 bp DNA ladder. 102
Figure 18 – Photograph of the 1% agarose gel from the electrophoresis assay conducted for the 10 DNA samples from Experiment Z1 after PCR amplification by PCR Experiment 1 and after purification. Order of the samples: 100 bp DNA ladder; Clones Z1.1-Z1.10; 100 bp DNA ladder. 103
Figure 19 – Photograph of the 2% agarose gel from the electrophoresis assay conducted for the 10 DNA samples from Experiment Z1 after PCR amplification by PCR Experiment 2 and after purification. Order of the samples: 100 bp DNA ladder; Clones Z1.1-Z1.10; 100 bp DNA ladder. 103
Figure 20 – Photograph of the 2% agarose gel from the electrophoresis assay conducted for the DNA samples from Experiment Z1 after PCR amplification by PCR Experiment 3 and before and after purification. Order of the samples: 100 bp DNA ladder; Control Before Purification; Control After Purification; Clones Z1.1 and Z1.2 Before Purification; Clones Z1.1 and Z1.2 After Purification; Clones Z1.6 and Z1.7 Before Purification; Clones Z1.6 and Z1.7 After Purification; 100 bp DNA ladder. 104

Figure 21 – Photograph of the 1% agarose gel from the electrophoresis assay conducted for the DNA samples from Experiment Z2 after PCR amplification and after purification. Order of the samples: 100 bp DNA ladder; Clones Z2.1-Z2.6. 105
Figure 22 – Photograph of the 1% agarose gel from the electrophoresis assay conducted for the DNA samples from Experiment Z3 after PCR amplification and before purification. Order of the samples: 100 bp DNA ladder; Clones Z3.1.1-Z3.1.4; Clones Z3.2.1-Z3.2.4; 100 bp DNA ladder. 106
Figure 23 – Photograph of the 1% agarose gel from the electrophoresis assay conducted for the DNA samples from Experiment Z3 after PCR amplification and after purification. Order of the samples: 100 bp DNA ladder; Clones Z3.1.1-Z3.1.5; Clones Z3.2.1-Z3.2.5..... 107
Figure 24 – Photograph of the 1% agarose gel from the electrophoresis assay conducted for the DNA samples from Experiment Z4 after PCR amplification and after purification. Order of the samples: 100 bp DNA ladder; Clones Z4.1-Z4.6. 108
Figure 25 – Example of the plates obtained for the titering of the amplified third round phage eluate pool on Experiment S1. 163
Figure 26 – Example of the plates obtained for the titering of the amplified third round phage eluate pool on Experiment Z1. 163
Figure 27 – Example of the plates obtained for the titering of the amplified third round phage eluate pool on Experiment S2. 164
Figure 28 – Example of the plates obtained for the titering of the amplified third round phage eluate pool on Experiment Z2. 164
Figure 29 – Example of the plates obtained for the titering of the amplified third round phage eluate pool on Experiment Z3. 165
Figure 30 – Example of the plates obtained for the titering of the amplified third round phage eluate pool on Experiment Z4. 165

Tables Index

Table 1 – Phage titers obtained for the third round amplified eluate pools of the surface-based panning procedure conducted against Streptavidin (Experiment S1). 73
Table 2 – Phage titers obtained for the third round amplified eluate pools of the surface-based panning procedure conducted against the Anti-Zika Virus NS1 Antibody [B4] (Experiment Z1)..... 74
Table 3 – Phage titers obtained for the third round amplified eluate pools of the solution-phase panning procedure conducted against Streptavidin (Experiment S2), using Protein G agarose beads in all three rounds and a subtractive panning step..... 75
Table 4 – Phage titers obtained for the third round amplified eluate pools of the solution-phase panning procedure conducted against the Anti-Zika Virus NS1 Antibody [B4] (Experiment Z2), using Protein G and Protein A agarose beads. 76
Table 5 – Phage titers obtained for the third round amplified eluate pools of the solution-phase panning procedure conducted against the Anti-Zika Virus NS1 Antibody [B4] (Experiment Z3.1) and against the Anti-Zika Virus NS1 Antibody [D11] (Experiment Z3.2), using Protein G agarose beads in all three rounds and a subtractive panning step. 77
Table 6 – Phage titers obtained for the third round amplified eluate pools of the solution-phase panning procedure conducted against the Anti-Zika Virus NS1 Antibody [D11] (Experiment Z4), using Protein A agarose beads in all three rounds and a subtractive panning step. 79
Table 7 - Amino acid sequences corresponding to the library inserts obtained for Experiment S1. . 109
Table 8 – Amino acid sequences corresponding to the library inserts obtained for Experiment S2.. 110
Table 9 – Amino acid sequences corresponding to the library inserts obtained for Experiment Z1.. 111
Table 10 – Amino acid sequences corresponding to the library inserts obtained for Experiment Z2.112
Table 11 – Amino acid sequences corresponding to the library inserts obtained for Experiment Z3.1. 113
Table 12 – Amino acid sequences corresponding to the library inserts obtained for Experiment Z3.2. 114
Table 13 – Amino acid sequences corresponding to the library inserts obtained for Experiment Z4.115
Table 14 – Volumes of reagents used on the three rounds of the positive control panning experiment (Step 1.1 and Step 1.2) and dilutions used in unamplified and amplified phage titering assays (Step 1.3 and Step 1.4, respectively), during the surface-based panning procedure against Streptavidin (Experiment S1). 141
Table 15 – Volumes of reagents used on the three rounds of the biopanning experiment (Step 1.1 and Step 1.2) and dilutions used in unamplified and amplified phage titering assays (Step 1.3 and Step 1.4, respectively), during the surface-based panning procedure against the Anti-Zika Virus NS1 Antibody [B4] (Experiment Z1). 141
Table 16 – Volumes of reagents used on the three rounds of the positive control panning experiment (Step 2.1, Step 3.1 and Step 3.2) and dilutions used in unamplified and amplified phage titering assays (Step 2.2 and Step 2.3, respectively), during the solution-based panning procedure against Streptavidin, using protein G agarose beads and a subtractive panning step (Experiment S2)..... 141
Table 17 – Volumes of reagents used on the three rounds of the biopanning experiment (Step 2.1) and dilutions used in unamplified and amplified phage titering assays (Step 2.2 and Step 2.3, respectively), during the solution-based panning procedure against the Anti-Zika Virus NS1 Antibody [B4], using protein A and protein G agarose beads (Experiment Z2)..... 142
Table 18 – Volumes of reagents used on the three rounds of the biopanning experiment (Step 2.1, Step 3.1 and Step 3.2) and dilutions used in unamplified and amplified phage titering assays (Step 2.2 and Step 2.3, respectively), during the solution-based panning procedure against the Anti-Zika Virus NS1 Antibody [B4], using protein G agarose beads and a subtractive panning step (Experiment Z3.1). .. 142

Table 19 – Volumes of reagents used on the three rounds of the biopanning experiment (Step 2.1, Step 3.1 and Step 3.2) and dilutions used in unamplified and amplified phage titering assays (Step 2.2 and Step 2.3, respectively), during the solution-based panning procedure against the Anti-Zika Virus NS1 Antibody [D11], using protein G agarose beads and a subtractive panning step (Experiment Z3.2). 143
Table 20 – Volumes of reagents used on the three rounds of the biopanning experiment (Step 2.1, Step 3.1 and Step 3.2) and dilutions used in unamplified and amplified phage titering assays (Step 2.2 and Step 2.3, respectively), during the solution-based panning procedure against the Anti-Zika Virus NS1 Antibody [D11], using protein A agarose beads and a subtractive panning step (Experiment Z4). ... 143
Table 21 – Volumes of reagents used in the ELISA assay conducted for the phage stocks amplified from the biopanning experiments performed against Streptavidin (Experiment S1 and Experiment S2).. 144
Table 22 – Volumes of reagents used in the ELISA assay conducted for the phage stocks amplified from the biopanning experiments performed against the Anti-Zika Virus NS1 Antibodies (Experiment Z1, Experiment Z2, Experiment Z3 and Experiment Z4). 145
Table 23 – Volumes and concentrations of reagents used in PCR Experiment 1. 146
Table 24 – Thermal cycling temperature and timing conditions used in PCR Experiment 1. 146
Table 25 – Volumes and concentrations of reagents used in PCR Experiment 2. 147
Table 26 – Volumes and concentrations of reagents used in PCR Experiment 3. 147
Table 27 – Thermal cycling temperature conditions used in PCR Experiment 3. 147
Table 28 – Absorbances registered on the ELISA assay conducted for the phage stocks amplified from the biopanning experiments performed against Streptavidin (Experiment S1 and Experiment S2).. 148
Table 29 – Absorbances registered on the ELISA assay conducted for the phage stocks amplified from the biopanning experiments performed against the Anti-Zika Virus NS1 Antibodies (Experiment Z1, Experiment Z2, Experiment Z3 and Experiment Z4). 149
Table 30 – Absorbances and corresponding DNA concentrations and purity ratios of the 10 clones and the eluate pool from Experiment S1. 150
Table 31 – Absorbances and corresponding DNA concentrations and purity ratios of the 10 clones and the eluate pool from Experiment S2. 150
Table 32 – Absorbances and corresponding DNA concentrations and purity ratios of the 10 clones from Experiment Z1. 150
Table 33 – Absorbances and corresponding DNA concentrations and purity ratios of the 10 clones from Experiment Z2. 151
Table 34 – Absorbances and corresponding DNA concentrations and purity ratios of the 10 clones and the eluate pool from Experiment Z3.1. 151
Table 35 – Absorbances and corresponding DNA concentrations and purity ratios of the 10 clones and the eluate pool from Experiment Z3.2. 151
Table 36 – Absorbances and corresponding DNA concentrations and purity ratios of the 10 clones from Experiment Z4. 152
Table 37 – Absorbances and corresponding DNA concentrations and purity ratios of the amplified and purified 10 clones and eluate pool from Experiment S1. 152
Table 38 – Absorbances and corresponding DNA concentrations and purity ratios of the amplified and purified 10 clones and eluate pool from Experiment S2. 152
Table 39 – Absorbances and corresponding DNA concentrations and purity ratios of the amplified and purified 10 clones from Experiment Z1 amplified by PCR Experiment 1. 153
Table 40 – Absorbances and corresponding DNA concentrations and purity ratios of the amplified and purified 10 clones from Experiment Z1 amplified by PCR Experiment 2. 153
Table 41 – Absorbances and corresponding DNA concentrations and purity ratios of the amplified and purified 10 clones from Experiment Z1 amplified by PCR Experiment 3. 153

Table 42 – Absorbances and corresponding DNA concentrations and purity ratios of the amplified and purified clones from Experiment Z2. 154
Table 43 – Absorbances and corresponding DNA concentrations and purity ratios of the amplified 10 clones from Experiment Z3.1. 154
Table 44 – Absorbances and corresponding DNA concentrations and purity ratios of the amplified and purified clones from Experiment Z3.1. 154
Table 45 – Absorbances and corresponding DNA concentrations and purity ratios of the amplified 10 clones from Experiment Z3.2. 155
Table 46 – Absorbances and corresponding DNA concentrations and purity ratios of the amplified and purified clones from Experiment Z3.2. 155
Table 47 – Absorbances and corresponding DNA concentrations and purity ratios of the amplified 10 clones from Experiment Z4. 155
Table 48 – Absorbances and corresponding DNA concentrations and purity ratios of the amplified and purified clones from Experiment Z4. 156
Table 49 – Nucleotide sequences obtained by Sanger Sequencing for the random 10 clones chosen for Experiment S1. 156
Table 50 – Nucleotide sequences corresponding to the library inserts obtained for Experiment S1. 156
Table 51 – Nucleotide sequences obtained by Sanger Sequencing for the random 10 clones chosen for Experiment S2. 157
Table 52 – Nucleotide sequences corresponding to the library inserts obtained for Experiment S2. 157
Table 53 – Nucleotide sequences obtained by Sanger Sequencing for the eluate pool and the random 10 clones chosen for Experiment Z1. 158
Table 54 – Nucleotide sequences corresponding to the library inserts obtained for Experiment Z1. 158
Table 55 – Nucleotide sequences obtained by Sanger Sequencing for the eluate pool and the random 10 clones chosen for Experiment Z2. 159
Table 56 – Nucleotide sequences corresponding to the library inserts obtained for Experiment Z2. 159
Table 57 – Nucleotide sequences obtained by Sanger Sequencing for the eluate pool and random 10 clones chosen for Experiment Z3.1. 160
Table 58 – Nucleotide sequences corresponding to the library inserts obtained for Experiment Z3.1. 160
Table 59 – Nucleotide sequences obtained by Sanger Sequencing for the eluate pool and random 10 clones chosen for Experiment Z3.2. 161
Table 60 – Nucleotide sequences corresponding to the library inserts obtained for Experiment Z3.2. 161
Table 61 – Nucleotide sequences obtained by Sanger Sequencing for the eluate pool and the random 10 clones chosen for Experiment Z4. 162
Table 62 – Nucleotide sequences corresponding to the library inserts obtained for Experiment Z4. 162

Abbreviations

IPTG – isopropyl-β-D-thiogalactoside
X-Gal – 5-Bromo-4-chloro-3-indolyl-β-D-galactoside
DMF – dimethyl formamide
MOI – multiplicity of infection
ABTS – azino-bis(3-ethylbenzothiazole sulfonic acid) diammonium salt
WHO – World Health Organization
ZIKV – Zika Virus
CDC – Centers for Disease Control and Prevention
FDA – Food and Drug Administration
DNA – deoxyribonucleic acid
RNA – ribonucleic acid
ssDNA – single stranded deoxyribonucleic acid
dsDNA – double stranded deoxyribonucleic acid
cDNA – complementary deoxyribonucleic acid
mRNA – messenger ribonucleic acid
ELISA – enzyme-linked immunosorbent assay
PCR – polymerase chain reaction
RT-PCR – reverse transcription polymerase chain reaction
GBS – Guillain–Barré syndrome
DEET – N,N-Diethyl-*meta*-toluamide
HIV – human immunodeficiency viruses
PRNT – plaque reduction neutralization test
IgG – immunoglobulin G
IgM – immunoglobulin M
PDT – Phage Display Technology
LB – lysogeny broth / Luria broth / Luria–Bertani medium
Fab – antigen-binding fragment
Fv – variable fragment
scFv – single-chain variable fragment
EDTA – ethylenediaminetetraacetic acid
PEG – polyethylene glycol
TBS – tris-buffered saline
TBST – tris-buffered saline plus Polysorbate 20
ZPIV – Zika Virus Purified Inactivated Vaccine
MAC-ELISA – IgM antibody capture enzyme-linked immunosorbent assay
PDT – Phage Display Technology
HOC – highly immunogenic outer capsid protein
SOC – small outer capsid protein
Fab – antigen-binding fragment
Fv – variable fragment
CDR – complementarity-determining regions
PVDF – polyvinylidene difluoride
CALI – chromophore-assisted laser inactivation
FMAT – fluorometric microvolume assay technology

CHAPTER 1. INTRODUCTION

1. Introduction
1.1. Zika Virus
1.1.1. Virology
1.1.2. Transmission
1.1.2.1. Mosquito
1.1.2.2. Sexual
1.1.2.3. Pregnancy
1.1.2.4. Blood Transfusions
1.1.3. Pathogenesis
1.1.4. Zika Fever
1.1.4.1. Vaccine Development
1.1.4.2. Treatment Strategies
1.1.4.3. Laboratory Diagnosis
1.2. Phage Display Technology
1.2.1. Brief History
1.2.2. Principle of the Technique
1.2.3. Bacteriophages – Phage Display Vectors
1.2.3.1. Filamentous Phages
1.2.3.1.1. M13 Filamentous Phages
1.2.4. Display of Foreign Peptides on Filamentous Phages
1.2.5. Types of Phage Display Systems
1.2.6. Types of Displayed Peptides and Proteins
1.2.6.1. Display of Antibody Fragments
1.2.7. General Principles of Selection
1.2.7.1. General Protocol
1.2.7.2. Affinity Selection
1.2.8. Applications
1.2.8.1. Disease Therapeutics
1.2.8.1.1. Transfusion Medicine
1.2.8.1.2. Autoimmune Diseases
1.2.8.1.3. Neurological Disorders
1.2.8.1.4. Tissue Targeting and Anti-Angiogenic Therapies
1.2.8.1.5. Molecular Imaging and Tumor Targeting
1.2.8.2. Target Receptors used in Affinity Selection
1.2.8.2.1. Epitope Mapping and Mimicking
1.2.8.2.2. Identification of New Receptors and Natural Ligands
1.2.8.2.3. Drug Discovery
1.2.8.2.4. Epitope Discovery
1.2.8.2.5. Selection of DNA-Binding Proteins
1.3. Thesis Objectives

1. Introduction

1.1. Zika Virus

The Zika virus, also known as ZIKV, is a member of the *Flaviviridae* family and belongs to the genus *Flavivirus*, to which Japanese encephalitis, West Nile, dengue and yellow fever viruses also belong (1). This virus is transmitted by the *Aedes* genus of mosquitos, such as *A. aegypti* and *A. albopictus*, which are active during daytime (2). ZIKV was first isolated in 1947 from the Zika Forest of Uganda, being named after the location where it was firstly found (1). Until the 1950s, its transmission was contained to a narrow equatorial belt from Africa to Asia. Yet, from 2007 to 2016, the virus managed to spread onto the Americas, leading to the 2015–2016 Zika epidemic (3).

Zika fever or Zika virus disease, the infection caused by the Zika virus, usually causes none to very mild symptoms, which are comparable to a very mild case of dengue fever (2). Nevertheless, this infection can lead to Guillain–Barré syndrome (GBS) in adults.

During its main outbreak, in January of 2016, the CDC issued recommendations when travelling to affected countries, such as enhancing precautions, and guidelines for pregnant women, for instance, considering postponing travelling (4,5). Following the USA, other governments and health agencies also issued analogous travel warnings (6–8).

1.1.1. Virology

As mentioned above, the Zika virus belongs to the family *Flaviviridae* and the genus *Flavivirus*. Similarly to other flaviviruses, Zika is enveloped and icosahedral, containing a nonsegmented, single-stranded, 10 kilobase, positive-sense RNA genome (9–12) (**Figure 1**).

The positive-sense RNA genome is directly translated into the viral proteins. Such as in other flaviviruses, the RNA genome encodes three structural proteins and seven nonstructural proteins, all in the form of a single polyprotein (Q32ZE1) (13). One structural protein, the envelope glycoprotein, encapsulates the virus and is responsible for the binding to the endosomal membrane of the host cell, in order to initiate endocytosis (14). The translation of the RNA genome leads to the formation of a nucleocapsid constituted by copies of the 12-kDa capsid protein. This nucleocapsid is enveloped within a host-derived membrane modified with two viral glycoproteins. The viral genome replicates by obtaining double-stranded RNA from the single-stranded positive-sense RNA (ssRNA(+)), and then by transcription and more replication to provide viral mRNAs and new single-stranded positive-sense RNA genomes (15).

Studies show that the vacuoles and mitochondria of cells infected with the Zika virus begin to swell after 6 hours, becoming severely swollen, leading to a form of programmed cell death known as paraptosis, which requires gene expression. A trans-membrane protein named IFITM3 is capable of protecting the cell from viral infection, since it is able to block the virus attachment. Therefore, when

levels of the IFITM3 protein are short, the cells are more vulnerable to Zika infection. After the cell is successfully infected by the virus, the latter rearranges the endoplasmic reticulum, leading to the formation of large vacuoles, which results in cell death (16).

The Zika virus has two lineages, the Asian and the African lineages (17). Some studies based on virus phylogeny have shown that the Zika virus being transmitted in the American continent was 89% identical to the African strain, although it showed a closer relation to the Asian genotype that spread during the 2013–2014 outbreak in the French Polynesia (17–19). Studies suggest that the Asian lineage was the first to evolve around 1928 (20).

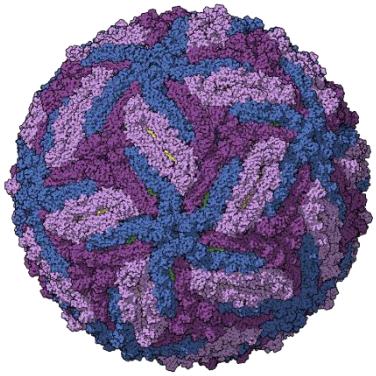

Figure 1 *– "Zika virus" capsid model, colored by chains* (21).

1.1.2. Transmission

Before the recent pandemic, monkeys were the main vertebrate hosts of this virus, through an enzootic mosquito-monkey-mosquito cycle, where transmission to humans and infection was occasional and rare, even in highly enzootic areas. Still, other arboviruses (viruses transmitted by arthropod vectors) began to spread in a mosquito–human–mosquito cycle and have become instituted as human diseases, such as the chikungunya virus (togavirus), and the yellow fever virus and the dengue fever virus (flaviviruses) (22). Although the origin of the pandemic is still unidentified, it is known that the prevalence of Dengue virus, a related arbovirus that infects the same species of mosquito vectors, has increased by urbanization and globalization (23).

Zika virus is mainly transmitted by *Aedes aegypti* mosquitoes, but it can also be spread by blood transfusions (24) and through sexual contact (25). The index of transmissibility (R0), a basic reproduction number, of the Zika virus is projected to be between 1.4 and 6.6 (26). An outbreak of Zika started in 2015 in Latin America and the Caribbean, with an extensive list of countries and territories experiencing local Zika virus transmission (27). The virus outbreak rapidly spread, and by September of 2018, more than 50 countries had experienced active local transmission of Zika (**Figure 2**).

Figure 2 *– Global map of Zika virus infection (Centers for Disease Control and Prevention, September of 2018)* (28).

1.1.2.1. Mosquito

The Zika virus is mainly transmitted by female *Aedes aegypti* mosquitoes, these being more active during daytime and feeding on blood to lay eggs (29). This virus can also be spread by other mosquito species of the genus *Aedes*, since it has been isolated from a couple of arboreal mosquito species, such as *A. africanus*, *A. apicoargenteus*, *A. furcifer*, *A. hensilli*, *A. luteocephalus*, and *A. vittatus*, having an extrinsic incubation period in these hosts of around 10 days (30). Still, the real extent of the Zika vectors is still not known, since the virus has also been detected in other species of *Aedes*, and in other species such as *Culex perfuscus*, *Mansonia uniformis* and *Anopheles coustani*, the latter ones not being confirmed as vectors.

Furthermore, an urban outbreak was reported in Gabon in 2007, where the tiger mosquito *A. albopictus* invaded the country and became the primary vector for the transmission of the Chikungunya and the Dengue viruses (31). Therefore, travelers carrying the virus can cause new outbreaks when going to regions where *A. albopictus* is common (32).

The distribution of the mosquito species that transmit Zika greatly impacts its potential societal risk, whereby the increment of the global trade and travel is leading to an expansion in the global distribution of the mainly carrier of Zika, *A. aegypti* (34). The species distribution is increasingly becoming more extensive, being found on parts of all continents except Antarctica, including North America and even the European periphery (Madeira, the Netherlands, and the northeastern Black Sea coast) (35), meaning that mosquitoes are adapting for perseverance in a northern climate (36). Studies suggest that the Zika virus seems to be contagious via mosquitoes for about a week after infection,

and it appears to be infectious for a longer period of time when transmitted via semen (2 weeks or more) (37).

Also, research shows that changes in precipitation and temperature might influence Zika virus to a greater extent than Dengue virus. Therefore, this virus is expected to be more prevalent in tropical areas. Yet, climate change and the rising global temperatures might lead to an expansion of the disease vector further north, permitting the Zika virus expansion to follow (38).

The Reverse Transcriptase – Polymerase Chain Reaction (RT-PCR) technique is usually employed to detect the presence of the virus in the mosquitoes, requiring genetic material to be analyzed. Near-infrared spectroscopy can also be used to identify chemical compounds characteristic of the virus. This technique consists in shining a light at the head and thorax of the mosquito, being a faster and cheaper method (33).

1.1.2.2. Sexual

Both men and women can transmit Zika to their sexual partners, although transmission from symptomatic men to women is found to be the most common case (39). During the 2015 Zika outbreak, sexual transmission of this virus was documented in Argentina, Australia, France, Italy, New Zealand, and the United States. Studies show that Zika can be found in semen several months after infection, whereby the viral RNA can be detected for up to one year after. It was found that this virus is able to replicate in the human testicles, infecting numerous testicular cell types, such as testicular macrophages, peritubular cells and germ cells, the spermatozoa precursors (40). Thereby, spermatozoa can be infectious, since it has been shown that several weeks post-symptoms onset the semen parameters can still be altered in patients (41). After Zika virus was isolated from semen samples, one patient had 10^5-fold times more virus in semen than blood or urine, two weeks after being infected (42). It is still unknown how long the Zika virus can remain in semen and why levels of this infectious virus in semen can be higher than in other body fluids. There has been transmission of the ZIKV disease by men with no symptoms of Zika virus infection (43). Studies show that oral, anal and vaginal sex can spread the disease (44). Nevertheless, sexual transmissions from women to their sexual partners have never been reported (43). Therefore, since ZIKV is still spreadable even if symptoms never develop, the CDC recommends that men who travelled to a country with Zika should use condoms or abstain from sexual intercourse for at least six months (45).

1.1.2.3. Pregnancy

Studies show that the Zika virus can be transmitted vertically, also referred as "mother-to-child" transmission, during pregnancy or delivery (46). Changes in the neuronal development of the unborn child have been associated to Zika infection during pregnancy (47). The development of

microcephaly in the unborn child is also shown to be connected to severe progression of infection during pregnancy, whereas neurocognitive disorders in adulthood can possibly be caused by mild infections (**Figure 3**) (48,49). In addition, other congenital brain abnormalities, severe brain malformations, eye development defects (chorioretinal scarring) and other birth defects caused by ZIKV have been reported (50). Less common systemic abnormalities have also been reported, such as abnormal accumulation of fluid in the fetus (hydrops fetalis) (51). All of these disturbances can cause intellectual problems, slow development, seizures, and vision and hearing problems in the future development (52). In fact, several abnormalities were witnessed in up to 42% of live births, although the full extent of birth defects caused by infection during pregnancy is still unclear (53). Also, Zika virus has been detected in breast milk, but there have been no reported cases of transmission from breastfeeding (54).

Additionally, some experiments with mice have shown that maternal immunity to dengue virus may boost fetal infection with Zika, exacerbate the microcephaly phenotype and enhance damage during pregnancy, although it is still unclear whether this also occurs in humans (55,56).

It is still not known if the stage of pregnancy at which the mother becomes infected affects the risk of the fetus developing abnormalities and if there are other risk factors that might also affect the outcome (57). Johansson MA *et al.* concluded that when the mother is infected during the first trimester, the risk of the baby developing microcephaly is approximately 1%, but that risk becomes unclear if infection happens after the first three months (58). Other studies have also shown that babies affected by Zika might appear healthy but have brain defects and that Zika infection in newborns can also cause brain damage (59).

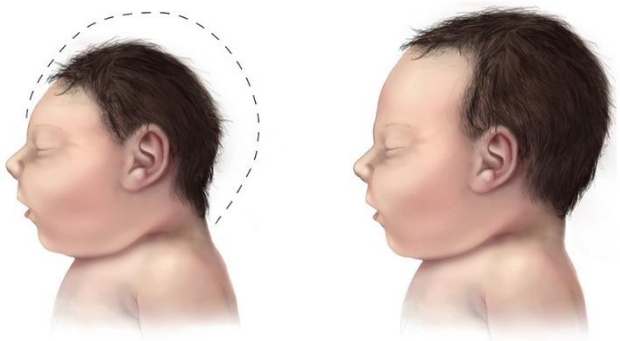

Figure 3 *– A baby with microcephaly (left) compared to a baby with a typical head size (right)* (48).

1.1.2.4. Blood Transfusions

Two cases of Zika transmission through blood transfusions have been reported in Brazil, the only situations reported globally as of April of 2016 (60). After these reports, the FDA recommended

the screening of potential blood donors and deferring possible high-risk donors for 4 weeks. During the French Polynesian Zika outbreak, a blood-donor screening study was conducted and a potential risk of Zika spreading through blood transfusions was found, since 2.8% of donors tested positive for Zika RNA and were all asymptomatic at the time of blood donation (61).

1.1.3. Pathogenesis

After finding a host, the Zika virus replicates in the midgut epithelial cells of the mosquito and then in its salivary gland cells. The virus is found in the saliva of the mosquito after about 5 to 10 days. When the saliva of the mosquito is inoculated into human skin, the Zika virus can then infect skin fibroblasts, epidermal keratinocytes and Langerhans cells. Then, it is theorized that the virus continues to spread to lymph nodes and into bloodstream (62). Although flaviviruses usually reproduce in the cytoplasm, Zika antigens have been found in the infected cell nuclei (63).

It is hypothesized that small head size (microcephaly) is caused by the viral protein NS4A, since it disrupts brain growth by hijacking a pathway that regulates the growth of new neurons (64). It is theorized that the virus might infect the neural progenitor cells, which are primary neural stem cells of the fetal brain (51). These brain stem cells are responsible for proliferation until the correct number of cells is achieved, and then for generating neurons through the process of neurogenesis (65). Li H *et al.* also concluded that the viral proteins NS4A and NS4B directly suppress neurogenesis. This might lead to an infection of the brain stem cells, which might induce cell death, decreasing the production of new neurons and leading to a smaller brain (66). Additionally, the infection of neural progenitor cells might also interfere with cell proliferation, setting off a reduction of the pool of progenitor cells (67). Moreover, in fruit flies, NS4A and NS4B viral proteins restrict eye growth, affecting the cells of the developing eye and leading to high rates of eye anomalies (68).

A considerable amount of cases of microcephaly have also been linked to inherited gene mutations, particularly mutations that might cause dysfunction of the mitotic spindle. Moreover, some studies suggest that the Zika virus might disturb the mitotic function, which can lead to an alteration in cell proliferation. Other studies propose that, after crossing the placenta, the virus might target the developing brain cells, leading to inflammation as a consequence of the immune response to cell infection (69).

1.1.4. Zika Fever

The Zika virus disease, also known as the Zika fever, is an infectious illness caused by the Zika virus (70). Although most infection cases present no symptoms, some patients can show some mild symptoms similar to those of Dengue fever (71). ZIKV disease symptoms generally include fever, headache, red eyes (conjunctivitis), muscle and joint pain and a maculopapular rash that usually are

present for less than seven days, meaning that admission into a hospital is rarely necessary (72). It is still unknown how long it takes to develop symptoms after a mosquito bite, but it is suggested that it varies from a few days to a week (73). There are no reported deaths by Zika fever during the initial infection. When the ZIKV infection occurs during pregnancy, it might cause microcephaly and other brain malformations in newborns, as already seen above (57). In adults, the disease has been shown to be connected to GBS, due to the virus ability to infect human Schwann cells (74). GBS is characterized by a rapid onset of muscle weakness, caused by damage of the peripheral nervous system by the immune system, which can progress to paralysis (75). However, identifying Zika as the cause of GBS is complicated, because both GBS and Zika infection can simultaneously occur in the same patient. Since Zika belongs to the same virus family as Dengue, it was suspected that it would cause similar bleeding disorders, although only one case of blood in semen (hematospermia) has been documented (76).

The diagnosis of this infection is based on testing the urine or saliva of patients for the presence of Zika virus RNA, or looking for antibodies in the blood after the presence of symptoms for more than a week (70,71). Since the disease is transmitted by a mosquito, prevention includes avoiding mosquito bites in areas where the disease occurs, by the use of insect repellents (such as DEET or picaridin) or mosquito nets, covering the body with clothing and getting rid of standing water, where mosquitoes usually reproduce (39).

The first documented outbreak of Zika virus among humans happened in 2007 in the Federated States of Micronesia. Then, another outbreak began in Brazil in 2015, and spread to the Americas, Pacific, Asia, and Africa, leading to the 2015-2016 Zika epidemic. In February of 2016, WHO declared it a Public Health Emergency of International Concern (77). Although the crisis greatly subsided by November of 2016, 84 countries still reported cases as of March of 2017 (78).

1.1.4.1. Vaccine Development

Nowadays, the main goal is to develop a safe and effective Zika virus vaccine, in order to prevent or minimize the complications and the symptoms of infection in humans, by producing specific antibodies against this virus that will prevent severe disease. One of the purposes of the vaccine will consist in protecting against congenital Zika syndrome during the virus outbreaks, since the Zika virus infection of pregnant women usually leads to congenital defects in the newborn. Similarly, one of the aims of the design of this vaccine would be limiting the consequences of the disease caused by this virus infection, such as reducing side effects like the Guillain-Barré syndrome, as well as reducing the chance of antibody-dependent enhancement of infection by Dengue virus, since the latter is closely related to Zika (79–82).

At present, no vaccines have been approved for clinical use, although there are a few in clinical trials, as of April of 2019 (83,84). Currently, the priority is the development of inactivated vaccines, since these are safer to use in pregnant women, as suggested by the World Health Organization (WHO) (85). Although an effective vaccine against Zika is not likely to be available for the next 10 years, 18 institutions and companies are currently working on its development (86). Actually, in June of 2016, a human clinical trial for a vaccine against Zika was granted by the Food and Drug Administration (FDA) for the first time (87). Also, in March of 2017, a DNA vaccine consisting of a plasmid, a small and circular piece of DNA, that is able to express the genes that originate the Zika virus envelope proteins, was authorized for phase 2 clinical trials in humans (88). This plasmid encodes the E and PrM proteins that constitute the outer coat of the Zika virus virion (89). Such vaccine is unable to cause infection, since it does not contain the full nucleotide sequence of the virus, and is designed to trigger the immune response of the body by causing the assembly of protein particles that mimic Zika virus (90).

Clinical trials for both subunit and inactivated vaccines were started in April of 2017 (91). Moreover, the Walter Reed Army Institute of Research is presently working on a purified inactivated vaccine (ZPIV) (92), which is composed of inactivated Zika particles, making the virus unable to replicate and cause disease in humans. The early clinical trials of this vaccine at Beth Israel Deaconess Medical Center showed promising results (93). Also, a live attenuated vaccine based on the approved dengue vaccine Dengvaxia is currently in Phase 1 clinical trials. In this vaccine, the virus is genetically modified in order not to cause disease in humans (94). Furthermore, Moderna Therapeutics is currently working on a modified mRNA vaccine containing the E and PrM proteins, which has been approved for Phase 1 and Phase 2 clinical trials (95).

Additionally, multiple viral vector-based vaccines, using safe and non-pathogenic viruses as vectors for immunogenic Zika virus proteins, are being developed at present. For example, in April of 2018, a vaccine using the Measles virus as a vector had a successful Phase 1 clinical trial (96). Likewise, another vaccine using adenovirus as a vector is currently undergoing Phase 1 clinical trials, since adenoviruses induce a strong immune response and have been previously successfully utilized as a vaccine platform for HIV, for example (97,98).

1.1.4.2. Treatment Strategies

Since there are still no vaccines or specific antiviral drugs for Zika disease, its treatment is mainly symptomatic. Symptoms are usually reduced with the use of analgesics and antipyretics; however the use of these drugs needs to be cautious as to avoid the induction of adverse effects, such as liver disease, allergies and nephropathy. Moreover, since the clinical diagnosis of Zika is sometimes not conclusive, as serological analysis presents the possibility of yielding an incorrect diagnostic, the

use of aspirin and other salicylates is not recommended, in order to avoid the induction of bleeding phenomena in patients with Dengue misdiagnosed as having a Zika infection.

On the other hand, the therapeutic approach to alleviate symptoms such as intense itching that usually follows the rash consists of appropriate skin hydration, cold baths and the use of refreshing lotions containing calamine or menthol, as well as avoiding excessive use of soap and hot baths. The use of older antihistamines is also sometimes recommended because of their sedation properties and their role in soothing the pruritus (99). The use of corticosteroids is not recommended as their efficacy in the reversion of these symptoms is unknown.

Guillain-Barré syndrome diagnosis is characterized by progressive weakness in two or more limbs and areflexia, with evolution within a maximum of four weeks. Also, other symptoms like increased protein and low cellularity (albumin-cytological dissociation) can be revealed by cerebrospinal fluid analysis. Considering the risk of evolution of respiratory muscle paralysis in patients with suspicion of GBS, they should be monitored in intensive care. Plasmapheresis or intravenous hyperimmune immunoglobulin are therapeutic options for this syndrome, despite of being quite expensive, because these two therapies shorten the time of recovery (100).

1.1.4.3. Laboratory Diagnosis

Currently, there are still no commercial tests for the serological diagnosis of ZIKV infections. Therefore, the diagnosis of acute infection has to be performed by reverse transcription and amplification by RT-PCR, of RNA directly extracted from serum of the patient, preferably collected until the sixth day after the onset of symptoms, or from saliva samples collected during the first 3 to 5 days. Also, Zika virus can be detected through molecular techniques applied in other body fluids, like urine and saliva (101,102). The evaluation of samples collected from the same patient shows that Zika is detected more frequently in saliva than in sera (103). On the other hand, urine samples can be collected and tested up to 14 days after the onset of infection, since it has been shown that the virus survives longer in the urine than in saliva or in sera (104).

Also, serologic detection of specific IgM and IgG antibodies against Zika virus can be used in the detection of this infection. Studies show that IgM antibodies can be found from the third day of illness, but IgG antibodies need to be examined in the convalescent serum (105). Nonetheless, the possibility of cross-reaction as a result of previous infections by other flaviviruses constitutes a problem with the use of serological tests (106–108). So, the incidence of Zika virus in areas where there was a previous transmission of Dengue virus embodies a diagnostic challenge. When performing a plaque reduction neutralization test (PRNT), it is difficult to differentiate probable cases of ZIKV infection in patients that were previously afflicted with dengue fever, even if the anti-ZIKV titers are always present

in higher amounts than the heterologous ones (non-ZIKV) (107). Still, in 2019, an improved diagnostic test that detects Zika infection in serum was granted market authorization by the FDA (109).

Numerous studies have reported both qualitative and quantitative assessments of the presence of anti-ZIKV antibodies in biological samples, even though the techniques used are not standardized techniques, being used in specific laboratory contexts. Therefore, the utilization of diagnostic tests is still fairly limited due to the fact that there are no commercial kits available on the market. Thus, Zika diagnosis is restricted to government institutions linked to health surveillance, and educational and research institutions. Still, the most sensitive and specific method that permits a diagnosis of ZIKV infections is the detection of viral genomes by RT-PCR. However, due to the limited circulation of the Zika virus, there is not a lot of knowledge about its real genetic diversity. Thus, there will always be a non-zero probability that the primers used in ZIKV genome amplifications may not allow for the intended amplifications, leading to an increase of false negative results (107,108).

1.2. Phage Display Technology

The Phage Display Technology (PDT) is a laboratory technique that focuses on the studying of protein–DNA, protein–peptide and protein–protein interactions, utilizing bacteriophages (or phages) to create a connection between proteins and the genetic information that encodes them (110). The PDT technique allows for a linkage between genotype and phenotype, since in this technology a gene encoding a protein of interest is inserted into a phage coat protein gene, leading to phages containing the gene for the protein of interest on their inside (in their genome), while displaying the protein or peptide on their outside (as one of their coat proteins). The peptide-displaying phages are then screened against other DNA sequences, peptides or proteins, with the aim of detecting possible interactions between the displayed peptides and these target molecules. Therefore, in a method named "*in vitro* selection", large libraries of peptides/proteins can be screened against diverse targets and then amplified, a process equivalent to natural selection.

In this technique, the most commonly used bacteriophages are M13 and fd filamentous phages, but T4, T7 and λ phages can also be utilized (111).

1.2.1. Brief History

George P. Smith first described the phage display technology in 1985, reporting the fusion of a capsid protein of a filamentous phage to a library of peptide sequences, demonstrating this way the display of peptides on the viral surface, which could be selected based on their binding affinities (112). Stephen Parmley and George Smith described biopanning for affinity selection in 1988, reporting that increasing rounds of selection would lead to the enrichment of clones present in very small quantities (113). Jamie Scott and George Smith studied the construction of large random peptide libraries

displayed on filamentous bacteriophages in 1990 (114). Then, several groups contributed for the development and improvement of the phage display technique, such as Greg Winter and John McCafferty, Lerner and Barbas, and Breitling and Dübel, who established the phage display of proteins such as antibodies for therapeutic protein engineering. In 2018, Smith and Winter won the Nobel Prize in Chemistry for their contribution to the advancement of this system, namely “for the phage display of peptides and antibodies”. George Pieczenik also described the same method for the generation of peptide libraries, patenting it as "Method and means for sorting and identifying biological information" and claiming priority from 1985.

1.2.2. Principle of the Technique

Phage display is a system that allows for the high-throughput screening of protein interactions. This technique is based on the presentation of randomized peptide sequences on the surface of bacteriophages. Using this technology, large peptide libraries can be displayed in the phage surface and used for affinity screening of specific target molecules. In the case of M13 filamentous phage display, DNA encoding a peptide or protein of interest is inserted into the pIII gene, encoding the minor coat protein, or into the pVIII gene, which encodes the major coat protein. In order to guarantee that the cDNA fragment is translated in the proper frame, multiple cloning sites are frequently applied so that the fragments can be inserted in all three possible reading frames. Then, a process of transduction occurs, where the phage gene and the insert DNA hybrid are inserted into *E. coli* bacterial cells from strains such as ER2738, XL1-Blue, TG1 or SS320. Furthermore, phagemid vectors, which consist of a simplified display construct vector, can also be used, leading to phage particles not being released from the *E. coli* cells until these are infected with a helper phage. Helper phages contribute for phage DNA packing and mature virions assembly with the protein fragment of interest, which can be part of their outer coating, either on the minor pIII or on the major pVIII coat protein.

The PDT technique consists of the immobilization of DNA fragments or protein targets to the surface of a microtiter plate well and the addition of a phage-displayed library to the latter, where phages that display a protein specific for the target on the surface will bind to that target and remain on the plate, while unbound phages will be removed by washing. The bound phages can be eluted and utilized to produce more phages, through bacterial infection with helper phages, leading to the production of a phage mixture that is enriched with the selected binding phages. This repeated cycle of steps is called “panning”, in which phages bound to a specific target go through several repeated cycles in order to produce a phage mixture enriched with the relevant phage-displaying peptides that specifically recognize target molecules with high sensitivity and selectivity. Then, the target-bound bacteriophages are amplified, where phages eluted in the final round of this method can be used for the infection of a suitable bacterial host, in order to produce more phagemids which are later collected.

The elution of the bound phages is performed by combining the use of a low-pH elution buffer with sonification, which helps to loose the peptide-target interaction and to detach the target molecule from the immobilization surface, allowing for a single-step selection of a high-affinity peptide (115). Then, the peptides are identified and characterized, and the corresponding DNA sequence is excised and sequenced to identify the interacting proteins or protein fragments (**Figure 4**). The use of a "bacterial packaging cell line" can effectively eliminate the need for the use of a helper phage (116).

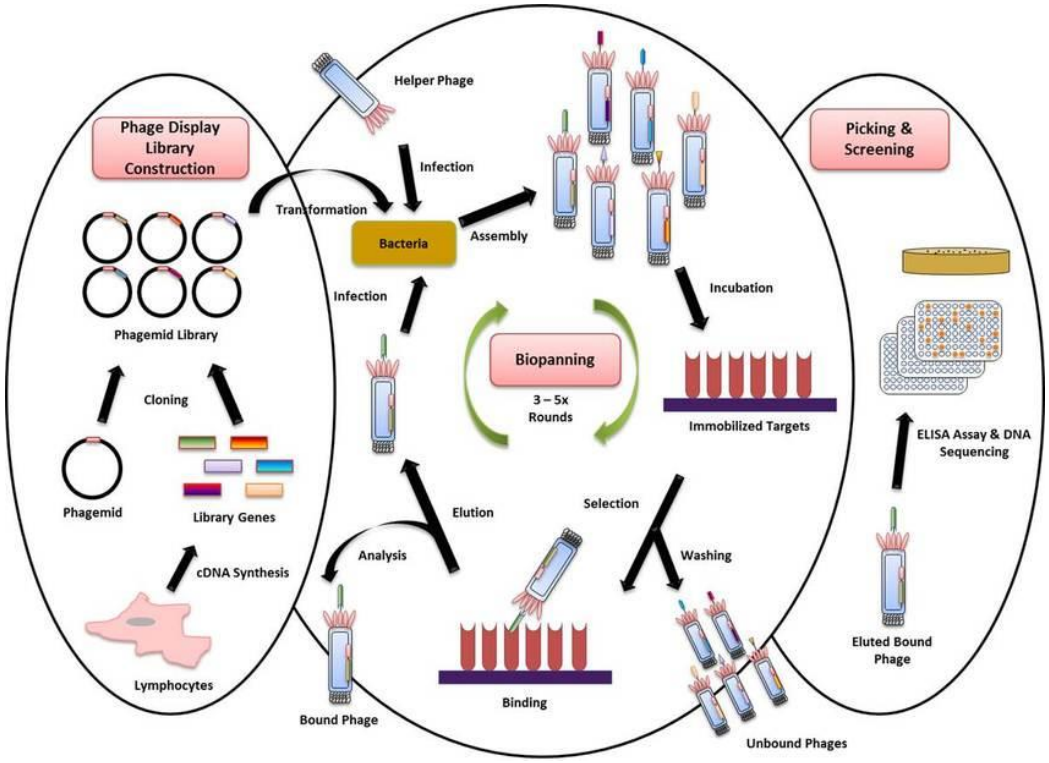

Figure 4 *– Principle of filamentous bacteriophage M13 phage display using a phagemid vector* (117).

1.2.3. Bacteriophages – Phage Display Vectors

Bacteriophages, also known as phages, are viruses that infect and replicate within bacteria and archaea. These viruses have a DNA or RNA genome encapsulated by proteins, and can have rather simple or elaborate structures. Their genomes might encode a small amount of genes (as few as four, for example, MS2) or be of a more considerable size, having as many as hundreds of genes. For their replication, phages inject their genome into a bacterium cytoplasm and then reproduce within it (118).

Phages constitute one of the most common and diverse parts of the biosphere are always found around anywhere bacteria exists, being very abundant viruses. There are more bacteriophages on Earth than every other organism combined, including bacteria, with their population on the planet having a projection of 10^{31} entities (119). It is also estimated that up to 70% of marine bacteria may be infected by bacteriophages (120).

Since the late 20th century that bacteriophages have been utilized to substitute antibiotics, in France, and in the former Soviet Union and Central Europe, constituting a possible new therapy against multi-drug-resistant strains of bacteria (118). In contrast, studies show that *Inoviridae* bacteriophages shelter bacteria from drugs meant to eliminate disease, leading to complications in the pneumonia and cystic fibrosis biofilms, consequently promoting persistent infection (121).

1.2.3.1. Filamentous Phages

Filamentous phages are a family of viruses (*Inoviridae*) that infect bacteria. The bacteriophages are about 6 nm in diameter and 1000-2000 nm in length, being named after their filamentous shape, which is long, thin and flexible, resembling a worm-like chain. Five types of viral proteins compose the coat of the phage virion, which during bacteriophage assembly are located in the inner membrane of the host bacteria. These proteins are added to the new phages as they exit through the membrane. Filamentous virions constitute an attractive model system for research of essential aspects of molecular biology and are also found to be a valuable instrument in nanotechnology and immunology (122–124).

1.2.3.1.1. M13 Filamentous Phages

The M13 phage is a member of the inovirus family of filamentous bacteriophages, being one of the Ff phages, like fd and f1. These Ff bacteriophages contain circular single-stranded DNA (ssDNA) in their interior. Their genome is composed of 6407 nucleotides encapsidated in roughly 2700 copies of the major coat protein p8, and capped with around 5 copies of each of the four different minor coat proteins, containing p3 and p6 at one end and p7 and p9 at the other end (**Figure 5**) (124–126). The minor coat protein p3 is the one responsible for attaching to the receptor at the tip of the F pilus of the host bacterium *Escherichia coli*. The life cycle of these phages is quite short, since the new assembled phages usually extrude the cell ten minutes after its infection. As Ff bacteriophages are chronic phages, they are able to release their progeny without killing or compromising the integrity of the host cells. Also, the infection of *E. coli* by these phagemids causes rather opaque turbid plaques, when compared to regular lysis plaques. However, infected cells seem to show a decrease in the cell growth rate. These M13 bacteriophages have been utilized in a various number of recombinant DNA processes, in phage display, in directed evolution and in nanostructures and nanotechnology applications (127–129).

The primary phage coat protein is called p8 and is composed of 50 amino acids, these being encoded by gene 8 in the phage genome. The phage coat is around 900 nm long and is constituted of roughly 2700 copies of p8, for a *wild type* M13 phage. The number of p8 copies is adjustable to the size of the single stranded genome it packages, making the dimensions of the phage coat flexible (130).

Roughly twice the natural DNA content of the phage seems to limit its size. Still, complete separation from the host *E. coli* is prevented if the phage protein p3 is deleted. When this happens, bacteriophages that are ten to twenty times the normal phage length containing several copies of the phage genome shed from the *E. coli* host bacteria.

Five copies of the surface-exposed protein p9 and a more hidden companion protein p7 are located at one end of the phage filament. Therefore, protein p8 forms the “tube” part of the phage, while proteins p9 and p7 form the "rounded" end part. Phage proteins p9 and p7 are considerably small, containing only 33 and 32 amino acids, respectively. If additional residues are added to the N-terminal portion of each protein, they will be displayed on the outside of the phage coat. Also, five copies of the surface-exposed protein p3 and a less visible accessory protein p6 are located at the other end of the phage filament. These proteins are responsible for the rounded shape of the tip of the phage and are the first proteins to interact with the *E. coli* host during bacterial infection. Moreover, the p3 protein is the last point of contact with the bacterial host as the new phages sprout from the bacterial surface.

These M13 bacteriophages replicate in *Escherichia coli* in the following way: first, the viral (+) strand DNA enters the cytoplasm; then, the complementary (-) strand is synthesized by bacterial enzymes; afterwards, a type II topoisomerase acts on double-stranded DNA and catalyzes the construction of negative supercoils in double-stranded DNA; the final product is a parental replicative form of the DNA. After this, host resources begin the transcription and translation of the viral genome, including the phage protein p2; p2 then nicks the (+) strand in the replicative form of the DNA; after, 3'-hydroxyl acts as a primer in the creation of new viral strand; then, p2 circularizes displaced viral (+) strand DNA. Subsequently, numerous new double-stranded replicative form molecules are produced, and the negative strand of this replicative form turns into the template of transcription; mRNAs are then translated into the phage proteins. The p2, p5 and p10 phage proteins in the cytoplasm also contribute to the replication process of the DNA, while the remaining phage proteins are synthesized and inserted into the cytoplasmic or outer membranes. Next, p5 dimers bind the newly synthesized single-stranded DNA and prevent their conversion to replicative form DNA, the timing and attenuation of p5 translation being crucial. Later, the synthesis of replicative form of DNA continues and the quantity of p5 proteins reaches the optimal concentration; then, DNA replication switches to synthesis of single-stranded (+) viral DNA; and finally, p5-DNA structures form, around 800 nm long and 8 nm round, and p5-DNA complexes are the substrate for the phage assembly reaction. Rarely, post-translation can be inserted into membranes by the major coat protein, even in those with missing translocation structures, and into liposomes with no protein content (131).

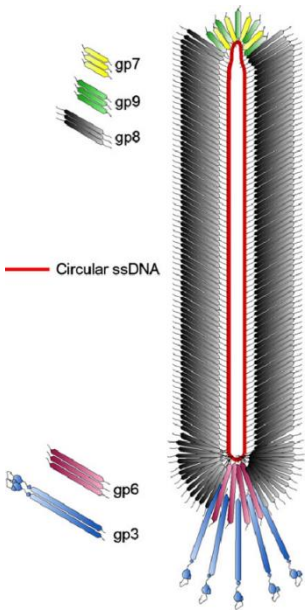

Figure 5 *– Schematic structure of bacteriophage M13* (132).

1.2.4. Display of Foreign Peptides on Filamentous Phages

The filamentous phage strains M13, fd, and f1 are the most utilized vectors in phage display, even though systems based on the bacteriophage T4 have also been tried (133,134). Foreign peptides are usually fused to three coat proteins: pIII, pVIII and pVI. The proteins pIII and pVIII are produced with N-terminal signal peptides, being sliced from the synthetized polypeptide chain absorbed in the inner membrane of the cell. The periplasmic N-terminal segment is separated from the cytoplasmic C-terminal segment by a single chain of amino acids in pIII and pVIII that traverses the inner membrane, leading to the incorporation of the proteins into the virions. Usually, these foreign peptides are merged to exposed regions of pVIII and pIII: the N-terminus of pVIII and the N-terminus and middle of pIII (135,136). Sometimes, when the pIII is used as the vector, the foreign peptide replaces the N-terminal domain of pIII, originating a hybrid protein incorporated into the virion that needs to be complemented by complete pIII molecules to ensure that the phage continues to be infectious. Likewise, when the pVIII protein presents a somewhat large foreign peptide, it also needs to be supplemented by *wild-type* pVIII molecules to ensure phage production (137,138).

When pIII and pVIII fusions are chosen, the foreign peptide needs to be spliced between the signal peptide and the portion of the coat protein responsible for merging with the phage. Therefore, it is important that the reading frame of the foreign DNA insert is rightly fused to the reading frame of the coat protein at vector-insert and insert-vector junctions. On the other hand, when foreign peptides are fused to the C-terminus of pVI, the two reading frames only need to be rightly merged at the vector-insert junction (139).

1.2.5. Types of Phage Display Systems

The most commonly used phage display systems consist of filamentous bacteriophages (f1, fd, M13), which have the majority of peptides and antibodies displayed at phage proteins pIII (140) and pVIII (141). The major coat protein pVIII is the product of the expression of gene 8, whereby almost 3000 copies of this protein are present in the bacteriophage, making it a useful method in enhancing the detection signal when a phage displayed antibody associates with an antigen. Moreover, the efficiency of display onto pVIII can be improved with the addition of modifications into this protein (141). The pVIII protein, known for preserving its functionality, is usually only used for the fusion of short (6–7 residues) peptides that do not contain the cysteine amino acid. On the other hand, the minor coat protein pIII contains 406 amino acid residues and is present in 3 to 5 copies at the phage tip, whereby most peptides and folded proteins are displayed as fusions to the pIII protein (142).

Hybrid phages and coat protein modifications constitute important tools in phage display, since they allowed for the resolution of one of the major limitations of this technology, the loss of coat protein functionality (141). The virions contain the complete *wild-type* bacteriophage genome and a copy of the fusion gene, which may occur as an insert in the phage genome (143) or as a phagemid vector containing the origins of replication for the phage and its host, an antibiotic-resistance gene and gene 3 with the appropriate cloning sites (144). Besides, a hybrid with helper phage in order to pack into the M13 particle is required by the phagemid encoding the polypeptide-pIII fusion. The helper phage should supply the structural proteins required for the production of a complete virion, while containing a slightly defective origin of replication (M13KO7 or VCSM13). Therefore, the phage surface will contain both *wild-type* pIII protein and polypeptide pIII fusion protein. The type of phagemid, the nature of the polypeptide fused to pIII, the phage growth conditions and the proteolytic cleavage of peptide-pIII fusions may all influence the ratio of *wild-type* pIII to polypeptide-pIII fusion protein, which might range 9 to 1 and 1000 to 1 (145). The polypeptide-pIII fusion protein to *wild-type* pIII ratio is responsible for ensuring that phage viability is not affected by the fusion protein. Nevertheless, attaining this ratio is not needed when a hyperphage is used, since the latter has the *wild-type* pIII phenotype, but because of the lack of a functional pIII gene, the only source of pIII for bacteriophage assembly is the fusion of pIII and antibody. Consequently, the use of a hyperphage leads to a 10-fold increase of the number of presented scFv and of the binding of phage to antigen, comparing to when using a M13KO7 helper phage. The latter is useful when single phages cannot be used to locate the desired antigen (146). Additionally, this hybrid phage system allows the display of large proteins with all five M13 coat proteins, as N-terminal fusions with pIII, pVIII, pVII and pIX (147–149) and as C-terminal fusions with pVI, pIII, and pVIII (144,150,151). Still, the expression of cDNA libraries may be complicated because of the naturally occurring stop codon in the 3'-region of reverse transcribed mRNAs, since expression in the M13 display system requires cDNA to not contain in-frame

translational stop codons. Also, another problem relies on the fact that cDNA needs to be in the same reading frame as the secretory leader sequence and the pIII protein, obstacle that might be solved by cDNA fragmentation prior to incorporation in the plasmid. However, this could result in the obtainment of a large number of phage clones with non-functional inserts.

Consequently, a T7 phage display system has been used as an alternative to M13 phage display, since it presents robustness and stability in conditions that would otherwise inactivate other phages (152–154). This technique presents several applications in comparison to the M13 phage display method, since it enables the display of inserts with stop codons on the C-terminal of the pX capsid protein, the display of small peptides with less than 50 residues in a large quantity and the display of larger peptides in a medium to low amount. Additionally, the advantages of applying this technique rely on the possibility to eliminate the need to secret the displayed peptides through the periplasm and the cell membrane, and on the fact that the capsid is not involved in the phage-to-host adsorption. Still, this method has been shown to restrict the possibility of post-translational modification of polypeptides in eukaryotic systems (152).

Another phage display method, the T4 HOC/SOC bipartite system, has been reported to be useful in the expression of cDNA, as it is able to display larger proteins in a big amount of copies and inserts with the stop codon on the N-terminal of the highly antigenic outer capsid protein (HOC) that occurs in 155 copies or on the C-terminal of the small outer capsid protein (SOC) that occurs in 810 copies (155). On the other hand, phage lambda allows for the display of higher molecular mass proteins as fusions to the N-terminal or the C-terminal of the pD head protein that appears in 405 copies, or as fusions to the C-terminal of the pV tail protein that appears in 6 copies (156,157). Additionally, this approach does not require translocation through the *Escherichia coli* membrane. So, the application of the phage lambda display system leads to a higher immune response, despite displaying a variety of proteins in multiple copies, when comparing to the filamentous phage display system.

1.2.6. Types of Displayed Peptides and Proteins

The most common type of phage-displayed molecules are “random” peptide libraries, based on the precisely-developed synthetic “mimotope” strategy (158,159). The DNA inserts are obtained from “degenerate” oligonucleotides. These are chemically synthesized through a process of addition of nucleotide mixtures, instead of single nucleotides, to an expanding nucleotide chain. Rather than having degeneracy at the level of single nucleotides, having it at the level of whole codons leads to a less biased representation of amino acids in the random peptides (160–162). A standard random peptide library has around a billion different phage clones, representing most of the 64 million possible 6-mer peptide sequences.

On the other hand, there are also “genomic” libraries, where the inserts are fragments of total chromosomal DNA, meaning all coding sequences in the genome of the organism are possibly represented among the displayed peptides. Likewise, in cDNA libraries, the inserts are DNA copies of mRNAs extracted from some tissue or cell population, meaning that a great multiplicity of coding sequences is possibly represented in an appropriately large cDNA library.

Frequently, in order to generate a library of sequence variants, some positions in the displayed domain are “randomized”, generally with the intention of selecting rare clones with enhanced function or clones in which the presented domain has acquired a novel function as a result of mutation.

1.2.6.1. Display of Antibody Fragments

The phage display technique allows for the use of different antibody fragments, including antigen-binding fragment (Fab), variable fragment (Fv), single-chain variable fragment (scFv) and modifications (163,164). Other types of antibodies can also be used in this technology, such as bivalent or bispecific diabodies (165), antibodies with one V-gene domain (166) and other oligomers (167). In antigen-binding fragments, V_H-C_H and V_L-C_L segments are linked by disulfide bonds, making radiolabeled Fabs a tool of extreme importance in tumor imaging (168). On the other hand, variable fragments and its modification, single-chain variable fragments, contain only V_L and V_H regions; the latter being usually the most used antibody fragment. In order to stabilize the V_L-V_H connection and to guarantee the antigen-binding site formation in these fragments, normally the $(Gly_4Ser)_3$ linker is employed (169,170). Thus, high binding affinity levels have been attained by fusion of several different single-chain variable fragments, since the expression of these segments on phage surface has been achieved without loss of antibody affinity. One example for this method is the CRAbs construct, which contains two scFv fragments specific to the same antigen, but to different adjacent epitopes, that are connected by a short linker amino acid sequence, whereby diabodies forming and dimerization of molecules might both occur (171,172).

The majority of antibodies are constituted by two heavy chains and a pair of light chains linked by noncovalent bonds and disulfide bridges. Yet, a different type of antibodies without any light chain in their structure was found in the serum of *Camelidae* (173), which bind to the antigen with a specific V_HH fragment that proved to be able to recognize unique conformational epitopes because of its long complementary-determining region 3.

Different antibody fragments have been expressed on the periplasm or cytoplasm of *E. coli*, where the *in vivo* refolding of the molecules produced by cytoplasmic expression is necessary to guarantee the correct activity and function of those antibody fragments. Moreover, Mahgoub IO *et al.* developed a method for the soluble expression of recombinant proteins in the cytoplasm of a strain of *E. coli*, whereby it was shown that the disruption of trxB and gor genes fused to the N-terminal of pET

32b plasmid sequences encoding two reductase enzymes enhanced the disulfide bond-dependent folding of heterologous proteins, promoting the formation of disulfide bonds in the cytoplasm of this bacterial strain (174). Also, the study described that the functional single-chain variable fragment that recognized MCF-7 cells, and was expressed in the bacterial cytoplasm, displayed improved binding characteristics and affinities when in comparison with the one expressed in the periplasm. Furthermore, the study also reported that fully functional molecules were allowed to be generated, since the periplasmic expression promoted V_H and V_L pairing, analogous conditions to those in the endoplasmic reticulum of the lymphocyte. The productivity of soluble scFv was strongly affected by the co-expression of FkpA and Skp, two periplasmic chaperones, but the secretory production was not significantly affected by cytoplasmic chaperones, for example TF SecB, GroELS and DnaKJE (175).

High quality and high affinity antigen-specific antibodies have been produced with the application of immune repertoires, whose source of V-genes are the IgG mRNA of immunized animals or human B-cells. Phage-displayed libraries can be obtained from spleen lymphocytes or from the peripheral blood through human immunization, providing phage-displayed antibodies to native T-cell receptors TCR-Vα (176), glycoproteins IIb/IIIa, red cell antigens D and B (177), platelet antigen HPA-Ia (178) and specific major histocompatibility complex/peptide construct (179). Moreover, the preparation of RNA from spleen material from hyperimmunized chickens (180), sheep (181), rabbits (182), cows and nonhuman primates (183) allows for the obtainment of highly diverse humanized immune libraries. Thus, this method has been employed into engineering a human antibody-producing XenoMouse strain, whereby the transgenic mice have most of the human antibody gene library on megabase-sized fragments from human heavy and kappa light chains and their immunization leads to the production of human-like antibodies in the B-cells (184). The fact that the produced antibodies undergo affinity maturation by the immune system constitutes one of the advantages of these immune libraries, through which high affinity antibodies can be generated even from small libraries (185,186). Still, the production of human antibodies has some limitations since predicting the response of the immune system is a difficult task. Also, every antigen requires the creation of new antibody library and the immunization process of animals is a very slow process. Furthermore, the lack of immune response to self or toxic antigens also constitutes a problem in this approach. Still, it has been reported that immune libraries might contain an elevated number of unimmunized clones, which supports the possibility for a sufficiently large immune library to be used in a similar way to a naïve library (187).

To form naïve libraries, several lymphoid sources, for example peripheral blood lymphocytes, bone marrow, spleen cells, tonsils or other animal sources, have been used to isolate V-genes derived from the IgM mRNA of B cells from non-immunized human donors (187). For instance, a library containing 1.4×10^{10} clones was constructed using lymphocytes obtained from about 40 non-immunized donors (188). Human monoclonal antibodies against red cell antigens B, D, E, H and Kbp

can be obtained from naïve libraries (177). Moreover, antibodies to tumor necrosis factor α (TNFα), bovine serum albumin, lysozyme, haptens, mucin or CD4 were produced using small sized human single-pot libraries containing 3×10^7 antibody clones. However, even though these antibodies presented good affinity and reactivity, it was low when compared to immune library antibodies (189). Single-pot libraries present some advantages, such as the ability to produce a single library for all antigens in a very short period of time, when comparing to obtaining antibodies from an immune library and the possibility of isolation of human antibodies to self, unimmunogenic or toxic antigens and direct isolation of high affinity antibodies if using large libraries (189,190). Still, these libraries also present some disadvantages, such as the possibly limited diversity of the IgM repertoire, the tendency to achieve increased cross-reactivity and the unknown history of the B cell donor. Also, when using a small sized naïve library, there might be a certain difficulty in obtaining high affinity antibodies. Furthermore, another problem relies on the fact that the quality, size and content of these libraries depends on V-gene repertoire size, since this level is not constant (191).

As another type of library, synthetic libraries do not use B-cells in antibody construction and are used to isolate a group of D and E antibodies (192). Polymerase chain reaction is used to obtain the antibody genes to randomize the hypervariable regions of a generic set of human germline encoded variable region genes (193,194). Semi-synthetic libraries consist of libraries in which the complementary determining regions contain changes in the V_H-CDR3 region. V_H-CDR3 is the most diverse loop in composition and length of all CDRs, being the most central to the antigen-binding site and randomized by PCR or oligonucleotide directed mutagenesis (194). One study reported that the randomization of light and heavy chain CDR3s and the differentiation of three CDR loops in one V-gene segment allowed for the construction of synthetic repertoires (195,196). These libraries present a series of advantages, such as the composition, which is not constrained by *in vivo* tolerance mechanisms, the diversity and variability of repertoires and the ability to manage and define the constituents. Also, these libraries could be of importance in cases where there is an antigen deficiency or toxicity, or when immunization is not possible and unimmunogenicity happens (197,198).

1.2.7. General Principles of Selection

The general principle of selection involves discarding an initial population of phage-displayed peptides according to previously defined criteria, in order to obtain a subpopulation with increased "fitness". Generally, in the first round of selection, the input amount is a very substantial initial library (10^9 clones, each typically represented by 100 phage particles) and the selected subpopulation is a very small fraction of the initial population (usually 10^6 particles), where the selected clones are usually overrepresented. This population is amplified by infection of fresh bacterial host cells, in order to make each individual phage in the selected subpopulation to be represented by millions of copies in the

amplified phage stock. The amplified population normally undergoes further rounds of selection, to obtain a narrower and fitter subset of the starting peptides.

There are two main parameters of selection: stringency, which consists of the degree to which peptides with higher fitness are favored over peptides with lower fitness, and yield, which constitutes the fraction of phage particles with a given fitness that survive the selection process. Both parameters can usually be manipulated in order to improve the efficacy of selection. The main goal of the selection process is to isolate peptides with high fitness. However, stringency should not be enhanced without bound, because increasing the stringency generally involves a decreased yield. In the first round of selection, where the phage input consists of all clones in a considerably large initial library, obtaining a high yield of the fittest clones is of great significance. The clones that are selected after the first round are amplified, meaning that each phage clone will be represented by millions of phages in the subsequent rounds. Then, in favor of high stringency, yield can be decreased. However, there is a limit to stringency, because there is an inevitable background yield of all the phages regardless of their fitness. So, stringency should not be set too high, because of the risk of the yield of a specifically selected phage falling below the background of a nonspecifically isolated phage, leading to the loss of the discrimination power in favor of high fitness (199).

1.2.7.1. General Protocol

The general protocol for the phage display screening, for identification of polypeptides that bind with high affinity to a target DNA sequence or protein, usually consists of the following set of steps. Firstly, the target molecule is immobilized on a solid support, such as the wells of a microtiter plate (200), PVDF membranes (201), column matrixes or immunotubes (202), magnetic beads (203) and whole cells (204). Then, a phage-displayed library is added, where the relevant peptides/proteins are expressed in the form of fusions with the viral particle coat protein. These proteins are displayed on the surface of the bacteriophage and correspond to the DNA sequence within the phage. After the addition of the library, phages are allowed time to bind to the immobilized molecules. The dish is then washed, where the phage-displayed proteins that show affinity to the target molecules remain attached, binding to the immobilized molecules, while the non-interacting phage displayed-proteins are washed away. Bound phages are then eluted and used to produce more phages by the infection of a suitable bacterial host. Following the bacterial-based phage amplification, an enriched mixture of the biding phage is obtained, which will contain significantly less non-binding phage than the initial mixture. These steps constitute a panning round and are repeated usually one or more times, in order to further enrich the phage library in binding proteins. Finally, the DNA contained in the selected binding phages is sequenced in order to identify and characterize the interacting proteins or protein fragments (**Figure 6**).

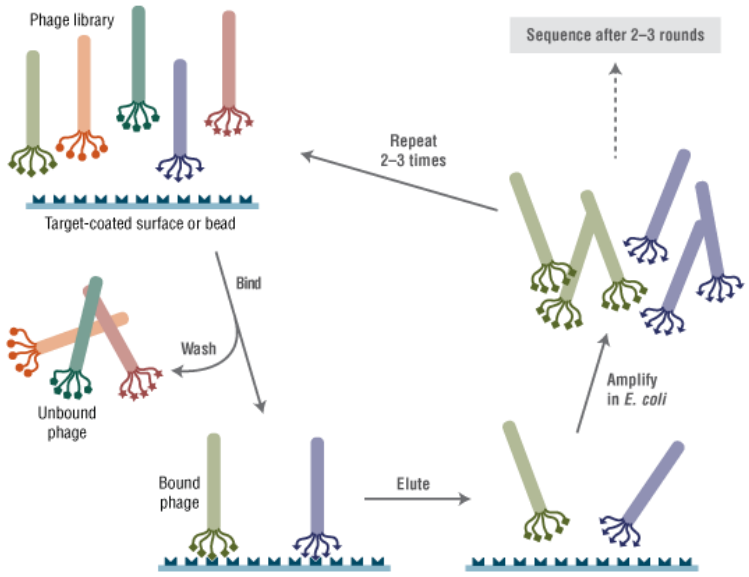

Figure 6 *– Panning with a pentavalent peptide library displayed on pIII* (205).

1.2.7.2. Affinity Selection

The phage display technique allows for the creation of libraries containing an elevated number of bacteriophage particles, each one encoding and displaying different molecules, presenting 10^6 – 10^{11} different ligands on a phage library with approximately 10^{12} phage particles. In order to enrich a specific molecule level, a method of biopanning is employed, in which the selection of the specific molecule binders is performed. This procedure consists of several rounds of a selection cycle, including steps of incubation, washing, amplification and selection of bound bacteriophages, which are essential to attain the ideal binding activity of the obtained displayed molecules. Enzyme-linked immunosorbent assay (ELISA) (206), chromophore-assisted laser inactivation (CALI) (207,208), and fluorometric microvolume assay technology (FMAT) (209) are tests that can be employed in order to examine this binding activity. The target concentration, the time of binding and washing and the type of solid support have been shown to affect the level of selection, in which the optimization of the biopanning procedure allows for the selection of proteins specific to unique targets (210).

1.2.8. Applications

The phage display technology presents innumerous applications, such as the identification of molecules that interact with certain proteins, which contain a library including all coding sequences of a cell, tissue or organism, and are immobilized on a plate in order to capture the binding phages and to determine the function or the mechanism of that protein. Phage display is also a system commonly utilized for *in vitro* protein evolution/engineering, using methods such as yeast, bacterial, ribosome or mRNA display, constituting an important tool in drug discovery. Moreover, the phage display

technique can also be employed in the discovery of new ligands (enzyme inhibitors, receptor agonists and antagonists) to target certain proteins (211–213). This system can also be applied to the identification of tumor antigens, which can be used in tumor diagnosis and therapeutic targeting (214), and of protein-DNA interactions, through the use of specially constructed DNA libraries including randomized segments (215). Furthermore, this approach has also been employed in the development of cancer treatments, through the adoptive cell transfer method, in which synthetic antibodies targeting tumor surface proteins are created and selected using the phage display technique, which are then used to create synthetic receptors for T-cells collected from the cancer patients (216).

Recently, numerous studies have used phage display for the study of infectious diseases, such as in the investigation of host–pathogen interactions, in epitope mapping and identification of potential vaccine candidate antigens and in the identification of bacterial adhesins. For example, new PDT approaches that are able to identify host receptors for microbial products have been developed, by employing panning *in vivo* in animal models or against *ex vivo* tissues or organs. Also, studies of synergistic relationships between opportunistic bacteria have been performed, by panning phage display libraries against one another, in order to explore interactions between microorganisms. Furthermore, phage display has been used in comparative genomics, with the number of sequenced microbial genomes increasing significantly in the last ten years. Thus, the panning of natural peptide libraries can be used in the identification and bioinformatic analysis of microbial genes, and in the comparison of the genes involved in pathogenicity between groups of closely related bacteria (217).

1.2.8.1. Disease Therapeutics

1.2.8.1.1. Transfusion Medicine

The application of the phage display technology in hematological medicine has been of significant importance. Thus far, reagents for *in vivo* imaging, targeted therapeutics and novel antibody reagents for cell subpopulation discrimination have been developed (218). Moreover, antibodies against red blood antigens used for hemagglutination assays were also obtained, namely anti-ABO, anti-Rh and anti-Kell antibodies (219). Blood group typing and the preparation of Rh(D)-immune globulin both require a large amount of anti-Rh(D) antibodies. The phage display technique appears to remain the best method for the obtainment of significant amounts of antibodies in a short period of time, since these can only be produced in humans and the availability of alloimmunized blood donors is diminishing. Furthermore, immunoglobulins expressed as Fab on the phage surface allow for the generation of highly sensitive (up to 15 times more than IgG) self-replication typing reagents. The phage display technology has also enabled the design of an anti-Rh(D) and anti-HPA-Ia bispecific diabody, which might be valuable in the diagnostic and treatment of neonatal alloimmune thrombocytopenia. Thus, the phage display approach allowed for the development of an accurate,

automated, inexpensive and sensitive hemagglutination assay for HPA-Ia (178). Additionally, this technology allows for the production of antibody reagents against fetal red blood cells (220). Likewise, antibodies against dendritic cells (221), hairy cells (222), paraproteins (223) and B and T cells (224) were obtained from a scFv naïve human library, in white blood cells. Besides, this technique has also allocated for the generation of antibodies against a multiplicity of differentiation antigens (225,226), AITP, GPIa, and GPIIIa platelets antigens (227), 11-dehydro-thromboxane B2 (11D-TX) (228) and clotting factors (229). Also, a phage display library from patients with chronic immune thrombocytopenic purpura was employed in the cloning of autoantibodies. Since the platelet GPIIb/IIIa specific H44L4 antibody obtained from this library can inhibit adenosine diphosphate-induced platelet aggregation and stay unbound to vitronectin receptor αvβ3, it can be useful in the prevention of cardiac ischemic complications in patients undergoing percutaneous coronary interventions (218).

1.2.8.1.2. Autoimmune Diseases

Phage display has also contributed to the investigation of several autoimmune diseases and their pathophysiology, since this technique allows for the cloning and characterization of human immune libraries (218). For example, affinity-selected phage clones specific to autoantibodies from patients suffering from autoimmune thrombocytopenia (AITP), a hematologic disorder caused by anti-platelet autoantibodies, were obtained by the screening of a random heptapeptide phage-displayed library (230). This technology has also proven to be a helping tool in the study of antigen-autoantibody reactions in acute anterior uveitis (231), thrombotic thrombocytopenic purpura (232), and other autoimmune ocular inflammatory disorders (233). Phage display has also contributed for the advancement in the investigation of autoimmune thyroid disease (234), autoimmune diabetes (235) and Wegener's granulomatosis (236). This technique has also been employed in the research of blistering skin diseases, such as pemphigus vulgaris (237) and pemphigus foliaceus (238). Additionally, phage display had a role in establishing that primary biliary cirrhosis and autoimmune cholangitis have a similar autoimmune targeting, whereby a protocol of biopanning was employed to generate phage clones that reacted with the E2 subunit of the pyruvate dehydrogenase complex, as these two diseases are serologic expressions derived from biliary ductular cells affecting autoimmune liver disease (239). The technique has also been applied in the research of Crohn's disease, as it was used to obtain galectin-3 mimotopes, which might be useful in the regulation of immune responses in Crohn's disease patients, since sera from patients with this disease contains more anti-galectin-3 IgG autoantibodies than sera from ulcerative colitis, primary biliary cirrhosis or autoimmune hepatitis patients, and healthy individuals (240). Also, different scFv against the toxic antigen (A-gliadin) and dietary antigens (α/βlactoglobulin) have been isolated due to the characterization of an antibody phage library from an individual suffering from celiac disease (241).

This multivalent technology also shows the possibility to be valuable in the design of potential diagnostic and therapeutic agents for autoimmune diseases. For instance, it has been shown that anti-huAChR Fab protects against nicotinic acetylcholine receptors (AChR) loss via antigenic modulation induced by myasthenia gravis serum antibodies, since these antibodies against AChR have been reported to cause loss of functional receptors at the neuromuscular junction (242). A cyclic molecule that has proven to be efficient in the prevention of antigenic modulation of AChR by the anti-main immunogenic region antibody, via *in vivo* inhibition of AChR binding, has been generated using the PMT LPE NYF SER PYH peptide (243).

Moreover, the phage display technique has also been employed in the production of human antibody therapeutics, in particular for autoimmune diseases (244). For example, a new treatment for the autoimmune disease rheumatoid arthritis, based on anti-TNFα antibodies, has been developed by the employment of this technology (225). The technique is also responsible for the discovery of a new drug for multiple sclerosis, another autoimmune disorder, based on an anti-CD52 antibody, that has been approved by the Food and Drug Administration (245,246).

1.2.8.1.3. Neurological Disorders

The phage display technology has also been of considerable importance on the development of therapies for several neurological disorders. An innovative immunotherapeutic strategy for botulism was designed, using a humanized-camel phage display library, in which a cell penetrating, humanized-single domain antibody proven to inhibit the botulinum neurotoxin is used (247). On the other hand, diseases like Creutzfeld-Jakob disease and Gerstmann-Sträussler-Scheinker syndrome can be caused by the accumulation of abnormal prion protein (PrPSc). Therefore, phage display libraries have been employed on the selection of human anti-prion scFv and Fab antibodies, since these were shown to inhibit *in vivo* the conformational change of normal prion protein (PrPC) in PrPSc (248).

This technique has also contributed for the improvement of research in the field of Huntington's and Parkinson diseases. For instance, proteins that bound to 2-methylnorharman, a structural and functional analog of MPP+, a toxin shown to induce Parkinson, have been studied using a phage display system (249). Also, a phage display library allowed the selection of the human single-chain variable fragment specific for the 17 N-terminal residues of huntingtin, as it was revealed that it could inhibit *in situ* expanded-repeat exon 1 analog aggregation in cellular models of Huntington's disease (250). Furthermore, this methodology also permitted the identification of a peptide that promotes the *in vitro* inhibition of polyglutamine aggregation (251). In addition, the technique has also been employed on the research of vaccines against Alzheimer's disease, constituting a possible method of production of anti-aggregating β-amyloid antibodies, since an epitope of the human β-

amyloid peptide has a regulatory function in the β-amyloid fibrils formation and disaggregation (252,253).

1.2.8.1.4. Tissue Targeting and Anti-Angiogenic Therapies

Phage displayed libraries have contributed to the characterization of the specific molecular diversity of the vascular endothelium, through the employment of *in vivo* biopanning protocols, which have allowed for the isolation of peptides analog to those found on several organs, such as the brain, uterus, breast, prostate, intestine, pancreas, kidney, lung and skin (254,255). This methodology can also contribute to the acceleration of bone and cartilage repair process, through the selection of skeletal stem cells (256). Moreover, an approach in which peptides that correspond to specific vascular beds are selected *in vivo* after intravenous administration of a phage displayed peptide library was described. This selection method has contributed to the development of angiogenesis-related tissue-specific targeting of tumor blood vessels or peptides. This phage display system might allow for the development of more effective and less toxic disease therapeutics, as it can contribute to the improvement of the delivery of cytotoxic drugs, proapoptotic peptides, cytokines and metalloprotease inhibitors (257). The methodology permitted the identification of peptides that bound to the extracellular domain of the LOX-1 receptor, this one being upregulated in dysfunctional endothelial cells related to atherogenesis and hypertension (258). The phage display system has also contributed for the discovery of a RGD-motif peptide analog to those present in angiogenic vasculature that was associated with a proapoptotic peptide, which managed to be successful in the treatment of arthritis (259). Likewise, another scientific study has reported that this technique was successfully utilized on the development of a therapeutic peptide for anti-obesity therapy, as it showed that the targeting of the proapoptotic CKGGRAKDC peptide to prohibitin protein in the adipose vasculature triggered the reduction of white fat (260). Also, phage displayed peptides have been identified as factors that might affect angiogenesis. Another research has identified molecules that exhibit *in vivo* anti-angiogenic and anti-tumor activity, namely peptides that have a role on the blocking of the interaction between MMP and avb3 integrin, and single-chain fragments that target the receptor-bound vascular endothelial growth factor (261,262). Thus, the phage display technology can be an important tool in tissue specific targeting, which can be of importance on the development of imaging techniques in cancer patients (263).

1.2.8.1.5. Molecular Imaging and Tumor Targeting

Diverse scientific studies have shown that phage displayed peptides can also be effectively used as tumor targeting agents. The first phage displayed recombinant antibody used as an anti-tumor agent was a scFv (MFE-23) molecule specific for a carcinoembryonic antigen (264). Recently, the phage

display technique has been of great interest in obtaining molecular imaging agents that can be utilized for the visualization of *in vivo* pathogenic processes (265,266). Phage displayed peptides appear to be better molecular imaging agents than labeled antibodies (radiolabeled, biotin-labeled, streptavidin-labeled), which have been used as tumor targeting and imaging agents for decades, since they present a smaller size, lack immunogenicity, allow for a rapid blood clearance, permit tissue penetration and promote increased diffusion, as opposed to labelled antibodies, which can cause adverse effects and lead to a decrease in natural immunity (267). Phage display technology has allowed for the isolation of several tumor targeting peptides, through the use of human B-cell lymphoma (268), glioblastoma (269), neuroblastoma (270), lung (271), hepatic (272), cervical (273), colon (274) gastric (275), breast (276), prostate (277) and thyroid (278) carcinoma cell cultures. Nevertheless, it has been reported that some peptides do not present *in vivo* function, such as peptides that recognize MDM2/p53 (279), IL-11 receptor (280), prostate specific antigens (281), heat shock protein 90 (282) and some growth factors (283). However, some phage display peptides have been reported to function as molecular imaging and tumor targeting agents *in vivo* (284), for example, the IAGLATPGWSHWLAL peptide that binds to prostate carcinoma (285). Another peptide, CPIEDRPMC, has been reported as a successful binding agent to five colon cancer cell lines: CaCo-2, SW480, RKO, DLD-1 and HT29. This RPMrel peptide, when fluorescein-conjugated, has the ability to stain tissue from colon adenocarcinoma *ex vivo*, while leaving normal tissues like colon, stomach, lung, liver, lung sarcoma and liver sarcoma unstained. The peptide, when conjugated to a mitochondrial toxin, was capable of inducing the death of HT29 cells (265). The peptide sequence CLSYYPSYC, which consists of a phosphatidylserine-recognizing moiety, was shown to be a promising anticancer drug as it can be used as an *in vivo* imaging molecule for apoptosis (286).

Moreover, the phage display technique allowed for the discovery of peptides that have been shown to inhibit tumor growth (271,287,288). For example, a heptapeptide labeled with 188-rhenium, NPNWGPR, has shown properties as a human tumor melanin-binding molecule, whereby its *in vivo* administration was shown to lead to the inhibition of tumor growth. Additionally, the radiolabeled peptide possesses the ability to only bind to extracellular melanin, which contributes to an increase of the safety of the therapy (289). Likewise, it was reported that the peptide K237-(HTM YYH HYQ HHL) obtained from a phage-displayed library was able to bind to the kinase domain receptor, which led to an inhibition of the growth of solid tumors implanted beneath breasts and to a reduction of the metastases to lungs (283). Furthermore, another peptide that can be used as an anti-tumor agent has been reported to promote the inhibition of tumor growth and to have a proapoptotic/cytotoxic effect. The LyP-1 peptide, of CGN KRT RGC sequence, has the ability to bind to tumor lymphatics, accumulating in breast cancer xenografts localizing specially in hypoxic areas and leading to treated tumors containing apoptotic cells and a lower amount of lymphatic vessels (290).

The phage display system also constitutes a tool for the design of novel nanoparticle-based diagnostics and therapeutics. Thus, a nanoparticle system based on the CERKA peptide, which binds to PyMT tumors and MDA-MB-435 human breast cancer xenografts, was reported to lead to a successful accumulation of the particles in the tumors. This approach may be valuable for tumor imaging and inhibiting tumor growth by blood vessel occlusion. An additional drug carrying function added to the peptide-nanoparticle complex might lead to an accumulation of the latter in tumor vessels and to the release of the drug, which contributes to an improved tumor growth inhibition (291). Also, the generation of peptides that are able to imitate carbohydrate ligands has been made possible by the screening of phage display libraries for binding to anti-carbohydrate antibodies. In the future, these peptides might be of considerable importance on the design of anti-cancer vaccines and on the inhibition of carbohydrate-dependent tumor metastasis (292).

Furthermore, the technology can be applied to the isolation of human monoclonal antibodies directed toward various antigens, such as tumor markers. In order to investigate numerous phage-derived antibodies, several clinical trials have been conducted over the years. For instance, it has been reported that a first generation of rabbit/human Fab and IgG1 that binds to the tyrosine kinase ROR1 receptor can function as a target in monoclonal antibodies-based therapy for mantle cell lymphoma and chronic lymphocytic leukemia (293). Another study has also described an *in vitro* immunization method towards inducing antigen-specific immune responses in human peripheral blood mononuclear cells, through the use of multiple antigen peptides instead of monovalent peptides, which allowed for the identification of four human monoclonal antibodies specific for tumor necrosis factor-α (TNF-α) (294). Additionally, the use of the phage display technique has allowed the discovery of a human antibody against psoriasin, a calcium-binding protein upregulated in various types of cancer that is frequently associated with reduced survival of the patients. The antibodies obtained by this technique can possibly be used in the diagnosis and treatment of breast cancer, oral squamous carcinomas or bladder cancer (295). In another case, the anti-human Cyr61 monoclonal antibodies 093G9 were shown to constitute a promising therapeutic for breast cancer (296). Moreover, the antibody phage technology was shown to be an important tool in the generation of F16 and P12 human recombinant antibodies, specific to the alternatively spliced domains A1 and D of the large isoform of glycoprotein tenascin-C, the latter suffering great overexpression in adult tissue undergoing tissue remodeling (297). Another study has successfully used (131)I-labeled antibodies specific to the A1 and D domains of tenascin-C in the treatment of glioma (298) and lymphoma (299). Furthermore, it has been reported that a generation of three human monoclonal antibodies (F8, B7 and D5) is also able to recognize the same epitope of the extra domain A, causing these antibodies to specifically recognize tumor cells. Thus, the anti-Ectodysplasin-A antibodies can be utilized as versatile tumor targeting agents and might be suitable for the development of effective and selective anti-cancer drugs. The phage-displayed

libraries have been consistently used for the isolation of human mAbs for various antigens, such as the alternatively spliced Ectodysplasin-A (EDA) domain of fibronectin, which consists of a marker of tumor angiogenesis. It was reported that an antibody derived from the library, 2H7 mAb, bound to a novel epitope on EDA, which differed from the mAb recognized by the clinical-stage F8 antibody. The described antibodies were utilized in the creation of chelating recombinant antibodies (CRAbs), such as anti-EDA CRAb (F8-10aa-2H7) and CRAb (F8-18aa-2H7), which were shown to accumulate selectively at the tumor site, turning these antibodies into a powerful tool in the development of improved anti-cancer therapeutics (300).

1.2.8.2. Target Receptors used in Affinity Selection

An immense diversity of target receptors has been utilized in the affinity-selection of peptides from phage-display libraries, including conventional receptors, such as antibodies and hormone receptors, and also plastic surfaces (301) and whole organs in living mice (302).

Even though most receptors recognize natural ligands (e.g. proteins), some of them are able to recognize different ligands like carbohydrates and some have no natural ligand at all (e.g. plastic surfaces).

1.2.8.2.1. Epitope Mapping and Mimicking

An “epitope” is an element on the surface of a ligand with which the receptor makes geometrical and chemical specific contact. Epitopes can be continuous, for protein ligands, including a few neighboring important amino acids in the primary sequence. For example, antibodies specific for continuous epitopes on protein antigens usually have three to four critical amino acids that establish contact over a six-residue segment. Still, typically, protein epitopes are more intricate. Several epitopes are discontinuous, containing critical binding residues that are distant in the primary sequence but close in the folded native conformation. Also, several epitopes are “conformation-dependent”, necessitating the setting of the overall protein structure to constrain them in a binding conformation.

Usually, mapping the epitope to a confined portion of the natural protein ligand is needed. Random peptide libraries can offer an inexpensive and easy approach to this objective when the epitopes are continuous and not conformation dependent (303–305). Random peptide ligands can be affinity selected by the receptor and then the sequence motif in the selected peptides is compared to the amino acid sequence of the natural ligand. Typically, the sequence motifs match the critical binding amino acids in the natural protein ligand, thus allowing the mapping of the epitope to a very specific part of the general natural ligand structure. This approach is typically inexpensive and easy, using replicable, widely available, all-purpose random peptide libraries and simple microbiological

procedures, when compared to other alternate epitope mapping methods, since these usually involve chemical synthesis of short peptide segments of the amino acid sequence of the ligand (306).

A random peptide library comprising a binding motif of more than six amino acids or representing conformation-dependent or discontinuous epitopes is very infrequent. Artificial ligands hardly ever stand an identifiable resemblance to any part of the natural protein ligand at the amino acid sequence level, though the receptors that recognize the epitopes frequently select ligands from random peptide libraries. So, sometimes a different approach is utilized, where a gene-specific library displaying 15-100 amino acid segments of the natural amino acid sequence is constructed, which sporadically can include small elements of secondary structure from the native protein (307,308). One advantage of these libraries is that occasionally they contain good ligands for receptors that fail to select ligands from random peptide libraries. Nevertheless, this method is much more difficult to employ than to just use all-purpose random peptide libraries, since it necessitates the construction of a specific library for each new ligand gene.

The affinity selection from random peptide libraries regularly chooses unforeseen ligands that do not match any linear epitope and that could not have been predicted from previous knowledge of the receptor and/or its natural ligand. This is more common when the natural epitope of the receptor is non-proteic or is a discontinuous or conformation-dependent protein epitope. Thus, a research team utilized the term “mimotope” when referring to small peptides that specifically bind to the binding site of the receptor (“mimicking” the epitope on the natural ligand), but without matching the natural epitope at the amino acid sequence level, including the situations where the natural ligand was non-proteic (309,310).

1.2.8.2.2. Identification of New Receptors and Natural Ligands

New receptors that bind to a ligand can be identified by using a ligand for a receptor as a “probe”. A few research teams identified novel SH3 domains through this method. These new domains are a family of homologous, around 60-residue, protein-binding modules that are part of a variety of signaling and cytoskeletal proteins (311–313). Firstly, a couple of cloned SH3 domains were used in the affinity-selection of specific ligands from random peptide libraries. After, these peptides were utilized in the probing of a conventional cDNA expression library for proteins that bind the peptide, where eighteen SH3 domains were identified, nine of which were formerly unidentified.

In other cases, finding the natural ligand for a receptor whose natural ligand is unknown might be achieved by simply identifying peptide ligands from a random peptide library. For example, a research team affinity-selected peptides that specifically bound to the Ca^{2+}-dependent binding protein S-100b, where it was shown that they shared a motif of eight amino acids and a similar motif in the R-

subunit of actin capping proteins was identified. The interaction of these two proteins was later revealed to be biologically significant.

1.2.8.2.3. Drug Discovery

Some receptors used in affinity selection can become targets of drug discovery, being the selected peptide ligands potential leads to new drugs. The peptides can work as receptor agonists or antagonists (for example, of enzymes or hormone receptors) or can also modulate the biological effect of the receptor. So, affinity selection can be seen as a traditional approach to drug discovery, since it consists of the screening of libraries of synthetic compounds or natural products for substances that bind the target receptor. Then, these substances can consequently become leads to new agonists, antagonists or modulators.

One of the advantages of affinity selection is the scale of search being way superior to when chemical libraries need to be screened compound by compound, since one allows for the search between billions of peptides versus tens of thousands of chemicals. Alternatively, peptides have poor pharmacological properties, since these are usually orally unavailable and rapidly degraded in the body by naturally occurring enzymes. One solution might be the synthesis of peptidomimetic compounds that mimic the essential pharmacological features of bioactive peptides on a nonpeptide scaffold. Still, the contribution of phage display to drug discovery will most likely be limited to applications where the peptides can serve as plausible therapeutics, for example in the field of vaccines.

Moreover, peptides constituted by D-amino acids are much less prone to degradation in the body than peptides constituted by the natural L-amino acids. So, a research team used the phage display technique to identify D-amino acid peptide ligands for target receptors (314). Firstly, the D isomer form of an SH3 domain was chemically synthesized, and then utilized for the affinity selection of ligands from a random peptide library, whose amino acids were the natural L isomers. Thus, the D-isomers of the peptides are ligands for the natural L-isomers of the receptor, being the latter the real targets of drug discovery.

1.2.8.2.4. Epitope Discovery

The peptides selected from a random peptide library are named “antigenic mimics” of the corresponding natural epitope (the antigenic determinant that produced the selector antibody) when the receptor used for affinity selection is an antibody. These peptides can be utilized in the immunization of naïve animals, where some of them are able to provoke the production of new antibodies that cross-react with the natural epitope, even though there was never a direct exposition to it. These peptides constitute “immunogenic mimics” and also antigenic mimics (315,316).

A peptide that binds its selector antibody (succeeding as an antigenic mimic) might not be able to cause cross-reacting antibodies when utilized in the immunization of naïve animals (not working as an immunogenic mimic). There are two possible reasons for the latter happening. Firstly, since most small peptides are flexible, they might adopt one conformation when binding the selector antibody, but numerous other conformations when eliciting new antibodies. This would lead to only a few of them actually cross-reacting with the authentic epitope. Secondly, peptides might be antigenic mimics without being true structural mimics. Peptides can bind to the selector antibody in an completely different way than they do to the original epitope, through the establishment of different interactions. For instance, peptides with the motif HPQ bind the biotin-binding pocket of streptavidin in a different way than biotin (317). Thus, these peptides would produce new antibodies that fit differently than the original selector antibody, hardly ever these antibodies cross-reacting with the authentic epitope.

Antigenic and immunogenic mimicry are the foundation of “epitope discovery”, a new method to disease diagnosis and vaccine development. The peptides obtained through epitope discovery can be used in two main ways.

Firstly, they can be used as antigenic mimics, serving as specific probes for antibodies that are the basis for a disease diagnosis, such as the way natural viral proteins are used in the current HIV tests. One of the advantages of using these peptides as diagnostic reagents over natural antigens is the fact that they are easy and inexpensive to discover and produce. Also, they can still be discovered and utilized when the natural antigens associated with the diseases are unknown. Moreover, they can focus on precise diagnostic specificities and reject potentially confusing signals from nondiagnostic determinants.

Secondly, they can be used as components of synthetic vaccines. For an antibody to be protective it has to react with a natural epitope on the actual pathogen, so only antigenic mimics that are also immunogenic mimics can be used in this situation.

1.2.8.2.5. Selection of DNA-Binding Proteins

One of the advantages of the phage display technology might be the possibility to help to design proteins that specifically bind a target DNA sequence. Rational design does not seem to have promising applications in this area, so a more promising approach is the construction of a library of randomized variants of a parent DNA binding domain displayed on filamentous phages, with randomization being focused on positions that make sequence specific contacts with the target DNA in the parent domain. Clones that bind a new target DNA sequence, different from the one recognized by the parent domain are affinity-selected from these libraries (318,319).

Research conducted using phage display has been used to map the DNA binding site of SATB1, a nuclear matrix protein that specifically binds to the minor groove of the MAR DNA sequence motif.

In this experiment, peptides were affinity-selected from a random peptide library using an MAR DNA sequence as the immobilized receptor. Conclusions showed that the predominant peptide shared 50% sequence identity with a nine-residue segment of the SATB1 sequence and was critical for DNA recognition (320). The phage display technique has also been used in the affinity-selection of an hexapeptide that showed binding preference for the single-stranded heptadeoxycytidilate (321).

1.3. Thesis Objectives

Current diagnostic tools for Zika infection and disease include serological/molecular studies, and antigen and/or genome detection. For symptomatic patients with Zika virus infection, Zika virus RNA can sometimes be detected early in the course of illness by RT-PCR. On the other hand, MAC-ELISA is utilized in the qualitative detection of Zika virus IgG and IgM antibodies in cerebrospinal fluid or serum. Nevertheless, results may be difficult to interpret due to possible cross-reaction with other flaviviruses and potential nonspecific reactivity. Moreover, these diagnostic methods are time-consuming and require specialized and expensive laboratory equipment. These tests also present low specificity, since cross-reactivity with other similar viruses is common and will originate false positive results. Usually, seven days of culture are necessary to validate the diagnosis and determine the infecting serotype. Therefore, no routine and accurate assay for the diagnosis of Zika virus infection is currently available.

The main purpose of this project was to develop an approach, based on the phage display technology, that would allow for an early, rapid and differential routine diagnosis of Zika. The objective was to identify and generate phage-displayed peptides that specifically recognized the disease target molecules with high sensitivity and selectivity, that would provide new insights into the development of robust bionanosensors as diagnostic tools for sensitive viral detection and serotyping. In this work, a commercially available phage-displayed peptide library was used for the detection of Zika-specific molecules, screening against two specific antibodies for Zika, in order to identify the peptides that will be used further in the development of bionanosensors as diagnostic tools for Zika infection, which will work as sensitive viral detection and serotyping tools. This type of innovative biosensing method will allow for a non-invasive, rapid, and in real time diagnosis of the disease.

Therefore, the goal of this project was to carry out a “panning” technique, where a commercial library of peptides displayed on bacteriophages would be screened against the specific antibodies for Zika, using two different methods: the “Surface Panning Procedure with Direct Target Coating”, in which the target molecules would be immobilized on the surface of a polystyrene plate; and the “Solution-Phase Panning with Affinity Bead Capture”, in which the phage library would react with the target molecules in solution and the target phage complexes would be captured in a matrix constituted by specific “Protein A/G Agarose Beads” to the target molecules. Then, the objective was for the

selected bacteriophage library to be amplified by bacterial infection in *Escherichia coli* and quantified using the “Phage Titering” technique. The aim was also for the selected bacteriophages to be validated by an ELISA test, in order to assess the binding affinity of the amplified phages. Also, the goal was for the selected DNA sequences to be amplified using the Polymerase Chain Reaction technique and quantified using agarose gel electrophoresis and UV spectrophotometry techniques. The final objective was for the obtained phage DNA to be sequenced, in order to determine the nucleotide sequences corresponding to the specific peptides for the target molecules.

CHAPTER 2. MATERIALS AND METHODS

2. Materials and Methods
2.1. General Materials
2.1.1. Phage Display Peptide Library Kit
2.1.2. *E. coli* ER2738 Host Strain
2.1.3. Anti-Zika Virus NS1 Antibodies
2.1.4. Media and Solutions
2.1.5. Laboratory Equipment
2.2. General Methods
2.2.1. Strain Maintenance
2.2.2. Avoiding Phage Contamination
2.2.3. Phage Titering
2.2.4. Storage of Phage Solutions
2.3. Surface Panning Procedure with Direct Target Coating
2.3.1. Biopanning against Streptavidin Target
2.3.2. Biopanning against Anti-Zika Virus NS1 Antibody Target
2.4. Solution-Phase Panning with Affinity Bead Capture
2.4.1. Biopanning against Streptavidin Target
2.4.2. Biopanning against Anti-Zika Virus NS1 Antibody Target
2.4.2.1. Biopanning with Protein A and Protein G Agarose Beads
2.4.2.2. Biopanning with Protein G Agarose Beads and Negative Selection Step
2.4.2.3. Biopanning with Protein A Agarose Beads and Negative Selection Step
2.5. Phage ELISA Binding Assay with Direct Target Coating
2.5.1. Plaque Amplification for ELISA
2.5.2. ELISA Assay
2.5.2.1. ELISA Assay against Streptavidin Target
2.5.2.2. ELISA Assay against Anti-Zika Virus NS1 Antibody Target
2.6. Sequencing of Phage DNA
2.6.1. Plaque Amplification for Sequencing
2.6.2. Rapid Purification of Sequencing Templates
2.6.3. DNA Quantification of PCR Templates
2.6.4. PCR Amplification
2.6.5. Purification of PCR Products
2.6.5.1. Ethanol/Isopropanol Precipitation
2.6.5.2. PCR Purification Kit
2.6.6. DNA Quantification of PCR Products
2.6.7. Agarose Gel Electrophoresis
2.6.8. Phage DNA Sequencing
2.6.8.1. Analysis of Results using Bioinformatic Tools

2. Materials and Methods

2.1. General Materials

2.1.1. Phage Display Peptide Library Kit

In all the experiments performed during this project, a Phage Display Peptide Library Kit was used, the Ph.D.™-12 Phage Display Peptide Library Kit (New England BioLabs, Inc.). The kit includes the following components: Ph.D.-12 Phage Display Peptide Library (100 µL, 1.0×10^{13} pfu/mL, supplied in TBS with 50% glycerol); -96 gIII 20-mer sequencing primer (5´-^{HO}CCC TCA TAG TTA GCG TAA CG-3´, 100 pmol, 1 pmol/µL); -28 gIII 22-mer sequencing primer (5´-^{HO}GTA TGG GAT TTT GCT AAA CAA C-3´, 100 pmol, 1 pmol/µL); *E. coli* K12 ER2738 host strain (supplied as 50% glycerol culture, not competent); streptavidin (lyophilized, 1.5 mg); biotin (100 µL, 10 mM). The Ph.D.-12 phage display peptide library consists of a combinatorial library with random dodecapeptides fused to the minor coat protein (pIII) of the filamentous M13 bacteriophage. The displayed 12-mer peptide is expressed pentavalently at the N-terminus of pIII, in which the first residue of the mature protein is the first randomized position. The peptide is followed by a short spacer sequence GGGS (Gly-Gly-Gly-Ser) and then the *wild-type pIII* sequence. The library contains approximately 10^9 electroporated sequences amplified once to yield roughly 100 copies of each sequence in 10 µL of the supplied phage.

2.1.2. *E. coli* ER2738 Host Strain

During the course of this work, the bacterial host strain used was the one provided with the Ph.D.-12 Phage Display Peptide Library Kit, namely the *Escherichia coli* K12 ER2738. This strain has the following genotype: *F´ proA$^+$B$^+$ lacI^q Δ(lacZ)M15 zzf::Tn10(Tet^R)/fhuA2 glnV Δ(lac-proAB) thi-1 Δ(hsdS-mcrB)5 [$r_k^-m_k^-$McrBC$^-$]*. The bacterial stock was provided as a suspension of *E. coli* ER2738, grown in LB medium, in 50% glycerol. This strain is resistant to the antibiotic tetracycline.

2.1.3. Anti-Zika Virus NS1 Antibodies

During this project, two anti-Zika virus antibodies were used, the Anti-Zika Virus NS1 antibody [B4] (IgG1 isotype, Abcam®) and the Anti-Zika Virus NS1 antibody [D11] (IgG1 isotype, Abcam®), two mouse monoclonal primary antibodies specific for different epitopes of the NS1 protein of Zika Virus, which are able to detect NS1 from both the Uganda and Suriname strains. These antibodies present insignificant cross-reactivity with NS1 proteins from Dengue Virus (all serotypes), Japanese Encephalitis Virus and Yellow Fever Virus, and little cross-reactivity with the NS1 protein from West Nile Virus. Both antibody stocks were supplied in a concentration of 1 mg/mL in 100% PBS buffer.

2.1.4. Media and Solutions

The streptavidin stock solution was prepared by dissolving 1.5 mg lyophilized streptavidin from the Phage Display Peptide Library Kit in 1 mL of 10 mM sodium phosphate (Merck) (pH 7.2) and 100 mM NaCl (Panreac), in order to obtain a final concentration of 1.5 mg/mL. The iodide buffer solution consisted of 10 mM Tris-HCl (Trizma® Base, Sigma-Aldrich) (pH 8.0), 1 mM EDTA (VWR Chemicals) and 4 M NaI (Riedel-de-Haën). The PEG/NaCl solution was prepared as 20% (w/v) PEG–8000 (Fisher Scientific) and 2.5 M NaCl (Panreac), and autoclaved. The TBS buffer solution was prepared as 50 mM Tris-HCl (Trizma® Base, Sigma-Aldrich) (pH 7.5) and 150 mM NaCl (Panreac), and autoclaved. The TBST 0.1% (v/v) solution was prepared by the addition of 1 mL of Tween® 20 (Fisher Scientific) to 999 mL of the TBS buffer solution. The TBST 0.5% (v/v) solution was prepared by the addition of 5 mL of Tween® 20 (Fisher Scientific) to 995 mL of the TBS buffer solution. The TBS plus 0.1 mM biotin solution was prepared by the addition of 50 µL of the 10 mM biotin stock solution provided in the Phage Display Peptide Library Kit to a total of 5 mL of previously prepared TBS buffer. The blocking buffer solution was prepared as 0.1 M $NaHCO_3$ (LabKem) (pH 8.6) and 5 mg/mL BSA (Sigma-Aldrich), and filter sterilized. The blocking buffer plus 0.1 µg/mL streptavidin solution was prepared by the addition of 10 µL of the 1.5 mg/mL streptavidin stock solution to a total of 150 mL of previously prepared blocking buffer. The tetracycline stock suspension was prepared as 20 mg/mL of tetracycline (Sigma-Aldrich) in 1:1 ethanol:water, whereby 200 mg of tetracycline were dissolved in a solution of 5 mL of ethanol and 5 mL of H_2O. The IPTG/X-Gal stock solution was prepared by the addition of 1.25 g IPTG (Thermo Fisher Scientific) and 1 g X-Gal (VWR Chemicals) to 25 mL of DMF (Thermo Fisher Scientific). LB medium was prepared by dissolving 25 g of LB Broth, Miller (Fisher Scientific) in 1 L of H_2O and autoclaved. Both LB/IPTG/X-Gal and LB+Tet plates were prepared as following: 25 g of LB Broth, Miller (Fisher Scientific) and 15 g of Bacteriological Agar (VWR Chemicals) were dissolved in 1 L of H_2O; the solution was autoclaved and cooled down until approximately 70 ^{o}C; 1 mL of the IPTG/X-Gal stock solution was added to it if preparing LB/IPTG/X-Gal plates; 1 mL of the tetracycline stock suspension was added to it if preparing LB+Tet plates; approximately 20 mL of the solution were poured into each plate and allowed to solidify. The Top Agar aliquots were prepared as following: 25 g of LB Broth, Miller (Fisher Scientific) and 7 g of Bacteriological Agar (VWR Chemicals) were dissolved in 1 L of H_2O; the solution was autoclaved and dispensed into 100 mL aliquots. The ABTS stock solution was prepared by dissolving 22 mg of ABTS in 100 mL of 50 mM sodium citrate (May and Baker) (pH 4.0) and filter sterilized. A buffer solution of 0.1 M $NaHCO_3$ (LabKem) (pH 8.6) was also prepared. The phage elution buffer solution was prepared as 0.2 M Glycine-HCl (Fisher Scientific) (pH 2.2) plus 1 mg/mL BSA (Sigma-Aldrich). The phage neutralizing buffer solution was prepared as 1 M Tris-HCl (Trizma® Base, Sigma-Aldrich) (pH 9.1). The TE (1×) buffer solution was prepared as 10 mM Tris (Trizma® Base, Sigma-Aldrich) and 1 mM EDTA (VWR Chemicals) (pH 8.0). The TAE (1×) buffer solution was prepared as 1 mM EDTA

(VWR Chemicals), 40 mM Tris (Trizma® Base, Sigma-Aldrich) and 20 mM acetic acid glacial (99-100%, Chem-Lab). The agarose gels were prepared by dissolving the appropriate amount of agarose (Sigma-Aldrich) in 100 mL of TAE Buffer (1×): 1 g of agarose for 1% and 2 g of agarose for 2% gels.

2.1.5. Laboratory Equipment

The Sigma 3-30K SuperSpeed Refrigerated Centrifuge and the Eppendorf™ MiniSpin Benchtop Centrifuge were used in all the centrifugation steps of this project. All the incubation steps performed during these experiments were carried out on a Heidolph™ Incubator 1000 / Unimax 1010 Incubator. All the shaking steps performed were conducted on a Heidolph™ Unimax 1010 Orbital Shaker. Whenever aseptic conditions were necessary, such as microorganism handling, an ESCO laminar flow cabinet was used to ensure a sterile working environment.

2.2. General Methods

2.2.1. Strain Maintenance

The *Escherichia coli* host strain ER2738 is a robust F^+ strain with a fast growth rate and is well-suited for M13 phage propagation. ER2738 is a $recA^+$ strain, but spontaneous *in vivo* recombination events with M13 or phagemid vectors were never observed. This strain presents supE (*GlnV*), being able to suppress amber (UAG) stop codons within the library with glutamine.

Since the M13 bacteriophage is a male-specific coliphage, all cultures for M13 propagation were inoculated from colonies grown on media selective for presence of the F-factor, instead of directly from the glycerol culture. The *E. coli* strain was plated and propagated in tetracycline-containing medium, so that the cells containing the F-factor could be selected, since the F-factor of ER2738 contains a mini-transposon, which confers tetracycline resistance. Tetracycline was not added to media during the phage amplification steps.

In order to prepare the ER2738 stock culture, 10 µL of the supplied *E. coli* glycerol culture stock was streaked out onto a LB+Tet plate. The plate was inverted and incubated at 37 °C overnight and stored wrapped with parafilm at 4 °C in the dark, for a maximum of 1 month.

2.2.2. Avoiding Phage Contamination

The library cloning vector M13KE has the lacZα-peptide cloning sequence inserted in the vicinity of the (+) strand origin of replication, resulting in a longer replication cycle, thus differing from the *wild-type* filamentous phage vector. The pIII coat protein mediates bacteriophage infectivity by binding to the F-pilus of the recipient bacterium, meaning that the display of foreign peptides as N-terminal fusions to pIII might attenuate the infectivity of the library phage when compared to the *wild-type* M13.

The selection of contaminating phage during the amplification steps between rounds of panning, in the absence of a correspondingly strong *in vitro* binding selection, can result in most of the phage pool being *wild-type* phage after three rounds of panning. In order to avoid and minimize the selection of any *wild-type* environmental bacteriophage, aerosol-resistant pipette tips were used in all the experiments.

M13 is not a lytic phage so, unlike phage lambda, plaques are caused by diminished cell growth instead of cell lysis and are turbid instead of clear. The library cloning vector M13KE is derived from the cloning vector M13mp19, which carries the lacZα gene, meaning that library phage plaques will appear blue when plated on media containing X-Gal and IPTG. On the contrary, *wild-type* filamentous phage will originate larger and fuzzier colorless plaques when plated on the IPTG/X-Gal media. Consequently, during all titering steps, the plating of the phage eluates was done exclusively on LB/IPTG/X-Gal media.

2.2.3. Phage Titering

After every round of the biopanning protocol, a phage titering procedure was carried out, in order to quantify the eluted bacteriophage pool and isolate single clones for phage DNA sequencing. This plaque assay was performed for the unamplified and the amplified phage stocks obtained in every round of panning. All the phage stocks were titered by diluting prior to infection, instead of diluting cells infected at a higher multiplicity of infection (MOI), since the number of plaques only increases linearly with added phage when the MOI is lower than 1 and cells are in significant excess. The phage plating was also performed at a lower MOI to ensure that each plaque contained only one DNA sequence.

The first step was to inoculate 10 mL of LB media and 10 µL of the tetracycline suspension with ER2738 from the stock plate and to incubate it at 37 °C, with shaking at 200 rpm, for five hours (mid-log phase, OD_{600} ~ 0.5). After this, one LB/IPTG/X-Gal plate per phage dilution was pre-warmed for one hour at 37 °C. While the bacteria were growing, Top Agar was melted in the microwave and 3 mL were dispensed into sterile centrifuge tubes, one per phage dilution, which were maintained at 45 °C. Then, 10^1 to 10^3-fold serial dilutions of phage in LB media were prepared, using 1 mL of LB as a final volume: for unamplified panning eluates, 10^1 to 10^6-fold dilutions were chosen; for amplified phage culture supernatants, 10^7 to 10^{12}-fold dilutions were used. When the ER2738 culture reached mid-log phase (approximately five hours), 200 µL of the latter were dispensed into sterile microcentrifuge tubes, one for each phage dilution. In order to carry out infection, 10 µL of each phage dilution were added to each corresponding tube, these being vortexed quickly and incubated at room temperature for five minutes. Then, the infected cells were transferred, one infection at a time, to the centrifuge tubes containing the 45 °C Top Agar. The tubes were vortexed quickly and the cultures were immediately

poured onto a pre-warmed LB/IPTG/X-Gal plate, one per infected culture. The plates were gently tilted and rotated, in order to spread the Top Agar evenly, and then cooled for five minutes. After this, the plates were inverted and incubated overnight at 37 °C. On the next day, the blue plaques on each plate were counted. The number of plaques of each plate was then multiplied by the dilution factor of that plate to obtain the corresponding phage titer in plaque forming units (pfu) per 10 µL.

2.2.4. Storage of Phage Solutions

Phage in suspension with NaCl/PEG was stored for a maximum of 4 weeks at 4 °C. Eluted unamplified phage was stored at 4 °C in neutralized buffer for a maximum of 1 week. Amplified phage was stored for a maximum of 2 weeks at 4 °C in neutral buffer. For long-term storage of the amplified phages, an equal volume of sterile glycerol (Pharmacia Biotech) was added to each phage aliquot, and these were vortexed and stored at -20 °C.

2.3. Surface Panning Procedure with Direct Target Coating

Firstly, a method of affinity partitioning involving the coating of a plastic surface with the target of interest was attempted. The coating, which was achieved by nonspecific hydrophobic and electrostatic interactions between the target and the plastic surface, was followed by washing away the excess antibody and by passing the pool of phage over the target-coated surface. This step was followed by washing of the excess phages, in order to collect only the specific target-binding phages. The biopanning procedure was carried out in polystyrene 96-well microtiter plates.

2.3.1. Biopanning against Streptavidin Target

A positive control surface panning experiment with direct target coating using streptavidin as the target (**Experiment S1**) was conducted in order to validate and optimize the panning protocol. The panning procedure was carried out following the same protocol as described on **Chapter 2.3.2**, but using streptavidin as the target. Two wells of a microtiter plate were coated with 150 µL of a solution of streptavidin in 0.1 M $NaHCO_3$ (pH 8.6) (**Step 1.1**), whereby another two wells were coated respectively with a streptavidin solution of 50 µg/mL (**Well S1.1**) and of 100 µg/mL (**Well S1.2**). In all blocking steps, the blocking buffer plus 0.1 µg/mL streptavidin solution was used, in order to complex any biotin or biotinylated protein in BSA. In all elution steps, the bound phage was eluted with the TBS plus 0.1 mM biotin solution for 60 minutes. Biotin was used as it is a known ligand for the target, competing with the bound phages for the immobilized target on the plate. Volumes of the reagents used in the several steps of this biopanning procedure are all specified in **Table 14** (in Annex 2), as well as the dilutions used in all phage titering steps. After 3 rounds of amplification, the expected consensus sequence for the streptavidin-binding peptides should include the motif His-Pro-Gln (HPQ).

2.3.2. Biopanning against Zika Virus NS1 Antibody Target

This biopanning procedure used the Anti-Zika Virus NS1 Antibody [B4] as the target and was carried out in three rounds (**Experiment Z1**). Volumes of the reagents used in the several steps of this biopanning procedure are all specified in **Table 15** (in Annex 2), as well as the dilutions used in all phage titering steps. In the first round, a 150 µL solution of 100 µg/mL of the target was prepared in 0.1 M $NaHCO_3$ (pH 8.6) (**Step 1.1**). This solution was then added to a microtiter well and swirled repeatedly until a complete wetting of the surface (**Well Z1**). In order to coat the well with the target, the microtiter plate was incubated overnight with gentle agitation, in a humidified container (sealable plastic box lined with damp paper towels) kept in cold conditions. A negative control surface-based panning experiment without the target was also included in this experiment, following the same biopanning procedure, but without the addition of Anti-Zika Virus NS1 Antibody [B4] to the well of the microtiter plate (**Step 1.1**). The latter was coated with 150 µL of 0.1 M $NaHCO_3$ (pH 8.6) buffer solution (**Well N1**). This negative control experiment was performed with the aim of checking for the possible existence of non-specific interactions between the library of bacteriophages and the plastic microtiter plate.

On the following day, ER2738 from the LB+Tet stock plate was inoculated in 10 mL of LB media and 10 µL of tetracycline suspension stock. This culture was incubated at 37 °C with vigorous shaking for approximately five hours, in order to be used for titering of the unamplified phage eluates. In the meantime, the coating solution from plate wells was poured off and the plate was slapped face down onto a clean paper towel to remove residual solution. After this step, each well was filled completely with 200 µL of blocking buffer solution and incubated for one hour at 4 °C. Subsequently, blocking solution was discarded, and plate wells were rapidly washed with 200 µL of TBST 0.1% six times. In order to avoid drying out the wells, their bottom and sides were coated with TBST by swirling. Solution was poured off and the plate was slapped face down onto a clean paper towel each time. After this, a 100-fold representation of the phage library (2×10^{11} phage from a library with 2×10^{9} clones – 1×10^{13} pfu/mL) was diluted in TBST 0.1% and added to each plate well to a total volume of 100 µL (**Step 1.2**). The plate was rocked gently for 60 minutes at room temperature. Nonbinding phages were discarded by pouring off excess solution and slapping the plate face down onto a clean paper towel. Wells were then washed ten times with 200 µL of TBST 0.1%, in order to completely remove the phages that did not bind to the target. Bound phages were then eluted with 100 µL of 0.2 M Glycine-HCl (pH 2.2) plus 1 mg/mL BSA, as this is a general elution buffer for nonspecific disruption of binding interactions. Elution mixtures were rocked gently for 20 minutes at room temperature. Phage eluates were then pipetted into microcentrifuge tubes and immediately neutralized with 15 µL of 1 M Tris-HCl (pH 9.1). The unamplified phage eluates were titered (**Step 1.3**) based on the titering protocol described before (**Chapter 2.2.3**). The remaining eluates were stored overnight at 4 °C and amplified the next day.

Additionally, 10 mL of LB media and 10 µL of tetracycline stock were inoculated with ER2738 and incubated overnight at 37 °C with gentle shaking for the amplification step.

The following day, the overnight bacterial culture was diluted 1:100 in erlenmeyer flasks (200 µL of culture in a total of 20 mL of LB media per flask). Each unamplified phage eluate was added to a flask and incubated with vigorous shaking for 4.5 hours at 37 °C. Cultures were then transferred to centrifuge tubes and centrifuged at 12000 g for 10 minutes at 4 °C. Pellets were discarded and supernatants transferred to fresh tubes. These tubes were centrifuged again under the same conditions. After this, the upper 80% of each supernatant (16 mL) was transferred to a fresh tube, to which 1/6 volume of 20% PEG/NaCl (2.7 mL) was added. Phages in the solutions were precipitated overnight at 4 °C.

On the next day, ER2738 from the LB+Tet stock plate was inoculated in 10 mL of LB media and 10 µL of tetracycline suspension stock. This culture was incubated at 37 °C with vigorous shaking for approximately five hours, in order to be used for titering of the amplified phage eluates. In the meantime, each PEG precipitation was centrifuged at 12000 g for 15 minutes at 4 °C. Solutions were then decanted and supernatants discarded. Tubes were re-spun for five minutes under the same conditions, and residual supernatants removed with a micropipette. Each phage pellet was then suspended in 1 mL of TBS buffer solution. The suspensions were transferred to microcentrifuge tubes and centrifuged at 18000 g for five minutes at 4 °C, in order to pellet residual cells. Supernatants (1 mL each) were subsequently transferred to fresh microcentrifuge tubes and phages reprecipitated by adding 1/6 volume (170 µL) of 20% PEG/NaCl. Each tube was incubated on ice for 60 minutes and then centrifuged at 18000 g for 10 minutes at 4 °C, and supernatants were discarded. Tubes were re-spun for five minutes under the same conditions and residual supernatants removed with a micropipette. Pellets were suspended in 200 µL of TBS and then microcentrifuged for one minute under the same conditions, in order to pellet any remaining insoluble material. Supernatants were transferred to fresh tubes, constituting the amplified phage eluates. These amplified first round phage eluates were titered (**Step 1.4**) based on the titering protocol described before (**Chapter 2.2.3**). The blue plaques from the titering plates were counted and this value was used to determine the phage titers in pfu/mL. These values were used to calculate the input volumes corresponding to the input titers for the second round of panning.

A second round of biopanning was carried out following the procedure used for the first round, using the calculated amount of first round amplified eluates as input phages (10^{11} virions). Amplified second round phage eluates were titered and the number of blue plaques was used to determine the phage titer in pfu/mL and to calculate the input volume corresponding to the input titer in the third round of panning. A third round of biopanning was carried out using the second round amplified eluates at an input titer equivalent to what was used in the first and second rounds (10^{11} virions).

Amplified third round phage eluates were titered and the number of blue plaques was used to determine the final third round phage titer in pfu/mL. Tween concentration was raised in the second and third rounds of biopanning, whereby TBST 0.5% was used in all wash steps.

2.4. Solution-Phase Panning with Affinity Bead Capture

A different panning approach was also tested as an alternative to directly coating a plate with the target molecule, in which the target reacted with the phage library in solution, followed by the affinity capture of the phage-target complexes onto an affinity matrix (bead) specific for the target molecule.

2.4.1. Biopanning against Streptavidin Target

A positive control solution-phase panning experiment with affinity bead capture using streptavidin as the target (**Experiment S2**) was conducted in order to validate and optimize this variant of the biopanning protocol. In this experiment, Protein G Agarose beads were used in all three rounds of panning, and a subtractive panning step was also included in the second round. The biopanning procedure was carried out following the same protocol as described on **Chapter 2.4.2.2**, but using streptavidin as the target. The final concentration of streptavidin on both **Step 2.1** and **Step 3.2** was 56.25 µg/mL (**Tube S2**). In all blocking steps, the blocking buffer plus 0.1 µg/mL streptavidin solution was used, in order to complex any biotin or biotinylated protein in BSA. In all elution steps, bound phages were eluted with the TBS plus 0.1 mM biotin solution for 60 minutes. Volumes of the reagents used in the several steps of this biopanning procedure are all specified in **Table 16** (in Annex 2), as well as the dilutions used in all phage titering steps. After 3 rounds of amplification, the expected consensus sequence for streptavidin-binding peptides should include the motif His-Pro-Gln (HPQ).

2.4.2. Biopanning against Anti-Zika Virus NS1 Antibody Target

Since the target used in this project was an antibody, Protein A and Protein G agarose beads were used for the capture of the antibody-phage complexes. In this case, using the anti-Zika NS1 [B4] antibody as the target, the selection of peptides specific for Protein A or Protein G was avoided by alternating rounds of panning between Protein A and Protein G agarose beads (**Chapter 2.4.2.1**). Then, an experiment where Protein G agarose was used in all biopanning rounds, including a negative selection strategy, was conducted for the anti-Zika NS1 [B4] antibody and the anti-Zika NS1 [D11] antibody (**Chapter 2.4.2.2**). An experiment where Protein A agarose was used in all biopanning rounds, including a negative selection strategy, was also conducted for the anti-Zika NS1 [D11] antibody (**Chapter 2.4.2.3**).

For these two last experiments, a negative selection step was employed in the beginning of the second round, in order to avoid the accidental selection of peptide sequences that specifically bound to the beads, in which the amplified first round phage eluate was pre-incubated with the agarose bead in the absence of target, and then the supernatant from this step was reacted with the target molecule in a positive selection step.

2.4.2.1. Biopanning with Protein A and Protein G Agarose Beads

At first, a solution-phase based biopanning with affinity bead capture was experimented for the anti-Zika NS1 [B4] antibody using both Protein A and Protein G agarose beads (**Experiment Z2**). Protein A beads were used in the first and third rounds of panning, and Protein G beads were used in the second round of panning, respectively. Both Protein A and G Agarose Beads (High Affinity) were from Abcam®, and were supplied as 50% slurry in 20% ethanol with very high binding capacity (>35 mg IgG/mL for Protein A and >30 mg IgG/mL for Protein G). Volumes of the reagents used in the several steps of this biopanning procedure are all specified in **Table 17** (in Annex 2), as well as the dilutions used in all phage titering steps.

For the first round of biopanning, ER2738 from the LB+Tet stock plate was inoculated in 10 mL of LB media and 10 µL of tetracycline suspension stock. This culture was incubated at 37 °C with vigorous shaking for approximately five hours, in order to be used for titering of the unamplified phage eluate. Then, 50 µL of the 50% aqueous suspension of protein A agarose affinity beads were transferred to a microcentrifuge tube and 1 mL of TBST 0.1% was added. The resin was suspended by gently vortexing the tube and then pelleted by centrifugation for 60 seconds at 10000 g. The supernatant was carefully pipetted away and discarded without disturbing the resin pellet. The resin was then suspended in 1 mL of blocking buffer solution and incubated for 60 minutes at 4 °C, vortexing occasionally. In the meantime, a 100-fold representation of the peptide library (equivalent to 2×10^{11} pfu from a library of complexity 2×10^{9}) and the antibody target were diluted to a final volume of 200 µL with TBST 0.1% (**Tube Z2**), being the final concentration of the target 50 µg/mL (**Step 2.1**). The tube was incubated for 20 minutes at room temperature. Following the blocking reaction, the resin was pelleted by centrifugation for 60 seconds at 10000 g and washed four times with 1 mL of TBST 0.1%, pelleting the resin each time. After the completion of the washing steps, the phage-target mixture was transferred to the microcentrifuge tube containing the previously washed resin. The solution was mixed gently and incubated for 15 minutes at room temperature, vortexing occasionally. After this step, the resin was pelleted again by centrifugation for 60 seconds at 10000 g and the supernatant was discarded. The resin was then washed 10 times with 1 mL of TBST 0.1%, pelleting it each time. Finally, the bound phages were eluted by suspending the resin in 1 mL of 0.2 M Glycine-HCl (pH 2.2) plus 1 mg/mL BSA, and incubating for 10 minutes at room temperature. The elution mixture was then

centrifuged for 60 seconds at 10000 g. The supernatant was carefully transferred to a clean microcentrifuge tube, without disturbing the pelleted resin, and immediately neutralized with 150 µL of 1 M Tris-HCl (pH 9.1). A negative control solution-phase panning experiment without the target was also included in this experiment, following the same biopanning procedure, but without the addition of Anti-Zika Virus NS1 [B4] Antibody to the mixture on **Step 2.1**, whereby only a 100-fold representation of the peptide library diluted to a final volume of 200 µL with TBST 0.1% was added to the microcentrifuge tube containing the resin (**Tube N2**). This negative control experiment was performed with the aim of checking for the possible existence of non-specific interactions between the library of bacteriophages and the affinity matrixes. The unamplified phage eluates were titered (**Step 2.2**) based on the titering protocol previously described (**Chapter 2.2.3**). The remaining eluates were stored overnight at 4 °C and amplified the next day. The amplification of the remaining phage eluates was conducted as described previously on **Chapter 2.3.2**. The amplified first round phage eluates were titered (**Step 2.3**) based on the titering protocol described before (**Chapter 2.2.3**). The blue plaques from the titering plates were counted and this value was used to determine the phage titer in pfu/mL. This value was used to calculate the input volume corresponding to the input titer in the second round of panning.

A second round of panning was carried out following the procedure used for the first round, using Protein G Agarose beads as the affinity matrix and the calculated amount of first round amplified eluate as input phage. The amplified second round phage eluates were titered and blue plaques from the titering plates were used to determine the phage titer in pfu/mL and to calculate the input volume corresponding to the input titer in the third round of panning. A third round of biopanning was carried out using the second round amplified eluate at an input titer equivalent to what was used in the first round (10^{11} virions). Protein A Agarose beads were used as the affinity matrix in this round. The amplified third round phage eluates were titered and the number of blue plaques from the titering plates was used to determine the final third round phage titer in pfu/mL. Tween concentration was raised in both the second and third rounds of biopanning, whereby TBST 0.5% was used in all binding and wash steps.

2.4.2.2. Biopanning with Protein G Agarose Beads and Negative Selection Step

As an alternative, a solution-phase based biopanning protocol with affinity bead capture was tried using Protein G agarose beads in all the three panning rounds (**Experiment Z3**). In order to avoid the selection of Protein G specific peptides, a negative selection step was employed during the second round of panning, in which the agarose beads were pre-incubated with the amplified first round phage eluate in the absence of target, and then the supernatant was reacted with the target molecule in a positive selection step. Two experiments following this protocol were conducted, **Experiment Z3.1**,

using the anti-Zika NS1 [B4] antibody as the target, and **Experiment Z3.2**, using the anti-Zika NS1 [D11] antibody as the target. In both experiments, different input volumes of anti-Zika antibody were tested. Volumes of the reagents used in the several steps of this biopanning procedure are all specified in **Table 18** (in Annex 2) for **Experiment Z3.1** and in **Table 19** (in Annex 2) for **Experiment Z3.2**, as well as the dilutions used in all phage titering steps.

For **Experiment Z3.1** and **Experiment Z3.2**, the first round of panning was carried out using the protocol described before (**Chapter 2.4.2.1**), but with the employment of Protein G agarose beads as the affinity matrix. The Tween concentration used in the binding and washing steps was 0.1% (v/v). On **Step 2.1**, the total concentration of anti-Zika antibody [B4] was 50 µg/mL for **Tube Z3.1.1** and 25 µg/mL for **Tube Z3.1.2**, and the total concentration of anti-Zika antibody [D11] was 50 µg/mL for **Tube Z3.2.1** and 25 µg/mL for **Tube Z3.2.2**. A negative control solution-phase panning experiment without the target was also included in this experiment, following the same biopanning procedure, but without the addition of Anti-Zika Virus NS1 [B4] Antibody to the resin mixture (**Tube N3.1**) and of Anti-Zika Virus NS1 [D11] Antibody to the resin mixture (**Tube N3.2**) on **Step 2.1**. This negative control experiment was performed with the aim of checking for the possible existence of non-specific interactions between the library of bacteriophages and the affinity matrixes. The unamplified and amplified phage eluates were titered based on the titering protocol previously described (**Chapter 2.2.3**).

For the second round of panning, Protein G Agarose beads were again employed, and a negative selection stage was applied. The calculated amount of the first round amplified eluate was used as input phage. The Tween concentration used in the binding and wash steps was 0.5% (v/v). An additional 50 µL of washed, blocked resin was prepared, whereby two aliquots of 50 µL of the 50% aqueous suspension of protein G agarose affinity beads per experiment were transferred to a microcentrifuge tube and 1 mL of TBST 0.5% was added to each. Resins were suspended by gently vortexing the tubes and then pelleting by centrifugation for 60 seconds at 10000 g. Supernatants were carefully pipetted away and discarded without disturbing the resin pellets. Resins were then suspended in 1 mL of blocking buffer solution and incubated for 60 minutes at 4 °C, vortexing occasionally. Resins were pelleted and washed 4 times with TBST 0.5%. After this, a 100-fold representation of the peptide library was diluted to a total volume of 200 µL of TBST 0.5% (**Step 3.1**) for both experiments. The diluted phage libraries were added to the washed and blocked resin aliquots and incubated for 15 minutes at room temperature with occasional vortexing. The resins were then microcentrifuged for 60 seconds at 10000 g and the supernatants were transferred to fresh microcentrifuge tubes. Then, the antibody targets were added to the supernatants (**Step 3.2**) and incubated for 20 minutes at room temperature. For **Experiment Z3.1**, anti-Zika antibody [B4] was added to a concentration of 50 µg/mL to **Tube Z3.1.1** and 25 µg/mL to **Tube Z3.1.2**. For **Experiment Z3.2**, anti-Zika antibody [D11] was added to a concentration of 50 µg/mL to **Tube Z3.2.1** and 25 µg/mL

to **Tube Z3.2.2**. The antibodies were not added to the resin mixtures on **Step 3.2** for the negative control tubes (**Tube N3.1** and **Tube N3.2**). The phage-target mixtures were then transferred to the remaining washed and blocked resin aliquots and the solutions were mixed gently and incubated for 15 minutes at room temperature, vortexing occasionally. After this step, the resins were pelleted again by centrifugation for 60 seconds at 10000 g and the supernatants were discarded. The resins were then washed 10 times with 1 mL of TBST 0.5%, pelleting the resins each time. Finally, the bound phages were eluted by suspending the resins in 1 mL of 0.2 M Glycine-HCl (pH 2.2) plus 1 mg/mL BSA and incubated for 10 minutes at room temperature. The elution mixtures were then centrifuged for 60 seconds at 10000 g. The supernatants were carefully transferred to clean microcentrifuge tubes, avoiding disturbing the pelleted resins, and immediately neutralized with 150 µL of 1 M Tris-HCl (pH 9.1).

The third round of panning was carried out using the protocol described before (**Chapter 2.4.2.1**), but with the employment of Protein G Agarose beads as the affinity matrix. The calculated amount of the second round amplified eluate was used as input phage. The Tween concentration used in the binding and washing steps was kept at 0.5% (v/v). On **Step 2.1**, for **Experiment Z3.1**, the total concentration of anti-Zika antibody [B4] was 50 µg/mL for **Tube Z3.1.1** and 25 µg/mL for **Tube Z3.1.2**. On the same **Step 2.1**, for **Experiment Z3.2**, the total concentration of anti-Zika antibody [D11] was 50 µg/mL for **Tube Z3.2.1** and 25 µg/mL for **Tube Z3.2.2**. The antibodies were not added to the resin mixtures on **Step 2.1** for the negative control tubes (**Tube N3.1** and **Tube N3.2**).

2.4.2.3. Biopanning with Protein A Agarose Beads and Negative Selection Step

Another solution-phase based biopanning protocol with affinity bead capture was tried using Protein A agarose beads in all the three panning rounds (**Experiment Z4**), using the anti-Zika NS1 [D11] antibody as the target. In order to avoid the selection of Protein A specific peptides, a negative selection step was employed during the second round of panning. In this protocol, two different input volumes of anti-Zika [D11] antibody were also tested. Volumes of the reagents used in the several steps of this biopanning procedure are all specified in **Table 20** (in Annex 2), as well as the dilutions used in all phage titering steps.

Experiment Z4 was carried out using the protocol described before (**Chapter 2.4.2.2**), but with the employment of Protein A agarose beads as the affinity matrix. In the first round of panning, the Tween concentration used in the binding and wash steps was 0.1% (v/v). On **Step 2.1**, the total concentration of anti-Zika antibody [D11] was 50 µg/mL for **Tube Z4.1** and 100 µg/mL for **Tube Z4.2**. A negative control solution-phase panning experiment without the target was once again included in this experiment, following the same biopanning procedure, but without the addition of Anti-Zika Virus NS1

[D11] Antibody to the resin mixture (**Tube N4**) on **Step 2.1**. The unamplified and amplified phage eluates were titered based on the titering protocol previously described (**Chapter 2.2.3**).

For the second round of panning, a negative selection stage was also applied. The calculated amount of the first round amplified eluate was used as input phage. For **Step 3.1**, a 100-fold representation of the peptide library was diluted to a total volume of 200 µL of TBST 0.5%. Then, on Step **3.2**, the anti-Zika antibody [D11] was added to the supernatants, to a concentration of 25 µg/mL on **Tube Z4.1** and a concentration of 50 µg/mL on **Tube Z4.2**. The antibody was not added to the resin mixture on the negative control **Tube N4**. For the third round of panning, the calculated amount of the second round amplified eluate was used as input phage. On **Step 2.1**, the total concentration of anti-Zika antibody [D11] was 25 µg/mL for **Tube Z4.1** and 50 µg/mL for **Tube Z4.2**. The antibody was again not added to the resin mixture on the negative control **Tube N4**. The Tween concentration used in the binding and wash steps for both rounds was 0.5% (v/v).

2.5. Phage ELISA Binding Assay with Direct Target Coating

In order to evaluate the target specificity of selected phage clones, a phage ELISA binding assay was conducted after every third round of biopanning for the experiments performed against the Streptavidin (**Experiment S1** and **Experiment S2**) and the Anti-Zika Virus NS1 Antibody (**Experiment Z1**, **Experiment Z2**, **Experiment Z3** and **Experiment Z4**) targets.

2.5.1. Plaque Amplification for ELISA

For every panning experiment, the third round amplified phage eluate pool and ten random individual phage clones were all amplified following the protocol described below.

In order to proceed to phage amplification, a 10 mL LB+Tet culture of ER2738 was inoculated from a colony. The overnight culture of ER2738 was diluted 1:100 in LB media, and 1 mL of diluted culture was dispensed into 11 culture tubes, one for each clone to be amplified (third round phage eluate and 10 third round random phage clones). A pipette tip was used to stab blue plaques from the third round amplified phage eluate titering plate and to transfer each of them to a tube containing the diluted culture. In order to prevent the occurrence of deletions, third round titering plates were incubated at 37 °C for no longer than 18 hours and then stored at 4 °C, and the plaques were picked within 1 day of plating. To ensure that each plaque contained a single DNA sequence, well separated plaques were picked. In the 11^{th} tube, 10 µL of the third round eluted phage pool were added to the 1 mL of diluted overnight culture. Tubes were incubated at 37 °C with shaking for five hours. After this, cultures were transferred to microcentrifuge tubes, and centrifuged at 18000 g for 60 seconds. Supernatants were transferred to fresh tubes and re-spun under the same conditions. The upper 80%

of the supernatants (800 µL, amplified phage stock) were transferred to fresh tubes and these were stored at 4 °C. On the same day, a 10 mL LB+Tet culture of ER2738 was inoculated from a colony.

The following day, an overnight culture of ER2738 was diluted 1:100 in 20 mL of LB media for each phage clone and phage pool to be characterized. After this, 5 µL of each amplified phage stock were added to a 20 mL diluted culture and incubated with vigorous aeration and agitation for five hours at 37 °C. Cultures were transferred to microcentrifuge tubes and spun at 12000 g for 10 minutes at 4 °C. Supernatants were then transferred to fresh tubes and pellets were discarded. Tubes were centrifuged again under the same conditions. After this, the upper 80% of each supernatant (16 mL) was transferred to a fresh tube, and 1/6 volume of 20% PEG/NaCl (3.5 mL) was added to each tube. Phages in the solutions were precipitated overnight at 4 °C.

On the next day, the PEG precipitations were centrifuged at 12000 g for 15 minutes at 4 °C. Solutions were then decanted and the supernatants discarded. Tubes were re-spun for five minutes under the same conditions, and residual supernatants were removed with a pipette. Pellets were then suspended in 1 mL of TBS buffer solution. Suspensions were transferred to microcentrifuge tubes and centrifuged at 18000 g for five minutes at 4 °C, in order to pellet residual cells. Supernatants were then transferred to fresh microcentrifuge tubes and phages were reprecipitated by adding 1/6 volume (170 µL) of 20% PEG/2.5 M NaCl to each tube. The tubes were incubated on ice for 60 minutes. Solutions were then centrifuged at 18000 g for 10 minutes at 4 °C and the supernatants were discarded. Tubes were re-spun under the same conditions and the residual supernatants were removed with a micropipette. Pellets were suspended in 50 µL of TBS buffer solution. The amplified phage stocks (third round amplified phage eluate pool and one random amplified phage clone for every panning procedure) were then titered following the phage titering protocol previously described (**Chapter 2.2.3**).

2.5.2. ELISA Assay

An ELISA assay was conducted for all the amplified third round phage eluates and for all the randomly selected amplified phage clones obtained after every biopanning experiment against a target. For ELISA characterization, a microtiter plate was coated with the target at high density, and each amplified phage stock was applied to the plate at a known concentration. The bound phages specific for the target were then detected with an anti-M13 antibody (anti-M13-HRP conjugate), the M13 Major Coat Protein Antibody (RL-PH1) HRP from Santa Cruz Biotechnology® (200 µg/mL in PBS, <0.1% sodium azide, 0.1% gelatin). This monoclonal mouse antibody is suitable for the detection of the M13 filamentous bacteriophage coat protein g8p, in the dilution 1:200 (dilution range of 1:100 to 1:1000).

2.5.2.1. ELISA Assay against Streptavidin Target

Phage stocks (phage pools and randomly selected phage clones) obtained from the amplification of the third round eluates from **Experiment S1** and **Experiment S2** were all examined for binding activity by an ELISA assay. Volumes of the reagents used in the several steps of this ELISA assay are all specified in **Table 21** (in Annex 2). The test was carried out following the protocol described on **Chapter 2.5.2.2**, but using streptavidin as the target, whereby one well of an ELISA plate for each phage clone and phage pool to be characterized was coated with 150 µL of a solution of 100 µg/mL of the streptavidin target in 0.1 M $NaHCO_3$ (pH 8.6) instead.

2.5.2.2. ELISA Assay against Anti-Zika Virus NS1 Antibody Target

Phage stocks (phage pools and randomly selected phage clones) obtained from the amplification of the third round eluates from **Experiment Z1**, **Experiment Z2**, **Experiment Z3** and **Experiment Z4** were all examined for binding activity by an ELISA assay. Volumes of the reagents used in the several steps of this ELISA assay are all specified in **Table 22** (in Annex 2).

Firstly, one well of an ELISA plate for each phage clone and phage pool to be characterized was coated with 150 µL of a solution of 100 µg/mL of the anti-Zika antibody target in 0.1 M $NaHCO_3$ (pH 8.6) and swirled repeatedly until the surface got completely wet (**Step 4.1**). For the experiments previously carried out with the anti-Zika antibody [B4] (**Experiment Z1**, **Experiment Z2** and **Experiment Z3.1**), this was the target added to the wells of the corresponding ELISA assay. For the experiments previously carried out with the anti-Zika antibody [D11] (**Experiment Z3.2** and **Experiment Z4**), this was the target respectively added to the wells of the corresponding ELISA assay. In order to coat the wells with the targets, the plate was incubated overnight with gentle agitation in an air-tight humidified container (sealable plastic box lined with damp paper towels) kept in cold conditions.

On the next day, the excess target solution was poured off and the plate was slapped face-down onto a clean paper towel to remove residual solution. After this step, each well was filled completely with 200 µL of blocking buffer solution and incubated for one hour at 4 °C. Also, in order to check for binding of the selected sequences to BSA-coated plastic, a test for background signal was performed, whereby one uncoated well of the ELISA plate per phage pool or clone to be characterized was also blocked (200 µL of blocking buffer). An uncoated row of wells of the ELISA plate was also blocked (200 µL of blocking buffer) for use in the dilution of the phage stocks before their addition to the target-coated plate, since the dilutions need to be done firstly in separated blocked wells and then transferred to the target coated wells. Next, the blocking buffer solution was discarded, and each well was rapidly washed with 200 µL TBST 0.5% six times, pouring off the solution and slapping the plate face-down onto a clean paper towel each time. In the separated blocked wells, the dilution of the selected phage stocks was carried out, whereby a 100-fold representation of the phage libraries

(2×10^{11} phage from a library with 2×10^{9} clones – 1×10^{13} pfu/mL) was diluted in a total of 200 µL of TBST 0.5% per well. Then, 100 µL from each of the diluted phage wells were transferred to the respective target coated wells and uncoated wells without target (**Step 4.2**). The plate was incubated at room temperature for 60 minutes with gentle agitation. Nonbinding phages were discarded by pouring off the excess solution and slapping the plate face down onto a clean paper towel. Wells were then washed six times with 200 µL TBST 0.5%, in order to completely remove phages that did not bind to the target. Then, the HRP-conjugated anti-M13 monoclonal antibody was diluted in blocking buffer to a final volume of 200 µL, using a 1:20 dilution. After this, 200 µL of diluted conjugate were added to each well and the plate was incubated at room temperature for 60 minutes with gentle agitation (**Step 4.3**). The nonbinding conjugate was discarded by pouring off the excess solution and slapping the plate face down onto a clean paper towel. Wells were again washed six times with 200 µL TBST 0.5%. The HRP substrate solution was prepared immediately prior to the detection step, by the addition of 36 µL of 30% H_2O_2 to 21 mL of ABTS stock solution. 200 µL of substrate solution were added to each well, and the plate was incubated for 60 minutes at room temperature with gentle agitation. The ELISA plate was read using a microplate reader (PerkinElmer VICTOR^3 1420 Multilabel Plate Reader) set at 410 nm. The software used in the readings was Wallac 1420 Workstation with the Absorbance Scale.

2.6. Sequencing of Phage DNA

In order to identify and characterize the selected binding sequences, the individual phage clones and third round phage pools that were previously chosen for the ELISA assay were also amplified and purified, as described below, for posterior DNA sequencing.

2.6.1. Plaque Amplification for Sequencing

For every biopanning experiment performed against Streptavidin (**Experiment S1** and **Experiment S2**), the ten phage clones previously selected for the ELISA assay were amplified for subsequent sequencing. As to every biopanning experiment performed against the Anti-Zika Virus NS1 Antibodies (**Experiment Z1**, **Experiment Z2**, **Experiment Z3** and **Experiment Z4**), the ten random phage clones and the third round eluted phage pools previously selected for ELISA were also amplified for subsequent sequencing. All the selected phage stocks were amplified following the protocol described previously on **Chapter 2.5.1** until the last centrifugation step mentioned on the second paragraph. Following this centrifugation, the upper 50% of the supernatants (500 µL, amplified phage stock) were transferred to fresh tubes and these were stored at 4 °C.

2.6.2. Rapid Purification of Sequencing Templates

In order to purify the obtained amplified phage stocks for posterior phage DNA sequencing, the following protocol was used, which produced templates of enough purity for dideoxy sequencing.

Firstly, 200 µL of 20% PEG/NaCl were added to each microcentrifuge tube containing 500 µL of the phage-containing supernatants. Tubes were inverted several times to mix and were incubated for 20 minutes at room temperature. Afterwards, they were centrifuged at 18000 g for 10 minutes at 4 °C and supernatants were posteriorly discarded. Tubes were re-spun briefly under the same conditions and remaining supernatants were carefully pipetted away. Pellets were then suspended thoroughly in 100 µL of iodide buffer solution by vigorously tapping the tube. Then, 250 µL of ethanol were added to each tube and the mixtures were incubated at room temperature only for 20 minutes, since short incubation at room temperature favorably precipitates single-stranded phage DNA, leaving most phage protein in solution. Tubes were then centrifuged at 18000 g for 10 minutes at 4 °C and supernatants were discarded. Pellets were washed with 500 µL of 70% ethanol (stored at –20 °C) and tubes were re-spun under the same conditions. Supernatants were discarded and pellets were air-dried briefly in an Eppendorf® ThermoStat Plus machine at 60 °C. Pellets were then suspended in 30 µL of TE buffer solution.

2.6.3. DNA Quantification of PCR Templates

In order to quantify the phage DNA in the samples for PCR amplification, all obtained phage stocks had their DNA quantified by UV/vis spectrophotometry, using a PerkinElmer Lambda 25 UV/Vis Spectrophotometer with PerkinElmer UV WinLab software for **Experiment S1**, **Experiment S2**, **Experiment Z1** and **Experiment Z2**, and a NanoDrop™ One Microvolume UV-Vis Spectrophotometer for **Experiment Z3** and **Experiment Z4**. Absorbance of the samples was measured at 260 nm, in order to determine the DNA concentration in the samples (A_{260} ssDNA = 33 µg/mL), and at 230 and 280 nm, in order to determine the samples purity, using the absorbance ratios at 260 and 280 nm ($A_{260/280}$) and at 260 and 230 nm ($A_{260/230}$) to assess the purity of the phage nucleic acids. The concentration of nucleic acids in each sample was determined using the Beer–Lambert law, which relates the amount of light absorbed to the concentration of the absorbing molecule. At a wavelength of 260 nm, the average extinction coefficient for single-stranded DNA is 0.027 $(\mu g/mL)^{-1}.cm^{-1}$. Thus, an Absorbance (A) of 1 corresponds to a concentration of 33 µg/mL for single-stranded DNA. For every measurement performed with the PerkinElmer spectrophotometer, 5 µL of each sample and 995 µL of H_2O were added to each quartz cuvette, diluting the samples 1:200 for the DNA quantification. The blank cell contained 995 µL of H_2O and 5 µL of TE buffer solution.

2.6.4. PCR Amplification

All the obtained phage DNA stocks were amplified via Polymerase Chain Reaction, using a BIO-RAD® iQ™5 Real-Time PCR Detection System (iCycler® Thermal Cycler). Forward and reverse primers were manually designed and ordered from IDT (Integrated DNA Technologies, Inc.). The forward and reverse primers were **5' CGC AAT TCC TTT AGT GGT ACC 3'** (100 µM, MW 6372.2 g/mol, T_m 53.6 °C) and **5' GCC CTC ATA GTT AGC GTA ACG 3'** (100 µM, MW 6406.2 g/mol, T_m 55.3 °C), respectively. The mean T_m (melting temperature) of the primers was 54.45 °C. They were diluted 1:10 in H_2O (1 µL of each primer in 9 µL of H_2O), in order to obtain a working concentration of 10 µM. The iQ™ Supermix (2x) from BIO-RAD®, which is a ready-to-use reaction master mix containing antibody-mediated hot-start iTaq DNA polymerase, dNTPs, $MgCl_2$, enhancers and stabilizers, was used in all PCR reactions. The total volume for all PCR reactions was 20 µL. The expected amplicon size for all amplified samples was 190 bp. The amplified third round phage eluate pool and 10 random individual phage clones for every panning experiment conducted against a target were amplified by PCR, this being considered **PCR Experiment 1**. Volumes and concentrations of the reagents used in the reaction are specified in **Table 23** (in Annex 2). Thermal cycling temperature and timing conditions are specified in **Table 24** (in Annex 2).

Another PCR reaction was conducted, in order to try to optimize and maximize the amount of products obtained from PCR. Therefore, different primer concentrations were tested in the PCR mixture. Individual phage clones from **Experiment Z1** were chosen and amplified by PCR using two different primer concentrations in the reagent mixture, 250 nM and 500 nM, this being considered **PCR Experiment 2**. Reactions were conducted under the same conditions as the **PCR Experiment 1** previously described. Negative controls were added, which contained all the PCR reagents except the DNA template to amplify. Two negative controls were performed for every primer concentration. Volumes and concentrations of the reagents used in this PCR reaction are specified in **Table 25** (in Annex 2).

Another PCR reaction using different thermal cycling conditions was also conducted, in order to optimize the PCR reaction and avoid the presence of non-specific PCR products. This reaction was performed under the same conditions as **PCR Experiment 1** and **PCR Experiment 2**, but with the addition of a Hot-Start step at 95 °C. Individual phage clones from **Experiment Z1** were chosen and amplified by PCR, this being considered **PCR Experiment 3**. A negative control was also added to this reaction. Volumes and concentrations of the reagents used in this PCR reaction are specified in **Table 26** (in Annex 2). Thermal cycling temperature conditions are all specified in **Table 27** (in Annex 2).

2.6.5. Purification of PCR Products

The purification of the obtained PCR products was attempted by using two different protocols.

2.6.5.1. Ethanol/Isopropanol Precipitation

Firstly, an ethanol/isopropanol DNA precipitation was attempted. For all **Experiment Z1** phage stocks amplified by PCR during **PCR Experiment 1**, the obtained samples were purified following this protocol. The first five amplified phage clones (samples Z1.1, Z1.2, Z1.3, Z1.4 and Z1.5) were precipitated using ethanol and following **Protocol 1**. The remaining five amplified phage clones (Z1.6, Z1.7, Z1.8, Z1.9 and Z1.10) were precipitated using isopropanol and following **Protocol 2**. These two experiments were performed in order to compare the purification efficacy between ethanol and isopropanol.

For the purification carried out following **Protocol 1**, 1 µL of 3 M sodium acetate and 20 µL of 100% ethanol (stored at −20 °C) were added to each 10 µL of PCR products, mixing the samples thoroughly. Then, samples were incubated at −20 °C for 30 minutes. Afterwards, samples were centrifuged at 20000 g for 20 minutes at 4 °C and the supernatants were discarded. Then, 500 µL of 70% ethanol (stored at −20 °C) were added to each sample in order to wash the solutions. The samples were centrifuged at 15000 g for 15 minutes at 4 °C and the supernatants were discarded again. Pellets were air-dried briefly in an Eppendorf® ThermoStat Plus machine at 60 °C for 15 minutes. Pellets were resuspended in 15 µL of TE buffer and stored at −20 °C.

For the purification carried out following **Protocol 2**, 1 µL of 3 M sodium acetate and 10 µL of 100% isopropanol were added to each 10 µL of PCR products, mixing the samples thoroughly. Then, the samples were incubated at room temperature for 10 minutes. Samples were centrifuged at 20000 g for 20 minutes at 20 °C and the supernatants were discarded. Pellets were washed with 500 µL of 70% isopropanol and centrifuged for 15000 g for 15 minutes at 20 °C. Supernatants were discarded again and then pellets were air-dried briefly in an Eppendorf® ThermoStat Plus machine at 60 °C for 15 minutes. Pellets were resuspended in 15 µL of TE buffer and stored at −20 °C.

2.6.5.2. PCR Purification Kit

Afterwards, the DNA purification using a PCR clean-up kit was performed, using the QIAGEN® "QIAquick® PCR Purification Kit / QIAquick® PCR & Gel Cleanup Kit", following the standard protocol described on Annex 1, provided by QIAGEN®. For all the remaining phage stocks amplified by PCR during **PCR Experiment 1** (**Experiment Z2**, **Experiment Z3**, **Experiment Z4**, **Experiment S1** and **Experiment S2**), a total 20 µL of each sample was purified following this protocol. All the amplified phage DNA strands obtained on **PCR Experiment 2** were also purified following this protocol. For the DNA templates obtained on **PCR Experiment 3**, only 15 µL of each sample were purified by this protocol.

2.6.6. DNA Quantification of PCR Products

In order to quantify the phage DNA in the samples after PCR amplification and purification, all the purified PCR products obtained on **PCR Experiment 1** had their DNA quantified by UV/vis spectrophotometry, using a PerkinElmer Lambda 25 UV/Vis Spectrophotometer with PerkinElmer UV WinLab software for **Experiment S1**, **Experiment S2**, **Experiment Z1** and **Experiment Z2**, and a NanoDrop™ One Microvolume UV-Vis Spectrophotometer for **Experiment Z3** and **Experiment Z4**, using the same methods as described before on **Chapter 2.6.3**. The purified PCR products obtained on **PCR Experiment 2** and on **PCR Experiment 3** also had their DNA quantified by this method using the PerkinElmer spectrophotometer. Absorbance of the samples was measured at 260 nm, in order to determine the DNA concentration (A260 dsDNA = 50 µg/mL), and at 230 and 280 nm, in order to determine their purity. At a wavelength of 260 nm, the average extinction coefficient for double-stranded DNA is 0.020 $(\mu g/mL)^{-1}.cm^{-1}$. Thus, an Absorbance (A) of 1 corresponds to a concentration of 50 µg/mL for double-stranded DNA. For every measurement, 5 µL of each sample were added to 995 µL of H_2O, diluting the samples 1:200 for the DNA quantification. For the **PCR Experiment 1** clones, the blank cell contained 995 µL of H_2O and 5 µL of TE buffer solution (**Experiment Z1**) / EB buffer solution (**Experiment Z2**, **Experiment Z3**, **Experiment Z4** and **Experiment S1** and **Experiment S2**). For the **PCR Experiment 2** and the **PCR Experiment 3** clones (**Experiment Z1**), the blank was measured using EB buffer solution.

2.6.7. Agarose Gel Electrophoresis

In order to verify the PCR products and confirm the size of the obtained PCR amplicons, an electrophoresis assay using agarose gel was conducted for all the samples. The assays were performed using the Thermo Scientific MiniCell® Primo™ Electrophoretic Gel System and the power supply Pharmacia LKB – EPS 500/400. All gels were run at 100 Volts (V) for 60 minutes. The molecular weight marker GeneRuler™ 100 bp DNA ladder (Fermentas) was used to check the size of the DNA bands and to approximately quantify the PCR products. In order to visualize the DNA bands, 1:6 of EZ Vision was added to each sample, whereby 1 µL of EZ Vision and 5 µL of sample/ladder were added to each well of the agarose gel. Gels were visualized on a Bio-Rad Gel Doc EQ Imaging System and a record was printed out. DNA templates obtained on **PCR Experiment 1** were run on a 1% agarose gel, whereas the ones obtained on **PCR Experiment 2** were run on a 2% agarose gel. For PCR products obtained on **PCR Experiment 3**, an electrophoresis experiment was also conducted in order to compare the DNA templates obtained before and after purification with the PCR Clean-Up Kit. Purified and unpurified samples obtained after this PCR experiment were both run on a 2% agarose gel.

2.6.8. Phage DNA Sequencing

The obtained PCR products were sequenced by Sanger Sequencing, a service provided by the StabVida company. For each clone, 3 µL of Forward Primer (10 pmol/µL – 10 µM) and 10 µL of DNA (≥20 µg/mL) were added to a microcentrifuge tube (YouTube It Reaction). The selected DNA sequences were then sent to the StabVida laboratories and identified by Sanger DNA sequencing.

2.6.8.1. Analysis of Results using Bioinformatic Tools

All the obtained sequencing data was analyzed using specific bioinformatic tools. Basic Local Alignment Search Tool (BLAST) was used for the identification of the obtained peptide sequences and to obtain information regarding those peptides. Expert Protein Analysis System (ExPASy) tool was used for translation of the obtained DNA sequences into the respective amino acid sequences. European Informatics Institute (EMBL-EBI) Nucleotide Sequence Translation tool was used for the translation of the obtained nucleic acid sequences to the corresponding peptide sequences. European Informatics Institute (EMBL-EBI) Multiple Sequence Alignment tool was used to align the obtained nucleotide sequences and find regions of similarity between the corresponding peptide sequences. A Plasmid Editor (ApE) tool was used to visualize and determine the size of the obtained DNA sequences and to write the reverse-complement counterpart of each DNA strand.

CHAPTER 3. RESULTS AND DISCUSSION

3. Results and Discussion
3.1. Surface Panning Procedure with Direct Target Coating
3.1.1. Biopanning against Streptavidin Target
3.1.2. Biopanning against Anti-Zika Virus NS1 Antibody Target
3.2. Solution-Phase Panning with Affinity Bead Capture
3.2.1. Biopanning against Streptavidin Target
3.2.2. Biopanning against Anti-Zika Virus NS1 Antibody Target
3.2.2.1. Biopanning with Protein A and Protein G Agarose Beads
3.2.2.2. Biopanning with Protein G Agarose Beads and Negative Selection Step
3.2.2.3. Biopanning with Protein A Agarose Beads and Negative Selection Step
3.3. Phage ELISA Binding Assay with Direct Target Coating
3.3.1. ELISA Assay against Streptavidin Target
3.3.2. ELISA Assay against Anti-Zika Virus NS1 Antibody Target
3.4. PCR Amplification of Phage DNA
3.4.1. DNA Quantification of PCR Templates
3.4.2. DNA Quantification of PCR Products
3.5. Agarose Gel Electrophoresis
3.6. Sequencing of Phage DNA

3. Results and Discussion

3.1. Surface Panning Procedure with Direct Target Coating

3.1.1. Biopanning against Streptavidin Target

This experiment corresponded to the positive control surface panning experiment with direct target coating using streptavidin as the target (**Experiment S1**) in two concentrations, 50 µg/mL for **S1.1** and 100 µg/mL for **S1.2**. The results of the titering of the amplified third round bacteriophage eluates are all specified in **Table 1**. An example of the plates obtained for the titering of the amplified third round phage eluate pool on this experiment is depicted on **Figure 25** (in Annex 3).

Table 1 *– Phage titers obtained for the third round amplified eluate pools of the surface-based panning procedure conducted against Streptavidin (Experiment S1).*

Experiment		Sample	Titering Dilution	Number of Plaques	pfu/mL
S1	S1.1	Amplified 3rd Round Phage Eluate Pool	10^9	45	4.5×10^{12}
			10^{10}	20	2×10^{13}
	S1.2	Amplified 3rd Round Phage Eluate Pool	10^9	70	7×10^{12}
			10^{10}	35	3.5×10^{13}

Analyzing the phage titering results obtained for **Experiment S1**, it can be concluded that a good amount of streptavidin-binding peptides were selected, since a significant amount of blue plaques could be found in all the corresponding titering plates. For **Experiment S1.1**, the plates obtained for the titering of the amplified third round phage eluate pool showed that this eluate had a concentration of approximately 10^{12}-10^{13} pfu/mL. Also, the lower titering dilution resulted in a higher amount of blue plaques and the higher titering dilution resulted in a lower amount of blue plaques, as it was expected. For **Experiment S1.2**, the plates obtained for the titering of the amplified third round phage eluate pool showed that this eluate also had a concentration of approximately 10^{12}-10^{13} pfu/mL, alike **S1.1**. Also, similarly to **S1.1**, the lower titering dilution resulted in a higher amount of blue plaques and the higher titering dilution resulted in a lower amount of blue plaques, as it was anticipated. Since a higher concentration of target was used in **S1.2** during the biopanning experiment, it was expected that the obtained eluate for this experiment would contain a higher amount of pfu/mL than the eluate of **S1.1**. Although both eluates showed similar concentrations, **S1.2** eluates still contained a slightly higher number of streptavidin-binding bacteriophages than **S1.1** eluates, which was the expected result. Therefore, the selection of streptavidin binding-peptides and the successful amplification of both eluates was achieved.

All titering plates for this experiment showed a significant number of colorless plaques, which was not predicted. The most likely explanation for white plaques is that the pool of phages became contaminated with an environmental M13-like phage during panning and amplification. Display of

foreign peptides as N-terminal fusions to the infectivity protein pIII, as in the PDT libraries, slightly attenuates infectivity of the library phage relative to wild-type M13. As a result, there is an *in vivo* selection for the contaminating phage during the amplification steps between rounds of panning. In the absence of a correspondingly strong *in vitro* binding selection during panning, even vanishingly small levels of contamination can result in a majority of the phage pool being a *wild-type* phage after 3 rounds of panning. This was not the case, since the obtained phage eluate pools yielded mostly blue plaques. Though, contamination is an extremely common problem with any phage display system, so only X-Gal/IPTG plates were used for all titering steps, and if white plaques were evident, only blue plaques were picked for sequencing. Also, since *wild-type* phages are preferentially amplified during the amplification steps, blue plaques for sequencing were picked directly after the third round elution step.

3.1.2. Biopanning against Anti-Zika Virus NS1 Antibody Target

This experiment corresponded to the surface panning experiment with direct target coating using the Anti-Zika Virus NS1 Antibody [B4] as the target (**Experiment Z1**). The results of the titering of the amplified third round bacteriophage eluates are all specified in **Table 2**. An example of the plates obtained for the titering of the amplified third round phage eluate pool on this experiment is depicted on **Figure 26** (in Annex 3).

Table 2 *– Phage titers obtained for the third round amplified eluate pools of the surface-based panning procedure conducted against the Anti-Zika Virus NS1 Antibody [B4] (Experiment Z1).*

Experiment	Sample	Titering Dilution	Number of Blue Plaques	pfu/mL
Z1	Amplified 3rd Round Phage Eluate Pool	10^{8}	210	2.1×10^{12}
		10^{9}	180	1.8×10^{13}
		10^{10}	350	3.5×10^{14}
		10^{11}	130	1.3×10^{15}

Analyzing the phage titering results obtained for **Experiment Z1**, it can be concluded that a good amount of [B4] antibody-binding peptides were selected, since a significant amount of blue plaques could be found in all the corresponding titering plates. The plates obtained for the titering of the amplified third round phage eluate pool showed that this eluate had a concentration of approximately 10^{12}-10^{15} pfu/mL, which means this experiment allowed the selection of a high number of bacteriophages with affinity for the Anti-Zika Virus NS1 Antibody [B4] and that their amplification was also successful. The lower titering dilutions resulted in a higher amount of blue plaques and the higher titering dilutions resulted in a lower amount of blue plaques, with only the 10^{10} titering dilution yielding an unexpected high number of blue plaques, which might be the result of possible minor errors

committed during the titering experiment. All titering plates for this experiment showed a significant number of colorless plaques, which was not predicted but can be explained as it was previously on **Chapter 3.1.1**.

In a typical round of biopanning, 2×10^{11} input phages are expected to react with the target, and between 10^3 and 10^7 total phages to be eluted off following washing. This corresponds to an enrichment of 10^4 to 10^8-fold per round. Since the library contained approximately 2×10^9 different clones, the eluted pool of phages should in theory be fully enriched in favor of binding sequences after only 2 or 3 rounds. Once this point is reached, further rounds of amplification and panning will result only in the selection of phages that have a growth advantage over the library phages. For example, vanishingly small levels of contaminating environmental *wild-type* phages (less than one part per billion) will completely overtake the pool if too many rounds of amplification are carried out, regardless of the strength of the *in vitro* selection. Therefore, it can be concluded that, since 10^{12}-10^{15} pfu/mL concentrations were achieved, this experiment allowed the selection of a high number of bacteriophages with affinity for the Anti-Zika Virus NS1 Antibody [B4].

3.2. Solution-Phase Panning with Affinity Bead Capture

3.2.1. Biopanning against Streptavidin Target

This experiment corresponded to the positive control solution-phase panning experiment with affinity bead capture using streptavidin as the target (**Experiment S2**), performed using Protein G agarose beads in all three rounds and a subtractive panning step. The results of the titering of the amplified third round bacteriophage eluates are all specified in **Table 3**. An example of the plates obtained for the titering of the amplified third round phage eluate pool on this experiment is depicted on **Figure 27** (in Annex 3).

Table 3 *– Phage titers obtained for the third round amplified eluate pools of the solution-phase panning procedure conducted against Streptavidin (Experiment S2), using Protein G agarose beads in all three rounds and a subtractive panning step.*

Experiment	Sample	Titering Dilution	Number of Blue Plaques	pfu/mL
S2	Amplified 3rd Round Phage Eluate Pool	10^9	50	5×10^{12}
		10^{10}	50	5×10^{13}

Analyzing the phage titering results obtained for **Experiment S2**, it can be concluded that a good amount of streptavidin-binding peptides were selected, since a significant amount of blue plaques could be found in all the corresponding titering plates. The plates obtained for the titering of the amplified third round phage eluate pool showed that this eluate had a concentration of approximately 10^{12}-10^{13} pfu/mL. Also, the lower titering dilution resulted in the same number of blue plaques as the higher titering dilution, which might be due to possible minor errors committed during

the phage titering experiment, possibly during the pipetting steps. However, both eluates showed good concentrations, which means streptavidin binding-peptides were selected and successfully amplified. All titering plates for this experiment showed a significantly lower number of colorless plaques, which indicates low level of contamination with *wild-type* phages.

3.2.2. Biopanning against Anti-Zika Virus NS1 Antibody Target

3.2.2.1. Biopanning with Protein A and Protein G Agarose Beads

This experiment corresponded to the solution-phase panning experiment with affinity bead capture using the Anti-Zika Virus NS1 Antibody [B4] as the target (**Experiment Z2**), and using Protein G and Protein A agarose beads. The results of the titering of the amplified third round bacteriophage eluates are all specified in **Table 4**. An example of the plates obtained for the titering of the amplified third round phage eluate pool on this experiment is depicted on **Figure 28** (in Annex 3).

Table 4 *– Phage titers obtained for the third round amplified eluate pools of the solution-phase panning procedure conducted against the Anti-Zika Virus NS1 Antibody [B4] (Experiment Z2), using Protein G and Protein A agarose beads.*

Experiment	Sample	Titering Dilution	Number of Plaques	pfu/mL
Z2	**Amplified 3rd Round Phage Eluate Pool**	**10^{8}**	85	8.5×10^{11}
		10^{9}	110	1.1×10^{13}
		10^{10}	60	6×10^{13}
		10^{11}	50	5×10^{14}

Analyzing the phage titering results obtained for **Experiment Z2**, it can be concluded that a good amount of [B4] antibody-binding peptides were selected, since a significant amount of blue plaques could be found in all the corresponding titering plates. The plates obtained for the titering of the amplified third round phage eluate pool showed that this eluate had a concentration of approximately 10^{11}-10^{14} pfu/mL, which means this experiment allowed the selection of a good number of bacteriophages with affinity for the Anti-Zika Virus NS1 Antibody [B4] and that their amplification was also successful. However, concentrations obtained in this experiment were slightly lower than the ones obtained for **Experiment Z1**. This was expected, since **Experiment Z1** selected a considerable amount of phages that non-specifically bound to the plate wells, leading to a higher pfu/mL value. The phage concentrations obtained for **Experiment Z2** were lower, since the use of agarose beads only allowed the selection of specific bacteriophages. The lower titering dilutions resulted in a higher amount of blue plaques and the higher titering dilutions resulted in a lower amount of blue plaques, with only the 10^{9} titering dilution yielding an unexpected high number of blue plaques, which is probably related to minor experimental errors. All titering plates for this experiment showed an

insignificant amount of colorless plaques, meaning the obtained phage pools had a low level of contamination with *wild-type* phages.

If the phage pools are not sufficiently diluted, the plaques will be confluent on the plate and it will look like there are no plaques at all (or a bluish tinge when using X-Gal plates). This was the case for some of the earliest titering plates, which lead to a posterior increase in the dilutions, in order to obtain well separated plaques. Occasionally after PEG precipitation, the phages will also clump and not dilute properly. This can result in plates containing too many plaques merged together. In order to avoid this, the phage was given sufficient time to resuspend after precipitation (more than 1 hour) and each dilution tube was vortexed very well (for approximately 10 seconds).

3.2.2.2. Biopanning with Protein G Agarose Beads and Negative Selection Step

This experiment corresponded to the solution-phase panning experiment with affinity bead capture using the Anti-Zika Virus NS1 Antibody [B4] (**Experiment Z3.1**) and the Anti-Zika Virus NS1 Antibody [D11] (**Experiment Z3.2**) as the targets (**Experiment Z3**), performed using Protein G agarose beads in all three rounds and a subtractive panning step. The results of the titering of the amplified third round bacteriophage eluates are all specified in **Table 5**. An example of the plates obtained for the titering of the amplified third round phage eluate pool on this experiment is depicted on **Figure 29** (in Annex 3).

Table 5 *– Phage titers obtained for the third round amplified eluate pools of the solution-phase panning procedure conducted against the Anti-Zika Virus NS1 Antibody [B4] (Experiment Z3.1) and against the Anti-Zika Virus NS1 Antibody [D11] (Experiment Z3.2), using Protein G agarose beads in all three rounds and a subtractive panning step.*

Experiment			Sample	Titering Dilution	Number of Plaques	pfu/mL
Z3	Z3.1	Z3.1.1	Amplified 3rd Round Phage Eluate Pool	10^8	50	5×10^{11}
				10^{10}	90	9×10^{13}
		Z3.1.2	Amplified 3rd Round Phage Eluate Pool	10^8	30	3×10^{11}
				10^{10}	10	1×10^{13}
	Z3.2	Z3.2.1	Amplified 3rd Round Phage Eluate Pool	10^8	100	1×10^{12}
				10^{10}	50	5×10^{13}
		Z3.2.2	Amplified 3rd Round Phage Eluate Pool	10^8	15	1.5×10^{11}
				10^{10}	25	2.5×10^{13}

Analyzing the phage titering results obtained for **Experiment Z3.1**, it can be concluded that a good amount of [B4] antibody-binding peptides were selected, since a significant amount of blue plaques could be found in all the corresponding titering plates. For **Experiment Z3.1.1**, the plates obtained for the titering of the amplified third round phage eluate pool showed that this eluate had a concentration of approximately 10^{11}-10^{13} pfu/mL, which means this experiment allowed the selection of a high number of bacteriophages with affinity for the Anti-Zika Virus NS1 Antibody [B4] and that

their amplification was also successful. However, the lower titering dilution resulted in a lower amount of blue plaques than the higher titering dilution, which was not expected and might be due to possible minor errors committed during the phage titering experiment. For **Experiment Z3.1.2**, the plates obtained for the titering of the amplified third round phage eluate pool showed that this eluate also had a concentration of approximately 10^{11}-10^{13} pfu/mL, which means this experiment also allowed the selection of a good number of bacteriophages with affinity for the Anti-Zika Virus NS1 Antibody [B4]. The lower titering dilution resulted in a higher amount of blue plaques and the higher titering dilution resulted in a lower amount of blue plaques, as it was predicted. Since a higher concentration of target was used in **Z3.1.1** during the biopanning experiment, it was expected that the obtained eluate for this experiment would contain a higher amount of pfu/mL than the eluate of **Z3.1.2**, which was achieved, as it can be observed in **Table 5**. All titering plates for this experiment showed an insignificant amount of colorless plaques, meaning the obtained phage pools had a low level of contamination with *wild-type* phages.

Analyzing the phage titering results obtained for **Experiment Z3.2**, it can be concluded that a good amount of [D11] antibody-binding peptides were selected, since a significant amount of blue plaques could be found in all the corresponding titering plates. For **Experiment Z3.2.1**, the plates obtained for the titering of the amplified third round phage eluate pool showed that this eluate had a concentration of approximately 10^{12}-10^{13} pfu/mL, which means this experiment allowed the selection of a high number of bacteriophages with affinity for the Anti-Zika Virus NS1 Antibody [D11] and that their amplification was also successful. The lower titering dilution resulted in a higher amount of blue plaques and the higher titering dilution resulted in a lower amount of blue plaques, as it was predicted. For **Experiment Z3.1.2**, the plates obtained for the titering of the amplified third round phage eluate pool showed that this eluate had a concentration of approximately 10^{11}-10^{13} pfu/mL, which means this experiment also allowed the selection of a good number of bacteriophages with affinity for the Anti-Zika Virus NS1 Antibody [D11]. However, the lower titering dilution resulted in a lower amount of blue plaques than the higher titering dilution, which was not expected and is probably related to minor experimental errors committed during this experiment. Since a higher concentration of target was used in **Z3.2.1** during the biopanning experiment, it was expected that the obtained eluate for this experiment would contain a higher amount of pfu/mL than the eluate of **Z3.2.2**, which was achieved, as it can be observed in **Table 5**. All titering plates for this experiment showed an insignificant amount of colorless plaques, meaning the obtained phage pools had again a low level of contamination with *wild-type* phages.

3.2.2.3. Biopanning with Protein A Agarose Beads and Negative Selection Step

This experiment corresponded to the solution-phase panning experiment with affinity bead capture using the Anti-Zika Virus NS1 Antibody [D11] as the target (**Experiment Z4**), performed using Protein A agarose beads in all three rounds and a subtractive panning step. The results of the titering of the amplified third round bacteriophage eluates are all specified in **Table 6**. An example of the plates obtained for the titering of the amplified third round phage eluate pool on this experiment is depicted on **Figure 30** (in Annex 3).

Table 6 *– Phage titers obtained for the third round amplified eluate pools of the solution-phase panning procedure conducted against the Anti-Zika Virus NS1 Antibody [D11] (Experiment Z4), using Protein A agarose beads in all three rounds and a subtractive panning step.*

Experiment		Sample	Titering Dilution	Number of Plaques	pfu/mL
Z4	Z4.1	Amplified 3rd Round Phage Eluate Pool	10^9	70	7×10^{12}
			10^{10}	15	1.5×10^{13}
	Z4.2	Amplified 3rd Round Phage Eluate Pool	10^9	25	2.5×10^{12}
			10^{10}	5	5×10^{12}

Analyzing the phage titering results obtained for **Experiment Z4**, it can be concluded that a good amount of [D11] antibody-binding peptides were selected, since a significant amount of blue plaques could be found in all the corresponding titering plates. For **Experiment Z4.1**, the plates obtained for the titering of the amplified third round phage eluate pool showed that this eluate had a concentration of approximately 10^{12}-10^{13} pfu/mL, which means this experiment allowed the selection of a great number of bacteriophages with affinity for the Anti-Zika Virus NS1 Antibody [D11] and that their amplification was successful. The lower titering dilutions resulted in a higher amount of blue plaques and the higher titering dilutions resulted in a lower amount of blue plaques, as it was predicted. For **Experiment Z4.2**, the plates obtained for the titering of the amplified third round phage eluate pool showed that this eluate had a concentration of approximately 10^{12} pfu/mL, which means this experiment also allowed the selection of a great number of bacteriophages with affinity for the Anti-Zika Virus NS1 Antibody [D11]. The lower titering dilutions resulted in a higher amount of blue plaques and the higher titering dilutions resulted in a lower amount of blue plaques, as it was again predicted. Since a higher concentration of target was used in **Z4.2** during the biopanning experiment, it was expected that the obtained eluate for this experiment would contain a higher amount of pfu/mL than the eluate of **Z4.1**, which was not achieved, since all the eluates presented similar concentrations of target-binding peptides. This might be explained by the possible selection of very high affinity target-binding peptides that were successfully amplified. All titering plates for this experiment showed an insignificant amount of colorless plaques, meaning the obtained phage pools had again a low level of contamination with *wild-type* phages.

3.3. Phage ELISA Binding Assay with Direct Target Coating

This assay was able to quickly determine whether a selected peptide clone had affinity for the target, without the need for an antibody specific for the target. This method does not allow for the quantification of the amount of target coated on the plate, and since the latter is present at a sufficiently high density to allow multivalent binding to the phage, this procedure did not determine whether the selected phage bound with high or low affinity. Thus, this protocol allowed only for the qualitative determination of relative binding affinities for a few selected clones in parallel. This method was also useful to distinguish between true target binding from binding to the plastic support, since the direct coating method of panning was one of the procedures used during this project.

Since the phage pool obtained by the end of the third round presented a very low concentration, it was necessary to amplify phage from both the eluted pool and individual phage plaques. An uncoated row of wells of the ELISA plate was also blocked (200 µL of blocking buffer) for use in the dilution of the phage stocks before their addition to the target-coated plate, since the dilutions need to be done firstly in separated blocked wells and then transferred to the target coated wells, to guarantee that phages are not absorbed onto the target during the course of performing dilutions, which would result in a sudden "falling-off" of signal as the phages are diluted.

3.3.1. ELISA Assay against Streptavidin Target

For the biopanning experiments performed against Streptavidin (**Experiment S1** and **Experiment S2**), the absorbance signals obtained by the readings of the plates of the ELISA assays are all specified on **Table 28** (in Annex 2). The registered absorbances are also graphically displayed on **Figure 7**.

Experiment S1 constituted a positive control surface panning experiment with direct target coating using streptavidin as the target, whereby on **Experiment S1.1** the plate well was coated with a solution of 50 µg/mL of streptavidin and on **Experiment S1.2** the plate well was coated with a solution of 100 µg/mL of the same target during biopanning.

Analyzing the signals obtained for the **S1.1** eluate pool sample, it can be observed that the well that was coated with 200 µg/mL of streptavidin yielded a higher signal than the well coated with 100 µg/mL of the same target, meaning that, as expected, this well contained a larger amount of bacteriophages that bound to streptavidin. The uncoated wells presented some background signal, which can be attributed to potential binding to the polystyrene surface of the plate wells. The **S1.1** phage clone sample generated similar results, with the uncoated wells presenting some background signal, and the higher concentration well showing a higher signal than the lower concentration well, which was also expected.

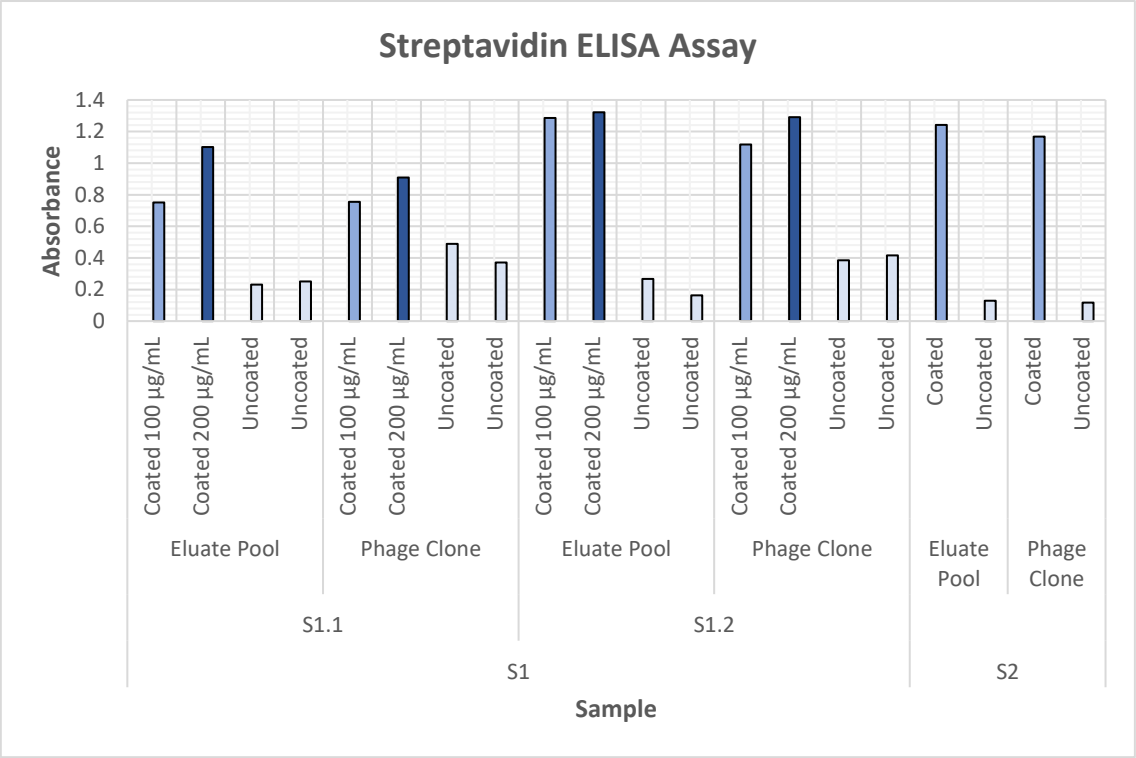

Figure 7 *– Absorbances registered on the ELISA assay conducted for the phage stocks amplified from the biopanning experiments performed against Streptavidin (Experiment S1 and Experiment S2).*

Then, when analyzing the signals obtained for the **S1.2** eluate pool sample, it can also be observed that the well coated with a higher concentration of streptavidin presented a slightly bigger signal than the well coated with a lower concentration, as it was predicted, meaning that the higher concentration well presented slightly more streptavidin-binding phages. The uncoated wells on this assay also yielded some background signal, which can be attributed to, again, possible binding to the plastic plate. For the **S1.2** phage clone sample, similar results were obtained, with the uncoated wells presenting some background signal and with the higher concentration well presenting a larger absorbance value, and consequently, more streptavidin-binding bacteriophages than the lower concentration well.

When comparing the results obtained for the **S1.1** and the **S1.2** experiments, it can be observed that the signals presented by the coated wells on **S1.2** are much larger than the signals presented by the coated wells on **S1.1**. This was expected, since during the biopanning experiment, the **S1.1** well was coated with a solution of 50 µg/mL of streptavidin, while the **S1.2** well was coated with double that concentration, a solution of 100 µg/mL of the same target. Thus, it was predicted that the eluates from **S1.2** would have a larger amount of streptavidin-binding phages then the eluates from **S1.1**, thus also leading to a higher ELISA signal from the **S1.2** samples and a lower signal for the **S1.1** samples.

All the uncoated wells presented some background signal. This can possibly be explained by the fact that, since the biopanning experiment was carried out against a polystyrene plate coated with the target (direct coating method), some peptides that specifically bound to the polystyrene surface were selected. These peptides will yield ELISA signals in the presence and absence of target, since the ELISA plate is also made of polystyrene, and are typically rich in aromatic residues (Phe, Tyr, Trp, His), which often alternate. The selection of plastic binders often occurs in the absence of a strong target preference for peptide sequences present in the library. So, in order to avoid the selection of these polystyrene-specific peptides, a bead capture protocol was then also experimented, where the phages reacted with the target in solution, and the phage-target complexes were then captured onto beads that specifically bound the target. Unbound phage was removed by extensively washing the beads in a microcentrifuge tube. Unlike polystyrene, neither the beads (crosslinked agarose) nor the microfuge tube (polypropylene) were likely to select specific peptide sequences from the library. Also, another disadvantage is that the direct target coating of a polystyrene plate can result in an inaccessible ligand binding site, either due to steric blocking or partial denaturation of the target along the surface.

Experiment S2 constituted a positive control solution-phase panning experiment with affinity bead capture using streptavidin as the target. When analyzing the signals obtained in the coated wells of the eluate pool and the phage clone samples, it can be observed that both wells yielded high absorbance signals, meaning that streptavidin-binding peptides were selected and present in a decent quantity in these samples. Also, the signals obtained for the uncoated wells decreased when compared to the uncoated wells of the previous samples, meaning that part of this background signal was actually caused by the selection of phage-displayed peptides that bound to the plastic surface. The significant diminution of this signal can be attributed to the use of the microcentrifuge tubes and the agarose beads in the biopanning experiment, instead of the polystyrene plates.

3.3.2. ELISA Assay against Anti-Zika Virus NS1 Antibody Target

For the biopanning experiments performed against the Anti-Zika Virus NS1 Antibodies (**Experiment Z1**, **Experiment Z2**, **Experiment Z3** and **Experiment Z4**), the absorbance signals obtained by the readings of the plates of the ELISA assays are all specified on **Table 29** (in Annex 2). The registered absorbances are also graphically displayed on **Figure 8**.

Experiment Z1 constituted a surface panning procedure with direct target coating using the Anti-Zika Virus NS1 Antibody [B4] as the target.

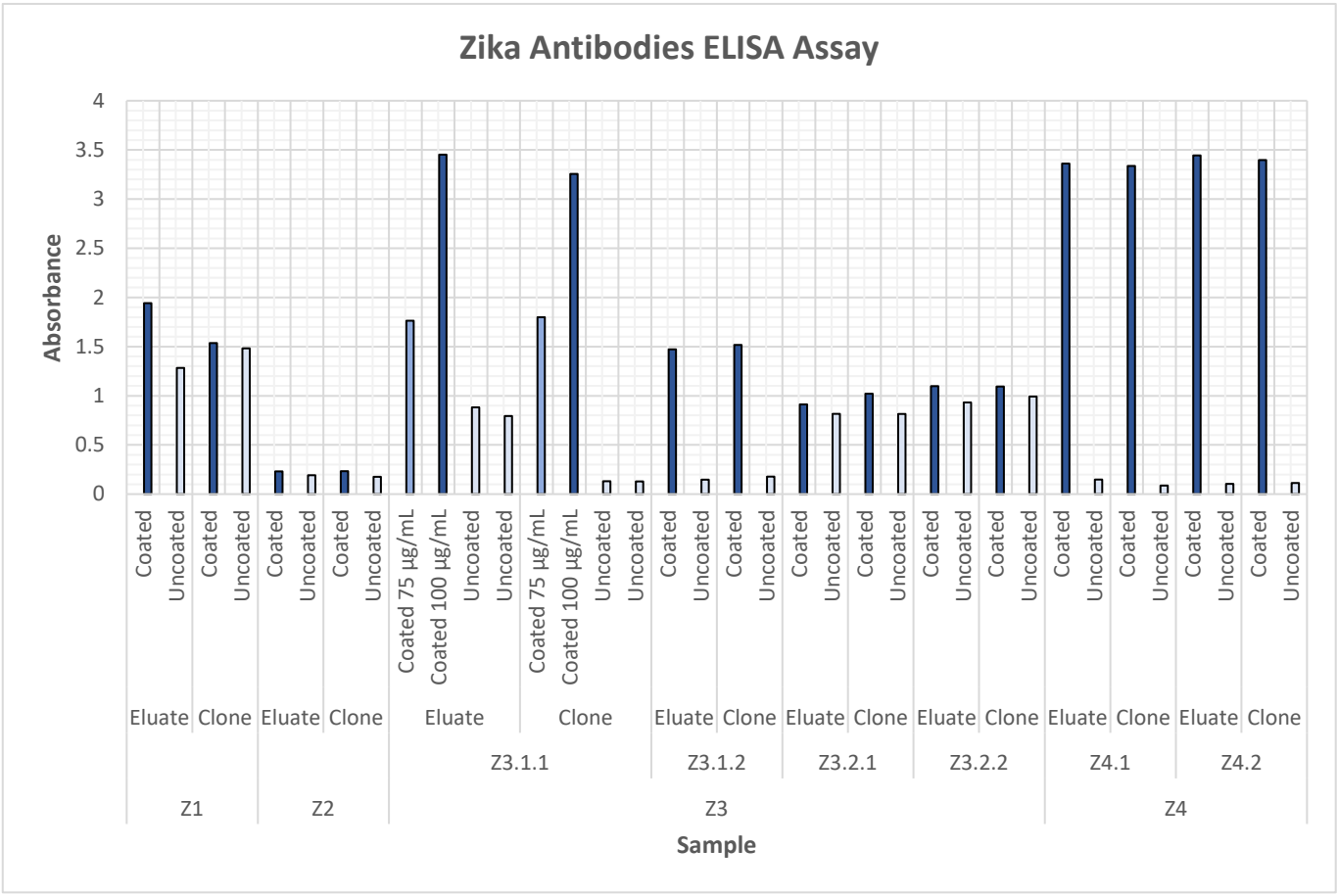

Figure 8 *– Absorbances registered on the ELISA assay conducted for the phage stocks amplified from the biopanning experiments performed against the Anti-Zika Virus NS1 Antibodies (Experiment Z1, Experiment Z2, Experiment Z3 and Experiment Z4).*

When analyzing the signals obtained for the **Z1** eluate pool sample, it can be observed that there is only a slight difference between the coated and uncoated wells, with the coated well presenting a slightly higher signal than the uncoated well. The **Z1** phage clone sample generated similar results, with the coated and uncoated wells generating almost the same signal, which was not expected. The signal presented by the uncoated wells might be possibly explained by the existance of some background signal, which can be attributed to potential non-specific interactions between the some of the phages and the plastic microtiter plate, meaning that the phages might have bound to the plastic support and not to the target, as it was previously explained on **Chapter 3.3.1**.

Experiment Z2 constituted a solution-phase based biopanning procedure with affinity bead capture, using both Protein A and Protein G agarose beads, and using the Anti-Zika Virus NS1 Antibody [B4] as the target. The solution-based biopanning results in enhanced accessibility of the ligand binding site to phage-displayed peptides, and prevents the partial denaturation of the target that happens when a plastic surface is used. When evaluating the signals yielded by both the eluate pool and the phage clone samples, it is detected that both coated and uncoated wells presented very low absorbance values, which was not expected. The uncoated wells show a lower signal for this

biopanning experiment, which means that using the agarose beads and the microcentrifuge tubes lessened the possible non-specific interactions between the bacteriophages and the plastic supports, since these were no longer used in the panning experiment. Both coated wells only show a slight absorbance signal, both for the eluate pool and the phage clone samples. This might be related to a possible low concentration of target-binding phages obtained by the end of the biopanning procedure, possibly due to minor errors committed during the performance of the experiment, possibly during the pipetting steps. Also, when characterizing phage clones by ELISA, it is difficult to add more than 10^{12} virions per 100 µL well. This corresponds to a phage concentration of only 16 nM. At this concentration, an unambiguously positive ELISA signal can only be observed if the binding affinity is in the micromolar range or better. Moreover, the iterative nature of phage selection permits identification of ligands with a broad range of affinities, from sub-nanomolar to 1 millimolar, so lower affinity ligands will not show a positive ELISA signal. In this case, maybe low affinity ligands were selected, and it might be necessary to increase the concentration of the selected ligand in the future, either by synthesizing a peptide corresponding to the selected sequence or by expressing the selected sequence as an N-terminal fusion to a smaller protein. Alternatively, a sandwich ELISA can be carried out in which the selected phage is immobilized and an excess of target is applied in the liquid phase. This procedure requires an antibody against the target protein, or some other means of detecting bound target protein. The wells are coated overnight with anti-M13 antibody (no HRP), washed and then serial dilutions of each phage clone (one clone per row) are added. After 1 hour, unbound phage is washed away and an excess of target protein (0.1 - 1 µM) in TBST is added. Then, incubation for 1-2 hours at room temperature follows, unbound target is washed away and then bound target is detected with an enzyme-linked antibody. Both these alternatives should be experimented in the future in order to increase the low ELISA signals.

Experiment Z3 constituted a solution-phase based biopanning procedure with affinity bead capture, using Protein G agarose beads and a negative selection step, using the anti-Zika NS1 [B4] antibody as the target in two concentrations in **Experiment Z3.1**, and the anti-Zika NS1 [D11] antibody as the target in two concentrations in **Experiment Z3.2**.

When examining the signals yielded by the eluate pool wells for **Z3.1.1**, the higher concentration sample in the biopanning **Z3.1**, it can be observed that the well coated with a higher concentration of target (100 µg/mL) produced a higher signal than the well coated with a lower concentration of the antibody (75 µg/mL), which was expected, since the first well was projected to have more target-binding phages then the second well. Some background signal can also be detected in the uncoated wells, but not to a great extent. When analyzing the signals yielded by the phage clone wells, similar results were obtained. The well coated with a higher concentration of target yielded a higher signal than the well coated with a lower concentration, as it was anticipated. Although, the

uncoated wells showed lower background signal for the phage clone wells than the eluate pool wells, which might be explained by the randomly selected phage clone presenting very low affinity to the plastic support. When examining the signals yielded by the sample wells for **Z3.1.2**, the lower concentration sample in the biopanning **Z3.1**, it can be observed that the eluate pool and the phage clone coated wells yielded a considerable signal, but still lower than the coated wells for **Z3.1.1**. This was already expected, since these samples were predicted to contain less target-binding phages than the samples on the previous experiment. During the biopanning experiment, the total concentration of anti-Zika antibody [B4] was 50 µg/mL for **Z3.1.1** and half that amount (25 µg/mL) for **Z3.1.2**, meaning that the samples in **Z3.1.1** were expected to have a higher concentration of target-binding phages than the samples in **Z3.1.2**. The uncoated wells also presented a low background signal.

The signals yielded by the sample wells for **Z3.2.1**, the higher concentration sample in the biopanning **Z3.2** show that, for both the eluate pool and the phage clone samples, the coated wells presented considerable signals, but the uncoated wells also presented background signal, comparable to the signal yielded by the sample wells. This might be explained by the possible selection of target-binding peptides that also presented affinity to the plastic support used in the ELISA experiment. The signals yielded by the sample wells for **Z3.2.2**, the lower concentration sample in the biopanning **Z3.2** show that again, for both the eluate pool and the phage clone samples, the coated wells presented significant signals, but once more comparable to the signal yielded by the uncoated wells. This background signal might be yet again explained by the possible selection of target-binding peptides that also presented affinity to the plastic support. It can also be observed that the signals obtained for the coated wells in **Z3.2.2** are slightly higher than the signals presented by the coated wells in **Z3.2.1**, which was not expected. Since the total concentration of anti-Zika antibody [D11] was 50 µg/mL for **Z3.2.1** and 25 µg/mL for **Z3.2.2** during the biopanning experiment, it was expected that the second sample wells would yield a lower signal than the first sample wells, since the **Z3.2.1** sample was expected to have double the target-binding phages than the **Z3.2.2** sample. Possible minor errors made during the experiments might be in the origin of these results.

When comparing the signals yielded by the coated wells in **Experiment Z3.1** with the signals yielded by the ones of **Experiment Z3.2**, it can be observed that all the signals obtained for the coated wells of the biopanning experiment performed with the [B4] Zika antibody (**Z3.1**) are significantly higher than the signals obtained for the coated wells of the biopanning experiment performed with the [D11] Zika antibody (**Z3.2**). This means that **Z3.1** samples contained more target-binding phages than **Z3.2** samples, meaning the commercial phage library used possibly contained more [B4] specific peptides than [D11] specific peptides. Also, since Protein G agarose beads were used, these might have more affinity to the [B4] antibody, then being more prone to selecting more [B4] binding peptides.

Thus, the biopanning experiment conducted against [B4] was probably able to select more target-binding bacteriophages than the experiment conducted against [D11].

Experiment Z4 constituted a solution-phase based biopanning procedure with affinity bead capture, using Protein A agarose beads and a negative selection step, and using the Anti-Zika Virus NS1 Antibody [D11] as the target in two different concentrations.

When examining the signals yielded by the samples in **Z4.1**, the lower concentration sample in the biopanning, it can be observed that, for both the eluate pool and the phage clone samples, the coated wells yielded a significantly higher absorbance signal than the uncoated wells, being the background signal almost non-existent. Then, it can be concluded that the samples contained a large amount of target-binding phages. When examining the signals yielded by the samples in **Z4.2**, the higher concentration sample in the biopanning, the same can be observed, with the coated wells yielding a significantly higher absorbance signal than the uncoated wells, meaning these samples also contained a large amount of target-binding phages. However, it was expected that samples in **Z4.2** to have yielded a higher signal than the samples in **Z4.1**, since a higher concentration of target was used for **Z4.2** and a lower concentration for **Z4.1** in the biopanning experiment. However, both samples showed considerably high comparable signals, which means that the library probably contained a large amount of [D11] binding peptides that were selected, that possibly presented very high affinity to the target, leading to the high signals yielded by all the samples. Also, since Protein A agarose beads were used, these might have more affinity to the [D11] antibody, then being more prone to selecting more [D11] binding peptides.

3.4. PCR Amplification of Phage DNA

3.4.1. DNA Quantification of PCR Templates

All DNA templates chosen for PCR amplification corresponded to ssDNA (single-stranded DNA) sequences obtained from the previously selected bacteriophages. Samples absorbance was measured at 260 nm, in order to determine the DNA concentration in the samples (A_{260} ssDNA = 33 µg/mL), and at 230 and 280 nm, in order to determine the samples purity, using the ratio of the absorbance at 260 and 280 nm ($A_{260/280}$) and at 260 and 230 nm ($A_{260/230}$) to assess the purity of the phage nucleic acids. Values of $A_{260/280}$ should be around 1.8 for pure DNA. $A_{260/230}$ values are usually higher for this same nucleic acid, being around 2.0-2.2 for pure DNA.

The measured ssDNA absorbances and corresponding concentrations and purity ratios for the 10 clones and the eluate pool chosen in **Experiment S1** are all specified in **Table 30** (in Annex 2).

Analyzing the samples measured concentrations, it can be observed that all clones presented concentrations of ssDNA between, approximately, 50 and 90 µg/mL, being the mean 74.07 µg/mL. Thus, it can be concluded that the DNA extraction from the selected bacteriophages was successful,

with all samples presenting considerable amounts of ssDNA. When analyzing the purity ratios for these samples, it can be noted that the purity ratios for $A_{260/280}$ are a bit lower than the expected 1.8 value for pure DNA. This indicates that the obtained DNA is not pure, with the low ratio probably being the result of a contaminant absorbing at 280 nm or less. These low ratios might have been caused by the presence of a reagent associated with the DNA extraction. The purity ratios for $A_{260/230}$ are a bit higher than the expected 2.0-2.2 values. This high ratio might have been the result of possible minor errors committed during the experiment, including the blank measurement being made on a dirty pedestal or the use of an inappropriate solution for the blank measurement.

The measured ssDNA absorbances and corresponding concentrations and purity ratios for the 10 clones and the eluate pool chosen in **Experiment S2** are all specified in **Table 31** (in Annex 2).

Analyzing the samples measured concentrations, it can be observed that all clones presented concentrations of ssDNA between, approximately, 105 and 135 µg/mL, being the mean 114.54 µg/mL. Thus, it can be concluded that the DNA extraction from the selected bacteriophages was successful, with all samples presenting considerable amounts of ssDNA. Also, it can also be determined that the DNA concentrations obtained for the **S2** clones were notably higher than the ones obtained for the **S1** clones, meaning this biopanning experiment allowed to obtain a higher quantity of target-binding bacteriophages and, consequently, a higher quantity of phage ssDNA. When analyzing the purity ratios for these samples, it can be noted that the purity ratios for $A_{260/280}$ are also lower than the expected 1.8 value for pure DNA. This indicates that the obtained DNA is not pure, with the low ratio probably being the result contamination of the sample by a reagent associated with the DNA extraction. The purity ratios for $A_{260/230}$ are considerably lower than the expected 2.0-2.2 values. This indicates that the obtained DNA is not pure, with the low ratio probably being the result of a contaminant absorbing at 230 nm or less. These low ratios might have been caused by contamination of the sample with reagents associated with the DNA extraction. Also, these low ratios might also be related to possible minor errors committed during the extraction procedure.

The measured ssDNA absorbances and corresponding concentrations and purity ratios for the 10 clones chosen in **Experiment Z1** are all specified in **Table 32** (in Annex 2).

Analyzing the samples measured concentrations, it can be observed that all clones presented concentrations of ssDNA between, approximately, 20 and 160 µg/mL, being the mean 68.739 µg/mL. Thus, it can be concluded that the DNA extraction from the selected bacteriophages was successful, with all samples presenting considerable amounts of ssDNA. When analyzing the purity ratios for these samples, it can be noted that the purity ratios for $A_{260/280}$ are a bit lower than the expected 1.8 value for pure DNA. This indicates that the obtained DNA is not pure, with the low ratio probably caused by the presence of residues of a reagent associated with the DNA extraction. The purity ratios for $A_{260/230}$ are a bit higher than the expected 2.0-2.2 values, specially for clones Z1.6, Z1.7 and Z1.8. These high

ratios might have been a result of the blank measurement being made on a dirty pedestal or by the use of an inappropriate solution for the blank measurement.

The measured ssDNA absorbances and corresponding concentrations and purity ratios for the 10 clones chosen in **Experiment Z2** are all specified in **Table 33** (in Annex 2).

Analyzing the samples measured concentrations, it can be observed that all clones presented concentrations of ssDNA between, approximately, 10 and 30 µg/mL, being the mean 18.70 µg/mL. Thus, it can be concluded that the DNA extraction from the selected bacteriophages was successful, with all samples presenting considerable amounts of ssDNA. Also, it can also be determined that the DNA concentrations obtained for the **Z2** clones were notably lower than the ones obtained for the **Z1** clones, meaning the first biopanning experiment allowed to obtain a higher quantity of phage ssDNA than the second experiment. When analyzing the purity ratios for these samples, it can be noted that the purity ratios for $A_{260/280}$ are around the expected 1.8 value for pure DNA, with some samples presenting even a higher value. However, the purity ratios for $A_{260/230}$ are considerably lower than the expected 2.0-2.2 values. This indicates that the obtained DNA is not pure, with the low ratio probably being the result of contamination of the sample by reagents associated with the DNA extraction. Also, these low ratios might also be related to possible minor errors committed during the extraction procedure.

The measured ssDNA absorbances and corresponding concentrations and purity ratios for the 10 clones and the eluate pool chosen in **Experiment Z3.1** are all specified in **Table 34** (in Annex 2).

Analyzing the samples measured concentrations, it can be observed that all clones presented concentrations of ssDNA between, approximately, 2 and 30 µg/mL, being the mean 15.67 µg/mL. Thus, it can be concluded that the DNA extraction from the selected bacteriophages was successful, with all samples presenting good amounts of ssDNA. Also, it can also be determined that the DNA concentrations obtained for the **Z3.1** clones were similar to the ones obtained for the **Z2** clones and notably lower than the ones obtained for the **Z1** clones. When analyzing the purity ratios for these samples, it can be noted that the purity ratios for $A_{260/280}$ are around the expected 1.8 value for pure DNA, with some samples presenting even a higher value. The purity ratios for $A_{260/230}$ are considerably lower than the expected 2.0-2.2 values for samples Z.3.1.6 to Z3.1.E. This indicates that the obtained DNA for these samples is not pure, with the low ratio probably being the result of contamination with reagents associated with the DNA extraction or of possible minor errors committed during the extraction procedure. Samples Z3.1.1 to Z3.1.5 presented the expected 2.0-2.2 values for the $A_{260/230}$ ratio, which indicates that the obtained DNA for these samples can be considered pure.

The measured ssDNA absorbances and corresponding concentrations and purity ratios for the 10 clones and the eluate pool chosen in **Experiment Z3.2** are all specified in **Table 35** (in Annex 2).

Analyzing the samples measured concentrations, it can be observed that all clones presented concentrations of ssDNA between, approximately, 6 and 25 µg/mL, being the mean 13.28 µg/mL. Thus, it can be concluded that the DNA extraction from the selected bacteriophages was successful, with all samples presenting good amounts of ssDNA. Also, it can also be determined that the DNA concentrations obtained for the **Z3.2** clones were similar to the ones obtained for the **Z2** and **Z3.1** clones and notably lower than the ones obtained for the **Z1** clones. Thus, it can be concluded that the first biopanning experiment allowed to obtain a higher quantity of phage ssDNA than the second and the third experiments. When analyzing the purity ratios for these samples, it can be noted that the purity ratios for $A_{260/280}$ are around the expected 1.8 value for pure DNA, with some samples presenting even a higher value. The purity ratios for $A_{260/230}$ are considerably lower than the expected 2.0-2.2 values for samples Z.3.2.6 to Z3.2.E again. This indicates that the obtained DNA for these samples is not pure, with the low ratio probably being the result of contamination of the sample with reagents associated with the DNA extraction. Also, these low ratios might also be due to possible minor errors committed during the extraction procedure. Values for the $A_{260/230}$ ratio presented by samples Z3.2.2 to Z3.2.5 were only a bit lower than the expected value. Only the sample Z3.2.1 presented a purity ratio within the expected range, which indicates that only the obtained DNA from this sample can be considered pure.

The measured ssDNA absorbances and corresponding concentrations and purity ratios for the 10 clones chosen in **Experiment Z4** are all specified in **Table 36** (in Annex 2).

Analyzing the samples measured concentrations, it can be observed that all clones presented concentrations of ssDNA between, approximately, 5 and 25 µg/mL, being the mean 11.67 µg/mL. Thus, it can be concluded that the DNA extraction from the selected bacteriophages was successful, with all samples presenting good amounts of ssDNA. Also, it can also be determined that the DNA concentrations obtained for the **Z4** clones were similar to ones obtained for the **Z2**, **Z3.1** and **Z3.2** clones and notably lower than the ones obtained for the **Z1** clones, meaning that the first biopanning experiment was the one that allowed to obtain a higher quantity of phage ssDNA. When analyzing the purity ratios for these samples, it can be noted that the purity ratios for $A_{260/280}$ are around the expected 1.8 value for pure DNA, with some samples presenting even a higher value. The purity ratios for $A_{260/230}$ are considerably lower than the expected 2.0-2.2 values. This indicates that the obtained DNA is not pure, with the low ratio probably being the result of contamination of the sample with reagents associated with the DNA extraction. Also, these low ratios might also be due to possible minor errors committed during the extraction procedure.

3.4.2. DNA Quantification of PCR Products

All DNA sequences obtained after PCR amplification corresponded to dsDNA (double-stranded DNA). Samples absorbance was measured again at 260 nm, in order to determine the DNA concentration in the samples (A260 dsDNA = 50 µg/mL), and at 230 and 280 nm, in order to determine the samples purity.

The measured dsDNA absorbances and corresponding concentrations and purity ratios for the 10 clones and eluate pool from **Experiment S1** after PCR amplification by the **PCR Experiment 1** and after purification by the technique described in **Chapter 2.6.5.2** are all specified in **Table 37** (in Annex 2). A comparison of the DNA concentrations obtained before PCR amplification and after PCR amplification and purification for the **Experiment S1** clones is graphically depicted in **Figure 9**.

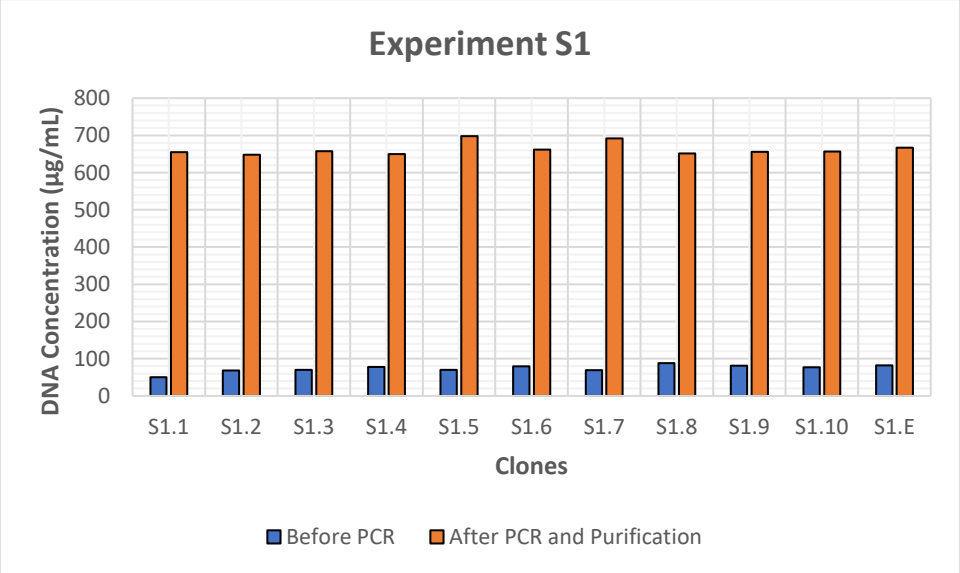

***Figure 9** – DNA concentrations obtained before PCR amplification and after PCR amplification and purification for the Experiment S1 clones.*

Analyzing the samples measured concentrations, it can be observed that all clones presented concentrations of dsDNA between, approximately, 650 and 700 µg/mL, being the mean 663 µg/mL. Thus, it can be concluded that the amplification of the extracted sequences from the selected bacteriophages was successful, with all samples presenting very high amounts of dsDNA. When analyzing the purity ratios for these samples, it can be noted that the purity ratios for $A_{260/280}$ are still lower than the expected 1.8 value for pure DNA. This indicates that the obtained DNA is not pure, with the low ratio probably being the result of contamination of the samples by a reagent associated with the purification. The purity ratios for $A_{260/230}$ are considerably lower than the expected 2.0-2.2 values, meaning that the obtained DNA is not pure, with the low ratio probably being again the result of contamination with reagents associated with the DNA purification. Thus, it can be concluded that the

purification method in this case was not successful, since both purity ratios are not within the expected values for pure DNA. However, there was no apparent loss of DNA caused by the use of the PCR purification kit. By analysis of **Figure 9**, it can be accessed that the amplification of the DNA templates was successful, since there was a considerable increase in the DNA concentration of all samples.

The measured dsDNA absorbances and corresponding concentrations and purity ratios for the 10 clones and eluate pool from **Experiment S2** after PCR amplification by the **PCR Experiment 1** and after purification by the technique described in **Chapter 2.6.5.2** are all specified in **Table 38** (in Annex 2). A comparison of the DNA concentrations obtained before PCR amplification and after PCR amplification and purification for the **Experiment S2** clones is graphically depicted in **Figure 10**.

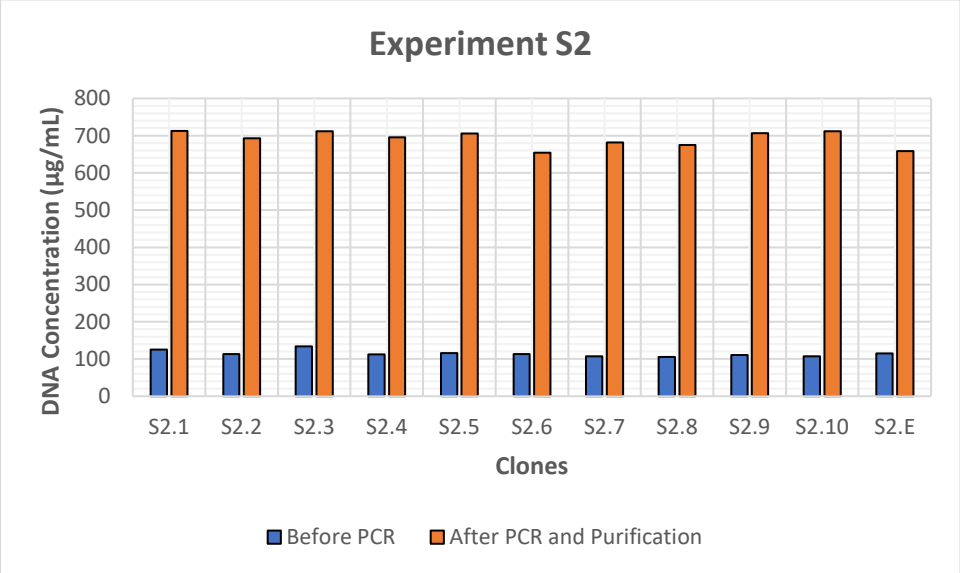

***Figure 10** – DNA concentrations obtained before PCR amplification and after PCR amplification and purification for the Experiment S2 clones.*

Analyzing the samples measured concentrations, it can be observed that all clones presented concentrations of dsDNA between, approximately, 650 and 715 µg/mL, being the mean 691.45 µg/mL. Thus, it can be concluded that the amplification of the extracted sequences from the selected bacteriophages was successful, with all samples presenting very high amounts of dsDNA. When analyzing the purity ratios for these samples, it can be noted that the purity ratios for $A_{260/280}$ are still lower than the expected 1.8 value for pure DNA. This indicates that the obtained DNA is not pure, with the low ratio probably being the result of contamination of the samples by reagents associated with the purification. The purity ratios for $A_{260/230}$ are still considerably lower than the expected 2.0-2.2 values, with only sample S2.9 presenting a higher value than expected, meaning that the obtained DNA is not pure, with the low ratio probably being the result of contamination of the sample with reagents associated with the DNA purification. The high ratio presented by sample S2.9 might be the result of

the measurement being made on a possibly dirty pedestal. Thus, it can be concluded that the purification method in this case was not successful, since both purity ratios are not within the expected values for pure DNA. Though, there was no apparent loss of DNA caused by the use of the PCR Clean-Up Kit. By analysis of **Figure 10**, it can be accessed that the amplification of the DNA templates was successful, since there was a considerable increase in the DNA concentration of all samples. Both **Experiment S1** and **Experiment S2** samples presented similar concentrations after the PCR amplification, meaning this process was successful for both streptavidin experiments.

The measured dsDNA absorbances and corresponding concentrations and purity ratios for the 10 clones from **Experiment Z1** after PCR amplification by the **PCR Experiment 1** and after purification by the technique described in **Chapter 2.6.5.1** are all specified in **Table 39** (in Annex 2). The measured dsDNA absorbances and corresponding concentrations and purity ratios for the 10 clones from **Experiment Z1** after PCR amplification by the **PCR Experiment 2** and after purification by the technique described in **Chapter 2.6.5.2** are all specified in **Table 40** (in Annex 2). The measured dsDNA absorbances and corresponding concentrations and purity ratios for the 10 clones from **Experiment Z1** after PCR amplification by the **PCR Experiment 3** and after purification by the technique described in **Chapter 2.6.5.2** are all specified in **Table 41** (in Annex 2). A comparison of the DNA concentrations obtained before PCR amplification and after PCR amplification by **PCR Experiment 1**, **PCR Experiment 2** and **PCR experiment 3** and purification for the **Experiment Z1** clones is graphically depicted in **Figure 11**.

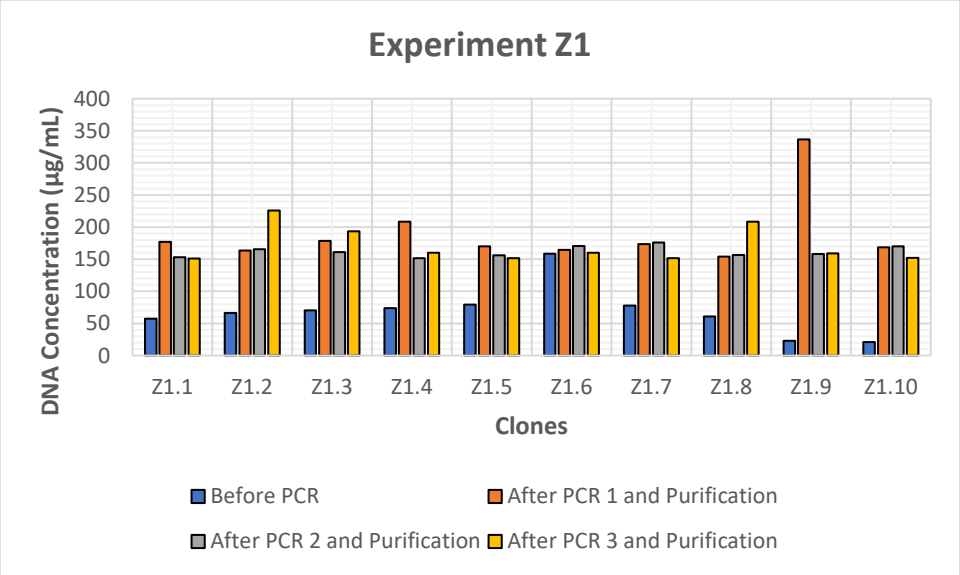

***Figure 11** – DNA concentrations obtained before PCR amplification and after PCR amplification by PCR Experiment 1, PCR Experiment 2 and PCR experiment 3 and purification for the Experiment Z1 clones.*

Analyzing the samples measured concentrations for the first 5 clones from **Experiment Z1** after PCR amplification by the **PCR Experiment 1** and after purification by the **Protocol 1** described in **Chapter 2.6.5.1**, it can be observed that all clones presented concentrations of dsDNA between, approximately, 160 and 210 µg/mL, being the mean 179.5 µg/mL. Thus, it can be concluded the amplification of the sequences by **PCR Experiment 1** was successful, with all samples presenting very high amounts of dsDNA. When analyzing the purity ratios for these samples, it can be noted that the purity ratios for $A_{260/280}$ are a still a bit lower than the expected 1.8 value for pure DNA. This indicates that the obtained DNA is not pure, with the low ratio probably being caused by contamination of the samples with a reagent associated with the ethanol purification method. On the other hand, the purity ratios for $A_{260/230}$ turned considerably lower than the expected 2.0-2.2 values, meaning that the obtained DNA is not pure, with the low ratio probably being again the result of contamination of the samples with reagents associated with the ethanol DNA purification method. Thus, it can be concluded that the ethanol purification method in **Protocol 1** was not successful, since both purity ratios are not within the expected values for pure DNA. Though, there was no apparent loss of DNA caused by this purification method.

Analyzing the samples measured concentrations for the last 5 clones from **Experiment Z1** after PCR amplification by the **PCR Experiment 1** and after purification by the **Protocol 2** described in **Chapter 2.6.5.1**, it can be observed that all clones presented concentrations of dsDNA between, approximately, 150 and 340 µg/mL, being the mean 199.4 µg/mL. Thus, it can be concluded the amplification of the sequences by **PCR Experiment 1** was successful, with all samples presenting very high amounts of dsDNA. When analyzing the purity ratios for these samples, it can be noted that the purity ratios for $A_{260/280}$ are a still a bit lower than the expected 1.8 value for pure DNA. This low ratio is probably caused by the contamination of the samples with a reagent associated with the isopropanol purification method. On the other hand, the purity ratios for $A_{260/230}$ turned considerably lower than the expected 2.0-2.2 values, with the low ratio again probably being the result of contamination of the samples with reagents associated with the isopropanol DNA purification method. Thus, it can be concluded that the ethanol purification method in **Protocol 2** was not successful, since both purity ratios are not within the expected values for pure DNA. However, there was no apparent loss of DNA caused by this purification method. Also, the second purification method allowed the yield of higher DNA concentrations for the last 5 clones when in comparison with the concentrations obtained for the first 5 clones after the first purification method. Thus, it can be concluded that the **Protocol 1** purification method was more effective than the **Protocol 2** purification method.

Analyzing the samples measured concentrations for the clones from **Experiment Z1** after PCR amplification by the **PCR Experiment 2** and after purification by the technique described in **Chapter 2.6.5.2**, it can be observed that all clones presented concentrations of dsDNA between, approximately,

150 and 180 µg/mL, being the mean 161.8 µg/mL. Thus, it can be concluded the amplification of the sequences by **PCR Experiment 2** was also successful, with all samples presenting very high amounts of dsDNA. However, the amplification by **PCR Experiment 1** allowed to obtain a higher concentration of DNA by the samples, meaning the first PCR experiment was more effective. The use of two different primer concentrations in the **PCR Experiment 2** (250 nM for the first 5 clones and 500 nM for the last 5 clones) did not seem to influence the obtained DNA concentrations, with all samples presenting similar final concentrations. When analyzing the purity ratios for these samples, it can be noted that the purity ratios for $A_{260/280}$ are a still a bit lower than the expected 1.8 value for pure DNA, probably being caused by contamination of the samples with a reagent associated with the purification method. On the other hand, the purity ratios for $A_{260/230}$ turned considerably lower than the expected 2.0-2.2 values, probably being the result of contamination with reagents associated with the DNA purification method again. Thus, it can be concluded that the purification method described in **Chapter 2.6.5.2** was not successful in this case, since both purity ratios are not within the expected values for pure DNA. Although there was no apparent loss of DNA caused by this purification method, it seems that the methods described in **Chapter 2.6.5.1** were more effective than this PCR Clean-Up Kit, since they allowed higher concentrations of DNA to be obtained.

Analyzing the samples measured concentrations for the clones from **Experiment Z1** after PCR amplification by the **PCR Experiment 3** and after purification by the technique described in **Chapter 2.6.5.2**, it can be observed that all clones presented concentrations of dsDNA between, approximately, 150 and 230 µg/mL, being the mean 171.3 µg/mL. Thus, it can be concluded the amplification of the sequences by **PCR Experiment 3** was also successful, with all samples presenting very high amounts of dsDNA. However, the amplification by **PCR Experiment 1** allowed to obtain a higher concentration of DNA by the samples, meaning this first PCR experiment was still more effective. So, it can be concluded that the inclusion of a Hot-Start step in the beginning of the **PCR Experiment 3** did not lead to an increase of the final obtained DNA concentrations. Also, by comparing the DNA concentrations, it can be concluded that **PCR Experiment 3** was more effective than **PCR Experiment 2**. When analyzing the purity ratios for these samples, it can be noted that the purity ratios for $A_{260/280}$ are a still a bit lower than the expected 1.8 value for pure DNA. On the other hand, the purity ratios for $A_{260/230}$ turned considerably lower than the expected 2.0-2.2 values. Thus, it can be concluded that the purification method described in **Chapter 2.6.5.2** was not successful in this case, since both purity ratios are not within the expected values for pure DNA and were probably caused by the presence of contaminants related to reagents used during this purification method. Although there was no apparent loss of DNA caused by this purification method, it seems that the methods described in **Chapter 2.6.5.1** were more effective than this PCR Clean-Up Kit, since they allowed higher concentrations of DNA to be obtained.

By analysis of **Figure 11**, it can be determined that all three PCR experiments allowed the amplification of the DNA samples. However, it can be concluded that **PCR Experiment 1** was still the most effective, allowing to achieve a mean DNA concentration after purification of 189.45 µg/mL. Thus, the temperature and timing conditions used in this experiment, as well as the reagents concentrations, were the most effective when amplifying the phage DNA.

The measured dsDNA absorbances and corresponding concentrations and purity ratios for the 10 clones from **Experiment Z2** after PCR amplification by the **PCR Experiment 1** and after purification by the technique described in **Chapter 2.6.5.2** are all specified in **Table 42** (in Annex 2). A comparison of the DNA concentrations obtained before PCR amplification and after PCR amplification and purification for the **Experiment Z2** clones is graphically depicted in **Figure 12**.

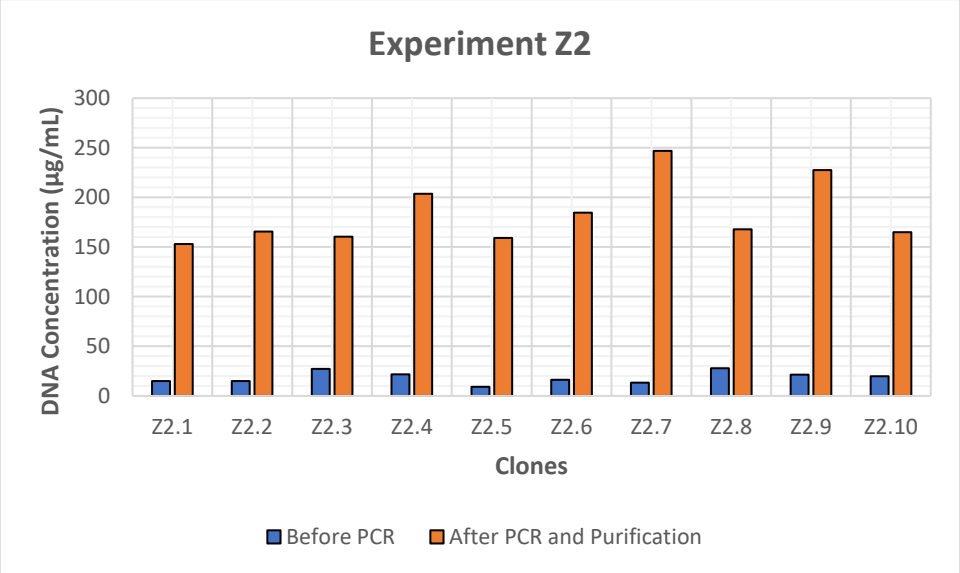

***Figure 12** – DNA concentrations obtained before PCR amplification and after PCR amplification and purification for the Experiment Z2 clones.*

Analyzing the samples measured concentrations, it can be observed that all clones presented concentrations of dsDNA between, approximately, 150 and 250 µg/mL, being the mean 183.35 µg/mL. Thus, it can be concluded the amplification of the extracted sequences from the selected bacteriophages was successful, with all samples presenting very high amounts of dsDNA. Also, it can be observed that the concentrations obtained in this experiment are similar to the ones obtained by all three PCR experiments for the Z1 clones, meaning **Experiment Z2** was also had a successful DNA amplification. When analyzing the purity ratios for these samples, it can be noted that the purity ratios for $A_{260/280}$ got considerably lower than the expected 1.8 value for pure DNA. This indicates that the obtained DNA is not pure and that there was a loss in purity, with the low ratio probably being the result of contamination of the samples with reagents used in the PCR Clean-Up Kit. The purity ratios

for $A_{260/230}$ are still considerably lower than the expected 2.0-2.2 values. Thus, it can be concluded that the purification method in this case was not successful, since both purity ratios are not within the expected values for pure DNA, with even a loss of purity highlighted by comparison of the $A_{260/280}$ ratios. Though, there was no apparent loss of DNA caused by the use of the PCR purification kit. By analysis of **Figure 12**, it can be accessed that the amplification of the DNA templates was successful, since there was a considerable increase in the DNA concentration of all samples. Both **Experiment Z1** and **Experiment Z2** samples presented similar concentrations after the PCR amplification, meaning this process was successful for both anti-Zika antibody experiments.

The measured dsDNA absorbances and corresponding concentrations and purity ratios for the 10 clones from **Experiment Z3.1** after PCR amplification by the **PCR Experiment 1** and before purification are all specified in **Table 43** (in Annex 2). The measured dsDNA absorbances and corresponding concentrations and purity ratios for the 10 clones from **Experiment Z3.1** after PCR amplification by the **PCR Experiment 1** and after purification by the technique described in **Chapter 2.6.5.2** are all specified in **Table 44** (in Annex 2). A comparison of the DNA concentrations obtained before PCR amplification and after PCR amplification before and after purification for the **Experiment Z3.1** clones is graphically depicted in **Figure 13**.

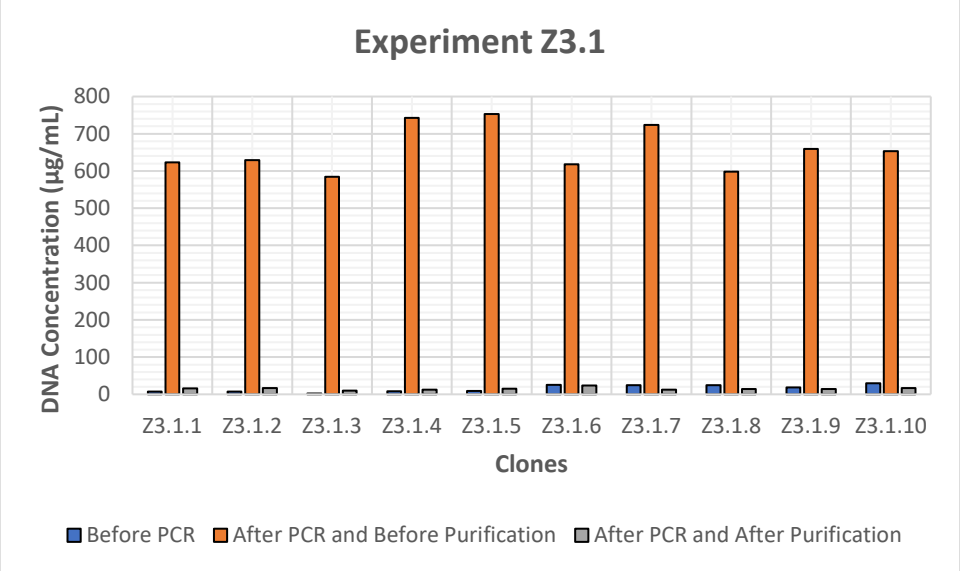

***Figure 13** – DNA concentrations obtained before PCR amplification and after PCR amplification before and after purification for the Experiment Z3.1 clones.*

Analyzing the samples measured concentrations before purification, it can be observed that all clones presented concentrations of dsDNA between, approximately, 580 and 750 µg/mL, being the mean 658.42 µg/mL. Thus, it can be concluded the amplification of the extracted sequences from the selected bacteriophages was successful, with all samples presenting very high amounts of dsDNA.

When analyzing the purity ratios for these samples, it can be noted that the purity ratios for $A_{260/280}$ got considerably lower than the expected 1.8 value for pure DNA. This indicates that the obtained DNA is not pure and that there was a loss in purity, with the low ratio probably being the result of contamination of the samples by reagents used in the PCR reaction. The purity ratios for $A_{260/230}$ also got considerably lower than the expected 2.0-2.2 values, probably being the result of contamination of the samples with reagents associated with the PCR amplification again.

Analyzing the samples measured concentrations after purification, it can be observed that all clones presented concentrations of dsDNA between, approximately, 10 and 25 µg/mL, being the mean 15.25 µg/mL. Thus, it can be concluded the purification of the obtained PCR products by the use of the PCR Clean-Up Kit lead to a significant loss in DNA concentration by the samples. This might be explained by a possible loss of product when using the purification kit, since the latter is usually used for the purification of 100 bp to 10 kbp PCR products. So, since the expected amplicon was 190 bp, it is likely that the DNA sequences were not retained on the column for being too small and were washed away with the contaminants. When analyzing the purity ratios for these samples, it can be noted that the purity ratios for $A_{260/280}$ got considerably higher and close to the expected 1.8 value for pure DNA. This indicates that there was an increase in the purity of the obtained DNA. The purity ratios for $A_{260/230}$ also got considerably higher, although still lower than the expected 2.0-2.2 values for most samples. Only samples Z3.1.3 and Z3.1.10 can be considered pure, since only these have both purity ratios in the expected range. The other samples probably present some form of contamination with reagents associated with the PCR amplification or with the purification method.

By analysis of **Figure 13**, it can be accessed that the amplification of the DNA templates was successful, since there was a considerable increase in the DNA concentration of all samples. The purification method was also able to increase the purity of the samples. However, pure DNA sequences were not achieved and this purification method lead to a drastic loss in DNA concentration, meaning that the DNA purification was not successful. Both **Experiment Z1** and **Experiment Z2** samples presented higher concentrations after the PCR amplification and purification than **Experiment Z3.1**, meaning this process was not as successful in amplifying and purifying the DNA templates selected in the anti-Zika antibody experiment.

The measured dsDNA absorbances and corresponding concentrations and purity ratios for the 10 clones from **Experiment Z3.2** after PCR amplification by the **PCR Experiment 1** and before purification are all specified in **Table 45** (in Annex 2). The measured dsDNA absorbances and corresponding concentrations and purity ratios for the 10 clones from **Experiment Z3.2** after PCR amplification by the **PCR Experiment 1** and after purification by the technique described in **Chapter 2.6.5.2** are all specified in **Table 46** (in Annex 2). A comparison of the DNA concentrations obtained

before PCR amplification and after PCR amplification before and after purification for the **Experiment Z3.2** clones is graphically depicted in **Figure 14**.

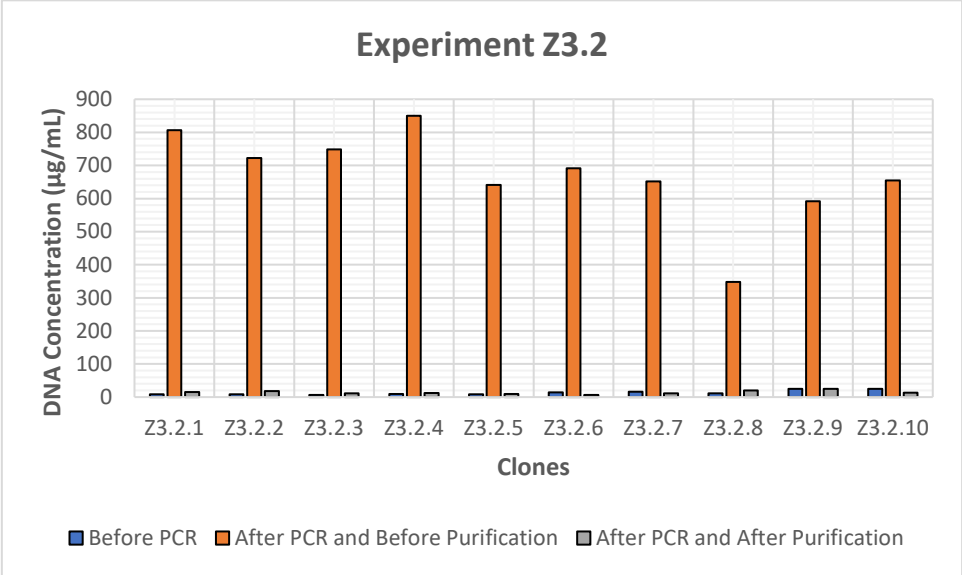

***Figure 14** – DNA concentrations obtained before PCR amplification and after PCR amplification before and after purification for the Experiment Z3.2 clones.*

Analyzing the samples measured concentrations before purification, it can be observed that all clones presented concentrations of dsDNA between, approximately, 350 and 850 µg/mL, being the mean 670.65 µg/mL. Thus, it can be concluded the amplification of the extracted sequences from the selected bacteriophages was successful, with all samples presenting very high amounts of dsDNA. When analyzing the purity ratios for these samples, it can be noted that the purity ratios for $A_{260/280}$ got a bit lower than the expected 1.8 value for pure DNA, with only sample Z3.2.8 presenting a higher value. This indicates that there was a loss in purity, with the low ratios probably being the result of contamination of the samples by reagents used in the PCR reaction. The purity ratios for $A_{260/230}$ also got considerably lower than the expected 2.0-2.2 values, with the low ratios probably being the result of contamination of the samples with reagents associated with the PCR amplification again.

Analyzing the samples measured concentrations after purification, it can be observed that all clones presented concentrations of dsDNA between, approximately, 6 and 25 µg/mL, being the mean 14.29 µg/mL. Thus, it can be concluded that the purification of the obtained PCR products by the use of the PCR Clean-Up Kit lead to a significant loss in DNA concentration by the samples. This might be explained by a possible loss of product when using the purification kit, as it was previously explained for the purified PCR products of **Experiment Z3.1**. When analyzing the purity ratios for these samples, it can be noted that the purity ratios for $A_{260/280}$ got considerably higher than the expected 1.8 value for pure DNA. This indicates that there was an increase in purity. The purity ratios for $A_{260/230}$ also got

considerably higher, although still lower than the expected 2.0-2.2 values. Only samples Z3.2.3, Z3.2.8 and Z3.2.9 can be considered pure, since only these samples have purity ratios in the expected range. The other samples presented lower ratios, probably being the result of contamination with reagents associated with the PCR amplification or with the purification method.

By analysis of **Figure 14**, it can be accessed that the amplification of the DNA templates was successful, since there was a considerable increase in the DNA concentration of all samples. The purification method was also able to increase the purity of the samples. However, pure DNA sequences were not achieved and this purification method lead to a drastic loss in DNA concentration, meaning that the DNA purification was not successful. Both **Experiment Z1** and **Experiment Z2** samples presented higher concentrations after the PCR amplification and purification than **Experiment Z3.2**, meaning this process was not as successful in amplifying and purifying the DNA templates selected in the anti-Zika antibody experiment. Still, this experiment yielded similar results to **Experiment Z3.1**.

The measured dsDNA absorbances and corresponding concentrations and purity ratios for the 10 clones from **Experiment Z4** after PCR amplification by the **PCR Experiment 1** and before purification are all specified in **Table 47** (in Annex 2). The measured dsDNA absorbances and corresponding concentrations and purity ratios for the 10 clones from **Experiment Z4** after PCR amplification by the **PCR Experiment 1** and after purification by the technique described in **Chapter 2.6.5.2** are all specified in **Table 48** (in Annex 2). A comparison of the DNA concentrations obtained before PCR amplification and after PCR amplification before and after purification for the **Experiment Z4** clones is graphically depicted in **Figure 15**.

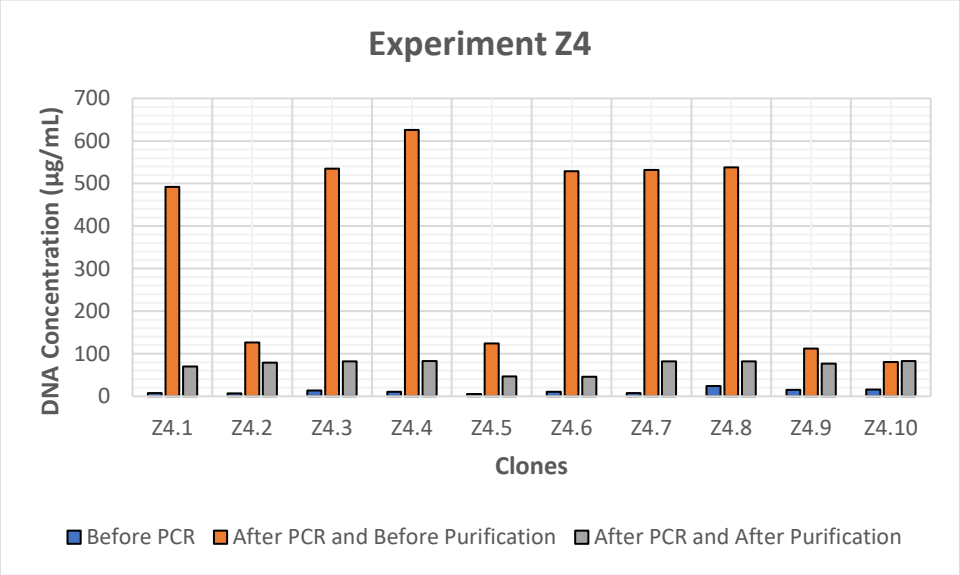

***Figure 15** – DNA concentrations obtained before PCR amplification and after PCR amplification before and after purification for the Experiment Z4 clones.*

Analyzing the samples measured concentrations before purification, it can be observed that all clones presented concentrations of dsDNA between, approximately, 80 and 630 µg/mL, being the mean 369.46 µg/mL. Thus, it can be concluded the amplification of the extracted sequences from the selected bacteriophages was successful, with all samples presenting very high amounts of dsDNA. When analyzing the purity ratios for these samples, it can be noted that the purity ratios for $A_{260/280}$ got a bit lower than the expected 1.8 value for pure DNA. This indicates that the obtained DNA is not pure and that there was a loss in purity, with the low ratio probably being the result of contamination of the samples by reagents used in the PCR reaction. The purity ratios for $A_{260/230}$ got a bit higher, but still lower than the expected 2.0-2.2 values, meaning that the obtained DNA is probably contaminated with reagents associated with the PCR amplification again.

Analyzing the samples measured concentrations after purification, it can be observed that all clones presented concentrations of dsDNA between, approximately, 45 and 85 µg/mL, being the mean 72.92 µg/mL. Thus, it can be concluded the purification of the obtained PCR products by the use of the PCR Clean-Up Kit lead to a significant loss in DNA concentration by the samples. This might be explained by a possible loss of product when using the purification kit, such as it was previously explained for the purified PCR products of **Experiment Z3.1** and of **Experiment Z3.2**. When analyzing the purity ratios for these samples, it can be noted that the purity ratios for $A_{260/280}$ got considerably higher, but still lower than the expected 1.8 value for pure DNA. This indicates that the obtained DNA is not pure and might still be contaminated with reagents used during the amplification or the purification method. The purity ratios for $A_{260/230}$ also got higher than the expected 2.0-2.2 values, and were probably the result of incorrect measurements. However, there was still an increase in purity of the samples.

By analysis of **Figure 15**, it can be accessed that the amplification of the DNA templates was successful, since there was a considerable increase in the DNA concentration of all samples. The purification method was also able to increase the purity of the samples. However, pure DNA sequences were not achieved and this purification method lead to a drastic loss in DNA concentration, meaning that the DNA purification was not successful. Both **Experiment Z1** and **Experiment Z2** samples presented higher concentrations after the PCR amplification and purification than **Experiment Z4**, meaning this process was not as successful in amplifying and purifying the DNA templates selected in the anti-Zika antibody experiment. However, this experiment yielded higher DNA concentrations than **Experiment Z3.1** and **Experiment Z3.2**.

3.5. Agarose Gel Electrophoresis

In order to confirm the size of the obtained PCR products, electrophoresis assays using agarose gels were conducted for all the samples. DNA products obtained on **PCR Experiment 1** were run on a 1% agarose gel, whereas the ones obtained on **PCR Experiment 2** were run on a 2% agarose gel. For

PCR products obtained on **PCR Experiment 3**, purified and unpurified samples obtained after this PCR experiment were both run on a 2% agarose gel.

The 10 DNA samples from **Experiment S1** after PCR amplification by the **PCR Experiment 1** and after purification by the technique described in **Chapter 2.6.5.2** were run on a 1% agarose gel. A photograph from this electrophoresis assay is shown on **Figure 16**.

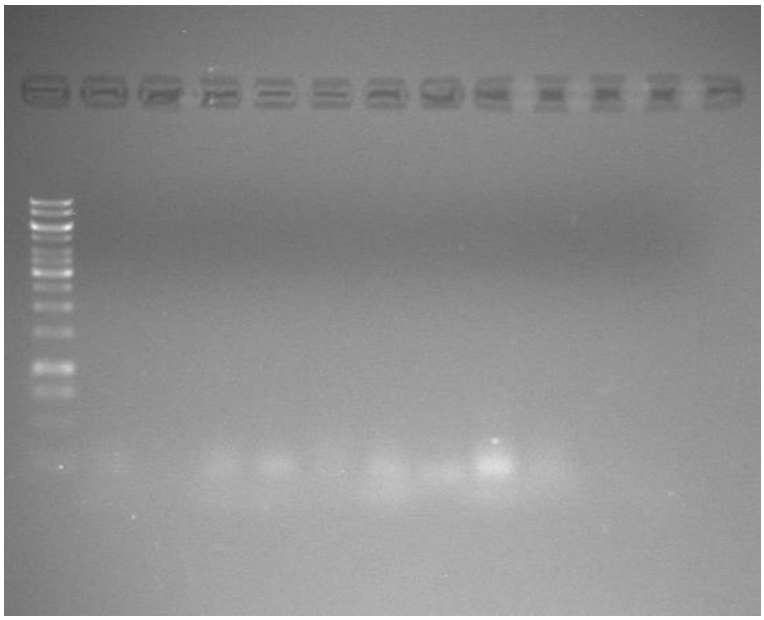

Figure 16 *– Photograph of the 1% agarose gel from the electrophoresis assay conducted for the 10 DNA samples from Experiment S1 after PCR amplification and after purification. Order of the samples: 100 bp DNA ladder; Clones S1.1-S1.10.*

When analyzing the agarose gel, it can be observed that all samples presented faint bands, with samples S1.2 and S1.10 presenting very faint bands. When in comparison with the DNA ladder, it can be seen that bands were positioned in between 100-200 bps, meaning that it can be concluded that the obtained DNA sequences were around the expected size (190 bps). Also, all samples seem to present a second unexpected band at around 100-80 bps, which might correspond to a possible contamination with primers dimers that might have occurred during the PCR amplification. Due to its apparent size, this contaminating band was probably not eliminated during the purification with the PCR Purification Kit, since it was possibly retained in the silica column used in the purification. Also, the size and density of the bands seem to indicate that the samples presented a good amount of DNA.

The 10 DNA samples from **Experiment S2** after PCR amplification by the **PCR Experiment 1** and after purification by the technique described in **Chapter 2.6.5.2** were run on a 1% agarose gel. A photograph from this electrophoresis assay is shown on **Figure 17**.

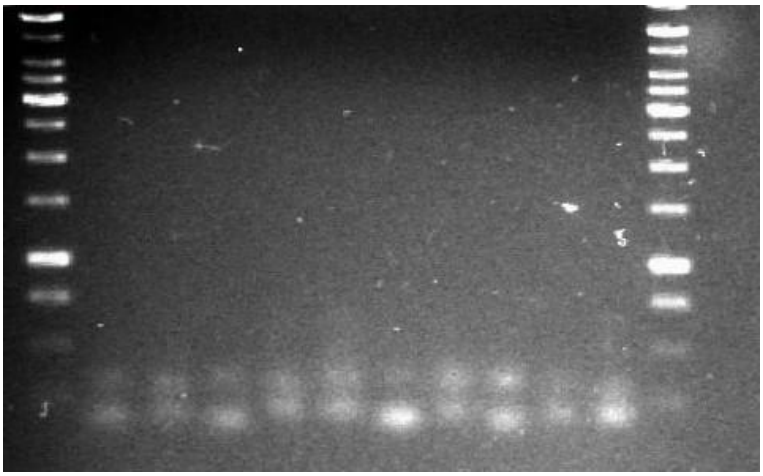

Figure 17 *– Photograph of the 1% agarose gel from the electrophoresis assay conducted for the 10 DNA samples from Experiment S2 after PCR amplification and after purification. Order of the samples: 100 bp DNA ladder; Clones S2.1-S2.10; 100 bp DNA ladder.*

When analyzing the agarose gel, it can be observed that all samples presented dense bands, which seems to indicate that the samples contain a high amount of DNA. When in comparison with the DNA ladder, it can be seen that bands were positioned in between 100-200 bps, meaning that it can be concluded that the obtained DNA sequences were around the expected size (190 bps). Also, all samples seem to present a second unexpected band, at around 100-80 bps, which might correspond again to a possible contamination with primers dimers that might have occurred during the PCR amplification, and were not eliminated during the purification method.

The 10 DNA samples from **Experiment Z1** after PCR amplification by the **PCR Experiment 1** and after purification by the technique described in **Chapter 2.6.5.1** were run on a 1% agarose gel. A photograph from this electrophoresis assay is shown on **Figure 18**.

When analyzing the agarose gel, it can be observed that all samples presented faint bands. When in comparison with the DNA ladder, it can be seen that bands were positioned in between 100-200 bps, meaning that it can be concluded that the obtained DNA sequences were around the expected size (190 bps). Also, all samples seem to present a second unexpected band at around 100-80 bps, which might again correspond to a possible contamination with primers dimers that might have occurred during the PCR amplification. The purification methods used for these samples (ethanol and isopropanol precipitation) were also not able to eliminate these primer dimers contaminants. Also, the size and density of the bands seem to indicate that the samples presented a good amount of DNA.

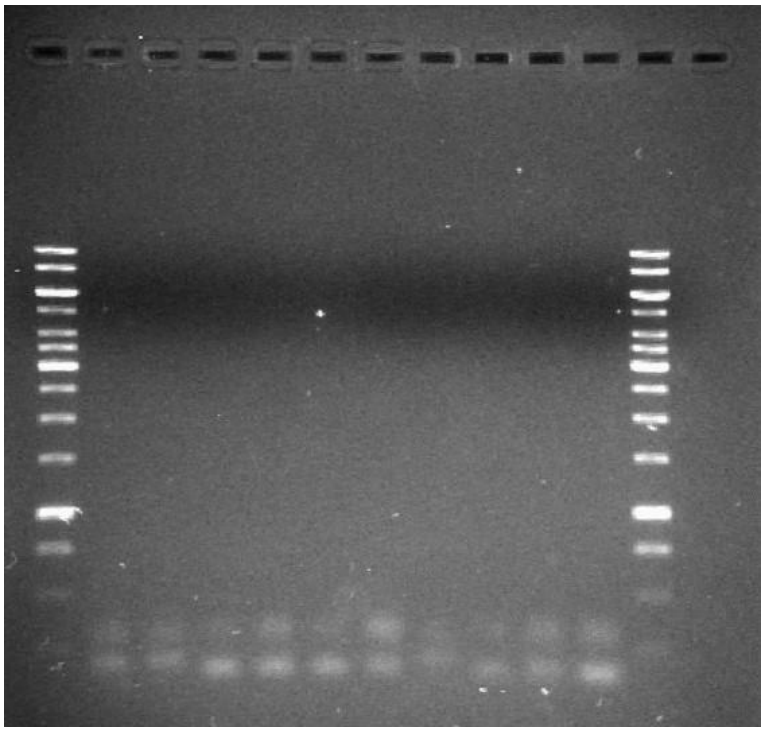

Figure 18 *– Photograph of the 1% agarose gel from the electrophoresis assay conducted for the 10 DNA samples from Experiment Z1 after PCR amplification by PCR Experiment 1 and after purification. Order of the samples: 100 bp DNA ladder; Clones Z1.1-Z1.10; 100 bp DNA ladder.*

The 10 DNA samples from **Experiment Z1** after PCR amplification by the **PCR Experiment 2** and after purification by the technique described in **Chapter 2.6.5.2** were run on a 2% agarose gel. A photograph from this electrophoresis assay is shown on **Figure 19**.

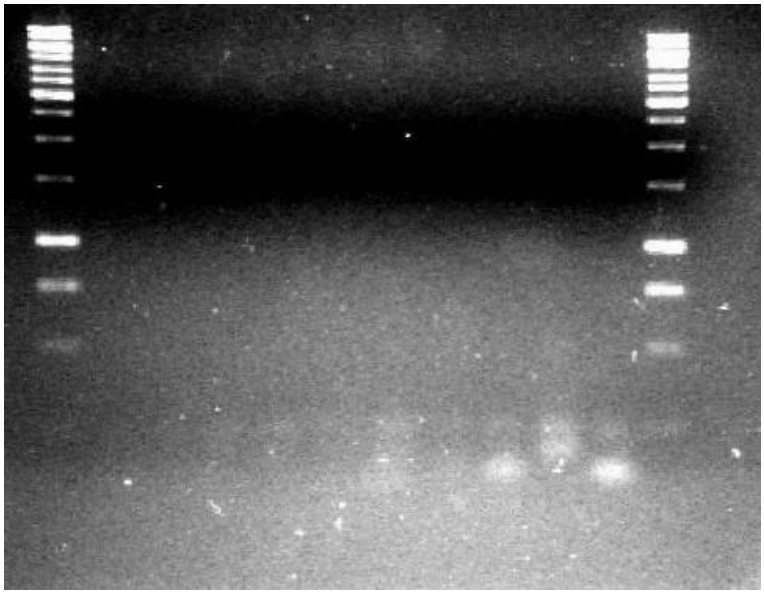

Figure 19 *– Photograph of the 2% agarose gel from the electrophoresis assay conducted for the 10 DNA samples from Experiment Z1 after PCR amplification by PCR Experiment 2 and after purification. Order of the samples: 100 bp DNA ladder; Clones Z1.1-Z1.10; 100 bp DNA ladder.*

When analyzing the agarose gel, it can be observed that all samples presented very faint bands, with samples Z1.6, Z1.8, Z1.9 and Z1.10 presenting denser bands. When in comparison with the DNA ladder, it can be seen that bands were positioned in between 100-200 bps, meaning that it can be concluded that the obtained DNA sequences were around the expected size (190 bps). Also, all samples seem to present a second unexpected band at around 100-80 bps, which might correspond to a possible contamination with primers dimers that might have occurred during the PCR amplification that were not eliminated during the purification with the PCR Purification Kit. Also, the size and density of the bands seem to indicate that the samples presented a good amount of DNA. It can also be concluded that the use of different primer concentrations during **PCR Experiment 2** did influence the final concentrations of DNA in the samples. A primer concentration of 250 nM was used during the PCR amplification of clones Z1.1-Z1.5, and it can be observed that these presented a lower density of the bands, meaning they contained a lower concentration of DNA. On the other hand, clones Z1.6-Z1.10 were amplified with a primer concentration of 500 nM, and it can be observed that these presented a higher density of the bands, meaning they contained a higher concentration of DNA.

DNA samples from **Experiment Z1** after PCR amplification by the **PCR Experiment 3** and before and after purification by the technique described in **Chapter 2.6.5.2** were run on a 2% agarose gel. A photograph from this electrophoresis assay is shown on **Figure 20**.

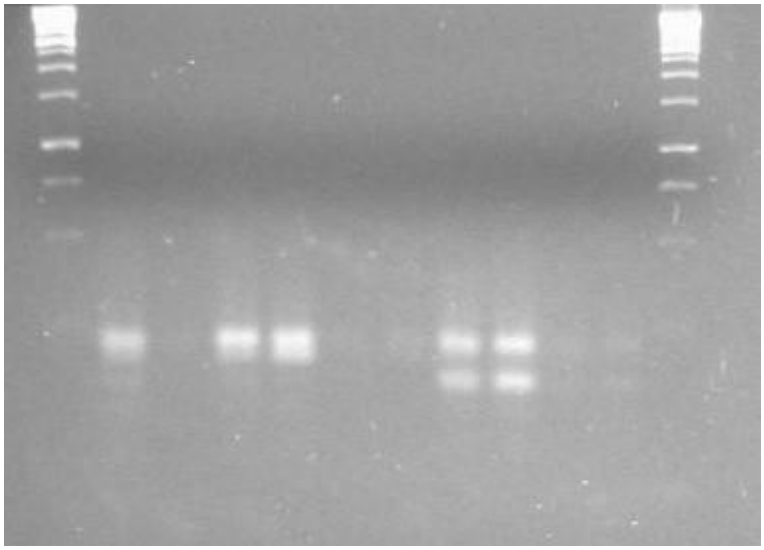

Figure 20 *– Photograph of the 2% agarose gel from the electrophoresis assay conducted for the DNA samples from Experiment Z1 after PCR amplification by PCR Experiment 3 and before and after purification. Order of the samples: 100 bp DNA ladder; Control Before Purification; Control After Purification; Clones Z1.1 and Z1.2 Before Purification; Clones Z1.1 and Z1.2 After Purification; Clones Z1.6 and Z1.7 Before Purification; Clones Z1.6 and Z1.7 After Purification; 100 bp DNA ladder.*

When analyzing the agarose gel, it can be observed that the bands corresponding to the samples before the use of the PCR Purification Kit were very dense bands. On the other hand, the

bands corresponding to the samples after the use of the purification method are shown to be very faint. So, it can be concluded that the **PCR Experiment 3** conditions allowed for a successful amplification of the DNA templates and that the use of the PCR Purification Kit lead to a significant decrease in the DNA concentration of the samples, which might be explained by the possible loss of the small sized PCR products through the silica columns. When in comparison with the DNA ladder, it can be seen that bands were positioned in between 100-200 bps, meaning that it can be concluded that the obtained DNA sequences were around the expected size (190 bps). Also, samples Z1.6 and Z1.7 seem to present a second unexpected band at around 100-80 bps, before and after purification, which might correspond to a possible contamination with primers dimers that might have occurred during the PCR amplification that were not eliminated during the purification method. The band corresponding to the control after PCR amplification and before purification shows some density, probably related to the presence of PCR reagents, such as dNTPs and primers. However, the band corresponding to the control after purification is extremely faint, meaning that the purification method is efficient in the elimination of contaminants of this sort.

DNA samples from **Experiment Z2** after PCR amplification by the **PCR Experiment 1** and after purification by the technique described in **Chapter 2.6.5.2** were run on a 1% agarose gel. A photograph from this electrophoresis assay is shown on **Figure 21**.

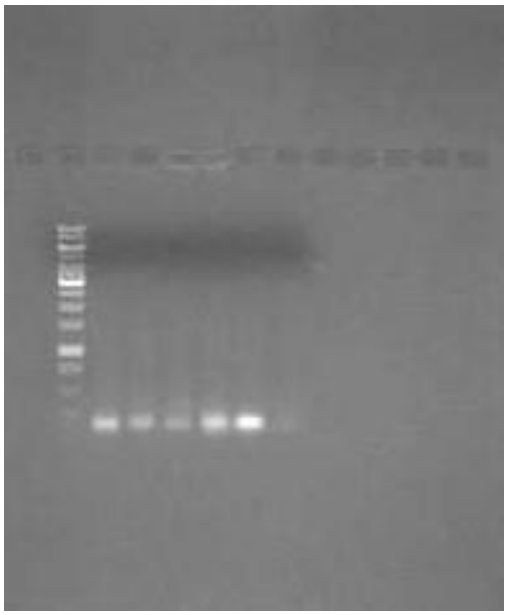

Figure 21 *– Photograph of the 1% agarose gel from the electrophoresis assay conducted for the DNA samples from Experiment Z2 after PCR amplification and after purification. Order of the samples: 100 bp DNA ladder; Clones Z2.1-Z2.6.*

When analyzing the agarose gel, it can be observed that samples presented fairly dense bands. When in comparison with the DNA ladder, it can be seen that bands were positioned in between 100-

200 bps, meaning that it can be concluded that the obtained DNA sequences were around the expected size (190 bps). Also, these samples do not present the second unexpected band at around 100-80 bps that occurred during the other experiments, meaning that primer dimers did not occur during this PCR amplification or that the purification of these PCR products was successful. Also, the size and density of the bands seem to indicate that the samples presented a good amount of DNA.

DNA samples from **Experiment Z3** after PCR amplification by the **PCR Experiment 1** and before purification by the technique described in **Chapter 2.6.5.2** were run on a 1% agarose gel. A photograph from this electrophoresis assay is shown on **Figure 22**.

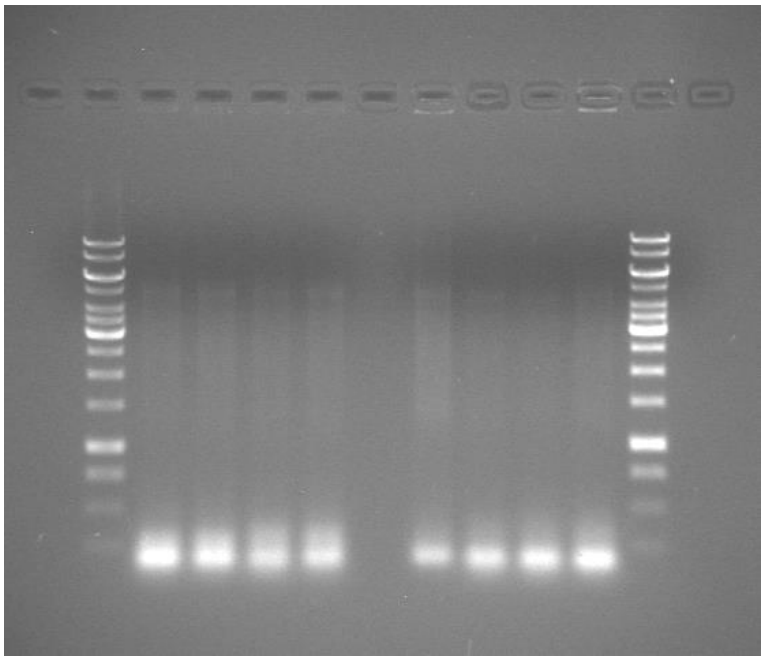

Figure 22 *– Photograph of the 1% agarose gel from the electrophoresis assay conducted for the DNA samples from Experiment Z3 after PCR amplification and before purification. Order of the samples: 100 bp DNA ladder; Clones Z3.1.1-Z3.1.4; Clones Z3.2.1-Z3.2.4; 100 bp DNA ladder.*

When analyzing the agarose gel, it can be observed that all samples presented very dense bands, which allows to conclude that amplification by this PCR experiment was successful, with products presenting very high concentrations of DNA. When in comparison with the DNA ladder, it can be seen that bands were positioned in between 100-200 bps, meaning that it can be concluded that the obtained DNA sequences were around the expected size (190 bps). An unexpected second band at around 100-80 bps is again not present, meaning that primer dimers did not form during the amplification method.

DNA samples from **Experiment Z3** after PCR amplification by the **PCR Experiment 1** and after purification by the technique described in **Chapter 2.6.5.2** were run on a 1% agarose gel. A photograph from this electrophoresis assay is shown on **Figure 23**.

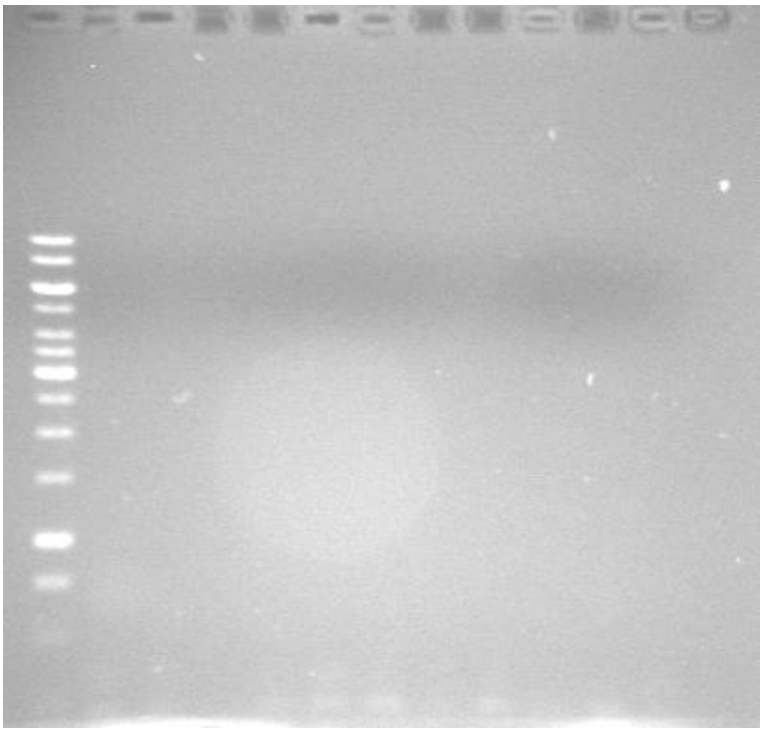

Figure 23 *– Photograph of the 1% agarose gel from the electrophoresis assay conducted for the DNA samples from Experiment Z3 after PCR amplification and after purification. Order of the samples: 100 bp DNA ladder; Clones Z3.1.1-Z3.1.5; Clones Z3.2.1-Z3.2.5.*

When analyzing the agarose gel, it can be observed that all samples presented very faint bands, which allows to conclude that the use of the PCR Purification Kit leads to a considerable decrease in the DNA amount of the samples, with products presenting very low concentrations of DNA. When in comparison with the DNA ladder, it can be seen that bands were again positioned in between 100-200 bps, meaning that the obtained DNA sequences corresponded to the expected amplicon (190 bps).

DNA samples from **Experiment Z4** after PCR amplification by the **PCR Experiment 1** and after purification by the technique described in **Chapter 2.6.5.2** were run on a 1% agarose gel. A photograph from this electrophoresis assay is shown on **Figure 24**.

When analyzing the agarose gel, it can be observed that all samples presented faint bands. When in comparison with the DNA ladder, it can be seen that bands were positioned in between 100-200 bps, meaning that it can be concluded that the obtained DNA sequences were around the expected size (190 bps). Also, the second unexpected band present in some of the other experiments is non-existent in this gel, meaning that primer dimers did not occur during this PCR experiment or that the purification with the PCR Purification Kit was successful. Also, the size and density of the bands seem to indicate that the samples present a low amount of DNA, probably related to the use of the purification method, since it was previously already seen that the use of this purification kit leads to a considerable decrease in the DNA concentration of the samples.

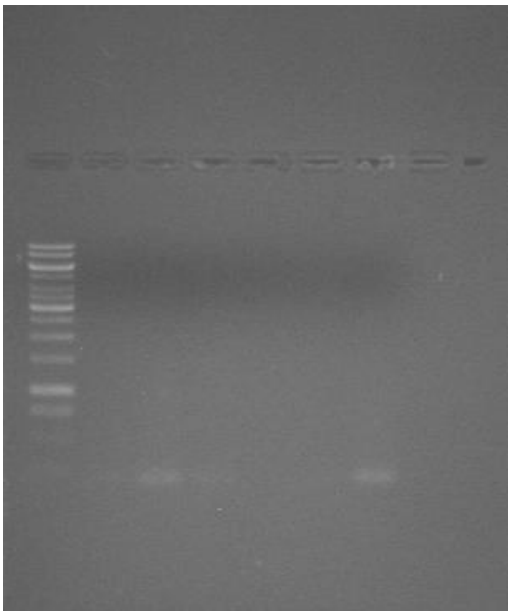

Figure 24 *– Photograph of the 1% agarose gel from the electrophoresis assay conducted for the DNA samples from Experiment Z4 after PCR amplification and after purification. Order of the samples: 100 bp DNA ladder; Clones Z4.1-Z4.6.*

3.6. Sequencing of Phage DNA

After the PCR experiment, the amplified nucleotide sequence should correspond to the depicted amplicon, with the forward primer highlighted in red and the reverse primer highlighted in blue. The library insert sequence of interest is highlighted in green, including the Gly-Gly-Gly spacer sequence. The amplified DNA sequence should contain 190 base pairs, as depicted.

5'CGCAATTCCTTTAGTGGTACCTTTCTATTCTCACTCT(NNK)$_{12}$GGTGGAGGTTCGGCCGAAACTGTTGAAAGTTGTTTAGCAAAATCCC
ATACAGAAAATTCATTTACTAACGTCTGGAAAGACGACAAAACTTTAGATCGTTACGCTAACTATGAGGGC3'
3'GCGTTAAGGAAATCACCATGGAAAGATAAGAGTGAGA(NNM)$_{12}$CCACCTCCAAGCCGGCTTTGACAACTTTCAACAAATCGTTTTA
GGGTATGTCTTTTAAGTAAATGATTGCAGACCTTTCTGCTGTTTTGAAATCTAGCAATGCGATTGATACTCCCG5'

For Sanger Sequencing, since the forward primer was used, the obtained nucleotide sequences should correspond to the depicted fragment, with the library insert sequence of interest highlighted in green, including the Gly-Gly-Gly spacer sequence. This DNA sequence should contain 169 base pairs, as depicted.

5'TTTCTATTCTCACTCT(NNK)$_{12}$GGTGGAGGTTCGGCCGAAACTGTTGAAAGTTGTTTAGCAAAATCCCATAC
AGAAAATTCATTTACTAACGTCTGGAAAGACGACAAAACTTTAGATCGTTACGCTAACTATGAGGGC3'

The sequence being read corresponds to the codon strand of the template. The randomized nucleotide sequence corresponds to a 36 base pair strand, with the third nucleotide of each codon in

the randomized region being G or T. When translated, the expected peptide sequences should contain 12 amino acids. Also, since TAG stop codons are suppressed by glutamine in ER2738 (*glnV*) and the library was amplified in this strain, TAG stop codons were considered a glutamine codon when translating.

Libraries often contain a small percentage (<1%) of clones containing multiple inserts of the randomized region. Preferential selection and amplification of these clones may occur when panning against targets whose ligand specificity spans a length greater than that specified by the insert. When interpreting sequence data, it was made sure that the sequence outside the restriction sites used for inserting the randomized sequence (*Acc65I* and *EagI*) matched the expected sequence, in order to identify the flanking regions of the library insert.

Experiment S1 constituted a positive control surface panning experiment with direct target coating using streptavidin as the target. Thus, after 3 rounds of enrichment/amplification, the consensus sequence for streptavidin-binding peptides should include the motif His-Pro-Gln (HPQ). The nucleotide sequences obtained by Sanger Sequencing for the random 10 clones chosen for this experiment are all specified in **Table 49** (in Annex 2). The nucleotide sequences corresponding to the library insert are all specified in **Table 50** (in Annex 2) and the corresponding translated amino acid sequences in **Table 7**.

Table 7 *- Amino acid sequences corresponding to the library inserts obtained for Experiment S1.*

Clone	Peptide Amino Acid Sequence
S1.1	ADRIFLRRNAAL
S1.2	XTDAXGGCCIFV
S1.3	XXDSDEYLQRPT
S1.4	QWNADRTIQGPL
S1.5	SADMWYQTYARP
S1.6	XXXXAMSSEEPP
S1.7	SSCSDFMVRSHW
S1.8	XGLHIPGEGCLL
S1.9	ADGWLQQLEWPP
S1.10	SALLTNCVQCLS

Most of the obtained nucleotide sequences corresponded to the previously depicted fragment and included the Gly-Gly-Gly spacer sequence. These DNA sequences contained around 169 base pairs, but none of them presented the exact expected number of base pairs, which might be explained by possible deletions that occurred during the whole amplification, purification and sequencing process. Also, none of the sequences presented the expected HPQ motif, meaning that the obtained sequences do not correspond to streptavidin-binding peptides. Since streptavidin-binding peptides were not

successfully selected, the method could not be validated yet. One reason for the streptavidin control experiment not yielding the HPQ consensus sequence might be the use of low pH glycine rather than biotin when eluting the phages. Due to the relatively low affinity of the peptide-streptavidin interaction, non-specific elution is incapable of selectively enriching for HPQ-containing peptides. In the future, in order to achieve the validation of the experiment, HPQ-containing peptides can be competitively eluted using the natural ligand biotin. If biotin is used to elute and still a consensus sequence a consensus sequence is not obtained, the most likely explanation is that not sufficiently rigorous washes were carried out. When washing, the wash buffer should be poured from a bottle in the plate and not gently pipetted in, and swirled for about 10 seconds each time. The number of phage eluted after the first round of biopanning should be in the range of 10^3 - 10^7 (closer to 10^3 for an ELISA well and closer to 10^7 for larger wells). If eluting more phage, the washing may not be enough and, as a result, sufficient enrichment will not be achieved. Also, 0.1 µg/mL streptavidin needs to be added to the blocking buffer to complex any contaminating biotin in the BSA, which could otherwise complex the streptavidin on the plate during the blocking step.

Experiment S2 constituted a positive control solution-phase panning experiment with affinity bead capture using streptavidin as the target. Thus, after 3 rounds of enrichment/amplification, the consensus sequence for streptavidin-binding peptides should again include the motif His-Pro-Gln (HPQ). The nucleotide sequences obtained by Sanger Sequencing for the random 10 clones chosen for this experiment are all specified in **Table 51** (in Annex 2). The nucleotide sequences corresponding to the library insert are all specified in **Table 52** (in Annex 2) and the corresponding translated amino acid sequences in **Table 8**.

Table 8 *– Amino acid sequences corresponding to the library inserts obtained for Experiment S2.*

Clone	Peptide Amino Acid Sequence
S2.1	XAXVEVVQQIPY
S2.2	GTDSLILADCLQ
S2.3	LIENSQFQCPAG
S2.4	HCQSCVWQRGAA
S2.5	CRESLQYGAAAG
S2.6	QLENSSILVPSQ
S2.7	QAVQISCITNDA
S2.8	SXQXXLCTMIPY
S2.9	XQNDQLIQYSHQ
S2.10	CFGDCVLMLGTP

Most of the obtained nucleotide sequences corresponded to the previously depicted fragment and included the Gly-Gly-Gly spacer sequence. These DNA sequences contained around 169 base pairs,

but none of them presented the exact expected number of base pairs, which might be explained by possible deletions that occurred during the amplification/purification/sequencing procedures. Also, none of the sequences presented the expected HPQ motif, meaning that the obtained sequences do not correspond to streptavidin-binding peptides. Since streptavidin-binding peptides were not successfully selected, the method could not be validated yet. In order to achieve the validation of the method in the future, the steps explained before should be conducted, including a solution-phase panning experiment with a biotinylated target and streptavidin surface plate capture.

Experiment Z1 constituted a surface panning procedure with direct target coating using the Anti-Zika Virus NS1 Antibody [B4] as the target. The nucleotide sequences obtained by Sanger Sequencing for the phage eluate pool and the random 10 clones chosen for this experiment are all specified in **Table 53** (in Annex 2). The nucleotide sequences corresponding to the library insert are all specified in **Table 54** (in Annex 2) and the corresponding translated amino acid sequences in **Table 9**.

Table 9 *– Amino acid sequences corresponding to the library inserts obtained for Experiment Z1.*

Clone	Peptide Amino Acid Sequence
Z1.1	EXMHXDSLVNFF
Z1.2	QXSLIRRLTMPR
Z1.3	XXXXXSCLANPI
Z1.4	XXXVXVVQLIPY
Z1.5	SAIQSNLCRLCQ
Z1.6	XNCQSCLANPIA
Z1.7	XNCQSCLANPIR
Z1.8	XNCQSCSSQILY
Z1.9	LQLKFVQQESHT
Z1.10	ELNGSCQCFISQ
Z1.Eluate	XXXCQSCLADPI

Most of the obtained nucleotide sequences corresponded to the previously depicted fragment and included the Gly-Gly-Gly spacer sequence. These DNA sequences contained around 169 base pairs, but none of them presented the exact expected number of base pairs, which might be explained by the occurrence of possible deletions. Also, by observation of **Table 9**, it can be concluded that some amino acid sequences present regions of similarity between them, with clones Z1.3, Z1.6 and Z1.7 presenting the CLANPI region and clones Z1.6, Z1.7, Z1.8 and Z1.Eluate presenting the CQSC region. However, most obtained amino acid sequences do not present regions of similarity, thus concluding that a consensus sequence was not selected. Thus, it can be determined that this experiment did not allow the selection of a consensus peptide with affinity to the Anti-Zika Virus NS1 Antibody [B4]. This might be explained by the selection of random peptides that established non-specific interactions with the plastic supports. Also, some sequences did not have the cloning sites, the full 36 nucleotide insert

or the expected Gly-Gly-Gly spacer sequence, which might be due to possible minor errors committed during the whole amplification, purification and sequencing process. Also, *wild-type* M13 contaminant phages might have been selected and amplified.

Experiment Z2 constituted a solution-phase based biopanning procedure with affinity bead capture, using both Protein A and Protein G agarose beads, and using the Anti-Zika Virus NS1 Antibody [B4] as the target. The nucleotide sequences obtained by Sanger Sequencing for the phage eluate pool and the random 10 clones chosen for this experiment are all specified in **Table 55** (in Annex 2). The nucleotide sequences corresponding to the library insert are all specified in **Table 56** (in Annex 2) and the corresponding translated amino acid sequences in **Table 10**.

Table 10 *– Amino acid sequences corresponding to the library inserts obtained for Experiment Z2.*

Clone	Peptide Amino Acid Sequence
Z2.1	XXLXSLSSAGPT
Z2.2	AAQKLFKQDPSQ
Z2.3	NCLKLFIQNAQQ
Z2.4	RLPREVFRLVPA
Z2.5	ASCCRIQGGSQL
Z2.6	ALKVSSCLIPQG
Z2.7	NCLKFFRLEPSQ
Z2.8	RNCFEKSQMVPA
Z2.9	QKLFSQSPVSGV
Z2.10	GMRREKSSMVPA
Z2.Eluate	QLIDRLLHPMPA

Most of the obtained nucleotide sequences corresponded to the previously depicted fragment and included the Gly-Gly-Gly spacer sequence. These DNA sequences contained around 169 base pairs, but none of them presented the exact expected number of base pairs, which might be explained by the occurrence of possible deletions. Also, by observation of **Table 10**, it can be concluded that some amino acid sequences present regions of similarity between them, with clones Z2.8 and Z2.10 presenting the MVPA region, clones Z2.4, Z2.8 and Z2.10 presenting the VPA region and clones Z2.4, Z2.8, Z2.10 and Z2.Eluate presenting the PA region. Then, it can be concluded that a consensus sequence was selected, since there are regions of similarity between some of the obtained amino acid sequences. Thus, it can be determined that this experiment allowed the selection of a peptide with affinity to the Anti-Zika Virus NS1 Antibody [B4]. The selection of peptides whose sequence did not have the common region might be related to a possible selection of random peptides that had affinity to the Protein A or the Protein G agarose beads, establishing non-specific interactions with these resins. Also, *wild-type* M13 contaminant phages might have been selected and amplified.

Experiment Z3.1 constituted a solution-phase based biopanning procedure with affinity bead capture, using Protein G agarose beads and a negative selection step, and using the Anti-Zika Virus NS1 Antibody [B4] as the target. The nucleotide sequences obtained by Sanger Sequencing for the phage eluate pool and the random 10 clones chosen for this experiment are all specified in **Table 57** (in Annex 2). The nucleotide sequences corresponding to the library insert are all specified in **Table 58** (in Annex 2) and the corresponding translated amino acid sequences in **Table 11**.

Table 11 *– Amino acid sequences corresponding to the library inserts obtained for Experiment Z3.1.*

Clone	Peptide Amino Acid Sequence
Z3.1.1	XXXXEFFRLVPA
Z3.1.2	XXXRESLRLVPA
Z3.1.3	GNAARSLQMVPA
Z3.1.4	EADQQLLHLVPA
Z3.1.5	KLPREVFRLVPA
Z3.1.6	ELTPRKSSMVPA
Z3.1.7	XSYAAESSMVPA
Z3.1.8	SSYAAESSMVPA
Z3.1.9	XSYAAESSMVPA
Z3.1.10	EAYARKSSMVPA
Z3.1.Eluate	XXXXAESSMVPA

All of the obtained nucleotide sequences corresponded to the previously depicted fragment and included the Gly-Gly-Gly spacer sequence. These DNA sequences contained around 169 base pairs, but none of them presented the exact expected number of base pairs, which might be explained by possible deletions that occurred during the whole amplification, purification and sequencing process. Also, by observation of **Table 11**, it can be concluded that all the amino acid sequences present regions of similarity between them, with all clones presenting the VPA region. Clones Z3.1.3, Z3.1.6, Z3.1.7, Z3.1.8, Z3.1.9, Z3.1.10 and Z3.1.Eluate presented the MVPA region and clones Z3.1.6, Z3.1.7, Z3.1.8, Z3.1.9, Z3.1.10 and Z3.1.Eluaute presented the SSMVPA region. Other regions of similarity can also be found, with clones Z3.1.1, Z2.1.2 and Z3.1.5 presenting the RLVPA region and clones Z3.1.7, Z3.1.8 and Z3.1.9 presenting the SYAAE region. Then, it can be concluded that a consensus sequence was selected, since there are regions of similarity between all of the obtained amino acid sequences. Also, this consensus region is similar to the one found in **Experiment Z2**. Thus, it can be determined that this experiment allowed the selection of a consensus peptide with affinity to the Anti-Zika Virus NS1 Antibody [B4], and avoided the selection of peptides specific to plastic supports or resin beads.

Experiment Z3.2 constituted a solution-phase based biopanning procedure with affinity bead capture, using Protein G agarose beads and a negative selection step, and using the Anti-Zika Virus NS1 Antibody [D11] as the target. The nucleotide sequences obtained by Sanger Sequencing for the phage

eluate pool and the random 10 clones chosen for this experiment are all specified in **Table 59** (in Annex 2). The nucleotide sequences corresponding to the library insert are all specified in **Table 60** (in Annex 2) and the corresponding translated amino acid sequences in **Table 12**.

Table 12 *– Amino acid sequences corresponding to the library inserts obtained for Experiment Z3.2.*

Clone	Peptide Amino Acid Sequence
Z3.2.1	GTGCVGXALDIR
Z3.2.2	GXXMRWEAVDIR
Z3.2.3	GNRNAWXAVDIR
Z3.2.4	WQXMRWEAVDIR
Z3.2.5	QGXXAWDAVDIA
Z3.2.6	GKXMLGNAVDIA
Z3.2.7	GXXNAWDAVDIX
Z3.2.8	RKXSVGEAVDIA
Z3.2.9	XASXAWXAVDIX
Z3.2.10	GQXXRGXLLHIR
Z3.2.Eluate	GNXNAWEAVDIR

All of the obtained nucleotide sequences corresponded to the previously depicted fragment and included the Gly-Gly-Gly spacer sequence. These DNA sequences contained around 169 base pairs, but none of them presented the exact expected number of base pairs, which might be explained by possible deletions that occurred during the whole amplification, purification and sequencing process. Also, by observation of **Table 12**, it can be concluded that all the amino acid sequences present regions of similarity between them, with all clones except for Z3.2.10 presenting the DIR/DIA/DI region. Clones Z3.2.1, Z3.2.2, Z3.2.3, Z3.2.4 and Z3.2.Eluate presented the DIR region and clones Z3.2.5, Z3.2.6 and Z3.2.8 presented the AVDIA region. Other regions of similarity can also be found, with clones Z3.2.7 and Z2.2.9 presenting the AVDI region and clones Z3.2.2, Z3.2.3, Z3.2.4 and Z3.2.Eluate presenting the AVDIR region. Then, it can be concluded that a consensus sequence was selected, since there are regions of similarity between most of the obtained amino acid sequences. Thus, it can be determined that this experiment allowed the selection of a consensus peptide with affinity to the Anti-Zika Virus NS1 Antibody [D11], and avoided the selection of peptides specific to plastic supports or resin beads.

Experiment Z4 constituted a solution-phase based biopanning procedure with affinity bead capture, using Protein A agarose beads and a negative selection step, and using the Anti-Zika Virus NS1 Antibody [D11] as the target. The nucleotide sequences obtained by Sanger Sequencing for the phage eluate pool and the random 10 clones chosen for this experiment are all specified in **Table 61** (in Annex 2). The nucleotide sequences corresponding to the library insert are all specified in **Table 62** (in Annex 2) and the corresponding translated amino acid sequences in **Table 13**.

Table 13 – Amino acid sequences corresponding to the library inserts obtained for Experiment Z4.

Clone	Peptide Amino Acid Sequence
Z4.1	XERDAWEAVDIR
Z4.2	INQDAWEAVDIR
Z4.3	GNGMRGKAVDIR
Z4.4	RERNAWEAVDIR
Z4.5	RGIKSHFSHTGK
Z4.6	RNGSVGRLLIFV
Z4.7	RNRNAWEAVDIR
Z4.8	REXNAWEAVDIR
Z4.9	RNXNAWEAVDIR
Z4.10	GNRNAWEAVDIR
Z4.Eluate	RNXNAWEAVDIR

All of the obtained nucleotide sequences corresponded to the previously depicted fragment and included the Gly-Gly-Gly spacer sequence. These DNA sequences contained around 169 base pairs, but none of them presented the exact expected number of base pairs, which might be explained by the occurrence of possible deletions. Also, by observation of **Table 13**, it can be concluded that all the amino acid sequences present regions of similarity between them, with all clones except for Z4.5 and Z4.6 presenting the AVDIR region. The clones Z4.1, Z4.2, Z4.4, Z4.7, Z4.8, Z4.9, Z4.10 and Z4.Eluate presented the region AWEAVDIR. Then, it can be concluded that a consensus sequence was selected, since there are regions of similarity between most of the obtained amino acid sequences. Also, this consensus region is similar to the one found in **Experiment Z3.2**. Thus, it can be determined that this experiment allowed the selection of a consensus peptide with affinity to the Anti-Zika Virus NS1 Antibody [D11], and avoided the selection of peptides specific to plastic supports or resin beads.

Conclusions and Future Work

The main purpose of this project was to identify and generate phage-displayed peptides that specifically recognized the Zika disease target molecules with high sensitivity and selectivity. In this project, a "panning" technique was carried out, where a commercial library of peptides displayed on bacteriophages was screened against two specific antibodies for Zika, using two different methods: the "Surface Panning Procedure with Direct Target Coating", in which the target molecules were immobilized on the surface of a polystyrene plate; and the "Solution-Phase Panning with Affinity Bead Capture", in which the phage library reacted with the target molecules in solution and the target phage complexes were affinity captured in a matrix constituted by specific "Protein A/G Agarose Beads" to the target molecule in a microcentrifuge tube. Then, the selected bacteriophage library was amplified by bacterial infection in *Escherichia coli* and quantified using the "Phage Titering" technique. The selected bacteriophages were validated through an ELISA test, in order to assess the binding affinity of the amplified phages. Also, the selected DNA sequences were amplified using the "Polymerase Chain Reaction" technique and quantified using agarose gel electrophoresis and UV spectrophotometry techniques. Finally, the obtained phage DNA was sequenced, in order to determine the nucleotide sequences corresponding to the specific peptides for the target molecules.

These experiments were able to yield consensus peptide sequences that bound to the two Zika-specific antibodies. These consensus peptide sequences will provide new insights into the development of bionanosensors as diagnostic tools for Zika infection, which will work as sensitive viral detection and serotyping tools. This type of innovative biosensing method will allow for a non-invasive, rapid, and in real time diagnosis of the disease.

In the future, candidate phages will continue to be validated. The phage-displayed peptide library is going to be precleared using antibodies specific for other serotypes and selected with antibodies from patients with the desired serotype. Disease-specific phages can be obtained by the screening of the selected ones with different sera from patients recovered from infection (including sera from individuals with other infectious diseases), with other diseases and with healthy sera too; and comparing phagotopes in several positive and negative sera using indirect ELISA. Also, the optimization of this technique is going to be performed in order to confirm and characterize the phage-displayed peptides that specifically recognize the target molecules with high sensitivity and selectivity. Functional assays with the candidate phages will also be performed in the future, in order to identify the peptides that will be used further in the development of bionanosensors as diagnostic tools for Zika infection.

Bibliography

1. Sikka V, Chattu VK, Popli RK, Galwankar SC, Kelkar D, Sawicki SG, et al. The Emergence of Zika Virus as a Global Health Security Threat: A Review and a Consensus Statement of the INDUSEM Joint working Group (JWG). Journal of Global Infectious Diseases [Internet]. 2016 Jan 1 [cited 2021 Sep 8];8(1):3. Available from: /pmc/articles/PMC4785754/

2. Malone RW, Homan J, Callahan M v., Glasspool-Malone J, Damodaran L, Schneider ADB, et al. Zika Virus: Medical Countermeasure Development Challenges. PLoS Neglected Tropical Diseases [Internet]. 2016 Mar 2 [cited 2021 Sep 8];10(3). Available from: /pmc/articles/PMC4774925/

3. Mehrjardi MZ. Is Zika Virus an Emerging TORCH Agent? An Invited Commentary. Virology : Research and Treatment [Internet]. 2017 [cited 2021 Sep 8];8:1–3. Available from: /pmc/articles/PMC5439991/

4. Zika Travel Information | Travelers' Health | CDC [Internet]. [cited 2021 Sep 8]. Available from: https://wwwnc.cdc.gov/travel/page/zika-information

5. Petersen EE. Interim Guidelines for Pregnant Women During a Zika Virus Outbreak — United States, 2016. MMWR Morbidity and Mortality Weekly Report. 2019 Jan 22;65(2):30–3.

6. Zika virus: Advice for those planning to travel to outbreak areas | ITV News [Internet]. [cited 2021 Sep 8]. Available from: https://www.itv.com/news/2016-01-22/zika-virus-advice-for-those-planning-to-travel-to-outbreak-area

7. Travel warning for Irish women over Zika virus [Internet]. [cited 2021 Sep 8]. Available from: https://www.rte.ie/news/2016/0122/762119-el-salvador-zika-virus/

8. Zika: Olympics plans announced by Rio authorities - BBC News [Internet]. [cited 2021 Sep 8]. Available from: https://www.bbc.com/news/world-latin-america-35394297

9. Faye O, Freire CCM, Iamarino A, Faye O, Oliveira JVC de, Diallo M, et al. Molecular Evolution of Zika Virus during Its Emergence in the 20th Century. PLoS Neglected Tropical Diseases [Internet]. 2014 [cited 2021 Sep 8];8(1):36. Available from: /pmc/articles/PMC3888466/

10. Cao-Lormeau V-M, Roche C, Teissier A, Robin E, Berry A-L, Mallet H-P, et al. Zika Virus, French Polynesia, South Pacific, 2013. Emerging Infectious Diseases [Internet]. 2014 [cited 2021 Sep 8];20(6):1085. Available from: /pmc/articles/PMC4036769/

11. Hayes EB. Zika Virus Outside Africa. Emerging Infectious Diseases [Internet]. 2009 Sep [cited 2021 Sep 8];15(9):1347. Available from: /pmc/articles/PMC2819875/

12. Kuno G, Chang G-JJ. Full-length sequencing and genomic characterization of Bagaza, Kedougou, and Zika viruses. Archives of Virology [Internet]. 2007 Feb 1 [cited 2021 Sep 8];152(4):687–96. Available from: https://zenodo.org/record/1232749

13. Cox BD, Stanton RA, Schinazi RF. Predicting Zika virus structural biology: Challenges and opportunities for intervention. Antiviral Chemistry & Chemotherapy [Internet]. 2015 Aug 1 [cited 2021 Sep 8];24(3–4):118. Available from: /pmc/articles/PMC5890524/

14. Dai L, Song J, Lu X, Deng Y-Q, Musyoki AM, Cheng H, et al. Structures of the Zika Virus Envelope Protein and Its Complex with a Flavivirus Broadly Protective Antibody. Cell Host & Microbe [Internet]. 2016 May 11 [cited 2021 Sep 8];19(5):696–704. Available from: http://www.cell.com/article/S1931312816301494/fulltext

15. Pierson TC, Diamond MS. Degrees of maturity: The complex structure and biology of flaviviruses. Current opinion in virology [Internet]. 2012 [cited 2021 Sep 8];2(2):168. Available from: /pmc/articles/PMC3715965/

16. Monel B, Compton AA, Bruel T, Amraoui S, Burlaud-Gaillard J, Roy N, et al. Zika virus induces massive cytoplasmic vacuolization and paraptosis-like death in infected cells. The EMBO Journal [Internet]. 2017 Jun 14 [cited 2021 Sep 8];36(12):1653. Available from: /pmc/articles/PMC5470047/

17. Enfissi A, Codrington J, Roosblad J, Kazanji M, Rousset D. Zika virus genome from the Americas. The Lancet [Internet]. 2016 Jan 16 [cited 2021 Sep 8];387(10015):227–8. Available from: http://www.thelancet.com/article/S0140673616000039/fulltext

18. Zanluca C, Melo VCA de, Mosimann ALP, Santos GIV dos, Santos CND dos, Luz K. First report of autochthonous transmission of Zika virus in Brazil. Memórias do Instituto Oswaldo Cruz [Internet]. 2015 [cited 2021 Sep 8];110(4):569. Available from: /pmc/articles/PMC4501423/

19. Lanciotti RS, Lambert AJ, Holodniy M, Saavedra S, Signor L del CC. Phylogeny of Zika Virus in Western Hemisphere, 2015. Emerging Infectious Diseases [Internet]. 2016 May 1 [cited 2021 Sep 8];22(5):933. Available from: /pmc/articles/PMC4861537/

20. A R, L D, D C, S S, R S, V A. Comparative analysis of protein evolution in the genome of pre-epidemic and epidemic Zika virus. Infection, genetics and evolution : journal of molecular epidemiology and evolutionary genetics in infectious diseases [Internet]. 2017 Jul 1 [cited 2021 Sep 8];51:74–85. Available from: https://pubmed.ncbi.nlm.nih.gov/28315476/

21. Sirohi D, Chen Z, Sun L, Klose T, Pierson TC, Rossmann MG, et al. The 3.8Å resolution cryo-EM structure of Zika Virus. Science (New York, NY) [Internet]. 2016 Apr 22 [cited 2021 Sep 9];352(6284):467. Available from: /pmc/articles/PMC4845755/

22. Fauci AS, Morens DM. Zika Virus in the Americas — Yet Another Arbovirus Threat. New England Journal of Medicine. 2016 Feb 18;374(7):601–4.

23. Gubler DJ. Dengue, Urbanization and Globalization: The Unholy Trinity of the 21st Century. Tropical Medicine and Health [Internet]. 2011 [cited 2021 Sep 7];39(4 Suppl):3. Available from: /pmc/articles/PMC3317603/

24. Vasquez AM. Survey of Blood Collection Centers and Implementation of Guidance for Prevention of Transfusion-Transmitted Zika Virus Infection — Puerto Rico, 2016. MMWR Morbidity and Mortality Weekly Report. 2019 Apr 15;65(14):375–8.

25. Oster AM. Update: Interim Guidance for Prevention of Sexual Transmission of Zika Virus — United States, 2016. MMWR Morbidity and Mortality Weekly Report. 2019 Mar 25;65(12).

26. Lessler J, Chaisson LH, Kucirka LM, Bi Q, Grantz K, Salje H, et al. Assessing the global threat from Zika virus. Science. 2016 Aug 12;353(6300).

27. FACTBOX - Zika virus spreads rapidly through Latin America [Internet]. [cited 2021 Sep 7]. Available from: https://news.trust.org/item/20160122152242-yxsmt/

28. Noorbakhsh F, Abdolmohammadi K, Fatahi Y, Dalili H, Rasoolinejad M, Rezaei F, et al. Zika virus infection, basic and clinical aspects: A review article. Iranian Journal of Public Health. 2019 Jan 16;48(1):20–31.

29. AI A, A N, H A. An updated review of Zika virus. Journal of clinical virology : the official publication of the Pan American Society for Clinical Virology [Internet]. 2016 Nov 1 [cited 2021 Sep 7];84:53–8. Available from: https://pubmed.ncbi.nlm.nih.gov/27721110/

30. Hayes EB. Zika Virus Outside Africa. Emerging Infectious Diseases [Internet]. 2009 Sep [cited 2021 Sep 7];15(9):1347. Available from: /pmc/articles/PMC2819875/

31. Grard G, Caron M, Mombo IM, Nkoghe D, Ondo SM, Jiolle D, et al. Zika Virus in Gabon (Central Africa) – 2007: A New Threat from Aedes albopictus? PLoS Neglected Tropical Diseases [Internet]. 2014 [cited 2021 Sep 7];8(2). Available from: /pmc/articles/PMC3916288/

32. L Z, G S, A M, D B, D T, S G, et al. Zika virus infections imported to Italy: clinical, immunological and virological findings, and public health implications. Journal of clinical virology : the official publication of the Pan American Society for Clinical Virology [Internet]. 2015 Feb 1 [cited 2021 Sep 7];63:32–5. Available from: https://pubmed.ncbi.nlm.nih.gov/25600600/

33. Shining a light on Zika | New Zealand Geographic [Internet]. [cited 2021 Sep 7]. Available from: https://www.nzgeo.com/stories/shining-a-light-on-zika/

34. Kraemer MU, Sinka ME, Duda KA, Mylne AQ, Shearer FM, Barker CM, et al. The global distribution of the arbovirus vectors Aedes aegypti and Ae. albopictus. eLife [Internet]. 2015 Jun 30 [cited 2021 Sep 7];4(JUNE2015). Available from: /pmc/articles/PMC4493616/

35. Aedes aegypti - Factsheet for experts [Internet]. [cited 2021 Sep 7]. Available from: https://www.ecdc.europa.eu/en/disease-vectors/facts/mosquito-factsheets/aedes-aegypti

36. Mosquitoes capable of carrying Zika virus found in Washington, D.C. | News | Notre Dame News | University of Notre Dame [Internet]. [cited 2021 Sep 7]. Available from: https://news.nd.edu/news/mosquitos-capable-of-carrying-zika-virus-found-in-washington-dc/

37. Zika outbreak: What you need to know - BBC News [Internet]. [cited 2021 Sep 7]. Available from: https://www.bbc.com/news/health-35370848

38. Carlson CJ, Dougherty ER, Getz W. An Ecological Assessment of the Pandemic Threat of Zika Virus. PLoS Neglected Tropical Diseases [Internet]. 2016 Aug 25 [cited 2021 Sep 7];10(8). Available from: /pmc/articles/PMC5001720/

39. Oster AM. Update: Interim Guidance for Prevention of Sexual Transmission of Zika Virus — United States, 2016. MMWR Morbidity and Mortality Weekly Report. 2019 Mar 25;65(12).

40. Matusali G, Houzet L, Satie A-P, Mahé D, Aubry F, Couderc T, et al. Zika virus infects human testicular tissue and germ cells. The Journal of Clinical Investigation [Internet]. 2018 Oct 1 [cited 2021 Sep 8];128(10):4697. Available from: /pmc/articles/PMC6159993/

41. Joguet G, Mansuy J-M, Matusali G, Hamdi S, Walschaerts M, Pavili L, et al. Effect of acute Zika virus infection on sperm and virus clearance in body fluids: a prospective observational study. The Lancet Infectious Diseases [Internet]. 2017 Nov 1 [cited 2021 Sep 8];17(11):1200–8. Available from: http://www.thelancet.com/article/S1473309917304449/fulltext

42. Mansuy JM, Dutertre M, Mengelle C, Fourcade C, Marchou B, Delobel P, et al. Zika virus: high infectious viral load in semen, a new sexually transmitted pathogen? The Lancet Infectious Diseases. 2016 Apr 1;16(4):405.

43. Brooks RB. Likely Sexual Transmission of Zika Virus from a Man with No Symptoms of Infection — Maryland, 2016. MMWR Morbidity and Mortality Weekly Report. 2019 Sep 2;65(34):915–6.

44. D'Ortenzio E, Matheron S, de Lamballerie X, Hubert B, Piorkowski G, Maquart M, et al. Evidence of Sexual Transmission of Zika Virus. https://doi.org/101056/NEJMc1604449 [Internet]. 2016 Apr 13 [cited 2021 Sep 9];374(22):2195–8. Available from: https://www.nejm.org/doi/10.1056/NEJMc1604449

45. Petersen EE. Update: Interim Guidance for Preconception Counseling and Prevention of Sexual Transmission of Zika Virus for Persons with Possible Zika Virus Exposure — United States, September 2016. MMWR Morbidity and Mortality Weekly Report. 2019 Oct 7;65(39):1077–81.

46. Rasmussen SA, Jamieson DJ, Honein MA, Petersen LR. Zika Virus and Birth Defects — Reviewing the Evidence for Causality. New England Journal of Medicine. 2016 May 19;374(20):1981–7.

47. Paploski IAD, Prates APPB, Cardoso CW, Kikuti M, Silva MMO, Waller LA, et al. Time Lags between Exanthematous Illness Attributed to Zika Virus, Guillain-Barré Syndrome, and Microcephaly, Salvador,

Brazil. Emerging Infectious Diseases [Internet]. 2016 Aug 1 [cited 2021 Sep 8];22(8):1438. Available from: /pmc/articles/PMC4982160/

48. Rubin EJ, Greene MF, Baden LR. Zika Virus and Microcephaly. New England Journal of Medicine. 2016 Mar 10;374(10):984–5.

49. Stanelle-Bertram S, Walendy-Gnirß K, Speiseder T, Thiele S, Asante IA, Dreier C, et al. Male offspring born to mildly ZIKV-infected mice are at risk of developing neurocognitive disorders in adulthood. Nature Microbiology 2018 3:10 [Internet]. 2018 Sep 10 [cited 2021 Sep 8];3(10):1161–74. Available from: https://www.nature.com/articles/s41564-018-0236-1

50. Kikuti M, Cardoso CW, Prates APB, Paploski IAD, Kitron U, Reis MG, et al. Congenital brain abnormalities during a Zika virus epidemic in Salvador, Brazil, April 2015 to July 2016. Eurosurveillance [Internet]. 2018 Nov 8 [cited 2021 Sep 8];23(45):1. Available from: /pmc/articles/PMC6234531/

51. Sarno M, Sacramento GA, Khouri R, Rosário MS do, Costa F, Archanjo G, et al. Zika Virus Infection and Stillbirths: A Case of Hydrops Fetalis, Hydranencephaly and Fetal Demise. PLoS Neglected Tropical Diseases [Internet]. 2016 Feb 25 [cited 2021 Sep 9];10(2). Available from: /pmc/articles/PMC4767410/

52. Boeuf P, Drummer HE, Richards JS, Scoullar MJL, Beeson JG. The global threat of Zika virus to pregnancy: epidemiology, clinical perspectives, mechanisms, and impact. BMC Medicine [Internet]. 2016 Aug 3 [cited 2021 Sep 9];14(1). Available from: /pmc/articles/PMC4973112/

53. Brasil P, Pereira JP, Jr., Moreira ME, Nogueira RMR, Damasceno L, et al. Zika Virus Infection in Pregnant Women in Rio de Janeiro. The New England journal of medicine [Internet]. 2016 Dec 15 [cited 2021 Sep 9];375(24):2321. Available from: /pmc/articles/PMC5323261/

54. Dupont-Rouzeyrol M, Biron A, O'Connor O, Huguon E, Descloux E. Infectious Zika viral particles in breastmilk. The Lancet. 2016 Mar 12;387(10023):1051.

55. Rathore APS, Saron WAA, Lim T, Jahan N, John AL st. Maternal immunity and antibodies to dengue virus promote infection and Zika virus–induced microcephaly in fetuses. Science Advances [Internet]. 2019 Feb 27 [cited 2021 Sep 8];5(2):3208. Available from: /pmc/articles/PMC6392794/

56. Brown JA, Singh G, Acklin JA, Lee S, Duehr JE, Chokola AN, et al. Dengue Virus Immunity Increases Zika Virus-Induced Damage during Pregnancy. Immunity [Internet]. 2019 Mar 19 [cited 2021 Sep 8];50(3):751. Available from: /pmc/articles/PMC6947917/

57. Rasmussen SA, Jamieson DJ, Honein MA, Petersen LR. Zika Virus and Birth Defects — Reviewing the Evidence for Causality. New England Journal of Medicine. 2016 May 19;374(20):1981–7.

58. Johansson MA, Mier-y-Teran-Romero L, Reefhuis J, Gilboa SM, Hills SL. Risk estimates for microcephaly related to Zika virus infection - from French Polynesia to Bahia, Brazil. bioRxiv [Internet]. 2016 May 2 [cited 2021 Sep 9];051060. Available from: https://www.biorxiv.org/content/10.1101/051060v1

59. França GVA, Schuler-Faccini L, Oliveira WK, Henriques CMP, Carmo EH, Pedi VD, et al. Congenital Zika virus syndrome in Brazil: a case series of the first 1501 livebirths with complete investigation. The Lancet. 2016 Aug 27;388(10047):891–7.

60. Vasquez AM. Survey of Blood Collection Centers and Implementation of Guidance for Prevention of Transfusion-Transmitted Zika Virus Infection — Puerto Rico, 2016. MMWR Morbidity and Mortality Weekly Report. 2019 Apr 15;65(14):375–8.

61. Musso D, Nhan T, Robin E, Roche C, Bierlaire D, Zisou K, et al. Potential for Zika virus transmission through blood transfusion demonstrated during an outbreak in French Polynesia, November 2013 to February 2014. Eurosurveillance [Internet]. 2014 Apr 10 [cited 2021 Sep 8];19(14):20761. Available from: https://www.eurosurveillance.org/content/10.2807/1560-7917.ES2014.19.14.20761

62. Chan JFW, Choi GKY, Yip CCY, Cheng VCC, Yuen K-Y. Zika fever and congenital Zika syndrome: An unexpected emerging arboviral disease. The Journal of Infection [Internet]. 2016 May 1 [cited 2021 Sep 8];72(5):507. Available from: /pmc/articles/PMC7112603/

63. Buckley A, Gould EA. Detection of Virus-specific Antigen in the Nuclei or Nucleoli of Cells Infected with Zika or Langat Virus. Journal of General Virology [Internet]. 1988 Aug 1 [cited 2021 Sep 8];69(8):1913–20. Available from: https://www.microbiologyresearch.org/content/journal/jgv/10.1099/0022-1317-69-8-1913

64. How maternal Zika virus infection results in newborn microcephaly – Scienmag: Latest Science and Health News [Internet]. [cited 2021 Sep 8]. Available from: https://scienmag.com/how-maternal-zika-virus-infection-results-in-newborn-microcephaly/

65. Rakic P. Evolution of the neocortex: Perspective from developmental biology. Nature reviews Neuroscience [Internet]. 2009 Oct [cited 2021 Sep 9];10(10):724. Available from: /pmc/articles/PMC2913577/

66. Li H, Saucedo-Cuevas L, Shresta S, Gleeson JG. The Neurobiology of Zika Virus. Neuron. 2016 Dec 7;92(5):949–58.

67. Merfeld E, Ben-Avi L, Kennon M, Cerveny KL. Potential mechanisms of Zika-linked microcephaly. Wiley Interdisciplinary Reviews Developmental Biology [Internet]. 2017 Jul 1 [cited 2021 Sep 9];6(4):273. Available from: /pmc/articles/PMC5516183/

68. Harsh S, Fu Y, Kenney E, Han Z, Eleftherianos I. Zika virus non-structural protein NS4A restricts eye growth in Drosophila through regulation of JAK/STAT signaling. Disease Models & Mechanisms [Internet]. 2020 Apr 1 [cited 2021 Sep 8];13(4). Available from: /pmc/articles/PMC7197722/

69. Bullerdiek J, Dotzauer A, Bauer I. The mitotic spindle: linking teratogenic effects of Zika virus with human genetics? Molecular Cytogenetics [Internet]. 2016 [cited 2021 Sep 9];9(1). Available from: /pmc/articles/PMC4837584/

70. Zika virus [Internet]. [cited 2021 Sep 9]. Available from: https://www.who.int/en/news-room/fact-sheets/detail/zika-virus

71. Zika virus disease [Internet]. [cited 2021 Sep 9]. Available from: https://www.ecdc.europa.eu/en/zika-virus-disease

72. Musso D, Nilles EJ, Cao-Lormeau VM. Rapid spread of emerging Zika virus in the Pacific area. Clinical Microbiology and Infection. 2014 Oct 1;20(10):O595–6.

73. Symptoms, Testing, & Treatment | Zika virus | CDC [Internet]. [cited 2021 Sep 9]. Available from: https://www.cdc.gov/zika/symptoms/

74. Dhiman G, Abraham R, Griffin DE. Human Schwann cells are susceptible to infection with Zika and yellow fever viruses, but not dengue virus. Scientific Reports [Internet]. 2019 Dec 1 [cited 2021 Sep 9];9(1). Available from: /pmc/articles/PMC6616448/

75. Frontera JA, da Silva IRF. Zika Getting on Your Nerves? The Association with the Guillain–Barré Syndrome. New England Journal of Medicine. 2016 Oct 20;375(16):1581–2.

76. Foy BD, Kobylinski KC, Foy JLC, Blitvich BJ, Rosa AT da, Haddow AD, et al. Probable Non–Vector-borne Transmission of Zika Virus, Colorado, USA. Emerging Infectious Diseases [Internet]. 2011 [cited 2021 Sep 9];17(5):880. Available from: /pmc/articles/PMC3321795/

77. WHO Director-General summarizes the outcome of the Emergency Committee regarding clusters of microcephaly and Guillain-Barré syndrome [Internet]. [cited 2021 Sep 9]. Available from: https://www.who.int/news/item/01-02-2016-who-director-general-summarizes-the-outcome-of-the-emergency-committee-regarding-clusters-of-microcephaly-and-guillain-barr%c3%a9-syndrome

78. 2019 Case Counts in the US | Zika Virus | CDC [Internet]. [cited 2021 Sep 9]. Available from: https://www.cdc.gov/zika/reporting/2019-case-counts.html/

79. Barouch DH, Thomas SJ, Michael NL. Prospects for a Zika Virus Vaccine. Immunity [Internet]. 2017 Feb 21 [cited 2021 Sep 7];46(2):176. Available from: /pmc/articles/PMC5357134/

80. Saiz J-C, Martín-Acebes MA, Bueno-Marí R, Salomón OD, Villamil-Jiménez LC, Heukelbach J, et al. Zika Virus: What Have We Learnt Since the Start of the Recent Epidemic? Frontiers in Microbiology [Internet]. 2017 Aug 22 [cited 2021 Sep 7];8(AUG). Available from: /pmc/articles/PMC5572254/

81. Priyamvada L, Hudson W, Ahmed R, Wrammert J. Humoral cross-reactivity between Zika and dengue viruses: implications for protection and pathology. Emerging Microbes & Infections [Internet]. 2017 [cited 2021 Sep 7];6(5):e33. Available from: /pmc/articles/PMC5520485/

82. Ghaffar KA, Ng LFP, Renia L. Fast Tracks and Roadblocks for Zika Vaccines. Vaccines [Internet]. 2018 Dec 1 [cited 2021 Sep 7];6(4). Available from: /pmc/articles/PMC6313897/

83. Abbink P, Stephenson KE, Barouch DH. Zika virus vaccines. Nature reviews Microbiology [Internet]. 2018 Oct 1 [cited 2021 Sep 7];16(10):594. Available from: /pmc/articles/PMC6162149/

84. Fernandez E, Diamond MS. Vaccination Strategies against Zika virus. Current opinion in virology [Internet]. 2017 Apr 1 [cited 2021 Sep 7];23:59. Available from: /pmc/articles/PMC5576498/

85. Wikan N, Smith DR. Zika virus: history of a newly emerging arbovirus. The Lancet Infectious Diseases. 2016 Jul 1;16(7):e119–26.

86. Zika virus: US scientists say vaccine “10 years away” - BBC News [Internet]. [cited 2021 Sep 7]. Available from: https://www.bbc.com/news/world-us-canada-35423288

87. Inovio set for first Zika vaccine human trial | FiercePharma [Internet]. [cited 2021 Sep 7]. Available from: https://www.fiercepharma.com/vaccines/inovio-set-for-first-zika-vaccine-human-trial

88. Phase 2 Zika Vaccine Trial Begins in U.S., Central and South America | NIH: National Institute of Allergy and Infectious Diseases [Internet]. [cited 2021 Sep 7]. Available from: https://www.niaid.nih.gov/news-events/phase-2-zika-vaccine-trial-begins-us-central-and-south-america

89. Dowd KA, Ko S-Y, Morabito KM, Yang ES, Pelc RS, DeMaso CR, et al. Rapid Development of a DNA Vaccine for Zika Virus. Science (New York, NY) [Internet]. 2016 Oct 14 [cited 2021 Sep 7];354(6309):237. Available from: /pmc/articles/PMC5304212/

90. Phase 2 Zika vaccine trial begins in U.S., Central and South America | National Institutes of Health (NIH) [Internet]. [cited 2021 Sep 7]. Available from: https://www.nih.gov/news-events/news-releases/phase-2-zika-vaccine-trial-begins-us-central-south-america

91. Fernandez E, Diamond MS. Vaccination Strategies against Zika virus. Current opinion in virology [Internet]. 2017 Apr 1 [cited 2021 Sep 7];23:59. Available from: /pmc/articles/PMC5576498/

92. Lecouturier V, Pavot V, Berry C, Donadieu A, Montfort A de, Boudet F, et al. An optimized purified inactivated Zika vaccine provides sustained immunogenicity and protection in cynomolgus macaques. NPJ Vaccines [Internet]. 2020 Dec 1 [cited 2021 Sep 7];5(1). Available from: /pmc/articles/PMC7067768/

93. Modjarrad K, Lin L, George SL, Stephenson KE, Eckels KH, de La Barrera RA, et al. Preliminary aggregate safety and immunogenicity results from three trials of a purified inactivated Zika virus vaccine candidate: phase 1, randomised, double-blind, placebo-controlled clinical trials. The Lancet. 2018 Feb 10;391(10120):563–71.

94. Zika Virus Vaccines | NIH: National Institute of Allergy and Infectious Diseases [Internet]. [cited 2021 Sep 7]. Available from: https://www.niaid.nih.gov/diseases-conditions/zika-vaccines

95. Fernandez E, Diamond MS. Vaccination Strategies against Zika virus. Current opinion in virology [Internet]. 2017 Apr 1 [cited 2021 Sep 7];23:59. Available from: /pmc/articles/PMC5576498/

96. Zika-Vaccine Dose Finding Study Regarding Safety, Immunogenicity and Tolerability (V186-001) - Full Text View - ClinicalTrials.gov [Internet]. [cited 2021 Sep 7]. Available from: https://clinicaltrials.gov/ct2/show/NCT02996890

97. A Study to Evaluate the Safety, Reactogenicity and Immunogenicity of Ad26.ZIKV.001 in Healthy Adult Volunteers - Full Text View - ClinicalTrials.gov [Internet]. [cited 2021 Sep 7]. Available from: https://clinicaltrials.gov/ct2/show/NCT03356561

98. Baden LR, Karita E, Mutua G, Bekker L-G, Gray G, Page-Shipp L, et al. Assessment of the Safety and Immunogenicity of 2 Novel Vaccine Platforms for HIV-1 Prevention: A Randomized Trial. Annals of internal medicine [Internet]. 2016 Mar 1 [cited 2021 Sep 7];164(5):313. Available from: /pmc/articles/PMC5034222/

99. Whitehorn J, Van VCN, Simmons CP. Dengue Human Infection Models Supporting Drug Development. The Journal of Infectious Diseases [Internet]. 2014 Jun 15 [cited 2021 Sep 7];209(Suppl 2):S66. Available from: /pmc/articles/PMC4036389/

100. V A, N V. Guillain-Barré syndrome. Primary care [Internet]. 2015 Jun 1 [cited 2021 Sep 7];42(2):189–93. Available from: https://pubmed.ncbi.nlm.nih.gov/25979580/

101. AC G, O O, E C, C G, M D-R. Detection of Zika virus in urine. Emerging infectious diseases [Internet]. 2015 [cited 2021 Sep 8];21(1):84–6. Available from: https://pubmed.ncbi.nlm.nih.gov/25530324/

102. D M, C R, TX N, E R, A T, VM C-L. Detection of Zika virus in saliva. Journal of clinical virology : the official publication of the Pan American Society for Clinical Virology [Internet]. 2015 Jul 1 [cited 2021 Sep 8];68:53–5. Available from: https://pubmed.ncbi.nlm.nih.gov/26071336/

103. Waggoner JJ, Pinsky BA. Zika Virus: Diagnostics for an Emerging Pandemic Threat. Journal of Clinical Microbiology [Internet]. 2016 Apr 1 [cited 2021 Sep 9];54(4):860. Available from: /pmc/articles/PMC4809954/

104. Interim Guidance for Zika Virus Testing of Urine — United States, 2016. MMWR Morbidity and Mortality Weekly Report. 2019 May 13;65(18):474.

105. RS L, OL K, JJ L, JO V, AJ L, AJ J, et al. Genetic and serologic properties of Zika virus associated with an epidemic, Yap State, Micronesia, 2007. Emerging infectious diseases [Internet]. 2008 Aug [cited 2021 Sep 8];14(8):1232–9. Available from: https://pubmed.ncbi.nlm.nih.gov/18680646/

106. KL M, DL H, N J, L L, ADT B, DJ S, et al. Flavivirus-induced antibody cross-reactivity. The Journal of general virology [Internet]. 2011 Dec [cited 2021 Sep 8];92(Pt 12):2821–9. Available from: https://pubmed.ncbi.nlm.nih.gov/21900425/

107. MR D, TH C, WT H, AM P, JL K, RS L, et al. Zika virus outbreak on Yap Island, Federated States of Micronesia. The New England journal of medicine [Internet]. 2009 Jun 11 [cited 2021 Sep 8];360(24):2536–43. Available from: https://pubmed.ncbi.nlm.nih.gov/19516034/

108. Lanciotti RS, Kosoy OL, Laven JJ, Velez JO, Lambert AJ, Johnson AJ, et al. Genetic and Serologic Properties of Zika Virus Associated with an Epidemic, Yap State, Micronesia, 2007 - Volume 14, Number 8—August 2008 - Emerging Infectious Diseases journal - CDC. Emerging Infectious Diseases [Internet]. 2008 Aug [cited 2021 Sep 8];14(8):1232–9. Available from: https://wwwnc.cdc.gov/eid/article/14/8/08-0287_article

109. Zika diagnostic test granted market authorization by FDA – Washington University School of Medicine in St. Louis [Internet]. [cited 2021 Sep 9]. Available from: https://medicine.wustl.edu/news/zika-diagnostic-test-granted-market-authorization-by-fda/

110. GP S. Filamentous fusion phage: novel expression vectors that display cloned antigens on the virion surface. Science (New York, NY) [Internet]. 1985 [cited 2021 Sep 10];228(4705):1315–7. Available from: https://pubmed.ncbi.nlm.nih.gov/4001944/

111. Malys N, Chang DY, Baumann RG, Xie D, Black LW. A Bipartite Bacteriophage T4 SOC and HOC Randomized Peptide Display Library: Detection and Analysis of Phage T4 Terminase (gp17) and Late σ Factor (gp55) Interaction. Journal of Molecular Biology. 2002 May 31;319(2):289–304.

112. Smith GP. Filamentous fusion phage: Novel expression vectors that display cloned antigens on the virion surface. Science. 1985;228(4705):1315–7.

113. Parmley SF, Smith GP. Antibody-selectable filamentous fd phage vectors: affinity purification of target genes. Gene. 1988 Dec 20;73(2):305–18.

114. Scott JK, Smith GP. Searching for peptide ligands with an epitope library. Science. 1990;249(4967):386–90.

115. Lunder M, Bratkovič T, Urleb U, Kreft S, Štrukelj B. Ultrasound in phage display: a new approach to nonspecific elution. BioTechniques. 2008 Jun 16;44(7):893–900.

116. Eliminating helper phage from phage display [Internet]. [cited 2020 May 18]. Available from: https://www.ncbi.nlm.nih.gov/pmc/articles/PMC1693883/

117. Leow C, Fischer K, Leow C, Cheng Q, Chuah C, McCarthy J. Single Domain Antibodies as New Biomarker Detectors. Diagnostics. 2017 Oct 17;7(4):52.

118. Keen EC. Phage Therapy: Concept to Cure. Frontiers in Microbiology [Internet]. 2012 [cited 2021 Sep 10];3(JUL). Available from: /pmc/articles/PMC3400130/

119. Novel Phage Therapy Saves Patient with Multidrug-Resistant Bacterial Infection [Internet]. [cited 2021 Sep 10]. Available from: https://health.ucsd.edu/news/releases/Pages/2017-04-25-novel-phage-therapy-saves-patient-with-multidrug-resistant-bacterial-infection.aspx

120. Wommack KE, Colwell RR. Virioplankton: Viruses in Aquatic Ecosystems. Microbiology and Molecular Biology Reviews [Internet]. 2000 Mar [cited 2021 Sep 10];64(1):69. Available from: /pmc/articles/PMC98987/

121. Sweere JM, Belleghem JD van, Ishak H, Bach MS, Popescu M, Sunkari V, et al. Bacteriophage trigger antiviral immunity and prevent clearance of bacterial infection. Science (New York, NY) [Internet]. 2019 Mar 29 [cited 2021 Sep 10];363(6434). Available from: /pmc/articles/PMC6656896/

122. Hay ID, Lithgow T. Filamentous phages: masters of a microbial sharing economy. EMBO Reports [Internet]. 2019 Jun [cited 2021 Sep 10];20(6). Available from: /pmc/articles/PMC6549030/

123. Mai-Prochnow A, Hui JGK, Kjelleberg S, Rakonjac J, McDougald D, Rice SA. 'Big things in small packages: the genetics of filamentous phage and effects on fitness of their host.' FEMS Microbiology Reviews [Internet]. 2015 Jul 1 [cited 2021 Sep 10];39(4):465–87. Available from: https://academic.oup.com/femsre/article/39/4/465/2467559

124. Roux S, Krupovic M, Daly RA, Borges AL, Nayfach S, Schulz F, et al. Cryptic inoviruses revealed as pervasive in bacteria and archaea across Earth's biomes. Nature Microbiology [Internet]. 2019 Nov 1 [cited 2021 Sep 10];4(11):1895. Available from: /pmc/articles/PMC6813254/

125. Smeal SW, Schmitt MA, Pereira RR, Prasad A, Fisk JD. Simulation of the M13 life cycle I: Assembly of a genetically-structured deterministic chemical kinetic simulation. Virology. 2017 Jan 1;500:259–74.

126. Rakonjac J, Das B, Derda R. Editorial: Filamentous Bacteriophage in Bio/Nano/Technology, Bacterial Pathogenesis and Ecology. Frontiers in Microbiology [Internet]. 2016 [cited 2021 Sep 10];7(DEC):2109. Available from: /pmc/articles/PMC5179506/

127. Khalil AS, Ferrer JM, Brau RR, Kottmann ST, Noren CJ, Lang MJ, et al. From the Cover: Single M13 bacteriophage tethering and stretching. Proceedings of the National Academy of Sciences of the United States of America [Internet]. 2007 Mar 20 [cited 2021 Sep 10];104(12):4892. Available from: /pmc/articles/PMC1829235/

128. Esvelt KM, Carlson JC, Liu DR. A System for the Continuous Directed Evolution of Biomolecules. Nature [Internet]. 2011 Apr 28 [cited 2021 Sep 10];472(7344):499. Available from: /pmc/articles/PMC3084352/

129. Suthiwangcharoen N, Li T, Li K, Thompson P, You S, Wang Q. M13 bacteriophage-polymer nanoassemblies as drug delivery vehicles. Nano Research 2011 4:5 [Internet]. 2011 Feb 17 [cited 2021 Sep 10];4(5):483–93. Available from: https://link.springer.com/article/10.1007/s12274-011-0104-2

130. Sattar S, Bennett NJ, Wen WX, Guthrie JM, Blackwell LF, Conway JF, et al. Ff-nano, short functionalized nanorods derived from Ff (f1, fd, or M13) filamentous bacteriophage. Frontiers in Microbiology [Internet]. 2015 [cited 2021 Sep 10];6(MAR). Available from: /pmc/articles/PMC4403547/

131. TA R, B J, U K. Protein transport across the eukaryotic endoplasmic reticulum and bacterial inner membranes. Annual review of biochemistry [Internet]. 1996 [cited 2021 Sep 10];65:271–303. Available from: https://pubmed.ncbi.nlm.nih.gov/8811181/

132. Ploss M, Kuhn A. Kinetics of filamentous phage assembly. Physical Biology. 2010;7(4).

133. Efimov VP, Nepluev I v., Mesyanzhinov V v. Bacteriophage T4 as a surface display vector. Virus Genes 1995 10:2 [Internet]. 1995 [cited 2021 Sep 11];10(2):173–7. Available from: https://link.springer.com/article/10.1007/BF01702598

134. Ren ZJ, Lewis GK, Wingfield PT, Locke EG, Steven AC, Black LW. Phage display of intact domains at high copy number: a system based on SOC, the small outer capsid protein of bacteriophage T4. Protein Science : A Publication of the Protein Society [Internet]. 1996 [cited 2021 Sep 11];5(9):1833. Available from: /pmc/articles/PMC2143533/?report=abstract

135. Smith GP. Filamentous fusion phage: Novel expression vectors that display cloned antigens on the virion surface. Science. 1985;228(4705):1315–7.

136. SF P, GP S. Antibody-selectable filamentous fd phage vectors: affinity purification of target genes. Gene [Internet]. 1988 Dec 20 [cited 2021 Sep 11];73(2):305–18. Available from: https://pubmed.ncbi.nlm.nih.gov/3149606/

137. J G, AE W, RN P. Multiple display of foreign peptides on a filamentous bacteriophage. Peptides from Plasmodium falciparum circumsporozoite protein as antigens. Journal of molecular biology [Internet]. 1991 Aug 20 [cited 2021 Sep 11];220(4):821–7. Available from: https://pubmed.ncbi.nlm.nih.gov/1880799/

138. VA P, GP S, X G, T Q. A library of organic landscapes on filamentous phage. Protein engineering [Internet]. 1996 [cited 2021 Sep 11];9(9):797–801. Available from: https://pubmed.ncbi.nlm.nih.gov/8888146/

139. LS J, JH M, A DK, D E, I V den B, YG G, et al. Surface expression and ligand-based selection of cDNAs fused to filamentous phage gene VI. Bio/technology (Nature Publishing Company) [Internet]. 1995 [cited 2021 Sep 11];13(4):378–82. Available from: https://pubmed.ncbi.nlm.nih.gov/9634780/

140. Cho W, Fowler JD, Furst EM. Targeted binding of the M13 bacteriophage to thiamethoxam organic crystals. Langmuir. 2012 Apr 10;28(14):6013–20.

141. Hess GT, Cragnolini JJ, Popp MW, Allen MA, Dougan SK, Spooner E, et al. M13 bacteriophage display framework that allows sortase-mediated modification of surface-accessible phage proteins. Bioconjugate Chemistry. 2012 Jul 18;23(7):1478–87.

142. Fagerlund A, Myrset AH, Kulseth MA. Construction and characterization of a 9-mer phage display pVIII-library with regulated peptide density. Applied Microbiology and Biotechnology. 2008 Oct;80(5):925–36.

143. Li L, Arumuganathan K, Gill KS, Song Y. Flow sorting and microcloning of maize chromosome 1. Hereditas. 2004;141(1):55–60.

144. Garbe D, Thiel I V., Mootz HD. Protein trans-splicing on an M13 bacteriophage: Towards directed evolution of a semisynthetic split intein by phage display. Journal of Peptide Science. 2010 Oct;16(10):575–81.

145. Oh M young, Joo H yoo, Hur B ung, Jeong Y ho, Cha S hoon. Enhancing phage display of antibody fragments using gIII-amber suppression. Gene. 2007 Jan 15;386(1–2):81–9.

146. Rondot S, Koch J, Breitling F, Dübel S. A helper phage to improve single-chain antibody presentation in phage display. Nature Biotechnology. 2001;19(1):75–8.

147. Sidhu SS, Weiss GA, Wells JA. High copy display of large proteins on phage for functional selections. Journal of Molecular Biology. 2000 Feb 18;296(2):487–95.

148. Løset GÅ, Bogen B, Sandlie I. Expanding the Versatility of Phage Display I: Efficient Display of Peptide-Tags on Protein VII of the Filamentous Phage. Neylon C, editor. PLoS ONE. 2011 Feb 24;6(2):e14702.

149. Løset GÅ, Roos N, Bogen B, Sandlie I. Expanding the Versatility of Phage Display II: Improved Affinity Selection of Folded Domains on Protein VII and IX of the Filamentous Phage. Neylon C, editor. PLoS ONE. 2011 Feb 24;6(2):e17433.

150. Fuh G, Pisabarro MT, Li Y, Quan C, Lasky LA, Sidhu SS. Analysis of PDZ domain-ligand interactions using carboxyl-terminal phage display. Journal of Biological Chemistry. 2000 Jul 14;275(28):21486–91.

151. Speck J, Arndt KM, Müller KM. Efficient phage display of intracellularly folded proteins mediated by the TAT pathway. Protein engineering, design & selection : PEDS. 2011 Jun;24(6):473–84.

152. Krumpe LRH, Atkinson AJ, Smythers GW, Kandel A, Schumacher KM, McMahon JB, et al. T7 lytic phage-displayed peptide libraries exhibit less sequence bias than M13 filamentous phage-displayed peptide libraries. Proteomics. 2006 Aug;6(15):4210–22.

153. Kang HT, Bang WK, Yu YG. Identification and characterization of a novel angiostatin-binding protein by the display cloning method. Journal of Biochemistry and Molecular Biology. 2004 Mar 31;37(2):159–66.

154. Ishi K, Sugawara F. A facile method to screen inhibitors of protein-protein interactions including MDM2-p53 displayed on T7 phage. Biochemical Pharmacology. 2008 May 1;75(9):1743–50.

155. Wu J, Tu C, Yu X, Zhang M, Zhang N, Zhao M, et al. Bacteriophage T4 nanoparticle capsid surface SOC and HOC bipartite display with enhanced classical swine fever virus immunogenicity: A powerful immunological approach. Journal of Virological Methods. 2007 Jan;139(1):50–60.

156. Cicchini C, Ansuini H, Amicone L, Alonzi T, Nicosia A, Cortese R, et al. Searching for DNA-protein interactions by lambda phage display. Journal of molecular biology. 2002 Sep 27;322(4):697–706.

157. Gao J, Wang Y, Liu Z, Wang Z. Phage display and its application in vaccine design. Vol. 60, Annals of Microbiology. BioMed Central; 2010. p. 13–9.

158. HM G, SJ R, TJ M. A priori delineation of a peptide which mimics a discontinuous antigenic determinant. Molecular immunology [Internet]. 1986 [cited 2021 Sep 11];23(7):709–15. Available from: https://pubmed.ncbi.nlm.nih.gov/2432410/

159. HM G, RH M, SJ B. Use of peptide synthesis to probe viral antigens for epitopes to a resolution of a single amino acid. Proceedings of the National Academy of Sciences of the United States of America [Internet]. 1984 Jul 1 [cited 2021 Sep 11];81(13):3998–4002. Available from: https://europepmc.org/articles/PMC345355

160. Saggio I, Gloaguen I, Poiana G, Laufer R. CNTF variants with increased biological potency and receptor selectivity define a functional site of receptor interaction. The EMBO Journal [Internet]. 1995 [cited 2021 Sep 11];14(13):3045. Available from: /pmc/articles/PMC394365/?report=abstract

161. Watkins JD, Beuerlein G, Wu H, McFadden PR, Pancook JD, Huse WD. Discovery of Human Antibodies to Cell Surface Antigens by Capture Lift Screening of Phage-Expressed Antibody Libraries. Analytical Biochemistry. 1998 Feb 15;256(2):169–77.

162. Haaparanta T, Huse WD. A combinatorial method for constructing libraries of long peptides displayed by filamentous phage. Molecular Diversity 1995 1:1 [Internet]. 1995 Sep [cited 2021 Sep 11];1(1):39–52. Available from: https://link.springer.com/article/10.1007/BF01715808

163. Carlsson F, Trilling M, Perez F, Ohlin M. A dimerized single-chain variable fragment system for the assessment of neutralizing activity of phage display-selected antibody fragments specific for cytomegalovirus. Journal of Immunological Methods. 2012 Feb 28;376(1–2):69–78.

164. Wen K, Nölke G, Schillberg S, Wang Z, Zhang S, Wu C, et al. Improved fluoroquinolone detection in ELISA through engineering of a broad-specific single-chain variable fragment binding simultaneously to 20 fluoroquinolones. Analytical and Bioanalytical Chemistry. 2012 Jul;403(9):2771–83.

165. Shimazaki K, Lepin EJ, Wei B, Nagy AK, Coulam CP, Mareninov S, et al. Diabodies targeting epithelial membrane protein 2 reduce tumorigenicity of human endometrial cancer cell lines. Clinical Cancer Research. 2008 Nov 15;14(22):7367–77.

166. Hughes DL, Stafford P, Hamaia SW, Harmer IJ, Schoolmeester A, Deckmyn H, et al. Platelet integrin α2 I-domain specific antibodies produced via domain specific DNA vaccination combined with variable gene phage display. Thrombosis and Haemostasis. 2005 Dec;94(6):1318–26.

167. KAWASAKI T, ONODERA K, KAMIJO S. Identification of Novel Short Peptide Inhibitors of Soluble 37/48 kDa Oligomers of Amyloid β42. Bioscience, Biotechnology, and Biochemistry. 2011 Aug 23;75(8):1496–501.

168. Heskamp S, Van Laarhoven HWM, Molkenboer-Kuenen JDM, Bouwman WH, Van Der Graaf WTA, Oyen WJG, et al. Optimization of IGF-1R SPECT/CT imaging using 111in-labeled F(ab)2 and Fab fragments of the monoclonal antibody R1507. Molecular Pharmaceutics. 2012 Aug 6;9(8):2314–21.

169. Markiv A, Beatson R, Burchell J, Durvasula R V., Kang AS. Expression of recombinant multi-coloured fluorescent antibodies in gor -/trxB -E. coli cytoplasm. BMC Biotechnology. 2011 Nov 30;11(1):117.

170. Tang YM, Ning BT, Cao J, Shen HQ, Qian BQ. Construction and expression of single-chain antibody derived from a new clone of monoclonal antibody against human CD14 in CHO Cells. Immunopharmacology and Immunotoxicology. 2007 Jul;29(3–4):375–86.

171. Neri D, Momo M, Prospero T, Winter G. High-affinity antigen binding by chelating recombinant antibodies (CRAbs). Journal of Molecular Biology. 1995;246(3):367–73.

172. Wright MJ, Deonarain MP. Phage display of chelating recombinant antibody libraries. Molecular Immunology. 2007 Apr 1;44(11):2860–9.

173. Hamers-Casterman C, Atarhouch T, Muyldermans S, Robinson G, Hammers C, Songa EB, et al. Naturally occurring antibodies devoid of light chains. Nature. 1993;363(6428):446–8.

174. Mahgoub IO. Expression and characterization of a functional single-chain variable fragment (scFv) protein recognizing MCF7 breast cancer cells in E. coli cytoplasm. Biochemical Genetics. 2012 Aug;50(7–8):625–41.

175. Sonoda H, Kumada Y, Katsuda T, Yamaji H. Effects of cytoplasmic and periplasmic chaperones on secretory production of single-chain Fv antibody in Escherichia coli. Journal of Bioscience and Bioengineering. 2011 Apr;111(4):465–70.

176. Dahan R, Tabul M, Chou YK, Meza-Romero R, Andrew S, Ferro AJ, et al. TCR-like antibodies distinguish conformational and functional differences in two- versus four-domain auto reactive MHC class II-peptide complexes. European Journal of Immunology. 2011 May;41(5):1465–79.

177. Hughes-Jones NC, Gorick BD, Bye JM, Finnern R, Scott ML, Voak D, et al. Characterization of human blood group scFv antibodies derived from a V gene phage-display library. British Journal of Haematology. 1994;88(1):180–6.

178. Watkins NA, Armour KL, Smethurst PA, Metcalfe P, Scott ML, Hughes DL, et al. Rapid phenotyping of HPA-1a using either diabody-based hemagglutination or recombinant IgG1-based assays. Transfusion. 1999;39(7):781–9.

179. Dogan I, Dorgham K, Chang HC, Parizot C, Lemaître F, Ferradini L, et al. Phage-displayed libraries of peptide/major histocompatibility complexes. European Journal of Immunology. 2004 Feb;34(2):598–607.

180. Finlay WJJ, Bloom L, Cunningham O. Optimized generation of high-affinity, high-specificity single-chain Fv antibodies from multiantigen immunized chickens. Methods in molecular biology (Clifton, NJ). 2011;681:383–401.

181. Charlton K, Harris WJ, Porter AJ. The isolation of super-sensitive anti-hapten antibodies from combinatorial antibody libraries derived from sheep. In: Biosensors and Bioelectronics. 2001. p. 639–46.

182. Hofer T, Tangkeangsirisin W, Kennedy MG, Mage RG, Raiker SJ, Venkatesh K, et al. Chimeric rabbit/human Fab and IgG specific for members of the Nogo-66 receptor family selected for species cross-reactivity with an improved phage display vector. Journal of Immunological Methods. 2007 Jan 10;318(1–2):75–87.

183. Chahboun S, Hust M, Liu Y, Pelat T, Miethe S, Helmsing S, et al. Isolation of a nanomolar scFv inhibiting the endopeptidase activity of botulinum toxin A, by single-round panning of an immune phage-displayed library of macaque origin. BMC Biotechnology. 2011 Nov 23;11.

184. Yang X-D, Jia X-C, Corvalan JRF, Wang P, Davis CG, Jakobovits A. Eradication of Established Tumors by a Fully Human Monoclonal Antibody to the Epidermal Growth Factor Receptor without Concomitant Chemotherapy. Vol. 59, CANCER RESEARCH. 1999.

185. Tabares-Da Rosa S, Rossotti M, Carleiza C, Carrión F, Pritsch O, Ahn KC, et al. Competitive selection from single domain antibody libraries allows isolation of high-affinity antihapten antibodies that are not favored in the llama immune response. Vol. 83, Analytical Chemistry. American Chemical Society; 2011. p. 7213–20.

186. Fu YY, Li ZG, Yang YW, Deng W, Duan W, Miao Q, et al. Isolation of single chain variable fragments against six esters of pyrethrins by subtractive phage display. Bioscience, Biotechnology and Biochemistry. 2009;73(7):1541–9.

187. Moon SA, Ki MK, Lee S, Hong ML, Kim M, Kim S, et al. Antibodies against non-immunizing antigens derived from a large immune scFv library. Molecules and Cells. 2011;31(6):509–13.

188. Vaughan TJ, Williams AJ, Pritchard K, Osbourn JK, Pope AR, Earnshaw JC, et al. Human Antibodies With Sub-Nanomolar Affinities Isolated From A Large Non-Immunized Phage Display Library. Nature Biotechnology. 1996 Mar;14(3):309–14.

189. Babel I, Barderas R, Peláez-García A, Casal JI. Antibodies on demand: A fast method for the production of human scFvs with minimal amounts of antigen. BMC Biotechnology. 2011 Jun 2;11:61.

190. Stoyanova V, Aleksandrov R, Lukarska M, Duhalov D, Atanasov V, Petrova S. Recognition of vipera ammodytes meridionalis neurotoxin vipoxin and its components using phage-displayed scFv and polyclonal antivenom sera. Toxicon. 2012 Oct 1;60(5):802–9.

191. Azzazy HME, Highsmith WE. Phage display technology: Clinical applications and recent innovations. Clinical Biochemistry. 2002 Sep;35(6):425–45.

192. Hughes-Jones N, Bye J, Gorick B, Marks J, Ouwehand W. Synthesis of Rh Fv phage-antibodies using VH and VL germline genes. British Journal of Haematology. 1999 Jun 1;105(3):811–6.

193. Knappik A, Ge L, Honegger A, Pack P, Fischer M, Wellnhofer G, et al. Fully synthetic human combinatorial antibody libraries (HuCAL) based on modular consensus frameworks and CDRs randomized with trinucleotides. Journal of Molecular Biology. 2000 Feb 11;296(1):57–86.

194. Krebs B, Rauchenberger R, Reiffert S, Rothe C, Tesar M, Thomassen E, et al. High-throughput generation and engineering of recombinant human antibodies. Journal of immunological methods. 2001 Aug 1;254(1–2):67–84.

195. Van Den Beucken T, Van Neer N, Sablon E, Desmet J, Celis L, Hoogenboom HR, et al. Building novel binding ligands to B7.1 and B7.2 based on human antibody single variable light chain domains. Journal of Molecular Biology. 2001 Jul 13;310(3):591–601.

196. Chen W, Zhu Z, Feng Y, Dimitrov DS. A large human domain antibody library combining heavy and light chain CDR3 diversity. Molecular Immunology. 2010 Jan;47(4):912–21.

197. Markovic-Plese S, Hemmer B, Zhao Y, Simon R, Pinilla C, Martin R. High level of cross-reactivity in influenza virus hemagglutinin-specific CD4+ T-cell response: Implications for the initiation of autoimmune response in multiple sclerosis. Journal of Neuroimmunology. 2005 Dec;169(1–2):31–8.

198. Chan CEZ, Chan AHY, Lim APC, Hanson BJ. Comparison of the efficiency of antibody selection from semi-synthetic scFv and non-immune Fab phage display libraries against protein targets for rapid development of diagnostic immunoassays. Journal of Immunological Methods. 2011 Oct 28;373(1–2):79–88.

199. and GPS, Petrenko VA. Phage Display. Chemical Reviews [Internet]. 1997 [cited 2021 Sep 11];97(2):391–410. Available from: https://pubs.acs.org/doi/abs/10.1021/cr960065d

200. Lomonosova A V., Laman AG, Fursova KK, Shepelyakovskaya AO, Vertiev Y V., Brovko FA, et al. Generation of scFv phages specific to Staphylococcus enterotoxin C1 by panning on related antigens. mAbs. 2011 Nov;3(6).

201. Liu B, Huang L, Sihlbom C, Burlingame A, Marks JD. Towards proteome-wide production of monoclonal antibody by phage display. Journal of Molecular Biology. 2002;315(5):1063–73.

202. Garet E, Cabado AG, Vieites JM, González-Fernández Á. Rapid isolation of single-chain antibodies by phage display technology directed against one of the most potent marine toxins: Palytoxin. Toxicon. 2010 Jul;55(8):1519–26.

203. Chang C, Takayanagi A, Yoshida T, Shimizu N. Screening of scFv-displaying phages recognizing distinct extracellular domains of EGF receptor by target-guided proximity labeling method. Journal of Immunological Methods. 2011 Sep 30;372(1–2):127–36.

204. Noronha EJ, Wang X, Ferrone S. Isolation of human tumor-associated cell surface antigen-binding scFvs. Vol. 178, Methods in molecular biology (Clifton, N.J.). Humana Press; 2002. p. 227–33.

205. Ph.D.™-12 Phage Display Peptide Library Kit | NEB [Internet]. [cited 2021 Sep 13]. Available from: https://international.neb.com/products/e8110-phd-12-phage-display-peptide-library-kit#Product%20Information

206. Chakravarthy B, Ménard M, Brown L, Atkinson T, Whitfield J. Identification of protein kinase C inhibitory activity associated with a polypeptide isolated from a phage display system with homology to PCM-1, the pericentriolar material-1 protein. Biochemical and Biophysical Research Communications. 2012 Jul 20;424(1):147–51.

207. Rubenwolf S, Niewöhner J, Meyer E, Petit-Frère C, Rudert F, Hoffmann PR, et al. Functional proteomics using chromophore-assisted laser inactivation. Proteomics. 2002;2(3):241–6.

208. Konthur Z, Crameri R. High-throughput applications of phage display in proteomic analyses. Vol. 2, Drug Discovery Today: TARGETS. Elsevier; 2003. p. 261–70.

209. Hallborn J, Carlsson R. Automated screening procedure for high-throughput generation of antibody fragments. BioTechniques. 2002 Dec;Suppl:30–7.

210. Almagro JC, Raghunathan G, Beil E, Janecki DJ, Chen Q, Dinh T, et al. Characterization of a high-affinity human antibody with a disulfide bridge in the third complementarity-determining region of the heavy chain. Journal of Molecular Recognition. 2012 Mar;25(3):125–35.

211. Lunder M, Bratkovič T, Kreft S, Trukelj B. Peptide inhibitor of pancreatic lipase selected by phage display using different elution strategies. Journal of Lipid Research. 2005;46(7):1512–6.

212. Bratkovič T, Lunder M, Popovič T, Kreft S, Turk B, Štrukelj B, et al. Affinity selection to papain yields potent peptide inhibitors of cathepsins L, B, H, and K. Biochemical and Biophysical Research Communications. 2005 Jul 8;332(3):897–903.

213. Lunder M, Bratkovič T, Doljak B, Kreft S, Urleb U, Štrukelj B, et al. Comparison of bacterial and phage display peptide libraries in search of target-binding motif. Applied Biochemistry and Biotechnology. 2005 Nov;127(2):125–31.

214. Hufton SE, Moerkerk PT, Meulemans E V., De Bruïne A, Arends JW, Hoogenboom HR. Phage display of cDNA repertoires: The pVI display system and its applications for the selection of immunogenic ligands. Journal of Immunological Methods. 1999 Dec 10;231(1–2):39–51.

215. Gommans WM, Haisma HJ, Rots MG. Engineering zinc finger protein transcription factors: The therapeutic relevance of switching endogenous gene expression on or off at command. Vol. 354, Journal of Molecular Biology. Academic Press; 2005. p. 507–19.

216. LÃ¸set GÃ, Berntzen G, Frigstad T, Pollmann S, Gunnarsen KS, Sandlie I. Phage Display Engineered T Cell Receptors as Tools for the Study of Tumor Peptideâ€“MHC Interactions. Frontiers in Oncology. 2015 Jan 12;4.

217. Bazan J, Całkosiñski I, Gamian A. Phage display - A powerful technique for immunotherapy. Human Vaccines and Immunotherapeutics. 2012;8(12):1817–28.

218. Marks JD, Ouwehand WH, Bye JM, Finnern R, Gorick BD, Voak D, et al. Human antibody fragments specific for human blood group antigens from a phage display library. Bio/Technology. 1993;11(10):1145–9.

219. Huie MA, Cheung MC, Muench MO, Becerril B, Kan YW, Marks JD. Antibodies to human fetal erythroid cells from a nonimmune phage antibody library. Proceedings of the National Academy of Sciences of the United States of America. 2001 Feb 27;98(5):2682–7.

220. Fitting J, Killian D, Junghanss C, Willenbrock S, Murua Escobar H, Lange S, et al. Generation of recombinant antibody fragments that target canine dendritic cells by phage display technology. Veterinary and Comparative Oncology. 2011 Sep;9(3):183–95.

221. Kreitman RJ, Tallman MS, Robak T, Coutre S, Wilson WH, Stetler-Stevenson M, et al. Phase I trial of anti-CD22 recombinant immunotoxin moxetumomab pasudotox (CAT-8015 or HA22) in patients with hairy cell leukemia. Journal of Clinical Oncology. 2012 May 20;30(15):1822–8.

222. O'Nuallain B, Allen A, Ataman D, Weiss DT, Solomon A, Wall JS. Phage display and peptide mapping of an immunoglobulin light chain fibril-related conformational epitope. Biochemistry. 2007 Nov 13;46(45):13049–58.

223. Maeda M, Ito Y, Hatanaka T, Hashiguchi S, Torikai M, Nakashima T, et al. Regulation of T cell response by blocking the ICOS signal with the B7RP-1-specific small antibody fragment isolated from human antibody phage library. mAbs. 2009;1(5):453–61.

224. Barth S, Huhn M, Matthey B, Tawadros S, Schnell R, Schinköthe T, et al. Ki-4(scFv)–ETA', a new recombinant anti-CD30 immunotoxin with highly specific cytotoxic activity against disseminated Hodgkin tumors in SCID mice. Blood. 2000 Jun 15;95(12):3909–14.

225. Löffler A, Kufer P, Lutterbüse R, Zettl F, Daniel PT, Schwenkenbecher JM, et al. A recombinant bispecific single-chain antibody, CD19 x CD3, induces rapid and high lymphoma-directed cytotoxicity by unstimulated T lymphocytes. Blood. 2000 Mar 15;95(6):2098–103.

226. Chu XX, Hou M, Peng J, Zhu YY, Ji XH, Wang L, et al. Effects of IgG and its F(ab')2 fragments of some patients with idiopathic thrombocytopenic purpura on platelet aggregation. European Journal of Haematology. 2006 Feb;76(2):153–9.

227. Tsuruta LR, Tomioka Y, Hishinuma T, Kato Y, Itoh K, Suzuki T, et al. Characterization of 11-dehydro-thromboxane B2 recombinant antibody obtained by phage display technology. Prostaglandins Leukotrienes and Essential Fatty Acids. 2003 Apr 1;68(4):273–84.

228. Suggett S, Kirchhofer D, Hass P, Lipari T, Moran P, Nagel M, et al. Use of phage display for the generation of human antibodies that neutralize factor IXa function. Blood Coagulation and Fibrinolysis. 2000;11(1):27–42.

229. Gevorkian G, Manoutcharian K, Almagro JC, Govezensky T, Dominguez V. Identification of autoimmune thrombocytopenic purpura-related epitopes using phage-display peptide library. Clinical Immunology and Immunopathology. 1998;86(3):305–9.

230. Kim Y, Caberoy NB, Alvarado G, Davis JL, Feuer WJ, Li W. Identification of Hnrph3 as an autoantigen for acute anterior uveitis. Clinical Immunology. 2011 Jan;138(1):60–6.

231. Luken BM, Kaijen PHP, Turenhout EAM, Kremer Hovinga JA, Van Mourik JA, Fijnheer R, et al. Multiple B-cell clones producing antibodies directed to the spacer and disintegrin/thrombospondin type-1 repeat 1 (TSP1) of ADAMTS13 in a patient with acquired thrombotic thrombocytopenic purpura. Journal of Thrombosis and Haemostasis. 2006 Nov;4(11):2355–64.

232. Zhang Y, Davis JL, Li W. Identification of tribbles homolog 2 as an autoantigen in autoimmune uveitis by phage display. Molecular Immunology. 2005 Jul;42(11):1275–81.

233. Latrofa F, Pichurin P, Guo J, Rapoport B, McLachlan SM. Thyroglobulin-thyroperoxidase autoantibodies are polyreactive, not bispecific: Analysis using human monoclonal autoantibodies. Journal of Clinical Endocrinology and Metabolism. 2003 Jan 1;88(1):371–8.

234. Farilla L, Tiberti C, Luzzago A, Yu L, Eisenbarth GS, Cortese R, et al. Application of phage display peptide library to autoimmune diabetes: identification of IA-2/ICA512bdc dominant autoantigenic epitopes. European Journal of Immunology. 2002 May 1;32(5):1420–7.

235. Finnern R, Pedrollo E, Fisch I, Wieslander J, Marks JD, Lockwood CM, et al. Human autoimmune anti-proteinase 3 scFv from a phage display library. Clinical and Experimental Immunology. 1997;107(2):269–81.

236. Payne AS, Ishii K, Kacir S, Lin C, Li H, Hanakawa Y, et al. Genetic and functional characterization of human pemphigus vulgaris monoclonal autoantibodies isolated by phage display. Journal of Clinical Investigation. 2005;115(4):888–99.

237. Ishii K, Lin C, Siegel DL, Stanley JR. Isolation of pathogenic monoclonal anti-desmoglein 1 human antibodies by phage display of pemphigus foliaceus autoantibodies. Journal of Investigative Dermatology. 2008;128(4):939–48.

238. Ikuno N, Scealy M, Davies JM, Whittingham SF, Omagari K, Mackay IR, et al. A comparative study of antibody expressions in primary biliary cirrhosis and autoimmune cholangitis using phage display. Hepatology. 2001;34(3):478–86.

239. Jensen-Jarolim E, Neumann C, Oberhuber G, Gscheidlinger R, Neuchrist C, Reinisch W, et al. Anti-Galectin-3 IgG autoantibodies in patients with Crohn's disease characterized by means of phage display peptide libraries. Journal of Clinical Immunology. 2001;21(5):348–56.

240. PHAGE ANTIBODY LIBRARY FROM CELIAC DISEASE PATIENT : Journal of Pediatric Gastroenterology and Nutrition [Internet]. [cited 2020 May 1]. Available from: https://journals.lww.com/jpgn/Fulltext/1999/05000/Phage_Antibody_Library_From_Celiac_Disease_Patient.118.aspx

241. Graus YF, De Baets MH, Van Breda Vriesman PJ, Burton DR. Anti-acetylcholine receptor Fab fragments isolated from thymus-derived phage display libraries from myasthenia gravis patients reflect predominant specificities in serum and block the action of pathogenic serum antibodies. Immunology Letters. 1997;57(1–3):59–62.

242. Venkatesh N, Im SH, Balass M, Fuchs S, Katchalski-Katzir E. Prevention of passively transferred experimental autoimmune myasthenia gravis by a phage library-derived cyclic peptide. Proceedings of the National Academy of Sciences of the United States of America. 2000 Jan 18;97(2):761–6.

243. Osbourn J, Jermutus L, Duncan A. Current methods for the generation of human antibodies for the treatment of autoimmune diseases. Drug discovery today. 2003 Sep 15;8(18):845–51.

244. Coles AJ, Cox A, Le Page E, Jones J, Trip SA, Deans J, et al. The window of therapeutic opportunity in multiple sclerosis: Evidence from monoclonal antibody therapy. Journal of Neurology. 2006 Jan;253(1):98–108.

245. Klotz L, Meuth SG, Wiendl H. Immune mechanisms of new therapeutic strategies in multiple sclerosis-A focus on alemtuzumab. Vol. 142, Clinical Immunology. 2012. p. 25–30.

246. Thanongsaksrikul J, Chaicumpa W. Botulinum neurotoxins and botulism: A novel therapeutic approach. Vol. 3, Toxins. 2011. p. 469–88.

247. Škrlj N, Čurin Šerbec V, Dolinar M. Single-chain Fv antibody fragments retain binding properties of the monoclonal antibody raised against peptide P1 of the human prion protein. Applied Biochemistry and Biotechnology. 2010 Mar;160(6):1808–21.

248. Gearhart DA, Toole PF, Beach JW. Identification of brain proteins that interact with 2-methylnorharman: An analog of the parkinsonian-inducing toxin, MPP+. Neuroscience Research. 2002 Nov 1;44(3):255–65.

249. Lecerf JM, Shirley TL, Zhu Q, Kazantsev A, Amersdorfer P, Housman DE, et al. Human single-chain Fv intrabodies counteract in situ huntingtin aggregation in cellular models of Huntington's disease. Proceedings of the National Academy of Sciences of the United States of America. 2001 Apr 10;98(8):4764–9.

250. Kenan DJ, Strittmatter WJ, Burke JR. Phage Display Screening for Peptides that Inhibit Polyglutamine Aggregation. Vol. 413, Methods in Enzymology. 2006. p. 253–73.

251. Solomon B. Active immunization against Alzheimer's β-amyloid peptide using phage display technology. Vaccine. 2007 Apr 20;25(16 SPEC. ISS.):3053–6.

252. Frenkel D, Katz O, Solomon B. Immunization against Alzheimer's β-amyloid plaques via EFRH phage administration. Proceedings of the National Academy of Sciences of the United States of America. 2000 Oct 10;97(21):11455–9.

253. Essler M, Ruoslahti E. Molecular specialization of breast vasculature: A breast-homing phage-displayed peptide binds to aminopeptidase P in breast vasculature. Proceedings of the National Academy of Sciences of the United States of America. 2002 Feb 19;99(4):2252–7.

254. Arap W, Haedicke W, Bernasconi M, Kain R, Rajotte D, Krajewski S, et al. Targeting the prostate for destruction through a vascular address. Proceedings of the National Academy of Sciences of the United States of America. 2002 Feb 5;99(3):1527–31.

255. Gothard D, Tare RS, Mitchell PD, Dawson JI, Oreffo ROC. In search of the skeletal stem cell: Isolation and separation strategies at the macro/micro scale for skeletal regeneration. Lab on a Chip. 2011 Apr 7;11(7):1206–20.

256. Arap W, Kolonin MG, Trepel M, Lahdenranta J, Cardó-Vila M, Giordano RJ, et al. Steps toward mapping the human vasculature by phage display. Nature Medicine. 2002 Feb;8(2):121–7.

257. White SJ, Nicklin SA, Sawamura T, Baker AH. Identification of peptides that target the endothelial cell-specific LOX-1 receptor. Hypertension. 2001;37(2 II):449–55.

258. Gerlag DM, Borges E, Tak PP, Ellerby HM, Bredesen DE, Pasqualini R, et al. Suppression of murine collagen-induced arthritis by targeted apoptosis of synovial neovasculature. Arthritis Research. 2001;3(6):357–61.

259. Kolonin MG, Saha PK, Chan L, Pasqualini R, Arap W. Reversal of obesity by targeted ablation of adipose tissue. Nature Medicine. 2004 Jun;10(6):625–32.

260. Dale L. Boger *,†, Joel Goldberg †, Steve Silletti ‡,§, Torsten Kessler ‡ and, Cheresh‡ DA. Identification of a Novel Class of Small-Molecule Antiangiogenic Agents through the Screening of Combinatorial Libraries Which Function by Inhibiting the Binding and Localization of Proteinase MMP2 to Integrin αVβ3. 2001.

261. Cooke SP, Boxer GM, Lawrence L, Pedley RB, Spencer DI, Begent RH, et al. A strategy for antitumor vascular therapy by targeting the vascular endothelial growth factor: receptor complex. Cancer research. 2001 May 1;61(9):3653–9.

262. Haubner R, Wester HJ, Burkhart F, Senekowitsch-Schmidtke R, Weber W, Goodman SL, et al. Glycosylated RGD-containing peptides: Tracer for tumor targeting and angiogenesis imaging with improved biokinetics. Journal of Nuclear Medicine. 2001;42(2):326–36.

263. Chester KA, Begent RHJ, Robson L, Keep PA, Pedley RB, Boden LIBiol JA, et al. Phage libraries for generation of clinically useful antibodies. The Lancet. 1994 Feb 19;343(8895):455–6.

264. Kelly KA, Jones DA. Isolation of a Colon Tumor Specific Binding Peptide Using Phage Display Selection. Neoplasia. 2003 Sep;5(5):437–44.

265. Pierce MC, Javier DJ, Richards-Kortum R. Optical contrast agents and imaging systems for detection and diagnosis of cancer. Vol. 123, International Journal of Cancer. 2008. p. 1979–90.

266. Reubi JC. Peptide receptors as molecular targets for cancer diagnosis and therapy. Vol. 24, Endocrine Reviews. 2003. p. 389–427.

267. McGuire MJ, Samli KN, Chang YC, Brown KC. Novel ligands for cancer diagnosis: Selection of peptide ligands for identification and isolation of B-cell lymphomas. Experimental Hematology. 2006 Apr;34(4):443–52.

268. Wu C, Lo SL, Boulaire J, Hong MLW, Beh HM, Leung DSY, et al. A peptide-based carrier for intracellular delivery of proteins into malignant glial cells in vitro. Journal of Controlled Release. 2008 Sep 10;130(2):140–5.

269. Characterization and development of a peptide (p160) with affinity for neuroblastoma cells. - PubMed - NCBI [Internet]. [cited 2020 May 4]. Available from: https://www.ncbi.nlm.nih.gov/pubmed/16741308

270. Chang DK, Lin CT, Wu CH, Wu HC. A novel peptide enhances therapeutic efficacy of liposomal anti-cancer drugs in mice models of human lung cancer. PLoS ONE. 2009 Jan 12;4(1):e4171.

271. Du B, Qian M, Zhou Z, Wang P, Wang L, Zhang X, et al. In vitro panning of a targeting peptide to hepatocarcinoma from a phage display peptide library. Biochemical and Biophysical Research Communications. 2006 Apr 14;342(3):956–62.

272. Robinson P, Stuber D, Deryckère F, Tedbury P, Lagrange M, Orfanoudakis G. Identification using phage display of peptides promoting targeting and internalization into HPV-transformed cell lines. Journal of Molecular Recognition. 2005 Mar;18(2):175–82.

273. Rasmussen UB, Schreiber V, Schultz H, Mischler F, Schughart K. Tumor cell-targeting by phage-displayed peptides. Cancer Gene Therapy. 2002;9(7):606–12.

274. Liang S, Lin T, Ding J, Pan Y, Dang D, Guo C, et al. Screening and identification of vascular-endothelial-cell-specific binding peptide in gastric cancer. Journal of Molecular Medicine. 2006 Sep 9;84(9):764–73.

275. Askoxylakis V, Zitzmann S, Mier W, Graham K, Krämer S, Von Wegner F, et al. Preclinical evaluation of the breast cancer cell-binding peptide, p160. Clinical Cancer Research. 2005 Sep 15;11(18):6705–12.

276. Zitzmann S, Mier W, Schad A, Kinscherf R, Askoxylakis V, Krämer S, et al. A new prostate carcinoma binding peptide (DUP-1) for tumor imaging and therapy. Clinical cancer research : an official journal of the American Association for Cancer Research. 2005 Jan 1;11(1):139–46.

277. Zitzmann S, Krämer S, Mier W, Hebling U, Altmann A, Rother A, et al. Identification and evaluation of a new tumor cell-binding peptide, FROP-1. Journal of Nuclear Medicine. 2007 Jun;48(6):965–72.

278. Pazgier M, Liu M, Zou G, Yuan W, Li C, Li C, et al. Structural basis for high-affinity peptide inhibition of p53 interactions with MDM2 and MDMX. Proceedings of the National Academy of Sciences of the United States of America. 2009 Mar 24;106(12):4665–70.

279. Zurita AJ, Troncoso P, Cardó-Vila M, Logothetis CJ, Pasqualini R, Arap W. Combinatorial screenings in patients: the interleukin-11 receptor alpha as a candidate target in the progression of human prostate cancer. Cancer research. 2004 Jan 15;64(2):435–9.

280. Pakkala M, Jylhäsalmi A, Wu P, Leinonen J, Stenman UH, Santa H, et al. Conformational and biochemical analysis of the cyclic peptides which modulate serine protease activity. Journal of Peptide Science. 2004 Jul;10(7):439–47.

281. Kim Y, Lillo AM, Steiniger SCJ, Liu Y, Ballatore C, Anichini A, et al. Targeting heat shock proteins on cancer cells: Selection, characterization, and cell-penetrating properties of a peptidic GRP78 ligand. Biochemistry. 2006 Aug 8;45(31):9434–44.

282. Lei H, An P, Song S, Liu X, He L, Wu J, et al. A novel peptide isolated from a phage display library inhibits tumor growth and metastasis by blocking the binding of vascular endothelial growth factor to its receptor KDR. Journal of Biological Chemistry. 2002.

283. Landon LA, Peletskaya EN, Glinsky V V, Karasseva N, Quinn TP, Deutscher SL. Combinatorial evolution of high-affinity peptides that bind to the Thomsen-Friedenreich carcinoma antigen. Journal of protein chemistry. 2003 Feb;22(2):193–204.

284. Newton JR, Kelly KA, Mahmood U, Weissleder R, Deutscher SL. In vivo selection of phage for the optical imaging of PC-3 human prostate carcinoma in mice. Neoplasia. 2006 Sep;8(9):772–80.

285. Thapa N, Kim S, So IS, Lee BH, Kwon IC, Choi K, et al. Discovery of a phosphatidylserine-recognizing peptide and its utility in molecular imaging of tumour apoptosis. Journal of Cellular and Molecular Medicine. 2008 Sep;12(5A):1649–60.

286. Zang L, Shi L, Guo J, Pan Q, Wu W, Pan X, et al. Screening and Identification of a peptide specifically targeted to NCI-H1299 from a phage display peptide library. Cancer Letters. 2009 Aug 18;281(1):64–70.

287. Koolpe M, Dail M, Pasquale EB. An ephrin mimetic peptide that selectively targets the EphA2 receptor. Journal of Biological Chemistry. 2002 Dec 6;277(49):46974–9.

288. Howell RC, Revskaya E, Pazo V, Nosanchuk JD, Casadevall A, Dadachova E. Phage display library derived peptides that bind to human tumor melanin as potential vehicles for targeted radionuclide therapy of metastatic melanoma. Bioconjugate Chemistry. 2007 Nov;18(6):1739–48.

289. Laakkonen P, Åkerman ME, Biliran H, Yang M, Ferrer F, Karpanen T, et al. Antitumor activity of a homing peptide that targets tumor lymphatics and tumor cells. Proceedings of the National Academy of Sciences of the United States of America. 2004 Jun 22;101(25):9381–6.

290. Simberg D, Duza T, Park JH, Essler M, Pilch J, Zhang L, et al. Biomimetic amplification of nanoparticle homing to tumors. Proceedings of the National Academy of Sciences of the United States of America. 2007 Jan 16;104(3):932–6.

291. Fukuda MN, Ohyama C, Lowitz K, Matsuo O, Pasqualini R, Ruoslahti E, et al. A peptide mimic of E-selectin ligand inhibits sialyl Lewis X-dependent lung colonization of tumor cells. Cancer Research. 2000 Jan 15;60(2):450–6.

292. Yang J, Baskar S, Kwong KY, Kennedy MG, Wiestner A, Rader C. Therapeutic potential and challenges of targeting receptor tyrosine kinase ROR1 with monoclonal antibodies in B-cell malignancies. PLoS ONE. 2011;6(6):e21018.

293. Fujiki T, Tsun A, Matsumoto SE, Yamashita M, Teruya K, Shirahata S, et al. Generation of a human anti-tumor necrosis factor-α monoclonal antibody by in vitro immunization with a multiple antigen peptide. Bioscience, Biotechnology and Biochemistry. 2010;74(9):1836–40.

294. Cyranka-Czaja A, Wulhfard S, Neri D, Otlewski J. Selection and characterization of human antibody fragments specific for psoriasin - A cancer associated protein. Biochemical and Biophysical Research Communications. 2012 Mar 9;419(2):250–5.

295. Lin J, Huo R, Wang L, Zhou Z, Sun Y, Shen B, et al. A novel anti-Cyr61 antibody inhibits breast cancer growth and metastasis in vivo. Cancer Immunology, Immunotherapy. 2012 May;61(5):677–87.

296. Brack SS, Silacci M, Birchler M, Neri D. Tumor-targeting properties of novel antibodies specific to the large isoform of tenascin-C. Clinical Cancer Research. 2006 May 15;12(10):3200–8.

297. Reardon DA, Akabani G, Edward Coleman R, Friedman AH, Friedman HS, Herndon JE, et al. Phase II Trial of Murine 131 I-Labeled Antitenascin Monoclonal Antibody 81C6 Administered Into Surgically Created Resection Cavities of Patients With Newly Diagnosed Malignant Gliomas . Journal of Clinical Oncology. 2002 Mar 1;20(5):1389–97.

298. Rizzieri DA, Akabani G, Zalutsky MR, Coleman RE, Metzler SD, Bowsher JE, et al. Phase 1 trial study of 131I-labeled chimeric 81C6 monoclonal antibody for the treatment of patients with non-Hodgkin lymphoma. Blood. 2004 Aug 1;104(3):642–8.

299. Villa A, Trachsel E, Kaspar M, Schliemann C, Sommavilla R, Rybak JN, et al. A high-affinity human monoclonal antibody specific to the alternatively spliced EDA domain of fibronectin efficiently targets tumor neo-vasculature in vivo. International Journal of Cancer. 2008 Jun 1;122(11):2405–13.

300. NB A, AH M, JE R, JM C, BK K. Characterization of phage that bind plastic from phage-displayed random peptide libraries. Gene [Internet]. 1995 Apr 14 [cited 2021 Sep 13];156(1):27–31. Available from: https://pubmed.ncbi.nlm.nih.gov/7737512/

301. Pasqualini R, Ruoslahti E. Organ targeting In vivo using phage display peptide libraries. Nature 1996 380:6572 [Internet]. 1996 Mar 28 [cited 2021 Sep 13];380(6572):364–6. Available from: https://www.nature.com/articles/380364a0

302. T C, JA W. In vitro selection from protein and peptide libraries. Trends in biotechnology [Internet]. 1994 [cited 2021 Sep 13];12(5):173–84. Available from: https://pubmed.ncbi.nlm.nih.gov/7764900/

303. Sioud M, Dybwad A, Jespersen L, Suleyman S, Natvig JB, Førre O. Characterization of naturally occurring autoantibodies against tumour necrosis factor-alpha (TNF-alpha): in vitro function and precise epitope mapping by phage epitope library. Clinical and Experimental Immunology [Internet]. 1994 [cited 2021 Sep 13];98(3):520. Available from: /pmc/articles/PMC1534487/?report=abstract

304. Böttger V, Stasiak PC, Harrison DL, Mellerick DM, Lane EB. Epitope Mapping of Monoclonal Antibodies to Keratin 19 Using Keratin Fragments, Synthetic Peptides and Phage Peptide Libraries. European Journal of Biochemistry [Internet]. 1995 Jul 1 [cited 2021 Sep 13];231(2):475–85. Available from: https://onlinelibrary.wiley.com/doi/full/10.1111/j.1432-1033.1995.0475e.x

305. HM G, SJ R, TJ M, G T, PG S. Strategies for epitope analysis using peptide synthesis. Journal of immunological methods [Internet]. 1987 Sep 24 [cited 2021 Sep 13];102(2):259–74. Available from: https://pubmed.ncbi.nlm.nih.gov/2443575/

306. Najar TA, Khare S, Varadarajan R. Rapid mapping of protein binding sites and conformational epitopes by coupling yeast surface display to chemical labeling and deep sequencing. Methods in Molecular Biology. 2018;1785:77–88.

307. Wang LF, Yu M. Random fragment libraries displayed on filamentous phage. Methods in molecular biology (Clifton, NJ). 1996;66:269–85.

308. HM G, SJ R, TJ M. A priori delineation of a peptide which mimics a discontinuous antigenic determinant. Molecular immunology [Internet]. 1986 [cited 2021 Sep 13];23(7):709–15. Available from: https://pubmed.ncbi.nlm.nih.gov/2432410/

309. HM G, RH M, SJ B. Use of peptide synthesis to probe viral antigens for epitopes to a resolution of a single amino acid. Proceedings of the National Academy of Sciences of the United States of America [Internet]. 1984 Jul 1 [cited 2021 Sep 13];81(13):3998–4002. Available from: https://europepmc.org/articles/PMC345355

310. Weng Z, Rickles RJ, Feng S, Richard S, Shaw AS, Schreiber SL, et al. Structure-function analysis of SH3 domains: SH3 binding specificity altered by single amino acid substitutions. Molecular and Cellular Biology [Internet]. 1995 Oct [cited 2021 Sep 13];15(10):5627. Available from: /pmc/articles/PMC230813/?report=abstract

311. Sparks AB, Quilliam LA, Thorn JM, Der CJ, Kay BK. Identification and characterization of Src SH3 ligands from phage-displayed random peptide libraries. Journal of Biological Chemistry. 1994 Sep 30;269(39):23853–6.

312. Sparks AB, Rider JE, Hoffman NG, Fowlkes DM, Quillam LA, Kay BK. Distinct ligand preferences of Src homology 3 domains from Src, Yes, Abl, Cortactin, p53bp2, PLCgamma, Crk, and Grb2. Proceedings of the National Academy of Sciences of the United States of America [Internet]. 1996 Feb 20 [cited 2021 Sep 13];93(4):1540. Available from: /pmc/articles/PMC39976/?report=abstract

313. TN S, LM M, DL M, MA M, MW B, PS K. Identification of D-peptide ligands through mirror-image phage display. Science (New York, NY) [Internet]. 1996 Mar 29 [cited 2021 Sep 13];271(5257):1854–7. Available from: https://pubmed.ncbi.nlm.nih.gov/8596952/

314. Lin C-W, Wu S-C. Identification of Mimotopes of the Japanese Encephalitis Virus Envelope Protein using Phage-Displayed Combinatorial Peptide Library. Microbial Physiology [Internet]. 2004 [cited 2021 Sep 13];8(1):34–42. Available from: https://www.karger.com/Article/FullText/82079

315. Dottavio D. Epitope mapping using phage-displayed peptide libraries. Methods in molecular biology (Clifton, NJ). 1996;66:181–93.

316. BA K. Binding to protein targets of peptidic leads discovered by phage display: crystal structures of streptavidin-bound linear and cyclic peptide ligands containing the HPQ sequence. Biochemistry [Internet]. 1995 [cited 2021 Sep 13];34(47):15421–9. Available from: https://pubmed.ncbi.nlm.nih.gov/7492542/

317. EJ R, CO P. Zinc finger phage: affinity selection of fingers with new DNA-binding specificities. Science (New York, NY) [Internet]. 1994 [cited 2021 Sep 13];263(5147):671–3. Available from: https://pubmed.ncbi.nlm.nih.gov/8303274/

318. Wu H, Yang WP, Barbas CF. Building zinc fingers by selection: toward a therapeutic application. Proceedings of the National Academy of Sciences [Internet]. 1995 Jan 17 [cited 2021 Sep 13];92(2):344–8. Available from: https://www.pnas.org/content/92/2/344

319. Durrin LK, Krontiris TG. The Thymocyte-Specific MAR Binding Protein, SATB1, Interacts in Vitro with a Novel Variant of DNA-Directed RNA Polymerase II, Subunit 11. Genomics. 2002 Jun 1;79(6):809–17.

320. Calcutt MJ, Kremer MT, Giblin MF, Quinn TP, Deutscher SL. Isolation and characterization of nucleic acid-binding antibody fragments from autoimmune mice-derived bacteriophage display libraries. Gene. 1993 Dec 27;137(1):77–83.

Annexes

Annex 1: QIAGEN® "QIAquick® PCR Purification Kit / QIAquick® PCR & Gel Cleanup Kit" Protocol

July 2018

Quick-Start Protocol

QIAquick® PCR Purification Kit
QIAquick® PCR & Gel Cleanup Kit

The QIAquick PCR Purification Kit and the QIAquick PCR & Gel Cleanup Kit (cat. nos. 28104, 28106, 28506 and 28115) can be stored at room temperature (15–25°C) for up to 12 months if not otherwise stated on label.

Further information

- *QIAquick Spin Handbook*: **www.qiagen.com/HB-1196**
- Safety Data Sheets: **www.qiagen.com/safety**
- Technical assistance: **support.qiagen.com**

Notes before starting

- This protocol is for the purification of up to 10 µg PCR products (100 bp to 10 kb in size).
- Add ethanol (96–100%) to Buffer PE before use (see bottle label for volume).
- All centrifugation steps are carried out at 17,900 x g (13,000 rpm) in a conventional table-top microcentrifuge at room temperature.
- Add 1:250 volume pH indicator I to Buffer PB. The yellow color of Buffer PB with pH indicator I indicates a pH ≤7.5. The adsorption of DNA to the membrane is only efficient at pH ≤7.5. If the purified PCR product is to be used in sensitive microarray applications, it may be beneficial to use Buffer PB without the addition of pH indicator I; do not add pH indicator I to buffer aliquots.
- Symbols: ● centrifuge processing; ▲ vacuum processing.

Sample to Insight

QIAGEN

1. Add 5 volumes Buffer PB to 1 volume of the PCR reaction and mix. If the color of the mixture is orange or violet, add 10 µl 3 M sodium acetate, pH 5.0, and mix. The color of the mixture will turn yellow.
2. Place a QIAquick column in ● a provided 2 ml collection tube or into ▲ a vacuum manifold. For details on how to set up a vacuum manifold, refer to the *QIAquick Spin Handbook*.
3. To bind DNA, apply the sample to the QIAquick column and ● centrifuge for 30–60 s or ▲ apply vacuum to the manifold until all the samples have passed through the column. ● Discard flow-through and place the QIAquick column back in the same tube.
4. To wash, add 750 µl Buffer PE to the QIAquick column ● centrifuge for 30–60 s or ▲ apply vacuum. ● Discard flow-through and place the QIAquick column back into the same tube.
5. Centrifuge the QIAquick column once more in the provided 2 ml collection tube for 1 min to remove residual wash buffer.
6. Place each QIAquick column in a clean 1.5 ml microcentrifuge tube.
7. To elute DNA, add 50 µl Buffer EB (10 mM Tris·Cl, pH 8.5) or water (pH 7.0–8.5) to the center of the QIAquick membrane and centrifuge the column for 1 min. For increased DNA concentration, add 30 µl elution buffer to the center of the QIAquick membrane, let the column stand for 1 min and then centrifuge.
8. If the purified DNA is to be analyzed on a gel, add 1 volume of Loading Dye to 5 volumes of purified DNA. Mix the solution by pipetting up and down before loading the gel.

Revision History

Revision no.	Description of change
R3 07/2018	Updated document title and introductory paragraph with additional applicable product QIAquick PCR & Gel Cleanup Kit. Also added additional product's related cat. nos.

Scan QR code for handbook.

For up-to-date licensing information and product-specific disclaimers, see the respective QIAGEN kit handbook or user manual.

Trademarks: QIAGEN®, Sample to Insight®, QIAquick® (QIAGEN Group). 1114321 07/2018 HB-0900-003 © 2018 QIAGEN, all rights reserved.

Annex 2: Tables

Table 14 *– Volumes of reagents used on the three rounds of the positive control panning experiment (Step 1.1 and Step 1.2) and dilutions used in unamplified and amplified phage titering assays (Step 1.3 and Step 1.4, respectively), during the surface-based panning procedure against Streptavidin (Experiment S1).*

Experiment S1		Concentration of Streptavidin on Step 1.1	Volume of Streptavidin on Step 1.1	Volume of 0.1 M $NaHCO_3$ (pH 8.6) on Step 1.1	Volume of Phage Library on Step 1.2	Volume of TBST on Step 1.2	Unamplified Phage Eluate Titering Dilutions on Step 1.3	Amplified Phage Eluate Titering Dilutions on Step 1.4
Round 1	**Well S1.1**	50 µg/mL	5 µL	145 µL	10 µL	90 µL	10^2, 10^4	10^8, 10^{10}
	Well S1.2	100 µg/mL	10 µL	140 µL	10 µL	90 µL	10^2, 10^4	10^8, 10^{10}
Round 2	**Well S1.1**	50 µg/mL	5 µL	145 µL	10 µL	90 µL	10^2, 10^4	10^8, 10^{10}
	Well S1.2	100 µg/mL	10 µL	140 µL	10 µL	90 µL	10^2, 10^4	10^8, 10^{10}
Round 3	**Well S1.1**	50 µg/mL	5 µL	145 µL	10 µL	90 µL	10^2, 10^4	10^8, 10^{10}
	Well S1.2	100 µg/mL	10 µL	140 µL	10 µL	90 µL	10^2, 10^4	10^8, 10^{10}

Table 15 *– Volumes of reagents used on the three rounds of the biopanning experiment (Step 1.1 and Step 1.2) and dilutions used in unamplified and amplified phage titering assays (Step 1.3 and Step 1.4, respectively), during the surface-based panning procedure against the Anti-Zika Virus NS1 Antibody [B4] (Experiment Z1).*

Experiment Z1		Volume of Anti-Zika Antibody on Step 1.1	Volume of 0.1 M $NaHCO_3$ (pH 8.6) on Step 1.1	Volume of Phage Library on Step 1.2	Volume of TBST on Step 1.2	Unamplified Phage Eluate Titering Dilutions on Step 1.3	Amplified Phage Eluate Titering Dilutions on Step 1.4
Round 1	**Well Z1**	15 µL	135 µL	10 µL	90 µL	10^1, 10^2, 10^3, 10^4	10^8, 10^9, 10^{10}, 10^{11}
	Well N1	0 µL	150 µL	10 µL	90 µL	10^1, 10^2, 10^3, 10^4	10^8, 10^{11}
Round 2	**Well Z1**	15 µL	135 µL	10 µL	90 µL	10^1, 10^2, 10^3, 10^4	10^8, 10^9, 10^{10}, 10^{11}
	Well N1	0 µL	150 µL	10 µL	90 µL	10^1, 10^2, 10^3, 10^4	10^8, 10^{11}
Round 3	**Well Z1**	15 µL	135 µL	10 µL	90 µL	10^1, 10^2, 10^3, 10^4	10^8, 10^9, 10^{10}, 10^{11}
	Well N1	0 µL	150 µL	10 µL	90 µL	10^1, 10^2, 10^3, 10^4	10^8, 10^{11}

Table 16 *– Volumes of reagents used on the three rounds of the positive control panning experiment (Step 2.1, Step 3.1 and Step 3.2) and dilutions used in unamplified and amplified phage titering assays (Step 2.2 and Step 2.3, respectively), during the solution-based panning procedure against Streptavidin, using protein G agarose beads and a subtractive panning step (Experiment S2).*

Experiment S2		Volume of Streptavidin on Step 2.1	Volume of Phage Library on Step 2.1	Volume of TBST on Step 2.1	Volume of Phage Library on Step 3.1	Volume of TBST on Step 3.1	Volume of Streptavidin on Step 3.2	Unamplified Phage Eluate Titering Dilutions on Step 2.2	Amplified Phage Eluate Titering Dilutions on Step 2.3
Round 1	**Well S2**	7.5 µL	10 µL	182.5 µL	-	-	-	10^2, 10^4	10^8, 10^{10}
Round 2	**Well S2**	-	-	-	10 µL	190 µL	7.5 µL	10^2, 10^4	10^8, 10^{10}
Round 3	**Well S2**	7.5 µL	10 µL	182.5 µL	-	-	-	10^2, 10^4	10^8, 10^{10}

Table 17 *– Volumes of reagents used on the three rounds of the biopanning experiment (Step 2.1) and dilutions used in unamplified and amplified phage titering assays (Step 2.2 and Step 2.3, respectively), during the solution-based panning procedure against the Anti-Zika Virus NS1 Antibody [B4], using protein A and protein G agarose beads (Experiment Z2).*

Experiment Z2		Volume of Anti-Zika Antibody on Step 2.1	Volume of Phage Library on Step 2.1	Volume of TBST on Step 2.1	Unamplified Phage Eluate Titering Dilutions on Step 2.2	Amplified Phage Eluate Titering Dilutions on Step 2.3
Round 1	**Tube Z2**	10 µL	10 µL	180 µL	10^2, 10^4	10^8, 10^9, 10^{10}, 10^{11}
	Tube N2	0 µL	10 µL	190 µL	10^2, 10^4	10^9, 10^{10}, 10^{11}
Round 2	**Tube Z2**	10 µL	10 µL	180 µL	10^2, 10^4	10^8, 10^9, 10^{10}, 10^{11}
	Tube N2	0 µL	10 µL	190 µL	10^2, 10^4	10^9, 10^{10}, 10^{11}
Round 3	**Tube Z2**	10 µL	10 µL	180 µL	10^2, 10^4	10^8, 10^9, 10^{10}, 10^{11}
	Tube N2	0 µL	10 µL	190 µL	10^2, 10^4	10^9, 10^{10}, 10^{11}

Table 18 *– Volumes of reagents used on the three rounds of the biopanning experiment (Step 2.1, Step 3.1 and Step 3.2) and dilutions used in unamplified and amplified phage titering assays (Step 2.2 and Step 2.3, respectively), during the solution-based panning procedure against the Anti-Zika Virus NS1 Antibody [B4], using protein G agarose beads and a subtractive panning step (Experiment Z3.1).*

Experiment Z3.1		Volume of Anti-Zika Antibody on Step 2.1	Volume of Phage Library on Step 2.1	Volume of TBST on Step 2.1	Volume of Phage Library on Step 3.1	Volume of TBST on Step 3.1	Volume of Anti-Zika Antibody on Step 3.2	Unamplified Phage Eluate Titering Dilutions on Step 2.2	Amplified Phage Eluate Titering Dilutions on Step 2.3
Round 1	**Tube Z3.1.1**	10 µL	10 µL	180 µL	-	-	-	10^2, 10^4	10^8, 10^{10}
	Tube Z3.1.2	5 µL	10 µL	185 µL	-	-	-	10^2, 10^4	10^8, 10^{10}
	Tube N3.1	0 µL	10 µL	190 µL	-	-	-	10^2, 10^4	10^9, 10^{11}
Round 2	**Tube Z3.1.1**	-	-	-	10 µL	190 µL	10 µL	10^2, 10^4	10^8, 10^{10}
	Tube Z3.1.2	-	-	-	10 µL	190 µL	5 µL	10^2, 10^4	10^8, 10^{10}
	Tube N3.1	-	-	-	10 µL	190 µL	0 µL	10^2, 10^4	10^9, 10^{11}
Round 3	**Tube Z3.1.1**	10 µL	10 µL	180 µL	-	-	-	10^2, 10^4	10^8, 10^{10}
	Tube Z3.1.2	5 µL	10 µL	185 µL	-	-	-	10^2, 10^4	10^8, 10^{10}
	Tube N3.1	0 µL	10 µL	190 µL	-	-	-	10^2, 10^4	10^9, 10^{11}

Table 19 *– Volumes of reagents used on the three rounds of the biopanning experiment (Step 2.1, Step 3.1 and Step 3.2) and dilutions used in unamplified and amplified phage titering assays (Step 2.2 and Step 2.3, respectively), during the solution-based panning procedure against the Anti-Zika Virus NS1 Antibody [D11], using protein G agarose beads and a subtractive panning step (Experiment Z3.2).*

Experiment Z3.2		Volume of Anti-Zika Antibody on Step 2.1	Volume of Phage Library on Step 2.1	Volume of TBST on Step 2.1	Volume of Phage Library on Step 3.1	Volume of TBST on Step 3.1	Volume of Anti-Zika Antibody on Step 3.2	Unamplified Phage Eluate Titering Dilutions on Step 2.2	Amplified Phage Eluate Titering Dilutions on Step 2.3
Round 1	Tube Z3.2.1	10 µL	10 µL	180 µL	-	-	-	10^2, 10^4	10^8, 10^{10}
	Tube Z3.2.2	5 µL	10 µL	185 µL	-	-	-	10^2, 10^4	10^8, 10^{10}
	Tube N3.2	0 µL	10 µL	190 µL	-	-	-	10^2, 10^4	10^9, 10^{11}
Round 2	Tube Z3.2.1	-	-	-	10 µL	190 µL	10 µL	10^2, 10^4	10^8, 10^{10}
	Tube Z3.2.2	-	-	-	10 µL	190 µL	5 µL	10^2, 10^4	10^8, 10^{10}
	Tube N3.2	-	-	-	10 µL	190 µL	0 µL	10^2, 10^4	10^9, 10^{11}
Round 3	Tube Z3.2.1	10 µL	10 µL	180 µL	-	-	-	10^2, 10^4	10^8, 10^{10}
	Tube Z3.2.2	5 µL	10 µL	185 µL	-	-	-	10^2, 10^4	10^8, 10^{10}
	Tube N3.2	0 µL	10 µL	190 µL	-	-	-	10^2, 10^4	10^9, 10^{11}

Table 20 *– Volumes of reagents used on the three rounds of the biopanning experiment (Step 2.1, Step 3.1 and Step 3.2) and dilutions used in unamplified and amplified phage titering assays (Step 2.2 and Step 2.3, respectively), during the solution-based panning procedure against the Anti-Zika Virus NS1 Antibody [D11], using protein A agarose beads and a subtractive panning step (Experiment Z4).*

Experiment Z4		Volume of Anti-Zika Antibody on Step 2.1	Volume of Phage Library on Step 2.1	Volume of TBST on Step 2.1	Volume of Phage Library on Step 3.1	Volume of TBST on Step 3.1	Volume of Anti-Zika Antibody on Step 3.2	Unamplified Phage Eluate Titering Dilutions on Step 2.2	Amplified Phage Eluate Titering Dilutions on Step 2.3
Round 1	Tube Z4.1	10 µL	10 µL	180 µL	-	-	-	10^2, 10^4	10^8, 10^{10}
	Tube Z4.2	20 µL	10 µL	170 µL	-	-	-	10^2, 10^4	10^8, 10^{10}
	Tube N4	0 µL	10 µL	190 µL	-	-	-	10^2, 10^4	10^9, 10^{11}
Round 2	Tube Z4.1	-	-	-	10 µL	190 µL	5 µL	10^2, 10^4	10^8, 10^{10}
	Tube Z4.2	-	-	-	10 µL	190 µL	10 µL	10^2, 10^4	10^8, 10^{10}
	Tube N4	-	-	-	10 µL	190 µL	0 µL	10^2, 10^4	10^9, 10^{11}
Round 3	Tube Z4.1	5 µL	10 µL	185 µL	-	-	-	10^2, 10^4	10^8, 10^{10}
	Tube Z4.2	10 µL	10 µL	180 µL	-	-	-	10^2, 10^4	10^8, 10^{10}
	Tube N4	0 µL	10 µL	190 µL	-	-	-	10^2, 10^4	10^9, 10^{11}

Table 21 *– Volumes of reagents used in the ELISA assay conducted for the phage stocks amplified from the biopanning experiments performed against Streptavidin (Experiment S1 and Experiment S2).*

Experiment		Sample	Well		Volume of Streptavidin on Step 4.1	Volume of $NaHCO_3$ on Step 4.1	Volume of Phage Stock on Step 4.2	Volume of TBST on Step 4.2	Volume of Anti-M13 Antibody on Step 4.3	Volume of Blocking Buffer on Step 4.3
S1	S1.1	Amplified 3rd Round Phage Eluate Pool	Coated	100 µg/mL	10 µL	140 µL	20 µL	80 µL	10 µL	190 µL
				200 µg/mL	20 µL	130 µL	20 µL	80 µL	10 µL	190 µL
			Uncoated		0 µL	0 µL	20 µL	80 µL	10 µL	190 µL
					0 µL	0 µL	20 µL	80 µL	10 µL	190 µL
		Amplified Random Phage Clone	Coated	100 µg/mL	10 µL	140 µL	20 µL	80 µL	10 µL	190 µL
				200 µg/mL	20 µL	130 µL	20 µL	80 µL	10 µL	190 µL
			Uncoated		0 µL	0 µL	20 µL	80 µL	10 µL	190 µL
					0 µL	0 µL	20 µL	80 µL	10 µL	190 µL
	S1.2	Amplified 3rd Round Phage Eluate Pool	Coated	100 µg/mL	10 µL	140 µL	20 µL	80 µL	10 µL	190 µL
				200 µg/mL	20 µL	130 µL	20 µL	80 µL	10 µL	190 µL
			Uncoated		0 µL	0 µL	20 µL	80 µL	10 µL	190 µL
					0 µL	0 µL	20 µL	80 µL	10 µL	190 µL
		Amplified Random Phage Clone	Coated	100 µg/mL	10 µL	140 µL	20 µL	80 µL	10 µL	190 µL
				200 µg/mL	20 µL	130 µL	20 µL	80 µL	10 µL	190 µL
			Uncoated		0 µL	0 µL	20 µL	80 µL	10 µL	190 µL
					0 µL	0 µL	20 µL	80 µL	10 µL	190 µL
S2		Amplified 3rd Round Phage Eluate Pool	Coated		10 µL	140 µL	25 µL	75 µL	10 µL	190 µL
			Uncoated		0 µL	0 µL	25 µL	75 µL	10 µL	190 µL
		Amplified Random Phage Clone	Coated		10 µL	140 µL	25 µL	75 µL	10 µL	190 µL
			Uncoated		0 µL	0 µL	25 µL	75 µL	10 µL	190 µL

Table 22 *– Volumes of reagents used in the ELISA assay conducted for the phage stocks amplified from the biopanning experiments performed against the Anti-Zika Virus NS1 Antibodies (Experiment Z1, Experiment Z2, Experiment Z3 and Experiment Z4).*

Experiment		Sample	Well		Volume of Anti-Zika Antibody on Step 4.1	Volume of $NaHCO_3$ on Step 4.1	Volume of Phage Stock on Step 4.2	Volume of TBST on Step 4.2	Volume of Anti-M13 Antibody on Step 4.3	Volume of Blocking Buffer on Step 4.3
Z1		Phage Pool	Coated		15 µL	135 µL	1 µL	99 µL	10 µL	190 µL
			Uncoated		0 µL	0 µL	1 µL	99 µL	10 µL	190 µL
		Phage Clone	Coated		15 µL	135 µL	1 µL	99 µL	2 µL	198 µL
			Uncoated		0 µL	0 µL	1 µL	99 µL	2 µL	198 µL
Z2		Phage Pool	Coated		15 µL	135 µL	2 µL	98 µL	10 µL	190 µL
			Uncoated		0 µL	0 µL	2 µL	98 µL	10 µL	190 µL
		Phage Clone	Coated		15 µL	135 µL	2 µL	98 µL	10 µL	190 µL
			Uncoated		0 µL	0 µL	2 µL	98 µL	10 µL	190 µL
Z3	Z3.1.1	Phage Pool	Coated	75 µg/mL	11.25 µL	138.75 µL	5 µL	95 µL	10 µL	190 µL
				100 µg/mL	15 µL	135 µL	10 µL	90 µL	10 µL	190 µL
			Uncoated		0 µL	0 µL	5 µL	95 µL	10 µL	190 µL
					0 µL	0 µL	10 µL	90 µL	10 µL	190 µL
		Phage Clone	Coated	75 µg/mL	11.25 µL	138.75 µL	5 µL	95 µL	10 µL	190 µL
				100 µg/mL	15 µL	135 µL	10 µL	90 µL	10 µL	190 µL
			Uncoated		0 µL	0 µL	5 µL	95 µL	10 µL	190 µL
					0 µL	0 µL	10 µL	90 µL	10 µL	190 µL
	Z3.1.2	Phage Pool	Coated		15 µL	135 µL	25 µL	75 µL	10 µL	190 µL
			Uncoated		0 µL	0 µL	25 µL	75 µL	10 µL	190 µL
		Phage Clone	Coated		15 µL	135 µL	25 µL	75 µL	10 µL	190 µL
			Uncoated		0 µL	0 µL	25 µL	75 µL	10 µL	190 µL
	Z3.2.1	Phage Pool	Coated		15 µL	135 µL	25 µL	75 µL	10 µL	190 µL
			Uncoated		0 µL	0 µL	25 µL	75 µL	10 µL	190 µL
		Phage Clone	Coated		15 µL	135 µL	25 µL	75 µL	10 µL	190 µL
			Uncoated		0 µL	0 µL	25 µL	75 µL	10 µL	190 µL
	Z3.2.2	Phage Pool	Coated		15 µL	135 µL	25 µL	75 µL	10 µL	190 µL
			Uncoated		0 µL	0 µL	25 µL	75 µL	10 µL	190 µL
		Phage Clone	Coated		15 µL	135 µL	25 µL	75 µL	10 µL	190 µL
			Uncoated		0 µL	0 µL	25 µL	75 µL	10 µL	190 µL
Z4	Z4.1	Phage Pool	Coated		10 µL	90 µL	10 µL	90 µL	20 µL	180 µL
			Uncoated		0 µL	0 µL	10 µL	90 µL	20 µL	180 µL
		Phage Clone	Coated		10 µL	90 µL	10 µL	90 µL	20 µL	180 µL
			Uncoated		0 µL	0 µL	10 µL	90 µL	20 µL	180 µL
	Z4.2	Phage Pool	Coated		10 µL	90 µL	10 µL	90 µL	20 µL	180 µL
			Uncoated		0 µL	0 µL	10 µL	90 µL	20 µL	180 µL
		Phage Clone	Coated		10 µL	90 µL	10 µL	90 µL	20 µL	180 µL
			Uncoated		0 µL	0 µL	10 µL	90 µL	20 µL	180 µL

Table 23 *– Volumes and concentrations of reagents used in PCR Experiment 1.*

Experiment Samples		Volume of iQ Supermix (2x)	Concentration of iQ Supermix (2x)	Volume of Forward Primer	Concentration of Forward Primer	Volume of Reverse Primer	Concentration of Reverse Primer	Volume of Phage DNA Template (100 ng)	Volume of H_2O
Z1		10 µL	1x	1 µL	500 nM	1 µL	500 nM	5 µL	3 µL
Z2		10 µL	1x	1 µL	500 nM	1 µL	500 nM	5 µL	3 µL
Z3	**Z3.1.1**	10 µL	1x	1 µL	500 nM	1 µL	500 nM	5 µL	3 µL
	Z3.1.2	10 µL	1x	1 µL	500 nM	1 µL	500 nM	5 µL	3 µL
	Z3.2.1	10 µL	1x	1 µL	500 nM	1 µL	500 nM	5 µL	3 µL
	Z3.2.2	10 µL	1x	1 µL	500 nM	1 µL	500 nM	5 µL	3 µL
Z4	**Z4.1**	10 µL	1x	1 µL	500 nM	1 µL	500 nM	5 µL	3 µL
	Z4.2	10 µL	1x	1 µL	500 nM	1 µL	500 nM	5 µL	3 µL
S1	**S1.1**	10 µL	1x	1 µL	500 nM	1 µL	500 nM	5 µL	3 µL
	S1.2	10 µL	1x	1 µL	500 nM	1 µL	500 nM	5 µL	3 µL
S2		10 µL	1x	1 µL	500 nM	1 µL	500 nM	5 µL	3 µL

Table 24 *– Thermal cycling temperature and timing conditions used in PCR Experiment 1.*

Experiment Samples		Initial DNA Denaturation at 95 °C	Amplification - 40 Cycles			Final Elongation at 72 °C	Final Hold at 4 °C
			Denaturation at 95 °C	Annealing at 60 °C	Extension/ Elongation at 72 °C		
Z1		5 minutes	1 minute	1 minute	1 minute	5 minutes	Indefinitely
Z2		5 minutes	1 minute	1 minute	1 minute	5 minutes	Indefinitely
Z3	**Z3.1.1**	5 minutes	1 minute	1 minute	1 minute	5 minutes	Indefinitely
	Z3.1.2	5 minutes	1 minute	1 minute	1 minute	5 minutes	Indefinitely
	Z3.2.1	5 minutes	1 minute	1 minute	1 minute	5 minutes	Indefinitely
	Z3.2.2	5 minutes	1 minute	1 minute	1 minute	5 minutes	Indefinitely
Z4	**Z4.1**	5 minutes	1 minute	1 minute	1 minute	5 minutes	Indefinitely
	Z4.2	5 minutes	1 minute	1 minute	1 minute	5 minutes	Indefinitely
S1	**S1.1**	5 minutes	1 minute	1 minute	1 minute	5 minutes	Indefinitely
	S1.2	5 minutes	1 minute	1 minute	1 minute	5 minutes	Indefinitely
S2		5 minutes	1 minute	1 minute	1 minute	5 minutes	Indefinitely

Table 25 *– Volumes and concentrations of reagents used in PCR Experiment 2.*

Sample	Volume of iQ Supermix (2x)	Concentration of iQ Supermix (2x)	Volume of Forward Primer	Concentration of Forward Primer	Volume of Reverse Primer	Concentration of Reverse Primer	Volume of Phage DNA Template (100 ng)	Volume of H_2O
Negative Control	10 µL	1x	0.5 µL	250 nM	0.5 µL	250 nM	0 µL	9 µL
Negative Control	10 µL	1x	0.5 µL	250 nM	0.5 µL	250 nM	0 µL	9 µL
Negative Control	10 µL	1x	1 µL	500 nM	1 µL	500 nM	0 µL	8 µL
Negative Control	10 µL	1x	1 µL	500 nM	1 µL	500 nM	0 µL	8 µL
Z1 Clones 1-5	10 µL	1x	0.5 µL	250 nM	0.5 µL	250 nM	5 µL	4 µL
Z1 Clone 5-10	10 µL	1x	1 µL	500 nM	1 µL	500 nM	5 µL	3 µL

Table 26 *– Volumes and concentrations of reagents used in PCR Experiment 3.*

Sample	Volume of iQ Supermix (2x)	Concentration of iQ Supermix (2x)	Volume of Forward Primer	Concentration of Forward Primer	Volume of Reverse Primer	Concentration of Reverse Primer	Volume of Phage DNA Template (100 ng)	Volume of H_2O
Negative Control	10 µL	1x	1 µL	500 nM	1 µL	500 nM	0 µL	8 µL
Z1 Clones	10 µL	1x	1 µL	500 nM	1 µL	500 nM	5 µL	3 µL

Table 27 *– Thermal cycling temperature conditions used in PCR Experiment 3.*

Sample	Hot-Start at 95 °C (Polymerase Activation)	Initial DNA Denaturation at 95 °C	Amplification - 40 Cycles			Final Elongation at 72 °C	Final Hold at 4 °C
			Denaturation at 95 °C	Annealing at 60 °C	Extension/ Elongation at 72 °C		
Negative Control	5 minutes	5 minutes	1 minute	1 minute	1 minute	5 minutes	Indefinitely
Z1 Clones	5 minutes	5 minutes	1 minute	1 minute	1 minute	5 minutes	Indefinitely

Table 28 *– Absorbances registered on the ELISA assay conducted for the phage stocks amplified from the biopanning experiments performed against Streptavidin (Experiment S1 and Experiment S2).*

Experiment		Sample	Well		Absorbance
S1	S1.1	Amplified 3rd Round Phage Eluate Pool	Coated	100 µg/mL	0.751 A
				200 µg/mL	1.102 A
			Uncoated		0.231 A
					0.251 A
		Amplified Random Phage Clone	Coated	100 µg/mL	0.755 A
				200 µg/mL	0.909 A
			Uncoated		0.489 A
					0.371 A
	S1.2	Amplified 3rd Round Phage Eluate Pool	Coated	100 µg/mL	1.286 A
				200 µg/mL	1.322 A
			Uncoated		0.267 A
					0.163 A
		Amplified Random Phage Clone	Coated	100 µg/mL	1.118 A
				200 µg/mL	1.291 A
			Uncoated		0.385 A
					0.416 A
S2		Amplified 3rd Round Phage Eluate Pool	Coated		1.242 A
			Uncoated		0.129 A
		Amplified Random Phage Clone	Coated		1.168 A
			Uncoated		0.117 A

Table 29 *– Absorbances registered on the ELISA assay conducted for the phage stocks amplified from the biopanning experiments performed against the Anti-Zika Virus NS1 Antibodies (Experiment Z1, Experiment Z2, Experiment Z3 and Experiment Z4).*

Experiment		Sample	Well		Absorbance
Z1		Amplified 3rd Round Phage Eluate Pool	Coated		1.942 A
			Uncoated		1.283 A
		Amplified Random Phage Clone	Coated		1.536 A
			Uncoated		1.482 A
Z2		Amplified 3rd Round Phage Eluate Pool	Coated		0.231 A
			Uncoated		0.192 A
		Amplified Random Phage Clone	Coated		0.233 A
			Uncoated		0.176 A
Z3	Z3.1.1	Amplified 3rd Round Phage Eluate Pool	Coated	75 µg/mL	1.763 A
				100 µg/mL	3.452 A
			Uncoated		0.882 A
					0.794 A
		Amplified Random Phage Clone	Coated	75 µg/mL	1.799 A
				100 µg/mL	3.256 A
			Uncoated		0.131 A
					0.129 A
	Z3.1.2	Amplified 3rd Round Phage Eluate Pool	Coated		1.472 A
			Uncoated		0.147 A
		Amplified Random Phage Clone	Coated		1.517 A
			Uncoated		0.178 A
	Z3.2.1	Amplified 3rd Round Phage Eluate Pool	Coated		0.912 A
			Uncoated		0.816 A
		Amplified Random Phage Clone	Coated		1.021 A
			Uncoated		0.815 A
	Z3.2.2	Amplified 3rd Round Phage Eluate Pool	Coated		1.098 A
			Uncoated		0.932 A
		Amplified Random Phage Clone	Coated		1.094 A
			Uncoated		0.992 A
Z4	Z4.1	Amplified 3rd Round Phage Eluate Pool	Coated		3.361 A
			Uncoated		0.148 A
		Amplified Random Phage Clone	Coated		3.337 A
			Uncoated		0.087 A
	Z4.2	Amplified 3rd Round Phage Eluate Pool	Coated		3.444 A
			Uncoated		0.104 A
		Amplified Random Phage Clone	Coated		3.397 A
			Uncoated		0.113 A

Table 30 *– Absorbances and corresponding DNA concentrations and purity ratios of the 10 clones and the eluate pool from Experiment S1.*

Sample	Absorbance at 230 nm	Absorbance at 260 nm	Absorbance at 280 nm	DNA Concentration (µg/mL)	$A_{(260/280)}$	$A_{(260/230)}$
S1.1	0.00295	0.00765	0.00665	50.49	1.1504	2.5932
S1.2	0.0048	0.01035	0.0091	68.31	1.1374	2.1563
S1.3	0.00465	0.0106	0.0093	69.96	1.1398	2.2796
S1.4	0.0048	0.01185	0.00985	78.21	1.2030	2.4688
S1.5	0.00395	0.0106	0.00875	69.96	1.2114	2.6835
S1.6	0.00545	0.01205	0.0105	79.53	1.1476	2.2110
S1.7	0.0043	0.01055	0.00905	69.63	1.1657	2.4535
S1.8	0.00555	0.01335	0.0112	88.11	1.1920	2.4054
S1.9	0.00495	0.0123	0.0104	81.18	1.1827	2.4848
S1.10	0.0039	0.01165	0.0094	76.89	1.2394	2.9872
S1.E	0.0038	0.0125	0.0085	82.5	1.4706	3.2895

Table 31 *– Absorbances and corresponding DNA concentrations and purity ratios of the 10 clones and the eluate pool from Experiment S2.*

Sample	Absorbance at 230 nm	Absorbance at 260 nm	Absorbance at 280 nm	DNA Concentration (µg/mL)	$A_{(260/280)}$	$A_{(260/230)}$
S2.1	0.0263	0.01895	0.0167	125.07	1.1347	0.7205
S2.2	0.0234	0.01715	0.0152	113.19	1.1283	0.7329
S2.3	0.02645	0.0203	0.01765	133.98	1.1501	0.7675
S2.4	0.02275	0.01705	0.015	112.53	1.1367	0.7495
S2.5	0.0232	0.0176	0.0155	116.16	1.1355	0.7586
S2.6	0.0228	0.01715	0.0152	113.19	1.1283	0.7522
S2.7	0.0224	0.0163	0.0143	107.58	1.1399	0.7277
S2.8	0.02165	0.016	0.01405	105.6	1.1388	0.7390
S2.9	0.02265	0.01675	0.01485	110.55	1.1279	0.7395
S2.10	0.02205	0.0162	0.0143	106.92	1.1329	0.7347
S2.E	0.02365	0.01745	0.0154	115.17	1.1331	0.7378

Table 32 *– Absorbances and corresponding DNA concentrations and purity ratios of the 10 clones from Experiment Z1.*

Sample	Absorbance at 230 nm	Absorbance at 260 nm	Absorbance at 280 nm	DNA Concentration (µg/mL)	$A_{(260/280)}$	$A_{(260/230)}$
Z1.1	0.0038	0.0087	0.0083	57.42	1.0482	2.2895
Z1.2	0.00345	0.01005	0.00925	66.33	1.0865	2.9130
Z1.3	0.0037	0.01065	0.0098	70.29	1.0867	2.8784
Z1.4	0.0044	0.01115	0.0104	73.59	1.0721	2.5341
Z1.5	0.0047	0.012	0.0111	79.2	1.0811	2.5532
Z1.6	0.0025	0.024	0.02645	158.4	0.9074	9.6000
Z1.7	0.00085	0.01175	0.0134	77.55	0.8769	13.8235
Z1.8	0.00085	0.00925	0.00945	61.05	0.9788	10.8824
Z1.9	0.0025	0.00345	0.0022	22.77	1.5682	1.3800
Z1.10	0.0029	0.00315	0.00235	20.79	1.3404	1.0862

Table 33 *– Absorbances and corresponding DNA concentrations and purity ratios of the 10 clones from Experiment Z2.*

Sample	Absorbance at 230 nm	Absorbance at 260 nm	Absorbance at 280 nm	DNA Concentration (µg/mL)	$A_{(260/280)}$	$A_{(260/230)}$
Z2.1	20.636	0.454	0.208	14.987	2.178	0.022
Z2.2	7.947	0.453	0.229	14.94	1.975	0.057
Z2.3	3.125	0.822	0.45	27.14	1.828	0.263
Z2.4	16.146	0.662	0.335	21.862	1.976	0.041
Z2.5	5.510	0.281	0.145	9.267	1.938	0.051
Z2.6	5.791	0.498	0.248	16.433	2.007	0.086
Z2.7	3.655	0.402	0.205	13.272	1.96	0.11
Z2.8	7.000	0.847	0.451	27.949	1.88	0.121
Z2.9	8.165	0.645	0.338	21.287	1.907	0.079
Z2.10	7.731	0.603	0.322	19.894	1.872	0.078

Table 34 *– Absorbances and corresponding DNA concentrations and purity ratios of the 10 clones and the eluate pool from Experiment Z3.1.*

Sample	Absorbance at 230 nm	Absorbance at 260 nm	Absorbance at 280 nm	DNA Concentration (µg/mL)	$A_{(260/280)}$	$A_{(260/230)}$
Z3.1.1	0.110	0.231	0.121	7.62	1.912	2.106
Z3.1.2	0.093	0.222	0.107	7.322	2.082	2.394
Z3.1.3	0.032	0.074	0.026	2.427	2.859	2.281
Z3.1.4	0.104	0.245	0.114	8.092	2.157	2.348
Z3.1.5	0.126	0.273	0.139	9.017	1.967	2.159
Z3.1.6	24.613	0.763	0.294	25.18	2.591	0.031
Z3.1.7	20.914	0.732	0.444	24.157	1.647	0.035
Z3.1.8	26.643	0.746	0.299	24.61	2.493	0.028
Z3.1.9	28.550	0.571	0.241	18.841	2.372	0.02
Z3.1.10	21.756	0.892	0.334	29.437	2.67	0.041
Z3.1.E	17.375	0.834	0.42	27.526	1.984	0.048

Table 35 *– Absorbances and corresponding DNA concentrations and purity ratios of the 10 clones and the eluate pool from Experiment Z3.2.*

Sample	Absorbance at 230 nm	Absorbance at 260 nm	Absorbance at 280 nm	DNA Concentration (µg/mL)	$A_{(260/280)}$	$A_{(260/230)}$
Z3.2.1	0.119	0.255	0.128	8.415	1.993	2.143
Z3.2.2	0.124	0.248	0.126	8.187	1.964	1.992
Z3.2.3	0.104	0.202	0.103	6.65	1.959	1.949
Z3.2.4	0.139	0.275	0.147	9.072	1.874	1.977
Z3.2.5	0.172	0.26	0.138	8.567	1.881	1.511
Z3.2.6	24.941	0.424	0.178	13.987	2.381	0.017
Z3.2.7	27.833	0.501	0.183	16.519	2.736	0.018
Z3.2.8	17.700	0.354	0.156	11.67	2.267	0.02
Z3.2.9	23.406	0.749	0.349	24.705	2.148	0.032
Z3.2.10	28.037	0.757	0.335	24.993	2.262	0.027
Z3.2.E	28.174	0.648	0.298	21.396	2.172	0.023

Table 36 *– Absorbances and corresponding DNA concentrations and purity ratios of the 10 clones from Experiment Z4.*

Sample	Absorbance at 230 nm	Absorbance at 260 nm	Absorbance at 280 nm	DNA Concentration (µg/mL)	$A_{(260/280)}$	$A_{(260/230)}$
Z4.1	19.167	0.23	0.08	7.582	2.868	0.012
Z4.2	1.149	0.208	0.106	6.88	1.963	0.181
Z4.3	3.038	0.398	0.211	13.139	1.883	0.131
Z4.4	7.634	0.313	0.152	10.333	2.06	0.041
Z4.5	5.091	0.168	0.087	5.53	1.923	0.033
Z4.6	5.569	0.323	0.148	10.66	2.178	0.058
Z4.7	3.095	0.229	0.117	7.56	1.956	0.074
Z4.8	6.667	0.74	0.409	24.405	1.807	0.111
Z4.9	8.018	0.449	0.228	14.816	1.971	0.056
Z4.10	7.354	0.478	0.251	15.769	1.906	0.065

Table 37 *– Absorbances and corresponding DNA concentrations and purity ratios of the amplified and purified 10 clones and eluate pool from Experiment S1.*

Sample	Absorbance at 230 nm	Absorbance at 260 nm	Absorbance at 280 nm	DNA Concentration (µg/mL)	$A_{(260/280)}$	$A_{(260/230)}$
S1.1	0.48255	0.0655	0.0655	655	1.0000	0.1357
S1.2	1.021	0.0648	0.06695	648	0.9679	0.0635
S1.3	0.2308	0.06575	0.0651	657.5	1.0100	0.2849
S1.4	1.1339	0.06495	0.0674	649.5	0.9636	0.0573
S1.5	0.25345	0.0698	0.0685	698	1.0190	0.2754
S1.6	1.07275	0.0662	0.068	662	0.9735	0.0617
S1.7	0.397	0.06915	0.06835	691.5	1.0117	0.1742
S1.8	0.83835	0.06515	0.06625	651.5	0.9834	0.0777
S1.9	0.7443	0.0656	0.0665	656	0.9865	0.0881
S1.10	0.81035	0.0657	0.0669	657	0.9821	0.0811
S1.E	0.5595	0.0667	0.06665	667	1.0008	0.1192

Table 38 *– Absorbances and corresponding DNA concentrations and purity ratios of the amplified and purified 10 clones and eluate pool from Experiment S2.*

Sample	Absorbance at 230 nm	Absorbance at 260 nm	Absorbance at 280 nm	DNA Concentration (µg/mL)	$A_{(260/280)}$	$A_{(260/230)}$
S2.1	0.06245	0.0713	0.0686	713	1.0394	1.1417
S2.2	0.4382	0.06925	0.0688	692.5	1.0065	0.1580
S2.3	0.03725	0.0712	0.0687	712	1.0364	1.9114
S2.4	0.08565	0.0695	0.0677	695	1.0266	0.8114
S2.5	0.1	0.07055	0.0677	705.5	1.0421	0.7055
S2.6	1.2329	0.0654	0.0678	654	0.9646	0.0530
S2.7	0.5981	0.0682	0.0681	682	1.0015	0.1140
S2.8	0.42805	0.0675	0.06715	675	1.0052	0.1577
S2.9	0.01435	0.0707	0.0685	707	1.0321	4.9268
S2.10	0.0701	0.07115	0.0686	711.5	1.0372	1.0150
S2.E	0.9572	0.06585	0.0675	658.5	0.9756	0.0688

Table 39 *– Absorbances and corresponding DNA concentrations and purity ratios of the amplified and purified 10 clones from Experiment Z1 amplified by PCR Experiment 1.*

Sample	Absorbance at 230 nm	Absorbance at 260 nm	Absorbance at 280 nm	DNA Concentration (µg/mL)	$A_{(260/280)}$	$A_{(260/230)}$
Z1.1	0.02345	0.0177	0.0158	177	1.1203	0.7548
Z1.2	0.0225	0.01635	0.01445	163.5	1.1315	0.7267
Z1.3	0.0248	0.01785	0.0158	178.5	1.1297	0.7198
Z1.4	0.02735	0.02085	0.0186	208.5	1.1210	0.7623
Z1.5	0.02275	0.017	0.015	170	1.1333	0.7473
Z1.6	0.02355	0.01645	0.015	164.5	1.0967	0.6985
Z1.7	0.0245	0.01735	0.01525	173.5	1.1377	0.7082
Z1.8	0.0214	0.0154	0.0137	154	1.1241	0.7196
Z1.9	0.0408	0.03365	0.03135	336.5	1.0734	0.8248
Z1.10	0.023	0.01685	0.01495	168.5	1.1271	0.7326

Table 40 *– Absorbances and corresponding DNA concentrations and purity ratios of the amplified and purified 10 clones from Experiment Z1 amplified by PCR Experiment 2.*

Sample	Absorbance at 230 nm	Absorbance at 260 nm	Absorbance at 280 nm	DNA Concentration (µg/mL)	$A_{(260/280)}$	$A_{(260/230)}$
Z1.1	0.02115	0.0153	0.01355	153	1.1292	0.7234
Z1.2	0.02305	0.01655	0.01465	165.5	1.1297	0.7180
Z1.3	0.02205	0.0161	0.01425	161	1.1298	0.7302
Z1.4	0.02055	0.01515	0.01355	151.5	1.1181	0.7372
Z1.5	0.02065	0.0156	0.014	156	1.1143	0.7554
Z1.6	0.02225	0.01705	0.0153	170.5	1.1144	0.7663
Z1.7	0.0258	0.0176	0.01555	176	1.1318	0.6822
Z1.8	0.02095	0.01565	0.01385	156.5	1.1300	0.7470
Z1.9	0.0216	0.0158	0.01435	158	1.1010	0.7315
Z1.10	0.02205	0.017	0.01545	170	1.1003	0.7710

Table 41 *– Absorbances and corresponding DNA concentrations and purity ratios of the amplified and purified 10 clones from Experiment Z1 amplified by PCR Experiment 3.*

Sample	Absorbance at 230 nm	Absorbance at 260 nm	Absorbance at 280 nm	DNA Concentration (µg/mL)	$A_{(260/280)}$	$A_{(260/230)}$
Z1.1	0.0205	0.0151	0.01365	151	1.1062	0.7366
Z1.2	0.02875	0.0226	0.02075	226	1.0892	0.7861
Z1.3	0.02555	0.01935	0.01715	193.5	1.1283	0.7573
Z1.4	0.02185	0.016	0.0144	160	1.1111	0.7323
Z1.5	0.0215	0.01515	0.01375	151.5	1.1018	0.7047
Z1.6	0.0212	0.016	0.01425	160	1.1228	0.7547
Z1.7	0.02105	0.01515	0.01365	151.5	1.1099	0.7197
Z1.8	0.02745	0.02085	0.01895	208.5	1.1003	0.7596
Z1.9	0.0219	0.0159	0.01415	159	1.1237	0.7260
Z1.10	0.0213	0.0152	0.0138	152	1.1014	0.7136

Table 42 *– Absorbances and corresponding DNA concentrations and purity ratios of the amplified and purified clones from Experiment Z2.*

Sample	Absorbance at 230 nm	Absorbance at 260 nm	Absorbance at 280 nm	DNA Concentration (µg/mL)	$A_{(260/280)}$	$A_{(260/230)}$
Z2.1	0.02085	0.0153	0.01365	153	1.1209	0.7338
Z2.2	0.0221	0.01655	0.01475	165.5	1.1220	0.7489
Z2.3	0.0214	0.01605	0.01405	160.5	1.1423	0.7500
Z2.4	0.0262	0.02035	0.01845	203.5	1.1030	0.7767
Z2.5	0.0215	0.0159	0.01395	159	1.1398	0.7395
Z2.6	0.02555	0.01845	0.01625	184.5	1.1354	0.7221
Z2.7	0.03105	0.0247	0.02275	247	1.0857	0.7955
Z2.8	0.02325	0.0168	0.01495	168	1.1237	0.7226
Z2.9	0.03505	0.02275	0.0211	227.5	1.0782	0.6491
Z2.10	0.02305	0.0165	0.01465	165	1.1263	0.7158

Table 43 *– Absorbances and corresponding DNA concentrations and purity ratios of the amplified 10 clones from Experiment Z3.1.*

Sample	Absorbance at 230 nm	Absorbance at 260 nm	Absorbance at 280 nm	DNA Concentration (µg/mL)	$A_{(260/280)}$	$A_{(260/230)}$
Z3.1.1	28.371	12.455	7.511	622.773	1.658	0.439
Z3.1.2	28.406	12.584	7.508	629.176	1.676	0.443
Z3.1.3	26.828	11.697	7.002	584.827	1.671	0.436
Z3.1.4	76.144	14.848	9.168	742.418	1.62	0.195
Z3.1.5	46.891	15.052	9.341	752.58	1.611	0.321
Z3.1.6	17.614	12.365	7.381	618.247	1.675	0.702
Z3.1.7	91.557	14.466	8.702	723.308	1.662	0.158
Z3.1.8	27.965	11.969	7.192	598.456	1.664	0.428
Z3.1.9	81.426	13.191	8.227	659.526	1.603	0.162
Z3.1.10	62.474	13.057	7.888	652.846	1.655	0.209

Table 44 *– Absorbances and corresponding DNA concentrations and purity ratios of the amplified and purified clones from Experiment Z3.1.*

Sample	Absorbance at 230 nm	Absorbance at 260 nm	Absorbance at 280 nm	DNA Concentration (µg/mL)	$A_{(260/280)}$	$A_{(260/230)}$
Z3.1.1	0.189	0.314	0.173	15.72	1.817	1.658
Z3.1.2	0.221	0.342	0.228	17.091	1.499	1.551
Z3.1.3	0.095	0.206	0.112	10.277	1.838	2.179
Z3.1.4	0.146	0.258	0.143	12.894	1.801	1.763
Z3.1.5	0.162	0.296	0.161	14.806	1.84	1.831
Z3.1.6	0.828	0.473	0.296	23.646	1.599	0.571
Z3.1.7	0.145	0.247	0.123	12.358	2.01	1.709
Z3.1.8	0.173	0.284	0.149	14.198	1.907	1.642
Z3.1.9	0.146	0.291	0.143	14.558	2.037	1.994
Z3.1.10	0.157	0.339	0.174	16.962	1.952	2.162

Table 45 *– Absorbances and corresponding DNA concentrations and purity ratios of the amplified 10 clones from Experiment Z3.2.*

Sample	Absorbance at 230 nm	Absorbance at 260 nm	Absorbance at 280 nm	DNA Concentration (µg/mL)	$A_{(260/280)}$	$A_{(260/230)}$
Z3.2.1	64.803	16.136	9.891	806.776	1.631	0.249
Z3.2.2	82.514	14.44	8.794	722.014	1.642	0.175
Z3.2.3	52.869	14.962	9.398	748.107	1.592	0.283
Z3.2.4	106.987	17.011	10.403	850.574	1.635	0.159
Z3.2.5	49.342	12.829	8.025	641.434	1.599	0.26
Z3.2.6	88.596	13.821	8.502	691.055	1.626	0.156
Z3.2.7	58.761	13.045	7.999	652.267	1.631	0.222
Z3.2.8	78.270	6.966	3.283	348.289	2.122	0.089
Z3.2.9	15.368	11.833	6.998	591.642	1.691	0.77
Z3.2.10	80.784	13.087	8.075	654.363	1.621	0.162

Table 46 *– Absorbances and corresponding DNA concentrations and purity ratios of the amplified and purified clones from Experiment Z3.2.*

Sample	Absorbance at 230 nm	Absorbance at 260 nm	Absorbance at 280 nm	DNA Concentration (µg/mL)	$A_{(260/280)}$	$A_{(260/230)}$
Z3.2.1	0.203	0.312	0.157	15.605	1.99	1.536
Z3.2.2	0.223	0.362	0.183	18.099	1.98	1.621
Z3.2.3	0.110	0.226	0.108	11.299	2.102	2.061
Z3.2.4	0.225	0.251	0.131	12.55	1.921	1.114
Z3.2.5	0.099	0.196	0.093	9.808	2.11	1.981
Z3.2.6	0.081	0.129	0.066	6.444	1.967	1.594
Z3.2.7	0.172	0.218	0.117	10.877	1.852	1.265
Z3.2.8	0.186	0.399	0.209	19.951	1.906	2.147
Z3.2.9	0.235	0.495	0.257	24.754	1.927	2.103
Z3.2.10	0.140	0.27	0.14	13.512	1.936	1.93

Table 47 *– Absorbances and corresponding DNA concentrations and purity ratios of the amplified 10 clones from Experiment Z4.*

Sample	Absorbance at 230 nm	Absorbance at 260 nm	Absorbance at 280 nm	DNA Concentration (µg/mL)	$A_{(260/280)}$	$A_{(260/230)}$
Z4.1	17.788	9.837	5.954	491.844	1.652	0.553
Z4.2	3.357	2.528	1.548	126.419	1.633	0.753
Z4.3	12.130	10.699	6.576	534.949	1.627	0.882
Z4.4	15.535	12.521	7.833	626.05	1.598	0.806
Z4.5	3.785	2.483	1.526	124.153	1.628	0.656
Z4.6	12.741	10.575	6.444	528.745	1.641	0.83
Z4.7	12.053	10.643	6.525	532.172	1.631	0.883
Z4.8	12.629	10.76	6.474	538.014	1.662	0.852
Z4.9	3.650	2.241	1.363	112.034	1.643	0.614
Z4.10	1.048	1.605	0.649	80.228	2.474	1.532

Table 48 *– Absorbances and corresponding DNA concentrations and purity ratios of the amplified and purified clones from Experiment Z4.*

Sample	Absorbance at 230 nm	Absorbance at 260 nm	Absorbance at 280 nm	DNA Concentration (µg/mL)	$A_{(260/280)}$	$A_{(260/230)}$
Z4.1	0.590	1.402	0.823	70.115	1.703	2.376
Z4.2	0.738	1.572	0.943	78.62	1.668	2.13
Z4.3	0.641	1.638	0.957	81.887	1.712	2.557
Z4.4	0.667	1.661	0.977	83.043	1.701	2.49
Z4.5	0.370	0.926	0.57	46.304	1.625	2.502
Z4.6	0.366	0.924	0.572	46.202	1.616	2.525
Z4.7	0.605	1.635	0.992	81.77	1.649	2.702
Z4.8	0.633	1.638	0.991	81.878	1.652	2.589
Z4.9	0.387	1.54	0.888	76.985	1.734	3.976
Z4.10	0.732	1.648	0.993	82.411	1.66	2.252

Table 49 *– Nucleotide sequences obtained by Sanger Sequencing for the random 10 clones chosen for Experiment S1.*

Clone	Nucleotide Sequence obtained by Sanger Sequencing
S1.1	5'GTGACAGGCTAGCTGACCGCATATTCCTCAGAAGGAATGCCGCGCTGGGTGGAGGTTCGGCCGAAACTGTTGAAAGTTGTTTAGCAAAATCCCATACAGAAAATTCATTTACTAACGTCTGGAAAGACGACAAAACTTTAGATCGTTACGCTAACTATGAGGGCAA3'
S1.2	5'CCCCGATGGNGAACGGATGCGTGNGGAGGCTGTTGCATATTCGTGGGTGGAGGTTCGGCCGAAACTGTTGAAAGTTGTTTAGCAAAATCCCATACAGAAAATTCATTTACTAACGTCTGGAAAGACGACAAAACTTTAGATCGTTACGCTAACTATGGAGGGCA3'
S1.3	5'GGATTCCGACGAATACTTATAGCGTCCGACTGGTGGAGGTTCGGCCGAAACTGTTGAAAGTTGTTTAGCAAAATCCCATACAGAAAATTCATTTACTAACGTCTGGAAAGACGACAAAACTTTAGATCGTTACGCTAACTATGAGGGCAAA3'
S1.4	5'GTCATCATGTAGTGGAATGCGGATCGTACTATCTAGGGGCCGCTGGGTGGAGGTTCGGCCGAAACTGTTGAAAGTTGTTTAGCAAAATCCCATACAGAAAATTCATTTACTAACGTCTGGAAAGACGACAAAACTTTAGATCGTTACGCTAACTATGAGGGCAA3'
S1.5	5'TGTCTCAGGCTATCTGCTGATATGTGGTATCAGACGTACGCACGACCTGGTGGAGGTTCGGCCGAAACTGTTGAAAGTTGTTTAGCAAAATCCCATACAGAAAATTCATTTACGAAAGTCTGGAAAGACGACAAAACTTTAGATCGTTACGCTAACTATGAGGGCAAT3'
S1.6	5'TGCTATGTCCTCAGAGGAGCCGCCTGGTGGAGGTTCGGCCGAAACTGTTGAAAGTTGTTTAGCAAAATCCCATACAGAAAATTCATTTACTAACGTCTGGAAAGACGACAAAACTTTAGATCGTTACGCTAACTATGAGGGCAA3'
S1.7	5'GGTCTCATCAGCAGCTGCTCCGATTTCATGGTTAGGAGTCATTGGGGTGGAGGTTCGGCCGAAACTGTTGAAAGTTGTTTAGCAAAATCCCATACAGAAAATTCATTTACTAACGTCTGGAAAGACGACAAAACTTTAGATCGTTACGCTAACTATGAGGGCAA3'
S1.8	5'GGACTGCATATTCCTGGCGAGGGATGCCTCCTGGGTGGAGGTTCGGCCGAAACTGTTGAAAGTTGTTTAGCAAAATCCCATACAGAAAATTCATTTACTAACGTCTGGAAAGACGACAAAACTTTAGATCGTTACGCTAACTATGAGGGCAA3'
S1.9	5'GTCTCATGCAGACGGATGGCTATAATGATTAGAGTGGCCGCCTGGTGGAGGTTCGGCCGAAACTGTTGAAAGTTGTTTAGCAAAATCCCATACAGAAAATTCATTTACTAACGTCTGGAAAGACGACAAAACTTTAGATCGTTACGCTAACTATGAGGGCAA3'
S1.10	5'CATCGGCCTTACTGACTAACTGCGTATAATGCCTATCGGGTGGAGGTTCGGCCGAAACTGTTGAAAGTTGTTTAGCAAAATCCCATACAGAAAATTCATTTACTAACGTCTGGAAAGACGACAAAACTTTAGATCGTTACGCTAACTATGAGGGCAAGG3'

Table 50 *– Nucleotide sequences corresponding to the library inserts obtained for Experiment S1.*

Clone	Nucleotide Sequence corresponding to the Random Peptide
S1.1	GCTGACCGCATATTCCTCAGAAGGAATGCCGCGCTG
S1.2	NGAACGGATGCGTGNGGAGGCTGTTGCATATTCGTG
S1.3	NNKNNGGATTCCGACGAATACTTATAGCGTCCGACT
S1.4	TAGTGGAATGCGGATCGTACTATCTAGGGGCCGCTG
S1.5	TCTGCTGATATGTGGTATCAGACGTACGCACGACCT
S1.6	NNKNNKNNKNNTGCTATGTCCTCAGAGGAGCCGCCT
S1.7	AGCAGCTGCTCCGATTTCATGGTTAGGAGTCATTGG
S1.8	NNKGGACTGCATATTCCTGGCGAGGGATGCCTCCTG
S1.9	GCAGACGGATGGCTATAATGATTAGAGTGGCCGCCT
S1.10	TCGGCCTTACTGACTAACTGCGTATAATGCCTATCG

Table 51 *– Nucleotide sequences obtained by Sanger Sequencing for the random 10 clones chosen for Experiment S2.*

Clone	Nucleotide Sequence obtained by Sanger Sequencing
S2.1	5'GNNNTNNNNNNGCANCTGTTGAAGTTGTTTAACAAATCCCATACGGTGGATGTTCTGCCTAAACTGTTGGAAATACGTTTAACCTTTCC ATCACTAAACATTCAATTACTGGNNTCTGGAAAGACGACAAAACTTTAGATCGTTACGCTAACTATGAGGGN3'
S2.2	5'GGTCTCGGGAACTGATTCACTGATTCTAGCTGACTGCCTACAGGGTGGAGGTTCTGCCGAAACTGTTGAAAGTTGTTTAGCATAATCCC ATACTGAACATTCATTTACGACAGTCTGGAAAGACGACAAAACTTTAGATCGTTACGCTAACTATGAGGGCAA3'
S2.3	5'TTCTGAGGGCATGCTTGATTGAAAATTCTTAATTCTGATGCCCAGCCGGGTAGGGAGGTTCGTGCCGAAACTGCAGGAAAGTTGTTTA GCAAAATCCCATACTGAACATTCATTTACTAGCAGTCTGGAAAGACGACAAAACTTTAGATCGTTACGCTAACTATGAGGGCAAAAA3'
S2.4	5'TTATCTTGGGCATTGCTAATCATGTGTTTGGTGACGTGGGGCGGCTGGTGGAGGTTCGGCCGAAACTGTTGAAAGTTGTTTAGCAAAA TCCCATACAGAAAATTCATTTACTAAAGTCTGGAAAGACGACAAAACTTTAGATCGTTACGCTAACTATGAGGGCAA3'
S2.5	5'GGTTCCATCAGGGACAGCTGCCGCGAAAGTCTTCAATATGGTGCCGCAGCGGGTGGTAGGTTCGTGCCGAAACTGCAGGAAAGTTGTT TAGCAAAATCCCATACAGAAAATTCATTTACTAACGTCTGGAAAGACGACAAAACTTTAGATCGTTACGCTAACTATGAGGGCAAG3'
S2.6	5'GTCTTCAGGGCATCTGACTCGAAAATTCTTCAATTCTGGTGCCCAGTCAGGGTGGAGGTTCGGCCGAAACTGTAGGAAAGTTGTTTAGC AAAATCCCATACTGAACATTCATTTACTAGCAGTCTGGAAAGACGACAAAACTTTAGATCGTTACGCTAACTATGAGGGCAAC3'
S2.7	5'CTCTCGGGCAGGCTGTTCAGATATCCTGTATAACTAATGATGCAGGTGGAGGTTCTGCCGAAACTGTTGGAAGTAGTTTAGCAAAATCC CTTACTGCACATTCATTTACTGGCATCTGGAAAGACGACAAAACTTTAGATCGTTACGCTAACTATGAGGGCAAA3'
S2.8	5'NNNNNNNNTCNTTCNNNATGATGNNNGTTGTGTACCATGATCCCCTACGGTGGATGCTCTTCCTAACCTGTGGAAGACGACTAACCTT TCCATCACTAAACATTCTATTACTAACGTCTGGAAAGACGACAAAACTTTAGATCGTTACGCTAACTATGAGGGCA3'
S2.9	5'TTTCCTAGGGCAACTATTGAAACGATTAGTTAATTCAGTATTCCCATCAGGGTGGAGGTTCGGCCGAAACTGTAGGAAAGTTGTTTAGC AAAATCCCATACAGAAAATTCATTTACTAACGTCTGGAAAGACGACAAAACTTTAGATCGTTACGCTAACTATGAGGGCAAA3'
S2.10	5'TTTCTCTTTGCTTCGGCGACTGCGTACTTATGCTGGGGACTCCTGGTGGAGGTTCGGCCGAAACTGTTGAAAGTTGTTTAGCAAAATCCC ATACAGAAAATTCATTTACTAACGTCTGGAAAGACGACAAAACTTTAGATCGTTACGCTAACTATGAGGGCAA3'

Table 52 *– Nucleotide sequences corresponding to the library inserts obtained for Experiment S2.*

Clone	Nucleotide Sequence corresponding to the Random Peptide
S2.1	NNNGCANCTGTTGAAGTTGTTTAACAAATCCCATAC
S2.2	GGAACTGATTCACTGATTCTAGCTGACTGCCTACAG
S2.3	TTGATTGAAAATTCTTAATTCTGATGCCCAGCCGGG
S2.4	CATTGCTAATCATGTGTTTGGTGACGTGGGGCGGCT
S2.5	TGCCGCGAAAGTCTTCAATATGGTGCCGCAGCGGGT
S2.6	TGACTCGAAAATTCTTCAATTCTGGTGCCCAGTCAG
S2.7	CAGGCTGTTCAGATATCCTGTATAACTAATGATGCA
S2.8	TCNNNATGATGNNNGTTGTGTACCATGATCCCCTAC
S2.9	NNKTGAAACGATTAGTTAATTCAGTATTCCCATCAG
S2.10	TGCTTCGGCGACTGCGTACTTATGCTGGGGACTCCT

Table 53 *– Nucleotide sequences obtained by Sanger Sequencing for the eluate pool and the random 10 clones chosen for Experiment Z1.*

Clone	Nucleotide Sequence obtained by Sanger Sequencing
Z1.1	5'CCCGNTATNAGGGAAANGATGCATANGGACTCGCTTGTGAATTTTTTTGGTGGAGGTTCGGCCGAAACTGTTGAAAGTTGTTTAGCA AAATCCCATACAGAAAATTCATTTACTAACGTCTGGAAAGACGACAAAACTTTAGATCGTTACGCTAACTATGAGGGCA3'
Z1.2	5'CCCCGAAANGAGGGCAATTNAGTCTAATTCGAAGGCTGACTATGCCGAGGGGTGGGAGGTTCGGCCGAAACTGTTGAAAGTTGTTT AGCAAAATCCCATACAGAAAATTCATTTACTANAGTCTGGAAAGACGACAAAACTTTAGATCGTTACGCTAACTATGAAGGGCA3'
Z1.3	5'NNNNNNNNCNNNTGNAGTTGTTTAGCTAATCCCATAGGTGGATGTTCTNCCGAAACTGTGGAAATTGTTTAACCTTTCCATTACTA AACATTCATTTAGGGCNNCTGGAAAGACGACAAAACTTTAGATCGTTACGCTAACTATGAGGGCA3'
Z1.4	5'NNNCNNNNNCTGTTGNNGTTGTTTAGCTAATCCCATACAGTGGATGTTCTTCCTAAACTGTGGAAATTGTTTAACCTTTCCATCACT ACACATTCTATTAGGGCNTCTGGAAAGACGACAAAACTTTAGATCGTTACGCTAACTATGAGGGCA3'
Z1.5	5'GTCTCTGCCATCTGATCGAATTTGTGTCGCCTATGCTGAGGTGGAAGTTCTGCCGAAACTGTGGAAGTTGTTTAGCAAAATCCCATACT GAACATTCATTTACTAGCAGTCTGGAAAGACGACAAAACTTTAGATCGTTACGCTAACTATGAGGGCAA3'
Z1.6	5'AACTGTTGAAGTTGTTTAGCTAATCCCATAGCGGTAGGAGGTCTCTGCCGAAACGTGCTTGGAAAGTTGTTTAGCAAAATCCCATACT GAACATTCATTTACTAACGTCTGGAAAGACGACAAAACTTTAGATCGTTACGCTAACTATGAGGGCTAA3'
Z1.7	5'AACTGTTGAAGTTGTTTAGCAAATCCCATACGAGTAGAAATTCACTTACTAACGTGCTGGAAAGTACGACTAAACTTTACATCGTTACG CTATCTATGAGGGCAGTCTGGAAAGACGACAAAACTTTAGATCGTTACGCTAACTATGAGGGCAA3'
Z1.8	5'AACTGTTGAAGTTGTTCTAGCTGAATCCTATACGGTAGAGAGGTCTCTGACGAAACTGCTTGGAAAGTTGTTTAGCAAAATCCCATAC AGAACATTCATTTACTAACGTCTGGAAAGACGACAAAACTTTAGATCGTTACGCTAACTATGAGGGCAA3'
Z1.9	5'GGGCCTACAGCTGAAGTTCGTTTAGCAGGAATCCCATACGGTAGGAGGTTCTGACGAACCTGCTTGGAAGTAGTTTAGCCTTTCCAAT ACTGAACATTCTTTGACTAGCAGTCTGGAAAGACGACAAAACTTTAGATCGTTACGCTAACTATGAGGGCAA3'
Z1.10	5'NCNGNTCTCAGGGAACTGAATGGAAGTTGTTGATGCTTCATCTCATAGGGTGGAGGCTCTGACTAAACTGTGGAAAGACGTTTAACA AAATCCCATACTAAAAATTCATTTACTGCAGTCTGGAAAGACGACAAAACTTTAGATCGTTACGCTAACTATGAGGGCA3'
Z1.Eluate	5'GNNNNANNNNNNCTGTTGAAGTTGTTTAGCAGATCCCATAGGTGGATGCTCTTACTAAACTGTGGAAATTGTTTAACCTTTCCATCA CTAAACATTCTATTAGGGNNTCTGGAAAGACGACAAAACTTTAGATCGTTACGCTAACTATGAGGGCA3'

Table 54 *– Nucleotide sequences corresponding to the library inserts obtained for Experiment Z1.*

Clone	Nucleotide Sequence corresponding to the Random Peptide
Z1.1	GAAANGATGCATANGGACTCGCTTGTGAATTTTTTT
Z1.2	CAATTNAGTCTAATTCGAAGGCTGACTATGCCGAGG
Z1.3	NNNNNNNNCNNNTGNAGTTGTTTAGCTAATCCCATA
Z1.4	CNNNNNNCTGTTGNNGTTGTTTAGCTAATCCCATAC
Z1.5	TCTGCCATCTGATCGAATTTGTGTCGCCTATGCTGA
Z1.6	NNNAACTGTTGAAGTTGTTTAGCTAATCCCATAGCG
Z1.7	NNNAACTGTTGAAGTTGTTTAGCAAATCCCATACGA
Z1.8	NNNAACTGTTGAAGTTGTTCTAGCTGAATCCTATAC
Z1.9	CTACAGCTGAAGTTCGTTTAGCAGGAATCCCATACG
Z1.10	GAACTGAATGGAAGTTGTTGATGCTTCATCTCATAG
Z1.Eluate	NANNNNNNCTGTTGAAGTTGTTTAGCAGATCCCATA

Table 55 *– Nucleotide sequences obtained by Sanger Sequencing for the eluate pool and the random 10 clones chosen for Experiment Z2.*

Clone	Nucleotide Sequence obtained by Sanger Sequencing
Z2.1	5'NNNNNCNNNNNNAANCTGNATTCTTTGAGTTCAGCAGGTCCTACAGGTGGATGTTCTGCCTAACCTGTGGANGACGACTAACAAAATC CAATACTAAAAATTCAATTACNGCNGTCTGGAAAGACGACAAAACTTTAGATCGTTACGCTAACTATGAGGGN3'
Z2.2	5'ATATTCTCAGGTCAGCTGCTTGAAAATTGTTCAAGCAGGATCCCAGTCAGGGTAGGAGGTCTCGGCCGAAACTGTTGAAAGTTGTTTAG CAAAATCCCATACTGAACATTCATTTACGAGCAGTCTGGAAAGACGACAAAACTTTAGATCGTTACGCTAACTATGAGGGCAAG3'
Z2.3	5'GGTCTCAGGAACTGCTTGAAATTGTTCATCTAGAATGCCCAGCAGGGTAGGAGGTTCGGCCGAAACTGTAGGAAAGTTGTTTAGCAAAA TCCCATACTGAACATTCATTTACTAGCGTCTGGAAAGACGACAAAACTTTAGATCGTTACGCTAACTATGAGGGCAAA3'
Z2.4	5'TCAGGGTAAGACTGCCGCGAGAAGTCTTCAGACTGGTGCCGGCGGGTGGAGGTTCGGCCGAAACTGTAGGAAAGTTGTTTAGCAAAAT CCCATACAGAAAATTCATTTACTAACGTCTGGAAAGACGACAAAACTTTAGATCGTTACGCTAACTATGAGGGCAAG3'
Z2.5	5'GGTTGCTCTTATGCATCCTGCTGCCGGATTTGAGGCGGCAGTTGACTGGTAGGAGGTTCGGCCGAAACTGTTGAAAGTTGTTTAGCAAA ATCCCATACAGAAAATTCATTTACTAACGTCTGGAAAGACGACAAAACTTTAGATCGTTACGCTAACTATGAGGGCAA3'
Z2.6	5'TTTCTCAGGGCAAGCTGCCTTGAAAGTTAGTTCATGCTTAATCCCATAGGGTGGGAGGTCTCGGCCGAAACTGTAGGAAAGTTGTTTAG CAAAATCCCATACAGAACATTCATTTACTAGCAGTCTGGAAAGACGACAAAACTTTAGATCGTTACGCTAACTATGAGGGCAAAC3'
Z2.7	5'GGTAGGGGGAAAGGGCAACTGCTTGAAATTCTTCAGACTGGAGCCCAGTCAGGGTGGATGTTCTGCCGAACCTGTGGAAGTAGTTTAG CCTTTCCATCACTACACATTCTATGACGGCATCTGGAAAGACGACAAAACTTTAGATCGTTACGCTAACTATGAGGGCAA3'
Z2.8	5'GGTTCATCAGGAGAAACTGCTTCGAAAAGTCTTAGATGGTGCCGGCGGGTGGAGGTTCGGCCGAAACTGTAGAAAGTTGTTTAGCAAA ATCCCATACAGAAAATTCATTTACTAACGTCTGGAAAGACGACAAAACTTTAGATCGTTACGCTAACTATGAGGGCAAG3'
Z2.9	5'AGTTGCTCAGGCATCTGCTTGAAAATTGTTCAGCTGAAGCCCAGTCAGCGGGGTAGAGAGGTTCTGCACGAAACTGTAGGAAAGTTGTT TAGCAAAATCCCATACAGAACATTCATTTACTAACGTCTGGAAAGACGACAAAACTTTAGATCGTTACGCTAACTATGAGGGCAAAA3'
Z2.10	5'ATTCTGAGGGCATGCGCCGCGAGAAGTCTTCGATGGTGCCGGCGGGTGGAGGTTCGGCCGAAACTGTTGAAAGTTGTTTAGCAAAATC CCATACAGAAAATTCATTTACTAACGTCTGGAAAGACGACAAAACTTTAGATCGTTACGCTAACTATGAGGGCAA3'
Z2.Eluate	5'TTCCTCAGGCAGCTTATTGATAGATTACTTCATCCGATGCCGGCGGGTGGAGGTTCGGCCGAAACTGTAGAAAGTTGTTTAGCAAAATC CCATACAGAAAATTCATTTACTAACGTCTGGAAAGACGACAAAACTTTAGATCGTTACGCTAACTATGAGGGCAA3'

Table 56 *– Nucleotide sequences corresponding to the library inserts obtained for Experiment Z2.*

Clone	Nucleotide Sequence corresponding to the Random Peptide
Z2.1	NNNAANCTGNATTCTTTGAGTTCAGCAGGTCCTACA
Z2.2	GCTGCTTGAAAATTGTTCAAGCAGGATCCCAGTCAG
Z2.3	AACTGCTTGAAATTGTTCATCTAGAATGCCCAGCAG
Z2.4	AGACTGCCGCGAGAAGTCTTCAGACTGGTGCCGGCG
Z2.5	GCATCCTGCTGCCGGATTTGAGGCGGCAGTTGACTG
Z2.6	GCCTTGAAAGTTAGTTCATGCTTAATCCCATAGGGT
Z2.7	AACTGCTTGAAATTCTTCAGACTGGAGCCCAGTCAG
Z2.8	AGAAACTGCTTCGAAAAGTCTTAGATGGTGCCGGCG
Z2.9	TGAAAATTGTTCAGCTGAAGCCCAGTCAGCGGGGTA
Z2.10	GGCATGCGCCGCGAGAAGTCTTCGATGGTGCCGGCG
Z2.Eluate	CAGCTTATTGATAGATTACTTCATCCGATGCCGGCG

Table 57 *– Nucleotide sequences obtained by Sanger Sequencing for the eluate pool and random 10 clones chosen for Experiment Z3.1.*

Clone	Nucleotide Sequence obtained by Sanger Sequencing
Z3.1.1	5'TGAGTTCTTCAGACTGGTGCCGGCGGGTGGAGGTTCGGCCGAAACTGTAGAAAGTTGTTTAGCAAAATCCCATACAGAAAATTCATTTACTAACGTCTGGAAAGACGACAAAACTTTAGATCGTTACGCTAACTATGAGGGCATTA3'
Z3.1.2	5'GCCGCGAAAGTCTTAGACTGGTGCCGGCGGGTGGAGGTTCGGCCGAAACTGTAGAAAGTTGTTTAGCAAAATCCCATACAGAAAATTCATTTACTAAATCTGGAAAGACGACAAAACTTTAGATCGTTACGCTAACTATGAGGGCAAC3'
Z3.1.3	5'TTCTGGAGGGAAACGCCGCGAGAAGTCTTCAGATGGTGCCGGCGGGTGGAGGTCTCGGCCGAAACTGTAGAAAGTTGTTTAGCAAAATCCCATACAGAAAATTCATTTACTAACGTCTGGAAAGACGACAAAACTTTAGATCGTTACGCTAACTATGAGGGCAAT3'
Z3.1.4	5'ACCTCTGAGGGAAGCTGACTGATAATTACTTCATCTGGTGCCGGCGGGTGGAGGTTCGGCCGAAACTGCAGGAAGTTGTTTAGCAAAATCCCATACTGAACATTCATTTACTAACGTCTGGAAAGACGACAAAACTTTAGATCGTTACGCTAACTATGAGGGCAA3'
Z3.1.5	5'TTTCTTCAGGGTAAGCTGCCGCGAGAAGTCTTCAGACTGGTGCCGGCGGGTGGAGGTTCGGCCGAAACTGTAGGAAAGTTGTTTAGCAAAATCCCATACAGAAAATTCATTTACTAACAGTCTGGAAAGACGACAAAACTTTAGATCGTTACGCTAACTATGAGGGCAAG3'
Z3.1.6	5'CCCCGAGCTTACGCCGCGGAAGTCTTCGATGGTGCCGGCGGGTGGAGGTTCGGCCGAAACTGTTGAAAGTTGTTTAGCAAAATCCCATACAGAAAATTCATTTACTAACGTCTGGAAAGACGACAAAACTTTAGATCGTTACGCTAACTATGAGGGCAAAAA3'
Z3.1.7	5'GGAGCTACGCCGCGGAGTCTTCGATGGTGCCGGCGGGTGGAGGTTCGGCCGAAACTGTTGAAAGTTGTTTAGCAAAATCCCATACAGAAAATTCATTTACTAACGTCTGGAAAGACGACAAAACTTTAGATCGTTACGCTAACTATGAGGGCAAAAA3'
Z3.1.8	5'TCGAGCTACGCCGCGGAGTCTTCGATGGTGCCGGCGGGTGGAGGTTCGGCCGAAACTGTTGAAAGTTGTTTAGCAAAATCCCATACAGAAAATTCATTTACTAACGTCTGGAAAGACGACAAAACTTTAGATCGTTACGCTAACTATGAGGGCAAAAA3'
Z3.1.9	5'GAGCTACGCCGCGGAGTCTTCGATGGTGCCGGCGGGTGGAGGTTCGGCCGAAACTGTTGAAAGTTGTTTAGCAAAATCCCATACAGAAAATTCATTTACTAACGTCTGGAAAGACGACAAAACTTTAGATCGTTACGCTAACTATGAGGGCATTTTT3'
Z3.1.10	5'GGTGCTGAGGCATACGCGCGGAAGTCTTCGATGGTGCCGGCGGGTGGAGGTTCGGCCGAAACGTGTTGAAAGTTGTTTAGCAAAATCCCATACAGAAAATTCATTTACTAACGTCTGGAAAGACGACAAAACTTTAGATCGTTACGCTAACTATGAGGGCAA3'
Z3.1.Eluate	5'CGCGGAGTCTTCGATGGTGCCGGCGGGTGGAGGTTCGGCCGAAACTGTTGAAAGTTGTTTAGCAAAATCCCATACAGAAAATTCATTTACTAACGTCTGGAAAGACGACAAAACTTTAGATCGTTACGCTAACTATGAGGGCAAAAA3'

Table 58 *– Nucleotide sequences corresponding to the library inserts obtained for Experiment Z3.1.*

Clone	Nucleotide Sequence corresponding to the Random Peptide
Z3.1.1	NNKNNKNNKNNTGAGTTCTTCAGACTGGTGCCGGCG
Z3.1.2	NNKNNKNGCCGCGAAAGTCTTAGACTGGTGCCGGCG
Z3.1.3	GGAAACGCCGCGAGAAGTCTTCAGATGGTGCCGGCG
Z3.1.4	GAAGCTGACTGATAATTACTTCATCTGGTGCCGGCG
Z3.1.5	AAGCTGCCGCGAGAAGTCTTCAGACTGGTGCCGGCG
Z3.1.6	GAGCTTACGCCGCGGAAGTCTTCGATGGTGCCGGCG
Z3.1.7	NGGAGCTACGCCGCGGAGTCTTCGATGGTGCCGGCG
Z3.1.8	TCGAGCTACGCCGCGGAGTCTTCGATGGTGCCGGCG
Z3.1.9	NNGAGCTACGCCGCGGAGTCTTCGATGGTGCCGGCG
Z3.1.10	GAGGCATACGCGCGGAAGTCTTCGATGGTGCCGGCG
Z3.1.Eluate	NNKNNKNNKNNCGCGGAGTCTTCGATGGTGCCGGCG

Table 59 *– Nucleotide sequences obtained by Sanger Sequencing for the eluate pool and random 10 clones chosen for Experiment Z3.2.*

Clone	Nucleotide Sequence obtained by Sanger Sequencing
Z3.2.1	5'NCCGNTANGAAGGGAACAGGATGCGTTGGGNAGGCTCTTGATATTCGTGGTGGAGGTTCGGCCGAAACTGTTGAAAGTTGTTTA GCAAAATCCCATACAGAAAATTCATTTACTAACGTCTGGAAAGACGACAAAACTTTAGATCGTTACGCTAACTATGAGGGCA3'
Z3.2.2	5'ACCGCACTGGGNAACNGATGCGTTGGGAGGCTGTTGATATTCGTGGTGGAGGTTCGGCCGAAACTGTTGAAAGTTGTTTAGCAAA ATCCCATACAGAAAATTCATTTACTAACGTCTGGAAAGACGACAAAACTTTAGATCGTTACGCTAACTATGAGGGCAT3'
Z3.2.3	5'ACCGGAANGAAGGCAACAGGAATGCGTGGGANGCTGTTGATATTCGTGGTGGAGGTTCGGCCGAAACTGTATGAAAGTTGTTTA GCAAAATCCCATACAGAAAATTCATTTACTAACGTCTGGAAAGACGACAAAACTTTAGATCGTTACGCTAACTATGAGAGGCA3'
Z3.2.4	5'CCGGGAACNGATGGCAANNGATGCGTTGGGAGGCTGTTGATATTCGTGGTGGAGGTTCGGCCGAAACTGTTGAAAGTTGTTTAG CAAAATCCCATACAGAAAATTCATTTACTAACGTCTGGAAAGACGACAAAACTTTAGATCGTTACGCTAACTATGAGGGCA3'
Z3.2.5	5'ACAGCNTTTAAGGAANNGNAGCGTGGGATGCTGTTGATATTGCTGGTGGAGGTTCGGCCGAAACTGTTGAAAGTTGTTTAGCAAA ATCCCATACAGAAAATTCATTTACTAACGTCTGGAAAGACGACAAAACTTTAGATCGTTACGCTAACTATGAGGGCAA3'
Z3.2.6	5'CCCGCAAATGAGGGAAGNGAATGCTTGGTAATGCTGTTGATATTGCTGGTGGAGGTTCGGCCGAAACTGTTGAAAGTTGTTTAGC AAAATCCCATACAGAAAATTCATTTACTAACGTCTGGAAAGACGACAAAACTTTAGATCGTTACGCTAACTATGAGGGCAA3'
Z3.2.7	5'ACGGNTCTCAGGGAANNGNAATGCGTGGGATGCTGTTGATATTCNTGGTGGAGGTTCGGCCGAAACTGTTGAAAGTTGTTTAGC AAAATCCCATACAGAAAATTCATTTACTAACGTCTGGAAAGACGACAAAACTTTAGATCGTTACGCTAACTATGAGGGCA3'
Z3.2.8	5'CCCGNATNGAGGAAGNCAAGCGTTGGGGAAGCTGTTGATATTGCTGGTGGAGGTTCGGCCGAAACTGTTGAAAGTTGTTTAGCA AAATCCCATACAGAAAATTCATTTACTAACGTCTGGAAAGACGACAAAACTTTAGATCGTTACGCTAACTATGAGGGCAA3'
Z3.2.9	5'CAGGGTNTGNGGCAAGTNNTGCGTGGGANGCTGTTGATATTNATGGTGGAGGTTCGGCCGAAACTGTTGAAAGTTGTTTAGCAA AATCCCATACAGAAAATTCATTTACTAACGTCTGGAAAGACGACAAAACTTTAGATCGTTACGCTAACTATGAGGGCAG3'
Z3.2.10	5'CCCGCAANGAGGGCAACNGNTGCGTGGGANGCTGTTGCATATTCGTGGTGGAGGTTCGGCCGAAACTGTTGAAAGTTGTTTAGC AAAATCCCATACAGAAAATTCATTTACTAACGTCTGGAAAGACGACAAAACTTTAGATCGTTACGCTAACTATGAGGGCA3'
Z3.2.Eluate	5'CCGGCAANGAGGGAACNGGAATGCGTGGGAGGCTGTTGATATTCGTGGTGGAGGTTCGGCCGAAACTGTTGAAAGTTGTTTAGC AAAATCCCATACAGAAAATTCATTTACTAACGTCTGGAAAGACGACAAAACTTTAGATCGTTACGCTAACTATGAGGGCA3'

Table 60 *– Nucleotide sequences corresponding to the library inserts obtained for Experiment Z3.2.*

Clone	Nucleotide Sequence corresponding to the Random Peptide
Z3.2.1	GGAACAGGATGCGTTGGGNAGGCTCTTGATATTCGT
Z3.2.2	GGGNAACNGATGCGTTGGGAGGCTGTTGATATTCGT
Z3.2.3	GGCAACAGGAATGCGTGGGANGCTGTTGATATTCGT
Z3.2.4	TGGCAANNGATGCGTTGGGAGGCTGTTGATATTCGT
Z3.2.5	TAAGGAANNGNAGCGTGGGATGCTGTTGATATTGCT
Z3.2.6	GGGAAGNGAATGCTTGGTAATGCTGTTGATATTGCT
Z3.2.7	GGGAANNGNAATGCGTGGGATGCTGTTGATATTCNT
Z3.2.8	AGGAAGNCAAGCGTTGGGGAAGCTGTTGATATTGCT
Z3.2.9	GNGGCAAGTNNTGCGTGGGANGCTGTTGATATTNAT
Z3.2.10	GGGCAACNGNTGCGTGGGANGCTGTTGCATATTCGT
Z3.2.Eluate	GGGAACNGGAATGCGTGGGAGGCTGTTGATATTCGT

Table 61 *– Nucleotide sequences obtained by Sanger Sequencing for the eluate pool and the random 10 clones chosen for Experiment Z4.*

Clone	Nucleotide Sequence obtained by Sanger Sequencing
Z4.1	5'CAGGGGGAAATGGANGGGAACGGGATGCGTGGGAGGCTGTTGATATTCGTGGTGGAGGTTCGGCCGAAACTGTTGAAAGTTGTTTAGCAAAATCCCATACAGAAAATTCATTTACTAACGTCTGGAAAGACGACAAAACTTTAGATCGTTACGCTAACTATGAGGGCA3'
Z4.2	5'AAGGAGNAATCAATTAACCAGGATGCGTGGGAGGCTGTTGATATTCGTGGTGGAGGTTCGGCCGAAACTGTTGAAAGTTGTTTAGCAAAATCCCATACAGAAAATTCATTTACTAACGTCTGGAAAGACGACAAAACTTTAGATCGTTACGCTAACTATGAGGGCA3'
Z4.3	5'TCAGGCAANGAGGGAACGGAATGCGTGGGAAGGCTGTTGATATTCGTGGTGGAGGTTCGGCCGAAACTGTTGAAAGTTGTTTAGCAAAATCCCATACAGAAAATTCATTTACTAACGTCTGGAAAGACGACAAAACTTTAGATCGTTACGCTAACTGATGAGGGCA3'
Z4.4	5'CCCGGGAATTGAAGGGAACGGAATGCGTGGGAGGCTGTTGATATTCGTGGTGGAGGTTCGGCCGAAACTGTTGAAAGTTGTTTAGCAAAATCCCATACAGAAAATTCATTTACTAACGTCTGGAAAGACGACAAAACTTTAGATCGTTACGCTAACTGATGAGGGCA3'
Z4.5	5'CACCGAGGAACTCGTGGAATTAAGTCTCATTTTTCGCATACTGGGAAGGGTGGAGGTTCGGCCGAAACTGTTGAAAGTTGTTTAGCAAAATCCCATACAGAAAATTCATTTACTAACGTCTGGAAAGACGACAAAACTTTAGATCGTTACGCTAACTATGAGGGCAA3'
Z4.6	5'ACCGATCNGAGGAACGGAAGCGTTGGGAGGCTGTTGATATTCGTGGGTGGGAGGTTCGGCCGAAACTGTTGAAAGTTGTTTAGCAAAATCCCATACAGAAAATTCATTTACTAACGTCTGGAAAGACGACAAAACTTTAGATCGTTACGCTAACTATGAGGGCAAAT3'
Z4.7	5'CCGGAGNAATNAAGGAACAGGAATGCGTGGGAGGCTGTTGATATTCGTGGTGGAGGTTCGGCCGAAACTGTTGAAAGTTGTTTAGCAAAATCCCATACAGAAAATTCATTTACTAACGTCTGGAAAGACGACAAAACTTTAGATCGTTACGCTAACTATGAGGGCA3'
Z4.8	5'CCCGGNANGAGGGAANGGAATGCGTGGGAGGCTGTTGATATTCGTGGTGGAGGTTCGGCCGAAACTGTTGAAAGTTGTTTAGCAAAATCCCATACAGAAAATTCATTTACTAACGTCTGGAAAGACGACAAAACTTTAGATCGTTACGCTAACTGATGAGGGCA3'
Z4.9	5'ACGGCAAATGAGGAACNGGAATGCGTGGGAGGCTGTTGATATTCGTGGTGGAGGTTCGGCCGAAACTGTTGAAAGTTGTTTAGCAAAATCCCATACAGAAAATTCATTTACTAACGTCTGGAAAGACGACAAAACTTTAGATCGTTACGCTAACTATGAGGGCA3'
Z4.10	5'TCCGGGGANTGCAAGGGAACCGGAATGCGTGGGAGGCTGTTGATATTCGTGGTGGAGGTTCGGCCGAAACTGTTGAAAGTTGTTTAGCAAAATCCCATACAGAAAATTCATTTACTAACGTCTGGAAAGACGACAAAACTTTAGATCGTTACGCTAACTATGAGGGCA3'
Z4.Eluate	5'CCCGGCTATNAGGAACAGNAATGCGTGGGAGGCTGTTGATATTCGTGGTGGAGGTTCGGCCGAAACTGTTGAAAGTTGTTTAGCAAAATCCCATACAGAAAATTCATTTACTAACGTCTGGAAAGACGACAAAACTTTAGATCGTTACGCTAACTATGAGGGCA3'

Table 62 *– Nucleotide sequences corresponding to the library inserts obtained for Experiment Z4.*

Clone	Nucleotide Sequence corresponding to the Random Peptide
Z4.1	NGGGAACGGGATGCGTGGGAGGCTGTTGATATTCGT
Z4.2	ATTAACCAGGATGCGTGGGAGGCTGTTGATATTCGT
Z4.3	GGGAACGGAATGCGTGGGAAGGCTGTTGATATTCGT
Z4.4	AGGGAACGGAATGCGTGGGAGGCTGTTGATATTCGT
Z4.5	CGTGGAATTAAGTCTCATTTTTCGCATACTGGGAAG
Z4.6	AGGAACGGAAGCGTTGGGAGGCTGTTGATATTCGTG
Z4.7	AGGAACAGGAATGCGTGGGAGGCTGTTGATATTCGT
Z4.8	AGGGAANGGAATGCGTGGGAGGCTGTTGATATTCGT
Z4.9	AGGAACNGGAATGCGTGGGAGGCTGTTGATATTCGT
Z4.10	GGGAACCGGAATGCGTGGGAGGCTGTTGATATTCGT
Z4.Eluate	AGGAACAGNAATGCGTGGGAGGCTGTTGATATTCGT

Annex 3: Figures

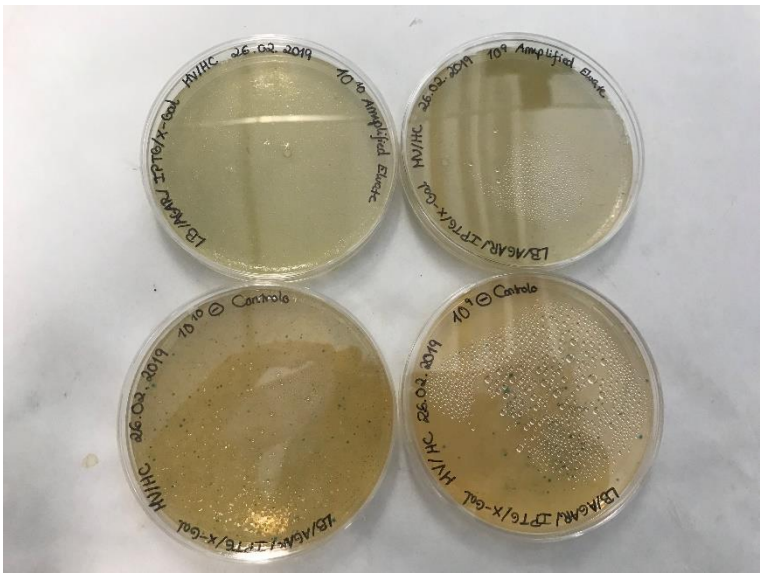

Figure 25 *– Example of the plates obtained for the titering of the amplified third round phage eluate pool on Experiment S1.*

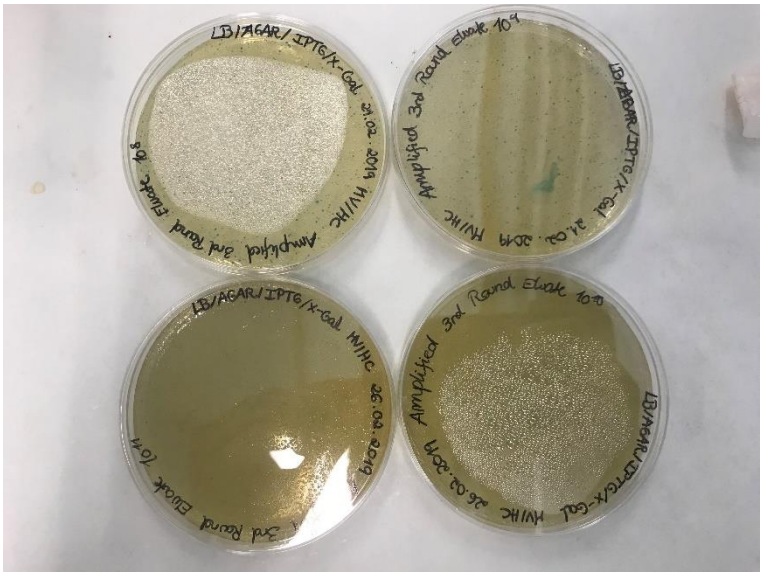

Figure 26 *– Example of the plates obtained for the titering of the amplified third round phage eluate pool on Experiment Z1.*

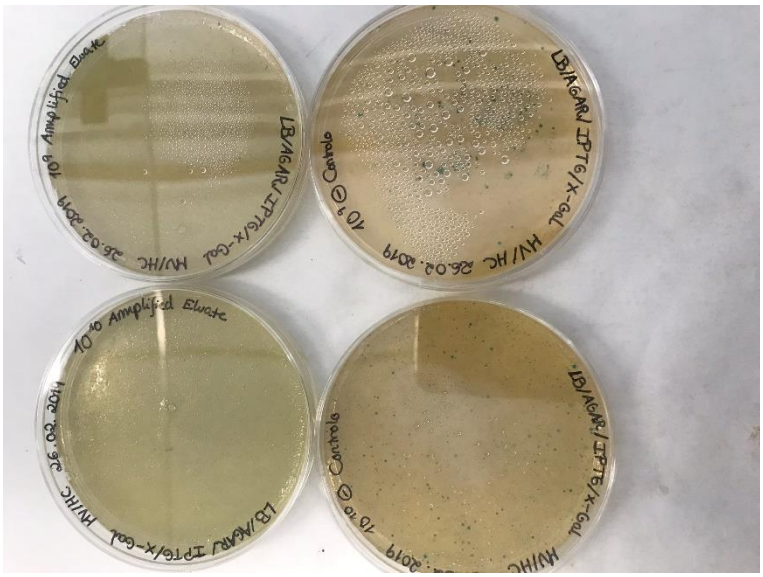

Figure 27 *– Example of the plates obtained for the titering of the amplified third round phage eluate pool on Experiment S2.*

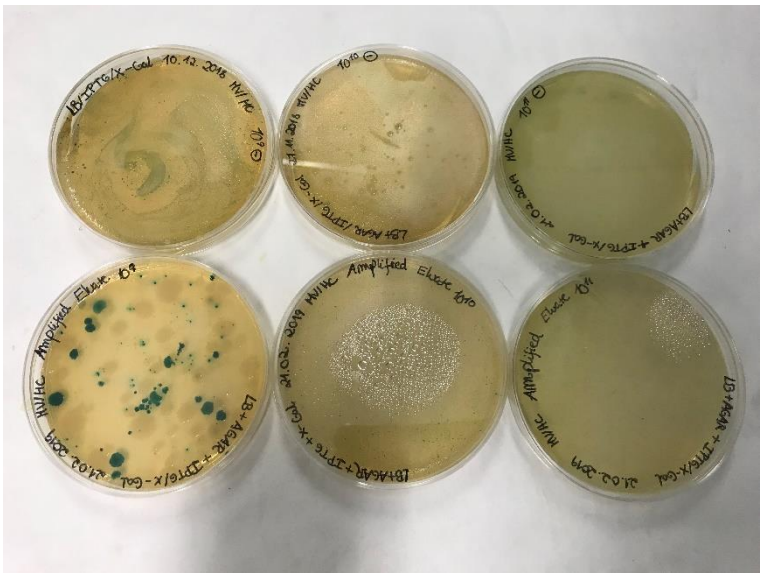

Figure 28 *– Example of the plates obtained for the titering of the amplified third round phage eluate pool on Experiment Z2.*

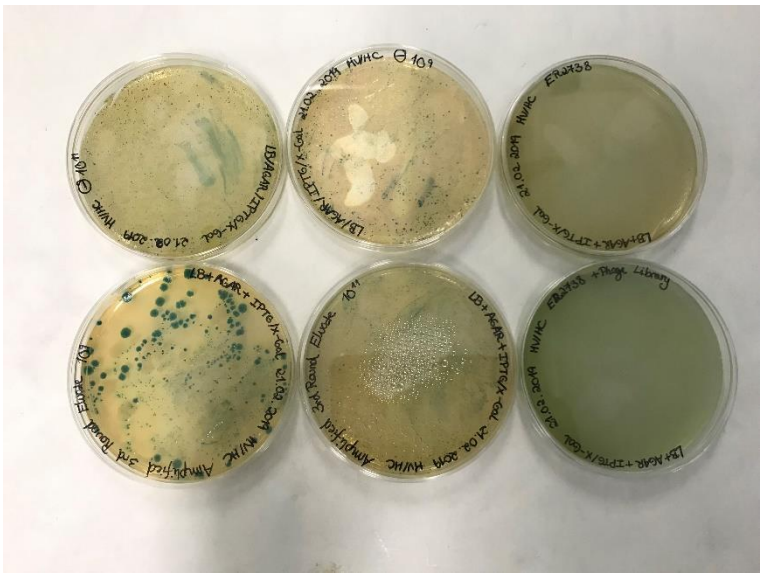

Figure 29 *– Example of the plates obtained for the titering of the amplified third round phage eluate pool on Experiment Z3.*

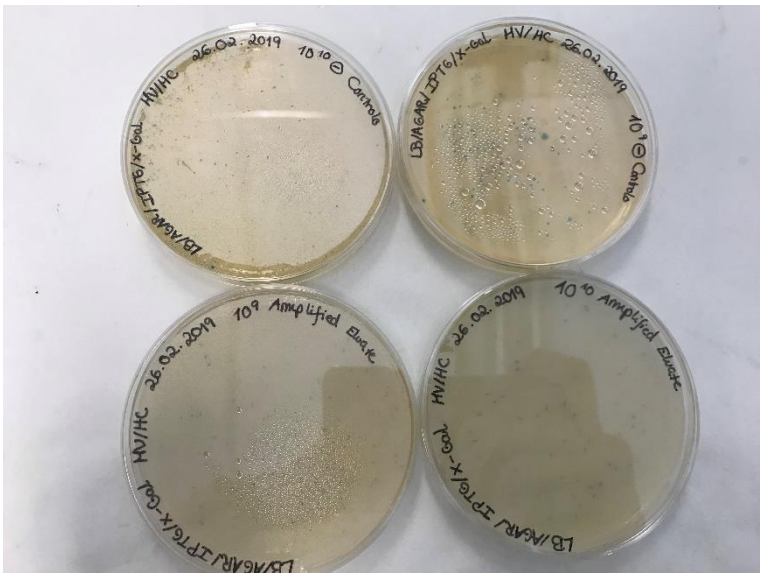

Figure 30 *– Example of the plates obtained for the titering of the amplified third round phage eluate pool on Experiment Z4.*